

August 2004

Revision 0

MAGNASTOR

(Modular Advanced Generation
Nuclear All-purpose STORAge)

SAFETY ANALYSIS REPORT

Docket No. 72-1031



Atlanta Corporate Headquarters, 3930 East Jones Bridge Road, Norcross, Georgia 30092 USA
Phone 770-447-1144, Fax 770-447-1797, www.nacintl.com

List of Effective Pages

Chapter 1

Page 1-i	Revision 0
Page 1-1	Revision 0
Page 1.1-1 thru 1.1-2.....	Revision 0
Page 1.2-1	Revision 0
Page 1.3-1 thru 1.3-15.....	Revision 0
Page 1.4-1	Revision 0
Page 1.5-1	Revision 0
Page 1.6-1 thru 1.6-2.....	Revision 0
Page 1.7-1 thru 1.7-2.....	Revision 0
Page 1.8-1	Revision 0

15 drawings (see Section 1.8)

Chapter 2

Page 2-i thru 2-ii	Revision 0
Page 2-1	Revision 0
Page 2.1-1 thru 2.1-4.....	Revision 0
Page 2.2-1 thru 2.2-7.....	Revision 0
Page 2.3-1 thru 2.3-9.....	Revision 0
Page 2.4-1 thru 2.4-8.....	Revision 0
Page 2.5-1	Revision 0
Page 2.6-1 thru 2.6-2.....	Revision 0

Chapter 3

Page 3-i thru 3-iii	Revision 0
Page 3-1	Revision 0
Page 3.1-1 thru 3.1-5.....	Revision 0
Page 3.2-1 thru 3.2-2.....	Revision 0
Page 3.3-1	Revision 0
Page 3.4-1 thru 3.4-27.....	Revision 0
Page 3.5-1 thru 3.5-27.....	Revision 0
Page 3.6-1 thru 3.6-9.....	Revision 0
Page 3.7-1 thru 3.7-85.....	Revision 0
Page 3.8-1	Revision 0
Page 3.9-1 thru 3.9-2.....	Revision 0

Chapter 3 Appendices

Page 3.A-i thru 3.A-ii.....	Revision 0
Page 3.A-1 thru 3.A-18.....	Revision 0
Page 3.B-1 thru 3.B-18	Revision 0
Page 3.C-1 thru 3.C-7	Revision 0
Page 3.D-1 thru 3.D-14.....	Revision 0
Page 3.E-1 thru 3.E-2.....	Revision 0

Chapter 4

Page 4-i thru 4-ii	Revision 0
Page 4-1	Revision 0
Page 4.1-1 thru 4.1-6.....	Revision 0
Page 4.2-1	Revision 0
Page 4.3-1	Revision 0
Page 4.4-1 thru 4.4-43.....	Revision 0
Page 4.5-1 thru 4.5-2.....	Revision 0
Page 4.6-1 thru 4.6-3.....	Revision 0
Page 4.7-1 thru 4.7-2.....	Revision 0

Chapter 4 Appendices

Page 4.A-i	Revision 0
Page 4.A-1 thru 4.A-10.....	Revision 0
Page 4.B-1 thru 4.B-3	Revision 0

Chapter 5

Page 5-i thru 5-iii	Revision 0
Page 5-1	Revision 0
Page 5.1-1 thru 5.1-4.....	Revision 0
Page 5.2-1 thru 5.2-11.....	Revision 0
Page 5.3-1 thru 5.3-2.....	Revision 0
Page 5.4-1 thru 5.4-2.....	Revision 0
Page 5.5-1 thru 5.5-14.....	Revision 0
Page 5.6-1 thru 5.6-12.....	Revision 0
Page 5.7-1 thru 5.7-3.....	Revision 0

Chapter 5 Appendices

Page 5.A-i thru 5.A-iii	Revision 0
Page 5.A-1 thru 5.A-4.....	Revision 0
Page 5.B-1 thru 5.B-4	Revision 0
Page 5.C-1 thru 5.C-37	Revision 0
Page 5.D-1 thru 5.D-32.....	Revision 0
Page 5.E-1 thru 5.E-9.....	Revision 0
Page 5.F-1 thru 5.F-2.....	Revision 0
Page 5.G-1 thru 5.G-38.....	Revision 0
Page 5.H-1 thru 5.H-51.....	Revision 0

Chapter 6

Page 6-i thru 6-ii	Revision 0
Page 6-1	Revision 0
Page 6.1-1 thru 6.1-6.....	Revision 0
Page 6.2-1 thru 6.2-4.....	Revision 0
Page 6.3-1 thru 6.3-9.....	Revision 0

List of Effective Pages (cont'd)

Page 6.4-1 thru 6.4-8.....	Revision 0	Page 9.3-1 thru 9.3-3.....	Revision 0
Page 6.5-1 thru 6.5-7.....	Revision 0		
Page 6.6-1	Revision 0	<u>Chapter 10</u>	
<u>Chapter 6 Appendices</u>		Page 10-i	Revision 0
Page 6.A-i thru 6.A-ii.....	Revision 0	Page 10-1	Revision 0
Page 6.A-1 thru 6.A-23.....	Revision 0	Page 10.1-1 thru 10.1-8.....	Revision 0
Page 6.B-1 thru 6.B-5	Revision 0	Page 10.2-1 thru 10.2-3.....	Revision 0
Page 6.C-1 thru 6.C-10	Revision 0	Page 10.3-1 thru 10.3-2.....	Revision 0
Page 6.D-1 thru 6.D-16.....	Revision 0	<u>Chapter 11</u>	
Page 6.E-1 thru 6.E-7.....	Revision 0	Page 11-i	Revision 0
Page 6.F-1 thru 6.F-9	Revision 0	Page 11-1 thru 11-10.....	Revision 0
Page 6.G-1 thru 6.G-27.....	Revision 0		
<u>Chapter 7</u>		<u>Chapter 12</u>	
Page 7-i	Revision 0	Page 12-i	Revision 0
Page 7-1	Revision 0	Page 12-1	Revision 0
Page 7.1-1 thru 7.1-5.....	Revision 0	Page 12.1-1 thru 12.1-8.....	Revision 0
Page 7.2-1 thru 7.2-2.....	Revision 0	Page 12.2-1 thru 12.2-21.....	Revision 0
Page 7.3-1	Revision 0	Page 12.3-1 thru 12.3-2.....	Revision 0
Page 7.4-1	Revision 0	<u>Chapter 13</u>	
<u>Chapter 8</u>		Page 13-i	Revision 0
Page 8-i thru 8-ii	Revision 0	Page 13-1	Revision 0
Page 8-1	Revision 0	Page 13A-i	Revision 0
Page 8.1-1 thru 8.1-3.....	Revision 0	Page 13A-1 thru 13A-28.....	Revision 0
Page 8.2-1	Revision 0	Page 13B-i.....	Revision 0
Page 8.3-1 thru 8.3-15.....	Revision 0	Page 13B-1 thru 13B-76	Revision 0
Page 8.4-1	Revision 0	Page 13C-i.....	Revision 0
Page 8.5-1 thru 8.5-2.....	Revision 0	Page 13C-1 thru 13C-20	Revision 0
Page 8.6-1 thru 8.6-2.....	Revision 0	<u>Chapter 14</u>	
Page 8.7-1 thru 8.7-2.....	Revision 0	Page 14-i	Revision 0
Page 8.8-1 thru 8.8-2.....	Revision 0	Page 14-1 thru 14-2.....	Revision 0
Page 8.9-1	Revision 0	Page 14.1-1 thru 14.1-8.....	Revision 0
Page 8.10-1 thru 8.10-7.....	Revision 0	Page 14.2-1	Revision 0
Page 8.11-1	Revision 0	<u>Chapter 15</u>	
Page 8.12-1 thru 8.12-3.....	Revision 0	Page 15-i	Revision 0
Page 8.13-1 thru 8.13-17.....	Revision 0	Page 15-1 thru 15-5.....	Revision 0
<u>Chapter 9</u>			
Page 9-i	Revision 0		
Page 9-1 thru 9-2.....	Revision 0		
Page 9.1-1 thru 9.1-17.....	Revision 0		
Page 9.2-1 thru 9.2-2.....	Revision 0		

Chapter 1 General Description

Table of Contents

1	GENERAL DESCRIPTION	1-1
1.1	Terminology.....	1.1-1
1.2	Introduction.....	1.2-1
1.3	General Description of MAGNASTOR.....	1.3-1
1.3.1	MAGNASTOR Components.....	1.3-1
1.3.2	Operational Features	1.3-6
1.4	MAGNASTOR Contents.....	1.4-1
1.5	Identification of Agents and Contractors.....	1.5-1
1.6	Generic Concrete Cask Arrays.....	1.6-1
1.7	References.....	1.7-1
1.8	License Drawings.....	1.8-1

List of Figures

Figure 1.3-1	Major Component Configuration for Loading the Concrete Cask	1.3-8
Figure 1.3-2	TSC and Basket.....	1.3-9
Figure 1.3-3	Concrete Cask	1.3-10
Figure 1.3-4	Transport Configuration of the Transport Cask.....	1.3-11
Figure 1.6-1	Typical ISFSI Storage Pad Layout	1.6-2

List of Tables

Table 1.3-1	Design Characteristics	1.3-12
Table 1.3-2	Physical Design Parameters of the TSC and Fuel Baskets.....	1.3-13
Table 1.3-3	TSC Fabrication Specification Summary	1.3-14
Table 1.3-4	Concrete Cask Fabrication Specification Summary	1.3-15

1 GENERAL DESCRIPTION

This Safety Analysis Report (SAR) describes the NAC International Inc. (NAC) MAGNASTOR System for the storage of spent fuel. It demonstrates that MAGNASTOR satisfies the requirements of the U.S. Nuclear Regulatory Commission (NRC) for spent nuclear fuel storage as prescribed in Title 10 of the Code of Federal Regulations, Part 72 (10 CFR 72) [1] and NUREG-1536 [2]. MAGNASTOR is a canister-based system that accommodates both the storage and transport of Pressurized Water Reactor (PWR) and Boiling Water Reactor (BWR) spent fuel.

The principal components of MAGNASTOR are:

- transportable storage canister (TSC)
- concrete cask
- transfer cask

The transportation component of MAGNASTOR, the MAGNASTOR Transport Cask, will be licensed in accordance with 10 CFR 71 [3].

The TSC is designed and fabricated to meet the requirements for storage in the concrete cask, for transport in the transport cask and to be compatible with the U.S. Department of Energy planning for permanent disposal in a Mined Geological Disposal System. The TSC incorporates a welded closure to preclude the loss of contents and to preserve the general health and safety of the public during long-term storage of spent fuel.

In long-term storage, the TSC is installed in a concrete cask, which provides structural protection and radiation shielding, as well as natural convection cooling. The concrete cask also provides protection during storage for the TSC under adverse environmental conditions.

The transfer cask is used to move the TSC between the workstations during TSC loading and preparation activities. It is also used to transfer the TSC to or from the concrete cask and to the transport cask.

This SAR is formatted in accordance with NRC Regulatory Guide 3.61 [4], except that Chapter 8, Materials Evaluation, is added in accordance with the requirement of Interim Staff Guidance (ISG)-15 [5], with the subsequent renumbering of the remaining chapters. The terminology used in this report is presented in Section 1.1. The term TSC refers to both the PWR and BWR TSCs where the discussion is common to both configurations. Discussion of features unique to the PWR and BWR configurations is addressed in subsections, as appropriate, within each chapter.

1.1 Terminology

This section lists and defines the terms used in this SAR.

Adapter Plate

A carbon steel plate assembly positioned on the top of the concrete cask or transport cask and used to align the transfer cask. It supports the operating mechanism for opening and closing the transfer cask shield doors.

Concrete Cask

A concrete cylinder that holds the TSC during storage. The concrete cask is formed around a steel inner liner and base and is closed by a lid.

Base

A carbon steel weldment incorporating the air inlets and the pedestal that supports the TSC inside of the concrete cask.

Lid

A thick concrete and carbon steel closure for the concrete cask. The lid precludes access to the TSC and provides radiation shielding.

Liner

A carbon steel shell that forms the inside diameter of the concrete cask. The liner serves as the inner form during concrete pouring and provides radiation shielding and structural protection for the TSC.

Standoffs (Channels)

Carbon steel weldments attached to the liner that assist in centering the TSC in the concrete cask and reducing the g-loading to the TSC and its contents in the nonmechanistic tip-over events.

Confinement System

The components of the TSC assembly that retain the spent fuel during storage.

Contents

Up to 37 PWR fuel assemblies or up to 87 BWR fuel assemblies. The fuel assemblies are confined in a TSC. Non-fuel hardware may be inserted into PWR fuel assemblies and BWR fuel assemblies may include channels.

Factor of Safety

An analytically determined value defined as the allowable stress or displacement of a material divided by its calculated stress or displacement.

Fuel Basket (Basket)

The structure inside the TSC that provides structural support, criticality control, and heat transfer paths for the fuel assemblies.

Fuel Tube

A carbon steel tube with a square cross-section. Fuel assemblies are loaded into the fuel tubes. A fuel tube may have neutron absorber material attached on its interior faces.

Neutron Absorber

A borated aluminum metal matrix or composite with neutron absorption capability.

Intact Fuel (Assembly or Rod) (Undamaged Fuel)

A fuel assembly with no fuel rod cladding defect or no known or suspected fuel rod cladding defects greater than pinhole leaks or hairline cracks. The fuel assembly can be handled by

normal means and any missing fuel rods have been replaced by solid stainless steel or zirconium-based alloy filler rods. Missing or damaged fuel assembly or fuel rod structural components have been evaluated to show that fuel pellets, and rods, are retained for all loading conditions.

MAGNASTOR (Modular Advanced Generation, Nuclear, All-purpose STORAGE)

The high-capacity system designed for safe, long-term spent fuel storage at a power reactor site or at an independent spent fuel storage installation.

Spent Nuclear Fuel (or Spent Fuel)

Irradiated fuel assemblies with the same configuration as when originally fabricated, consisting generally of the end fittings, fuel rods, guide tubes, and integral hardware. For PWR fuel, a thimble plug, an in-core instrument thimble, a burnable poison rod insert, or a control element assembly (CEA) is considered to be a component of standard fuel. For BWR fuel, the channel is considered to be integral hardware. Solid filler rods, burnable poison rods, burnable poison rod assemblies, thimble plugs, control element assemblies and stainless steel rod inserts may be inserted in PWR fuel assemblies.

Transport Cask

The packaging consisting of a transport cask body with a closure lid and energy-absorbing impact limiters. The transport cask is used to transport a TSC containing spent fuel. The cask body and closure lid provide the containment boundary during transport.

Transfer Cask

A shielded device used to lift and handle the TSC during fuel loading and closure operations, as well as to transfer the TSC in/out of the concrete cask during storage or in/out of the transport cask for transport. The transfer cask includes two lifting trunnions and two shield doors that can be opened to permit the vertical transfer of the TSC into and from the concrete and transport casks.

Trunnions

Two low-alloy steel components used to lift the transfer cask in a vertical orientation via a lifting assembly.

TSC (Transportable Storage Canister)

The stainless steel cylindrical shell, bottom-end plate, and closure lid that contain the fuel basket structure and the spent fuel contents.

Closure Lid

A thick, stainless steel disk installed directly above the fuel basket following fuel loading. The closure lid provides the confinement boundary for storage and operational shielding during TSC closure.

Drain and Vent Ports

Penetrations located in the closure lid to permit draining, drying, and helium backfilling of the TSC.

Port Cover

The stainless steel plates covering the vent and drain ports that are welded in place following draining, drying, and backfilling operations.

1.2 Introduction

MAGNASTOR is a spent fuel dry storage system consisting of a concrete cask and a welded stainless steel TSC with a welded closure to safely store spent fuel. The TSC is stored in the central cavity of the concrete cask and is compatible with the MAGNASTOR Transport Cask for future off-site shipment. The concrete cask provides structural protection, radiation shielding, and internal airflow paths that remove the decay heat from the TSC contents by natural air circulation. MAGNASTOR is designed and analyzed for a 50-year service life.

The loaded TSC is moved to and from the concrete cask using the transfer cask. The transfer cask provides radiation shielding during TSC closure and preparation activities. The TSC is transferred into the concrete cask by positioning the transfer cask, with the loaded TSC, on top of the concrete cask, opening the shield doors, and lowering the TSC into the concrete cask. Figure 1.3-1 depicts the major components of MAGNASTOR in such a configuration.

MAGNASTOR is designed to safely store up to 37 PWR or up to 87 BWR spent fuel assemblies in separate fuel basket assemblies. These capacities, combined with enhanced operational features, assure that MAGNASTOR reduces the time required and the personnel dose received on a per-assembly basis when placing spent fuel into dry storage. The fuel specifications and parameters that establish the design basis for the PWR and BWR fuel assemblies are presented in Chapter 2. The spent fuel considered in the design includes fuel assemblies that have different overall lengths. The PWR and BWR fuel assembly populations are divided into two groups based on fuel assembly length, and are accommodated by two different lengths of TSCs. The concrete cask and transfer cask are a fixed height and can accommodate both lengths of TSC. The designations and corresponding lengths of the TSCs are shown on the License Drawings.

For PWR fuel, the integral hardware in a fuel assembly can increase its overall length, resulting in the need to use the longer TSC. Spacers may be used in a given TSC to allow loading of fuel that is significantly shorter than the TSC length. The BWR fuel assembly groups are evaluated for the effects of the zirconium alloy channel that surrounds the fuel assembly in reactor operations.

The system design and analyses are in accordance with 10 CFR 72, ANSI/ANS 57.9 [6], the applicable sections of the ASME Boiler and Pressure Vessel Code (ASME Code), and the American Concrete Institute (ACI) code [7]. The analysis demonstrates that MAGNASTOR meets the regulatory requirements of 10 CFR 72 and the guidance of NUREG-1536 [2].

1.3 General Description of MAGNASTOR

MAGNASTOR provides for the long-term storage of PWR and BWR fuel assemblies as listed in Chapter 2 and subsequent transport using a MAGNASTOR transport cask. During long-term storage, the system provides an inert environment, passive structural shielding, cooling and criticality control, and a welded confinement boundary. The structural integrity of the system precludes the release of contents in any of the design basis normal conditions and off-normal or accident events, thereby assuring public health and safety during use of the system.

1.3.1 MAGNASTOR Components

The design and operation of the principal components of MAGNASTOR and the associated auxiliary equipment are described in this section. The design characteristics of three principal components of the system are presented in Table 1.3-1.

This list shows the auxiliary equipment generally needed to use MAGNASTOR.

- automated, remote, and /or manual welding equipment to perform TSC field closure welding operations
- an engine-driven or towed frame or a heavy-haul trailer to move the concrete cask to and from the storage pad and to position the concrete cask on the storage pad
- draining, drying, helium backfill, and water cooling systems for preparing the TSC and contents for storage
- hydrogen monitoring equipment to confirm the absence of explosive or combustible gases during TSC closure welding
- an adapter plate and a hydraulic supply system
- a lifting yoke for lifting and handling the transfer cask and rigging equipment for lifting and handling system components

In addition to these items, the system requires utility services (electric, helium, air, clean borated water, nitrogen gas supply, etc.), standard torque wrenches, tools and fittings, and miscellaneous hardware.

The loaded TSC may be placed into the MAGNASTOR transport cask for offsite transport. The contents of MAGNASTOR for transport shall comply with the content conditions specified in the 10 CFR 71 Certificate of Compliance (CoC).

1.3.1.1 Transportable Storage Canister (TSC)

Two lengths of TSCs accommodate all evaluated PWR and BWR fuel assemblies. The TSC is designed for transport per 10 CFR 71. The load conditions in transport produce higher stresses

in the TSC than are produced during storage conditions, except for TSC lifting. Consequently, transport load conditions establish the design basis for the TSC and, therefore, the TSC design is conservative with respect to storage conditions.

The stainless steel TSC assembly holds the fuel basket structure and confines the contents (see Figure 1.3-2). The TSC is defined as the confinement boundary during storage. The welded closure lid prevents the release of contents under normal conditions and off-normal or accident events. The fuel basket assembly provides the structural support and a heat transfer path for the fuel assemblies, while maintaining a subcritical configuration for all of the evaluated normal conditions and off-normal or accident events.

The major components of the TSC assembly are the shell, base plate, closure lid, and port covers, which provide the confinement boundary during storage. The TSC component dimensions and materials of fabrication are provided in Table 1.3-1. The TSC overall dimensions and design parameters for the two lengths of TSCs are provided in Table 1.3-2.

The TSC consists of a cylindrical stainless steel shell with a welded stainless steel bottom plate at its closed end and a 9-in thick stainless steel closure lid at its open end. The stainless steel shell and bottom plate are dual-certified Type 304/304L. The closure lid is Type 304 stainless steel. A fuel basket assembly is placed inside the TSC. The closure lid is positioned inside the TSC on the lifting lugs above the basket assembly following fuel loading. After the closure lid is placed on the TSC, the TSC is moved to a workstation, and the closure lid is welded to the TSC. The vent and drain ports are penetrations through the lid, which provide access for auxiliary systems to drain, dry, and backfill the TSC. The drain port has a threaded fitting for installing the drain tube. The drain tube extends the full length of the TSC and ends in a sump in the base plate. The vent port also provides access to the TSC cavity for draining, drying, and backfilling operations. Following completion of backfilling, the port covers are installed and welded in place.

The TSC is designed, fabricated, and inspected to the requirements of the ASME Boiler and Pressure Vessel Code (ASME Code), Section III, Division 1, Subsection NB [8], except as noted in the Alternatives to the ASME Code noted in Table 2.1-2.

Refer to Table 1.3-3 for a summary of the TSC fabrication requirements.

1.3.1.2 Fuel Baskets

Each TSC contains either a PWR or BWR fuel basket, which positions and supports the stored fuel. As described in the following sections, the design of the basket is similar for the PWR and BWR configurations. The fuel basket for each fuel type is designed, fabricated, and inspected to

the requirements of the ASME Code, Section III, Division 1, Subsection NG [9], except as noted in Table 2.1-2.

The structural components of both the PWR and BWR baskets are fabricated from ASME SA537, Class 1, carbon steel. To minimize corrosion and preclude significant generation of combustible gases during fuel loading, the assembled basket is coated with electroless nickel plating using an immersion process. Following coating, the neutron absorber panels and the stainless steel retainers are installed on the basket structure as shown on the License Drawings. The principal dimensions and materials of fabrication of the fuel basket are provided in Table 1.3-1.

Both fuel basket designs minimize horizontal surfaces that could entrain water and provide an open path for water flow to the drain tube and sump in the bottom of the TSC. The fuel baskets are supported from the baseplate by 3-in high spacers at the corner of the fuel tubes enabling the TSC to fill and drain evenly.

Spacers may be used to limit the movement of the spent fuel assemblies during storage or in subsequent transport operations.

PWR Fuel Basket

The PWR fuel basket design is an arrangement of square fuel tubes held in a right-circular cylinder configuration using support weldments that are bolted to the outer fuel tubes. The design parameters for the two lengths of PWR fuel baskets are provided in Table 1.3-2.

Fuel tubes support an enclosed neutron absorber sheet on up to four interior sides of the fuel tube. The neutron absorber panels, in conjunction with minimum TSC cavity water boron levels, provide criticality control in the basket. Each neutron absorber panel is covered by a sheet of stainless steel to protect the material during fuel loading and to keep it in position. The neutron absorber and stainless steel cover are secured to the fuel tube using edge clips spot-welded in the four corners of the fuel tubes and weld posts, approximately centered along the length of the fuel tube.

Each PWR fuel basket has a capacity of 37 fuel assemblies in an aligned configuration. Square tubes are assembled in an array where the tubes function as independent fuel positions and as sidewalls for the adjacent fuel positions in what is called a developed cell array. Consequently, the 37 fuel positions are developed using only 21 tubes. The array is surrounded by weldments that serve both as sidewalls for some perimeter fuel positions and as the structural load path from the array to the TSC shell wall. Each PWR basket fuel tube has a nominal 8.86-in square opening. Each developed cell fuel position has a nominal 8.76-in square opening.

BWR Fuel Basket

The BWR fuel basket design is an arrangement of square fuel tubes held in a right-circular cylinder configuration using support weldments that are bolted to the outer fuel tubes. The design parameters for the two lengths of BWR fuel baskets are provided in Table 1.3-2.

Each fuel tube supports an enclosed neutron absorber sheet on up to four interior sides of the fuel tube, which provides criticality control in the basket. The neutron absorber is covered by a sheet of stainless steel to protect the material during fuel loading and to keep it in position. The neutron absorber and stainless steel cover are secured to the fuel tube using edge clips spot-welded in the four corners of the fuel tubes and weld posts, approximately centered along the length of the fuel tube.

Each BWR fuel basket has a capacity of 87 fuel assemblies in an aligned configuration. Square tubes are assembled in an array where the tubes function as independent fuel positions and as sidewalls for the adjacent fuel positions in what is called a developed cell array. Consequently, the 87 fuel positions are developed using only 45 tubes. The array is surrounded by weldments that serve both as sidewalls for some perimeter fuel positions and as the structural load path from the array to the TSC shell wall. Each BWR basket fuel tube has a nominal 5.86-in square opening. Each developed cell fuel position has a nominal 5.77-in square opening.

1.3.1.3 Concrete Cask

The concrete cask is the storage overpack for the TSC and it is designed to hold both lengths of TSCs. The concrete cask provides structural support, shielding, protection from environmental conditions, and natural convection cooling of the TSC during long-term storage. The principal dimensions and materials of fabrication of the concrete cask are shown in Table 1.3-1.

The concrete cask is a reinforced concrete structure with a structural steel inner liner and base. The reinforced concrete wall and steel liner provide the neutron and gamma radiation shielding for the stored spent fuel. Inner and outer reinforcing steel (rebar) assemblies are encased within the concrete. The reinforced concrete wall provides the structural strength to protect the TSC and its contents in natural phenomena events such as tornado wind loading and wind-driven missiles and during non-mechanistic tip-over events (refer to Figure 1.3-3). The concrete surfaces remain accessible for inspection and maintenance over the life of the cask, so that any necessary restoration actions may be taken to maintain shielding and structural conditions.

The concrete cask provides an annular air passage to allow the natural circulation of air around the TSC to remove the decay heat from the contents. The lower air inlets and upper air outlets are steel-lined penetrations in the concrete cask body. Each air inlet/outlet is covered with a

screen. The weldment baffle directs the air upward and around the pedestal that supports the TSC. Decay heat is transferred from the fuel assemblies to the TSC wall by conduction, convection, and radiation. Heat is removed by conduction and convection from the TSC shell to the air flowing upward through the annular air passage and exhausting out through the air outlets. The passive cooling system is designed to maintain the peak fuel cladding temperature below acceptable limits during long-term storage [10]. The concrete cask thermal design also maintains the bulk concrete temperature below the American Concrete Institute (ACI) limits under normal operating conditions. The inner liner of the concrete cask incorporates standoffs that provide lateral support to the TSC in side impact accident events.

A carbon steel and concrete lid is bolted to the top of the concrete cask. The lid reduces skyshine radiation and provides a cover to protect the TSC from the environment and postulated tornado missiles.

Fabrication of the concrete cask requires no unique or unusual forming, concrete placement, or reinforcement operations. The concrete portion of the cask is constructed by placing concrete between a reusable, exterior form and the steel liner. Reinforcing bars are used near the inner and outer concrete surfaces to provide structural integrity. The structural steel liner and base are shop fabricated. Refer to Table 1.3-4 for the fabrication specifications for the concrete cask.

Daily visual inspection of the air inlet and outlet screens assures that airflow through the cask meets licensed requirements. As an alternative to daily visual inspections, the loaded concrete cask in storage may include the capability to measure air temperature at the four outlets. Each air outlet may be equipped with a remote temperature detector mounted in the outlet air plenum. The air temperature-monitoring system, designed to provide verification of heat dissipation capabilities, can be designed for remote or local read-out capabilities at the option of the licensee. The temperature-monitoring system can be installed on all or some of the concrete casks at the Independent Spent Fuel Storage Installation (ISFSI) facility. Alternatively, daily visual inspections of air inlet/outlet screens for blockage can be performed as described in the Technical Specifications.

1.3.1.4 Transfer Cask

The transfer cask is designed, fabricated, and tested to meet the requirements of ANSI N14.6 [11] as a special lifting device. The transfer cask provides biological shielding and structural protection for a loaded TSC, and is used to lift and move the TSC between workstations. The transfer cask is also used to shield the vertical transfer of a TSC into a concrete cask or transport cask.

The transfer cask design incorporates three retaining blocks, pin-locked in place, to prevent a loaded TSC from being inadvertently lifted through its top opening. The transfer cask has retractable bottom shield doors. During TSC loading and handling operations, the shield doors are closed and secured. After placement of the transfer cask on the concrete cask or transport cask, the doors are retracted using hydraulic cylinders and a hydraulic supply. The TSC is then lowered into a concrete cask for storage or into a transport cask for offsite shipment. Refer to Figure 1.3-1 for the general arrangement of the transfer cask, TSC, and concrete cask during loading and Table 1.3-1 for the principal dimensions and materials of fabrication of the transfer cask.

Sixteen penetrations, eight at the top and eight at the bottom, are available to provide a water supply to the transfer cask annulus. Penetrations not used for water supply or draining are capped. The transfer cask annulus is isolated using inflatable seals located between the transfer cask inner shell and the TSC near the upper and lower ends of the transfer cask.

During TSC closure operations, clean water is added through these penetrations into the annulus region to remove heat generated by the spent fuel contents. The cooling water circulation is maintained through completion of TSC activities and is terminated to allow movement of the transfer cask for TSC transfer operations.

A similar process of clean water circulation is used during in-pool fuel loading to minimize contamination of the TSC outside surfaces.

The transfer cask penetrations can also be used for the introduction of forced air or gas at the bottom of the transfer cask to achieve cooling of the TSC contents in case of the failure of the cooling water system. Alternately, the loaded TSC may be returned to the spent fuel pool for in-pool cooling.

1.3.1.5 Transport Cask

The transport cask is designed to transport a loaded TSC containing either PWR or BWR spent fuel. The TSC is loaded into the transport cask cavity in the transport cask, which is closed with a bolted stainless steel lid. A spacer may be used in the transport cask cavity to axially position the TSC and limit its potential movement. Refer to Figure 1.3-4 for the transport configuration of the MAGNASTOR transport cask.

1.3.2 Operational Features

In storage, MAGNASTOR does not require any active operational systems. The principal MAGNASTOR operational activities are loading, welding, and preparing the TSC for storage

and transferring the TSC to the concrete cask. The transfer cask is designed to meet the requirements of these operations. The transfer cask holds the TSC during fuel loading operations, provides biological shielding during TSC closure and preparation, and positions the TSC for transfer into the concrete cask. The lid design of the TSC assures structural integrity, while reducing the time and dose involved in TSC closure.

The detailed generic step-by-step operating procedures for the loading and transferring of MAGNASTOR are presented in Chapter 9. The following is a list of the major loading activities. This list assumes that the empty TSC is installed in the transfer cask.

- Fill the TSC with water or borated water if required.
- Lift the transfer cask over the pool and start the flow of water to the transfer cask annulus and lower the cask to the bottom of the pool.
- Load the selected spent fuel assemblies into the TSC.
- Install the closure lid.
- Remove the transfer cask from the pool and place it in the cask preparation workstation.
- Decontaminate the transfer cask.
- Lower the TSC water level and weld the closure lid to the TSC shell. Examine the weld.
- Drain the remaining pool water from the TSC.
- Dry the TSC cavity.
- Establish a helium backfill.
- Install the vent and drain port covers and weld them to the closure lid.
- Install the TSC lifting system.
- Install the adapter plate on the concrete cask.
- Lift and place the transfer cask on the transfer adapter.
- Attach the TSC lifting system to the crane hook and raise the TSC off of the shield doors.
- Open the shield doors.
- Lower the TSC into the concrete cask (see Figure 1.3-1).
- Remove the transfer cask, transfer adapter, and TSC lifting systems.
- Install the lid on the concrete cask.
- Move the loaded concrete cask to the storage pad.
- Move the concrete cask to its designated location on the storage pad.

The TSC unloading and spent fuel removal from the TSC are essentially the reverse of these steps, except that weld removal and cooldown of the contents is required. This typical sequence of operations, and individual steps, may be modified by the approved site procedure to accommodate specific site requirements, as long as the requirements of the Technical Specifications and the CoC are met.

Figure 1.3-1 Major Component Configuration for Loading the Concrete Cask

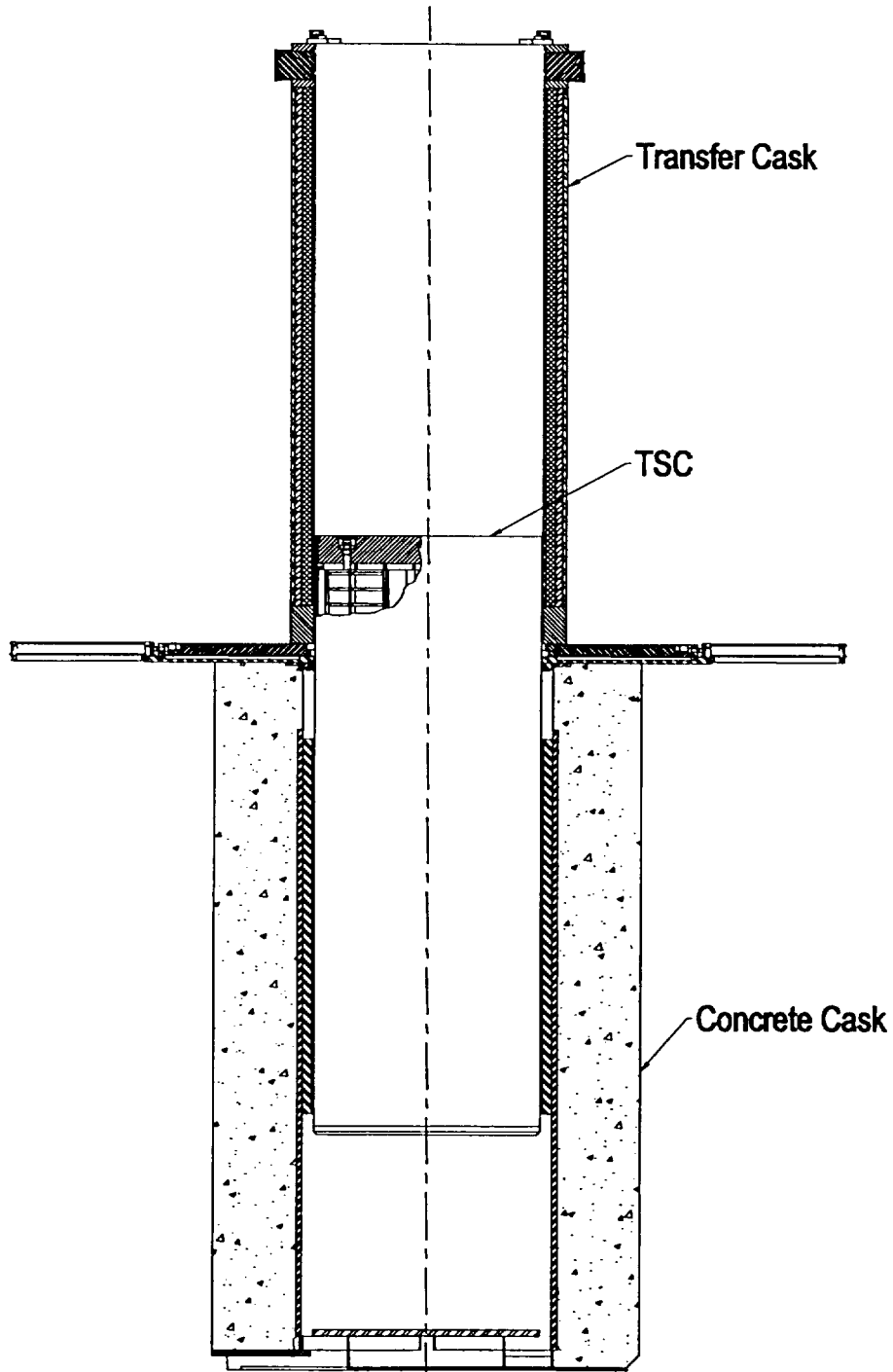


Figure 1.3-2 TSC and Basket

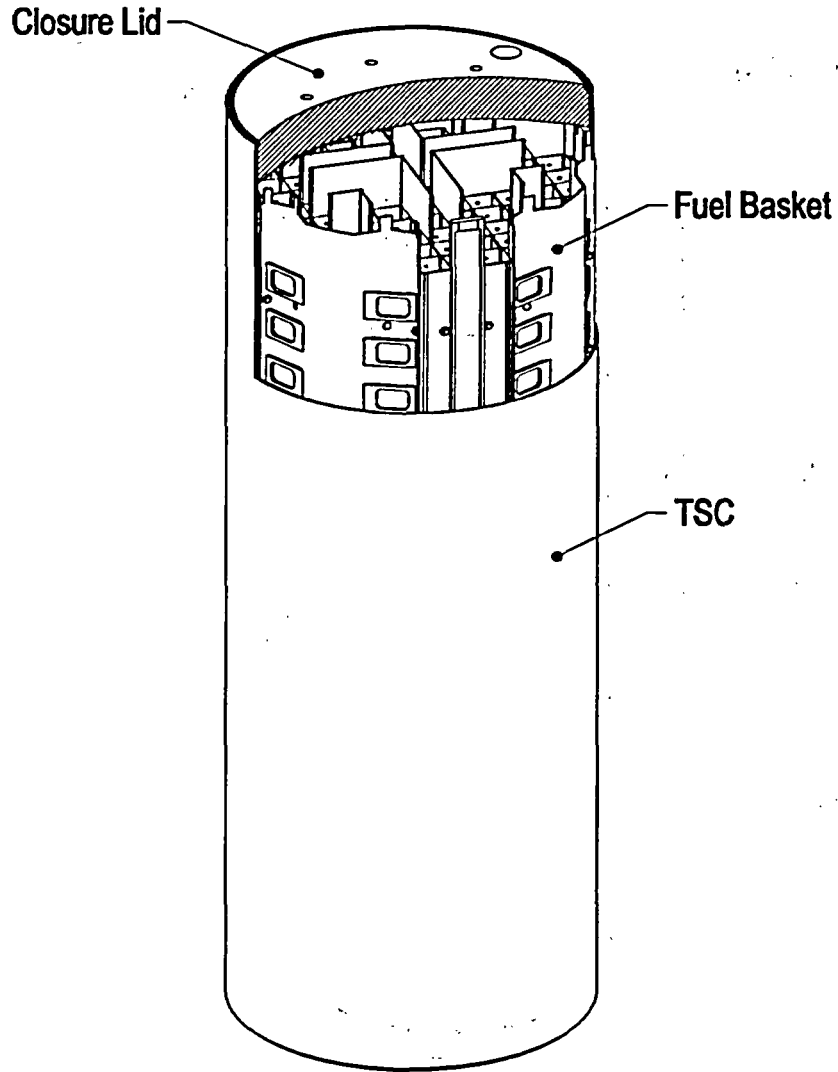


Figure 1.3-3 Concrete Cask

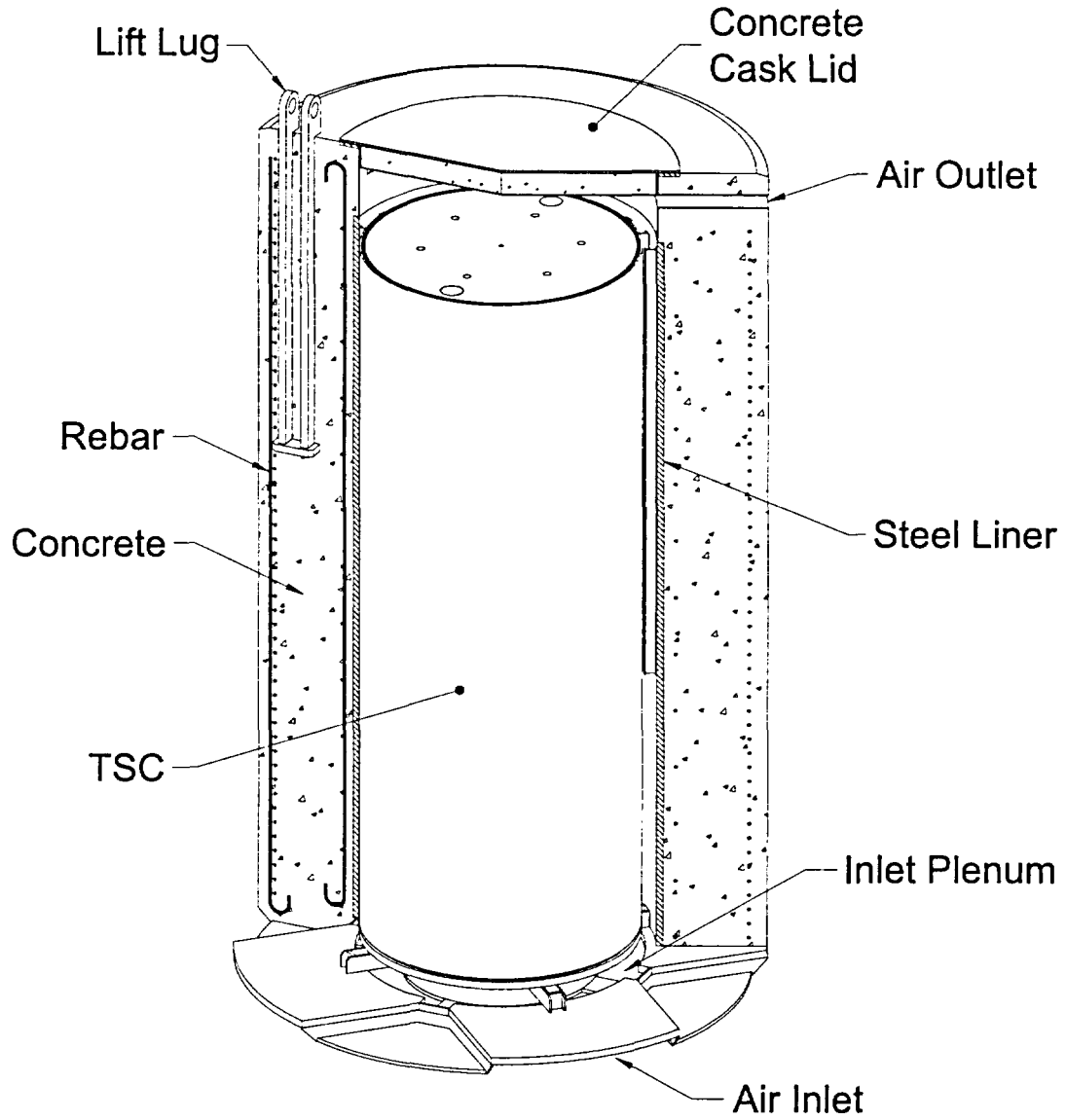


Figure 1.3-4 Transport Configuration of the Transport Cask

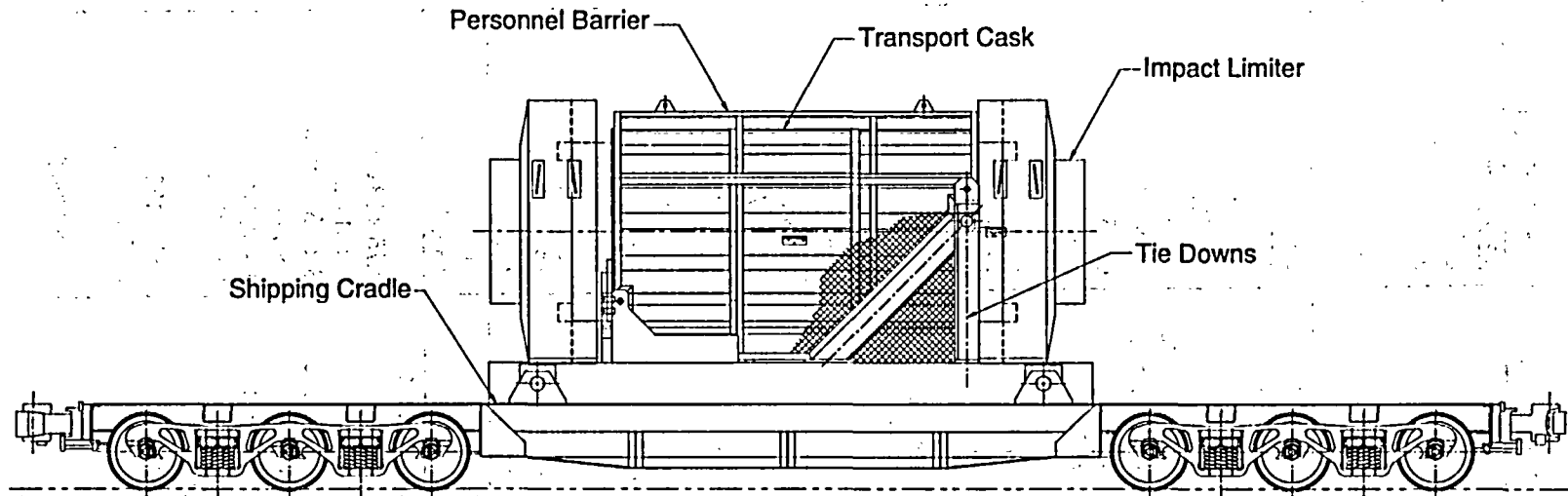


Table 1.3-1 Design Characteristics

	Design Characteristic	Nominal Value (in) ^{a)}	Material
TSC	Shell	0.5 x 72 dia.	Stainless Steel
	Bottom	2.75	Stainless Steel
	Closure Lid	9	Stainless Steel
	Length		
	Group 1 & 3	184.8	
Group 2 & 4	191.8		
Fuel Basket	PWR Fuel Tube Wall	0.31	Carbon Steel
	BWR Fuel Tube Wall	0.25	Carbon Steel
	Neutron Absorber	0.125 (PWR)	Metallic Composite/Matrix
		0.1 (BWR)	
	Neutron Absorber Retainer	0.015	Stainless Steel
	Support Plates & Gussets	0.5 to 0.75	Carbon Steel
	Support Bars (PWR)	0.875	Carbon Steel
	Support Plate (BWR)	0.75	Carbon Steel
	Length		
	Group 1 & 3	172.5	
	Group 2 & 4	179.5	
	Assembly dia.	69.8	
	# of Fuel Tubes/Fuel Loading Positions		
PWR	21/37		
BWR	45/87		
Transfer Cask	Outer Shell	1.25 x 88 dia.	Low Alloy Steel
	Inner Shell	0.75 x 74.5 dia.	Low Alloy Steel
	Retaining Block	8 x 8.75 x 1.50	Stainless Steel
	Trunnions	9.5 dia.	Low Alloy Steel
	Bottom Forging	12 x 88 dia.	Low Alloy Steel
	Top Forging	14 x 88 dia.	Low Alloy Steel
	Shield Doors	5.0	Low Alloy Steel
	Door Rails	5.25 x 7.5 x 52.0	Low Alloy Steel
	Gamma Shield	3.2	Lead
	Neutron Shield	2.25	NS-4-FR, Solid Synthetic Polymer
Transfer Adapter	Base Plate	2.0	Carbon Steel
	Guide Ring	2.5 x 79 dia.	Carbon Steel
Concrete Cask	Weldment Structures		
	Liner	1.75 x 83 dia	Carbon Steel
	Top Flange	1 x 91 dia.	Carbon Steel
	Standoffs (Channels)	3 x 7.5 (s-beam)	Carbon Steel
	Pedestal Plate	2 x 72 dia.	Carbon Steel
	Bottom Weldment	1 x 128 in	Carbon Steel
	Inlet Top	2 x 136 dia.	Carbon Steel
	Concrete Cask		
	Concrete Shell	26.5 x 136 dia.	Type II Portland Cement
	Lid	6.75 x 88 dia.	Carbon Steel
	Rebar	various lengths	Type II Portland Cement Carbon Steel

^{a)} Thickness unless otherwise indicated.

Table 1.3-2 Physical Design Parameters of the TSC and Fuel Baskets

Component	Characteristic	Parameter	Nominal Value
TSC	Canister Weldment	Shell Outside Diameter (in)	72
		Shell Thickness (in)	0.5
		Bottom Thickness (in)	2.75
	Length	Group 1 & 3 (in)	184.8
		Group 2 & 4 (in)	191.8
Capacity (# of fuel assemblies)	PWR	37	
	BWR	87	
Fuel Basket	Length (in)	Group 1 & 3 (in)	172.5
		Group 2 & 4 (in)	179.5
	Diameter	Assembly Diameter (in)	70.76
	Number of Fuel Tubes/Fuel Loading Positions	PWR	21/37
BWR		45/87	

Table 1.3-3 TSC Fabrication Specification Summary

Materials

- All materials shall be in accordance with the referenced drawings and meet the applicable ASME Code sections.

Welding

- Welds shall be in accordance with the referenced drawings.
- Filler metals shall be appropriate ASME Code materials.
- Welders and welding operators shall be qualified in accordance with ASME Code Section IX [12].
- Welding procedures shall be written and qualified in accordance with ASME Code Section IX.
- Personnel performing weld examinations shall be qualified in accordance with the NAC International Quality Assurance Program and SNT-TC-1A [13].
- Weld inspection and examination requirements and acceptance criteria are specified in Chapter 10.

Fabrication

- Cutting, welding, and forming shall be in accordance with ASME Code, Section III, NB-4000 [8] unless otherwise specified. Code stamping is not required.
- Surfaces shall be cleaned to a surface cleanliness classification C, or better, as defined in ANSI N45.2.1 [14], Section 2.
- Fabrication tolerances shall meet the requirements of the referenced drawings after fabrication.

Packaging

- Packaging and shipping shall be in accordance with ANSI N45.2.2 [15].

Quality Assurance

- The TSC shall be fabricated under a quality assurance program that meets 10 CFR 72, Subpart G, and 10 CFR 71, Subpart H.

Table 1.3-4 Concrete Cask Fabrication Specification Summary

Materials

- Concrete mix shall be in accordance with the requirements of ACI 318 and ASTM C94 [16].
- Type II Portland Cement, ASTM C150 [17].
- Fine aggregate ASTM C33 [18] or C637 [19].
- Coarse aggregate ASTM C33.
- If concrete temperatures of general or local areas exceed 200°F but would not exceed 300°F, aggregates are selected that are acceptable for concrete in this temperature range. The following criteria for fine and coarse aggregates are acceptable.
 - Satisfy ASTM C33 requirements and other requirements referenced in ACI 349 [20] for aggregates.
 - Demonstrate a coefficient of thermal expansion (tangent in temperature range of 70°F to 100°F) no greater than 6×10^{-6} in./in./°F, or be one of the following minerals: limestone, dolomite, marble, basalt, granite, gabbro, or rhyolite.
- Admixtures
 - Water Reducing and Superplasticizing ASTM C494 [21].
 - Pozzolanic Admixture (loss on ignition 6% or less) ASTM C618 [22].
- Compressive strength 4000 psi minimum at 28 days.
- Specified air entrainment per ACI 318.
- All steel components shall be of the material as specified in the referenced drawings.

Construction

- A minimum of two samples for each concrete cask shall be taken in accordance with ASTM C172 [23] and ASTM C31 [24] for the purpose of obtaining concrete slump, density, air entrainment, and 28-day compressive strength values. The two samples shall not be taken from the same batch or truck load.
- Test specimens shall be tested in accordance with ASTM C39 [25].
- Formwork shall be in accordance with ACI 318.
- All sidewall formwork shall remain in place in accordance with the requirements of ACI 318.
- Grade, type, and details of all reinforcing steel shall be in accordance with the referenced drawings.
- Embedded items shall conform to ACI 318 and the referenced drawings.
- The placement of concrete shall be in accordance with ACI 318.
- Surface finish shall be in accordance with ACI 318.
- Welding and inspection requirements and acceptance criteria are specified in Chapter 10.

Quality Assurance

The concrete cask shall be constructed under a quality assurance program that meets 10 CFR 72, Subpart G.

1.4 MAGNASTOR Contents

MAGNASTOR is designed to store up to 37 PWR fuel assemblies or up to 87 BWR fuel assemblies in a pressurized helium atmosphere. PWR fuel assemblies may be stored with inserted burnable poison rod assemblies, thimble plugs or control element assemblies. Stainless steel rod inserts for guide tube dashpots may also be inserted. BWR fuel assemblies may be stored with or without channels. Assemblies may contain solid filler rods or burnable absorber rods replacing fuel rods in the assembly lattice. Steel filler rods must be unirradiated. The design content conditions are specified in the CoC for MAGNASTOR. Unenriched fuel assemblies are not evaluated and are not included as allowable contents. Assemblies may contain unenriched axial end blankets.

1.5 Identification of Agents and Contractors

The prime contractor for the MAGNASTOR design is NAC. All design, analysis, licensing, and procurement activities are performed by NAC in accordance with its approved Quality Assurance Program, as described in Chapter 14. Fabrication of the steel components will be by qualified vendors. A qualified concrete contractor will perform construction of the concrete cask. All vendors and contractors will be selected and their performance monitored in accordance with the NAC Quality Assurance Program. All MAGNASTOR fabrication and assembly activities will be performed in accordance with quality assurance programs that meet the requirements of 10 CFR 72, Subpart G.

NAC as a contractor, or the licensee, may perform construction of the ISFSI and MAGNASTOR loading operations on site in accordance with the NAC or licensee quality assurance program, as appropriate. The licensee will perform decommissioning of the ISFSI in accordance with the licensee quality assurance program.

NAC is a private corporation founded in 1968, whose primary focus is the tracking, inspection, handling, storage, and transportation of spent nuclear fuel. NAC is recognized in the industry as an expert in all aspects of the design, licensing, and operation of spent fuel handling, inspection, storage, and transport equipment, as well as in the management of spent fuel inventories.

Within the past 15 years, NAC has completed fabrication or has under construction the following transportation and/or storage systems.

Part 71 (Transport Casks)

- 8 NAC-LWT
- 16 TRUPACT-II
- 6 RH-TRU 72B
- 2 NAC-STC

Part 72 (Storage System Casks and Components)

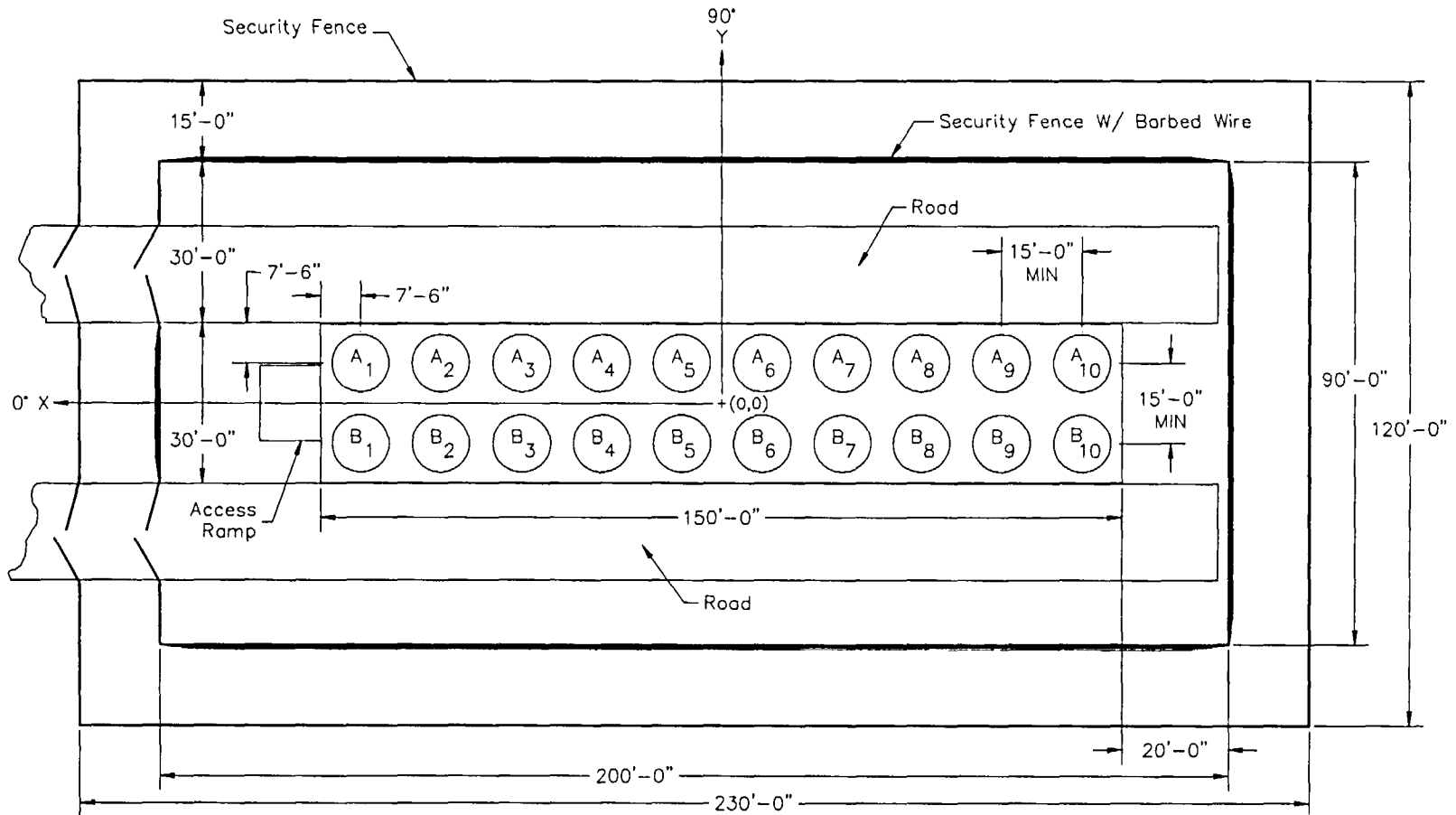
- 7 UMS[®]/MPC transfer casks
- 2 NAC-I28 S/T metal casks
- 1 NAC-I26 S/T metal cask
- > 173 UMS[®]/MPC TSCs
- > 179 UMS[®]/MPC concrete casks

1.6 Generic Concrete Cask Arrays

A typical ISFSI storage pad layout for 20 MAGNASTOR systems is provided in Figure 1.6-1. As shown in this figure, roads parallel the sides of the pad to facilitate transfer of the concrete cask from the transporter to the designated storage position on the pad. Alternately, a ramp or low-profile concrete pad may be used to allow access for a motorized or towed frame for concrete cask transfer and placement. Loaded concrete casks are placed in the vertical orientation on the pad in a linear array. Array sizes could accommodate from 1 to more than 200 casks. Figure 1.6-1 shows the minimum concrete cask spacing and representative site dimensions. Actual spacing and facility dimensions are dependent on the general site layout, access roads, site boundaries, and transfer equipment selection, but must conform to the spacing specified in the Technical Specifications.

The reinforced concrete storage pad is capable of sustaining the transient loads from the cask transporter and the general loads of the stored casks. If necessary, the pad can be constructed in phases to specifically meet utility-required expansions.

Figure 1.6-1 Typical ISFSI Storage Pad Layout



1.7 References

1. 10 CFR 72, "Licensing Requirements for the Independent Storage of Spent Nuclear Fuel and High-Level Radioactive Waste and Reactor-Related Greater Than Class C Waste," Code of Federal Regulations, US Nuclear Regulatory Commission, Washington, DC.
2. NUREG-1536, "Standard Review Plan for Dry Cask Storage Systems," US Nuclear Regulatory Commission, Washington, DC, January 1997.
3. 10 CFR 71; "Packaging and Transportation of Radioactive Materials," Code of Federal Regulations, US Nuclear Regulatory Commission, Washington, DC.
4. Regulatory Guide 3.61, "Standard Format and Content for a Topical Safety Analysis Report for a Spent Fuel Dry Concrete Cask," US Nuclear Regulatory Commission, Washington, DC, February 1989.
5. ISG-15, "Materials Evaluation," US Nuclear Regulatory Commission, Washington, DC, Revision 0, January 10, 2001.
6. ANSI/ANS 57.9-1992, "Design Criteria for an Independent Spent Fuel Storage Installation (Dry Type)," American Nuclear Society, La Grange Park, IL, May 1992.
7. ACI 318, "Building Code Requirements for Structural Concrete," American Concrete Institute, Farmington Hills, MI.
8. ASME Boiler and Pressure Vessel Code, Section III, Subsection NB, "Class I Components," American Society of Mechanical Engineers, New York, NY, 2001 Edition with 2003 Addenda.
9. ASME Boiler and Pressure Vessel Code, Section III, Subsection NG, "Core Support Structures," American Society of Mechanical Engineers, New York, NY, 2001 Edition with 2003 Addenda.
10. ISG-11, "Cladding Considerations for the Transport and Storage of Spent Fuel," US Nuclear Regulatory Commission, Washington, DC, Revision 3, November 17, 2003.
11. ANSI N14.6-1993, "American National Standard for Radioactive Materials – Special Lifting Devices for Shipping Containers Weighing 10,000 Pounds (4,500 kg) or More," American National Standards Institute, Inc., Washington, DC, June 1993.
12. ASME Boiler and Pressure Vessel Code, Section IX, "Qualification Standards for Welding and Brazing Procedures, Welders, Brazers, and Welding and Brazing Operators," American Society of Mechanical Engineers, New York, NY, 2001 Edition with 2003 Addenda.
13. Recommended Practice No. SNT-TC-1A, "Personnel Qualification and Certification in Nondestructive Testing," The American Society for Nondestructive Testing, Inc., Columbus OH, edition as invoked by the applicable ASME Code.

14. ANSI N45.2.1, "Cleaning of Fluid Systems and Associated Components During Construction Phase of Nuclear Power Plants," American National Standards Institute, Inc., Washington, DC.
15. ANSI N45.2.2-1978, "Packaging, Shipping, Receiving, Storage, and Handling of Items for Nuclear Power Plants," American National Standards Institute, Inc., Washington, DC.
16. ASTM C94^{a)}, "Standard Specification for Ready-Mixed Concrete," American Society for Testing and Materials, West Conshohocken, PA.
17. ASTM C150^{a)}, "Standard Specification for Portland Cement," American Society for Testing and Materials, West Conshohocken, PA.
18. ASTM C33^{a)}, "Standard Specification for Concrete Aggregates," American Society for Testing and Materials, West Conshohocken, PA.
19. ASTM C637^{a)}, "Specification for Aggregates for Radiation-Shielding Concrete," American Society for Testing and Materials, West Conshohocken, PA.
20. ANSI/ACI 349-90, "Code Requirements for Nuclear Safety Related Concrete Structures" American Concrete Institute, Farmington Hills, MI
21. ASTM C494^{a)}, "Standard Specification for Chemical Admixtures for Concrete," American Society for Testing and Materials, West Conshohocken, PA.
22. ASTM C618^{a)}, "Specification for Fly Ash and Raw or Calcined Natural Pozzolan for Use as a Mineral Admixture in Portland Cement Concrete," American Society for Testing and Materials, West Conshohocken, PA.
23. ASTM C172^{a)}, "Standard Practice for Sampling Freshly Mixed Concrete," American Society for Testing and Materials, West Conshohocken, PA.
24. ASTM C31^{a)}, "Method of Making and Curing Concrete Test Specimens in the Field," American Society for Testing and Materials, West Conshohocken, PA.
25. ASTM C39^{a)}, "Standard Test Method for Compressive Strength of Cylindrical Concrete Specimens," American Society for Testing and Materials, West Conshohocken, PA.

^{a)} Current edition of testing standards at time of fabrication/construction is to be used.

1.8 License Drawings

This section presents the list of License Drawings for MAGNASTOR.

Drawing Number	Title	Revision No.
71160-551	Fuel Tube Assembly, MAGNASTOR – 37 PWR	1
71160-560	Assembly, Standard Transfer Cask, MAGNASTOR	1
71160-561	Structure, Weldment, Concrete Cask, MAGNASTOR	2
71160-562	Reinforcing Bar and Concrete Placement, Concrete Cask, MAGNASTOR	2
71160-571	Details, Neutron Absorber, Retainer, MAGNASTOR – 37 PWR	1
71160-572	Details, Neutron Absorber, Retainer, MAGNASTOR – 87 BWR	1
71160-574	Basket Support Weldments, MAGNASTOR – 37 PWR	1
71160-575	Basket Assembly, MAGNASTOR – 37 PWR	1
71160-581	Shell Weldment, Canister, MAGNASTOR	1
71160-584	Details, Canister, MAGNASTOR	1
71160-585	TSC Assembly, MAGNASTOR	1
71160-590	Loaded Concrete Cask, MAGNASTOR	2
71160-591	Fuel Tube Assembly, MAGNASTOR – 87 BWR	1
71160-598	Basket Support Weldments, MAGNASTOR – 87 BWR	1
71160-599	Basket Assembly, MAGNASTOR - 87 BWR	1

Figure Withheld Under 10 CFR 2.390



Figure Withheld Under 10 CFR 2.390

 NAC INTERNATIONAL	
ASSEMBLY, STANDARD TRANSFER CASK, MAGNASTOR	
71160	550

A

Figure Withheld Under 10 CFR 2.390

 NAC INTERNATIONAL	
ASSEMBLY, STANDARD TRANSFER CASK, MAGNASTOR	
71160	560

Figure Withheld Under 10 CFR 2.390

PLATE	
PLATE	NO. OF SHEETS
NAC INTERNATIONAL	
STRUCTURE, WELDMENT, CONCRETE CASK, MAGNASTOR	
71160	561
	1 of 1

Figure Withheld Under 10 CFR 2.390

 NAC INTERNATIONAL	
STRUCTURE, WELDMENT, CONCRETE CASK, MAGNASTOR	
71160	561
- 2 - 41	

A

Figure Withheld Under 10 CFR 2.390

 NAC INTERNATIONAL	
STRUCTURE, WELDMENT, CONCRETE CASK, MAGNASTOR	
71160	561 3

A

Figure Withheld Under 10 CFR 2.390

 NAC INTERNATIONAL	
STRUCTURE, WELDMENT, CONCRETE CASK, MAGNASTOR	
71160	561

A

Figure Withheld Under 10 CFR 2.390

	24(10)	
	25(10)	
DESCRIPTION	DESCRIPTION	
	 NAC INTERNATIONAL	
	REINFORCING BAR AND CONCRETE PLACEMENT, CONCRETE CASK, MAGNASTOR	
71160	562	7

Figure Withheld Under 10 CFR 2.390

 NAC INTERNATIONAL	
REINFORCING BAR AND CONCRETE PLACEMENT, CONCRETE CASK, MAGNASTOR	
71160	562
	2

A

Figure Withheld Under 10 CFR 2.390

SHEET	
SHEET/STAMP	
DRAWING NO. IN SHOP FILE	
NAC INTERNATIONAL	
DETAILS, NEUTRON ABSORBER, RETAINER, MAGNASTOR - 37 PWR	
71160	571

Figure Withheld Under 10 CFR 2.390

SHEET	
SHEET/SLIP	
Drawing No. 88-200-1000	
NAC INTERNATIONAL	
DETAILS, NEUTRON ABSORBER, RETAINER, MAGNASTOR - 87 BWR	
71160	572

Figure Withheld Under 10 CFR 2.390

PLATE	
DAR	
AS SUPPLIER	
 NAC INTERNATIONAL	
BASKET SUPPORT WELDMENTS, MAGNASTOR - 37 PWR	
71160	574
1	2

A

Figure Withheld Under 10 CFR 2.390

 NAC INTERNATIONAL	
BASKET SUPPORT WELDMENTS, MAGNASTOR - 37 PWR	
71160	574
	2 2

Figure Withheld Under 10 CFR 2.390

71160-330-01	
71160-330-01	
NAC INTERNATIONAL	
BASKET ASSEMBLY, MAGNASTOR - 37 PWR	
71160...	575
1	3

Figure Withheld Under 10 CFR 2.390

 NAC INTERNATIONAL	
BASKET ASSEMBLY, MAGNASTOR - 37 PWR	
71160	575

Figure Withheld Under 10 CFR 2.390

 NAC INTERNATIONAL	
BASKET ASSEMBLY, MAGNASTOR - 37 PWR	
71160	575 1

Figure Withheld Under 10 CFR 2.390

	PLATE	
	PLATE	
	DESCRIPTION	
	 NAC INTERNATIONAL	
	SHELL WELDMENT, CANISTER, MAGNASTOR	A
	71160	581

Figure Withheld Under 10 CFR 2.390

 NAC INTERNATIONAL	
SHELL WELDMENT, CANISTER, MAGNASTOR	
71160	581
- 2 - of 2	

A

Figure Withheld Under 10 CFR 2.390

	QUICK CONNECT COUPLING	
	PLATE / DRG NO	
	DESCRIPTION	
	NAC INTERNATIONAL	
	DETAILS, CANISTER, MAGNASTOR	
	71160	584

Figure Withheld Under 10 CFR 2.390

71160-585-80	
NAC INTERNATIONAL	
TSC ASSEMBLY, MAGNASTOR	
DATE	
2/04	
2/04	
2/04	
2/04	
2/04	
2/04	
2/04	71160
2/04	585
	1
	1

Figure Withheld Under 10 CFR 2.390

 NAC INTERNATIONAL	
TSC ASSEMBLY, MAGNASTOR	
71160	585 7

Figure Withheld Under 10 CFR 2.390

71160-563-01	
71160-563-01	
NAC INTERNATIONAL	
LOADED CONCRETE CASK, MAGNASTOR	
71160	590

Figure Withheld Under 10 CFR 2.390

PLATE	
PLATE	
NAC INTERNATIONAL	
FUEL TUBE ASSEMBLY, MAGNASTOR - 87 BWR	
71160	591

Figure Withheld Under 10 CFR 2.390

DRAWING NO.		PLATE
DESCRIPTION		PLATE
 NAC INTERNATIONAL		
BASKET SUPPORT WELDMENTS, MAGNASTOR - 87 BWR		
DATE	71160	598
BY		1

Figure Withheld Under 10 CFR 2.390

 NAC INTERNATIONAL	
BASKET SUPPORT WELDMENTS, MAGNASTOR - 87 BWR	
71160	598

A

Figure Withheld Under 10 CFR 2.390

71160-599-59	
71160-599-59	
Description	
NAC INTERNATIONAL	
BASKET ASSEMBLY, MAGNASTOR - 87 BWR	
71160	599

Figure Withheld Under 10 CFR 2.390

 NAC INTERNATIONAL	
BASKET ASSEMBLY, MAGNASTOR - 67 BWR	
71160	599
	2 of 3

Figure Withheld Under 10 CFR 2.390

 NAC INTERNATIONAL	
BASKET ASSEMBLY, MAGNASTOR - 87 BWR	
71160	599

A

Chapter 2 Principal Design Criteria

Table of Contents

2	PRINCIPAL DESIGN CRITERIA	2-1
2.1	MAGNASTOR System Design Criteria	2.1-1
2.2	Spent Fuel To Be Stored	2.2-1
2.2.1	PWR Fuel Evaluation	2.2-1
2.2.2	BWR Fuel Evaluation	2.2-2
2.3	Design Criteria for Environmental Conditions and Natural Phenomena	2.3-1
2.3.1	Tornado Missiles and Wind Loadings	2.3-1
2.3.2	Water Level (Flood) Design	2.3-2
2.3.3	Seismic Design	2.3-3
2.3.4	Snow and Ice Loadings	2.3-4
2.3.5	Combined Load Criteria	2.3-5
2.3.6	Environmental Temperatures	2.3-6
2.4	Safety Protection Systems	2.4-1
2.4.1	General	2.4-1
2.4.2	Confinement Barriers and Systems	2.4-2
2.4.3	Concrete Cask Cooling	2.4-2
2.4.4	Protection by Equipment	2.4-3
2.4.5	Protection by Instrumentation	2.4-3
2.4.6	Nuclear Criticality Safety	2.4-3
2.4.7	Radiological Protection	2.4-5
2.4.8	Fire Protection	2.4-6
2.4.9	Explosion Protection	2.4-6
2.4.10	Auxiliary Structures	2.4-6
2.5	Decommissioning Considerations	2.5-1
2.6	References	2.6-1

List of Figures

Figure 2.2-1 Schematic of PWR Fuel Preferential Loading Pattern..... 2.2-4
Figure 2.2-2 82-Assembly-BWR Basket Pattern..... 2.2-5

List of Tables

Table 2.1-1 MAGNASTOR System Design Criteria 2.1-2
Table 2.1-2 ASME Code Alternatives for MAGNASTOR Components 2.1-3
Table 2.2-1 PWR Fuel Assembly Characteristics 2.2-6
Table 2.2-2 BWR Fuel Assembly Characteristics..... 2.2-7
Table 2.3-1 Load Combinations for the Concrete Cask..... 2.3-8
Table 2.3-2 Load Combinations for the TSC..... 2.3-8
Table 2.3-3 Structural Design Criteria for Components Used in the TSC..... 2.3-9
Table 2.4-1 Safety Classification of MAGNASTOR Components..... 2.4-8

2 PRINCIPAL DESIGN CRITERIA

MAGNASTOR is a canister-based spent fuel dry storage cask system designed in accordance with the requirements of 10 CFR 72 [10], Subpart L, Approval of Spent Fuel Storage Casks. It is designed to store a variety of intact PWR and BWR spent fuel assemblies and to be compatible with the MAGNASTOR Transportation System. This chapter presents the principal design criteria for MAGNASTOR components.

2.1 MAGNASTOR System Design Criteria

The design of MAGNASTOR ensures that the stored spent fuel is maintained subcritical in an inert environment, within allowable temperature limits, and is retrievable. The acceptance testing and maintenance program specified in Chapter 10 ensures that the system is, and remains, suitable for the intended purpose. The MAGNASTOR design criteria appear in Table 2.1-1.

Approved alternatives to the ASME Code for the design procurement, fabrication, inspection, and testing of MAGNASTOR TSCs and spent fuel baskets are listed in Table 2.1-2.

Proposed alternatives to ASME Code, Section III, 2001 Edition with Addenda through 2003, including alternatives listed in Table 2.1-2, may be used when authorized by the Director of the Office of Nuclear Material Safety and Safeguards or designee. The request for such alternatives should demonstrate the following.

- The proposed alternatives would provide an acceptable level of quality and safety, or
- Compliance with the specified requirements of ASME Code, Section III, Subsections NB and NG, 2001 Edition with Addenda through 2003, would result in hardship or unusual difficulty without a compensating increase in the level of quality and safety.

Requests for alternatives shall be submitted in accordance with 10 CFR 72.

Table 2.1-1 MAGNASTOR System Design Criteria

Parameter	Criteria
Design Life	50 years
Design Code – Confinement	
TSC	ASME Code, Section III, Subsection NB [1] for confinement boundary
TSC Cavity Atmosphere	Helium
Gas Pressure	7.0 atmospheres gauge (103 psig)
Design Code - Nonconfinement	
Fuel Basket	ASME Code, Section III, Subsection NG [2] and NUREG/CR-6322 [3]
Concrete Cask	ACI-349 [4], ACI-318 [5]
Transfer Cask	ANSI N14.6 [6]
Thermal	
Maximum Fuel Cladding Temperature	752°F (400°C) for Normal, Off-Normal, and Transfer [7] 1058°F (570°C) for Accident [8]
Ambient Temperature	
Normal (average annual ambient)	100°F
Off-Normal (extreme cold; extreme hot)	-40°F; 106°F
Accident	133°F
Concrete Temperature	
Normal Conditions	≤150°F (bulk); ≤ 300°F (local) [9]
Off-Normal/Accident Conditions	≤ 350°F local/ surface [4]
Radiation Protection/Shielding	
Owner-Controlled Area Boundary Dose [10]	
Normal/Off-Normal Conditions	25 mrem (Annual Whole Body) [10]
Accident Whole Body Dose	5 rem (Whole Body) [10]

Table 2.1-2 ASME Code Alternatives for MAGNASTOR Components

Component	Reference ASME Code Section/Article	Code Requirement	Exception, Justification and Compensatory Measures
TSC and Fuel Basket	NCA-1000, NCA-2000, NCA-3000, NCA-4000, NCA-5000, NCA-8000, NB-1110, and NG-1110	Requirements for Code stamping of NB components and preparation of Code Design Specifications, Design Reports, Overpressure Protection Report (TSC only), and Data Reports, and Quality Assurance requirements in accordance with Code requirements.	Code stamping is not required for the TSC or fuel baskets. Code Design Specifications, Design Reports, Overpressure Protection Report, and Data Reports are not required. The TSC and Fuel Basket are designed, procured, fabricated, inspected and tested in accordance with a QA Program meeting 10 CFR 72, Subpart G. Authorized Nuclear Inspection Agency Services are not required.
TSC Pressure-Retaining Materials	NB-2000	Pressure-retaining material to be provided by ASME-approved Material Organization.	Materials will be supplied with Certified Material Test Reports by NAC approved suppliers.
TSC Closure Lid-to-Shell Weld	NB-4243	Full penetration welds required for Category C joints.	The closure lid-to-shell weld is not a full penetration weld. The design and analysis of the closure lid weld utilizes a 0.8 stress reduction factor in accordance with ASME Code Case N-595-4 [23].
Port Cover-to-Closure Lid Weld.	NB-5230	Radiographic (RT) examination required.	In accordance with ASME Code Case N-595-4, root and final surface liquid penetrant (PT) examination to be performed per ASME Code, Section V, Article 6. (Note: Final surface PT only to be performed if weld completed in single pass). PT acceptance criteria are to be in accordance with NB-5350.)
TSC Closure Lid-to-Shell Weld	NB-5230	Radiographic (RT) examination required.	In accordance with ASME Code Case N-595-4, the TSC closure lid-to-shell weld is to be inspected by progressive surface liquid penetrant (PT) examination of the root, midplane and final surface layers. The progressive PT examination of the weld will be performed in accordance with ASME Code, Section V, Article 6, and acceptance criteria per NB-5350.

Table 2.1-2 ASME Code Alternatives for MAGNASTOR Components (continued)

Component	Reference ASME Code Section/Article	Code Requirement	Exception, Justification and Compensatory Measures
TSC	NB-6111	All completed pressure retaining systems shall be pressure tested.	In accordance with the alternative rules of ASME Code Case N-595-4, the welded TSC vessel (i.e., shell and base plate) shall be leak tested prior to loading in accordance with ASME Code, Section V, Article 10 to leaktight criteria as defined by ANSI N14.5.
TSC	NB-7000	Pressure vessels shall be protected from the consequences of pressure conditions exceeding design pressure.	No overpressure protection is provided. The function of the TSC is to confine radioactive contents without release under normal conditions, or off-normal and accident events of storage. The TSC is designed to withstand the maximum internal pressure considering 100% fuel rod failure and maximum accident condition temperatures.
TSC	NB-8000	States requirements for nameplates, stamping and reports per NCA-8000.	The TSC is marked and identified to ensure proper identification of the contents. Code stamping is not required.
TSC Basket Assembly Structural Materials	NG-2000	Core support structural materials are to be provided by an ASME approved Material Organization.	Fuel basket structural materials with Certified Material Test Reports to be supplied by NAC approved suppliers.
TSC Basket Assembly Structural Components	NG-8000	Requirements for nameplates, stamping and reports per NCA-8000.	The TSC basket structural assembly is marked and identified to ensure component traceability in accordance with NAC's QA Program.

2.2 Spent Fuel To Be Stored

MAGNASTOR is designed to safely store up to 37 PWR or up to 87 BWR spent fuel assemblies, contained within a TSC. The fuel assemblies are grouped into two groups of PWR and two groups of BWR fuel assemblies on the basis of fuel assembly length. Refer to Chapter 1 for the fuel assembly length groupings. For TSC spent fuel content loads less than a full basket, empty fuel positions shall include an empty fuel cell insert.

Intact PWR and BWR fuel assemblies having parameters as shown in Table 2.2-1 and Table 2.2-2, respectively, may be stored in MAGNASTOR.

The minimum initial enrichment limits are shown in Table 2.2-1 and Table 2.2-2 for PWR and BWR fuel, respectively, and exclude the loading of fuel assemblies enriched to less than 1.3 wt% ²³⁵U, including unenriched fuel assemblies. Fuel assemblies with unenriched axial end-blankets may be loaded into MAGNASTOR.

2.2.1 PWR Fuel Evaluation

The limiting parameters of the PWR fuel assemblies authorized for loading in MAGNASTOR are shown in Table 2.2-1. The maximum initial enrichments listed are based on a minimum soluble boron concentration of 2,500 ppm in the spent fuel pool water. Lower soluble boron content is allowed at lower maximum enrichment. The maximum initial enrichment authorized represents the peak fuel rod enrichment for variably enriched PWR fuel assemblies. Each TSC may contain up to 37 intact PWR fuel assemblies. The maximum TSC decay heat load for the storage of PWR fuel assemblies is 40.0 kW. Uniform and preferential loading patterns are allowed in the PWR basket. The uniform loading pattern permits assemblies with a maximum heat load 1.08 kW/assembly. The preferential loading pattern contains peak heat loads of 1.35 kW, as indicated in the following pattern and in Figure 2.2-1.

Zone Description (Figure 2.2-1)	Designator	Heat Load (W/assy)	# Assemblies
Inner Ring	A	1,081	9
Middle Ring	B	1,350	12
Outer Ring	C	879	16

The minimum cool times are determined based on the maximum decay heat load of the contents. Refer to Chapter 5 for the minimum cool-time requirement for PWR spent fuel based on fuel assembly initial enrichment and burnup.

The design of MAGNASTOR is based on bounding PWR fuel assembly parameters that maximize the source terms for the shielding, the reactivity for criticality evaluations, and the fuel weight used for the structural evaluations. These bounding parameters are selected from the variety of spent fuel assemblies that are candidates for storage and transport in MAGNASTOR. The bounding fuel assembly values are established based primarily on how the principal parameters are combined, and on the loading conditions (or restrictions) established for a group of fuel assemblies based on its parameters.

As shown in Table 2.2-1, PWR fuel assemblies may contain a thimble plug (flow mixer), a burnable poison rod assembly (BPRA), a control element assembly (CEA), and/or solid filler rods. As shown in Table 2.2-1, the evaluation of PWR fuel assemblies includes thimble plugs, burnable poison rods, CEAs, or stainless steel rods inserted in guide tube positions. Empty fuel rod positions are filled with a solid filler rod or a solid neutron absorber rod.

2.2.2 BWR Fuel Evaluation

The limiting parameters of the BWR fuel assemblies authorized for loading in MAGNASTOR are shown in Table 2.2-2. Each TSC may contain up to 87 intact BWR fuel assemblies. To increase allowed assembly enrichments over those determined for the 87-assembly basket configuration, an optional 82-assembly loading pattern may be used. The required assembly locations in the 82-assembly pattern are shown in Figure 2.2-2. The minimum initial enrichment represents the peak planar-average enrichment. The maximum decay heat load per TSC for the storage of BWR fuel assemblies is 38.0 kW (average of 0.437 kW/assembly). The minimum cooling times are determined based on the maximum decay heat load of the contents. Refer to Chapter 5 for the minimum cool-time requirement for spent fuel based on fuel assembly initial enrichment and burnup.

The design of MAGNASTOR is based on bounding BWR fuel assembly parameters that maximize the source terms for the shielding evaluation, the reactivity for the criticality evaluation, and the fuel weight for the structural evaluations. These bounding parameters are selected from the assemblies that are candidates for storage and transport in MAGNASTOR. The bounding fuel assembly values are established based primarily on how the principal parameters are combined, and on the loading conditions or restrictions established for a group of fuel assemblies based on its parameters.

As shown in Table 2.2-2, the BWR assemblies may be channeled with a zirconium-based alloy channel, or they may be unchanneled. BWR fuel assemblies with stainless steel channels are not authorized as contents.

Empty fuel rod positions are filled with a solid filler rod or a solid neutron absorber rod.

Figure 2.2-1 Schematic of PWR Fuel Preferential Loading Pattern

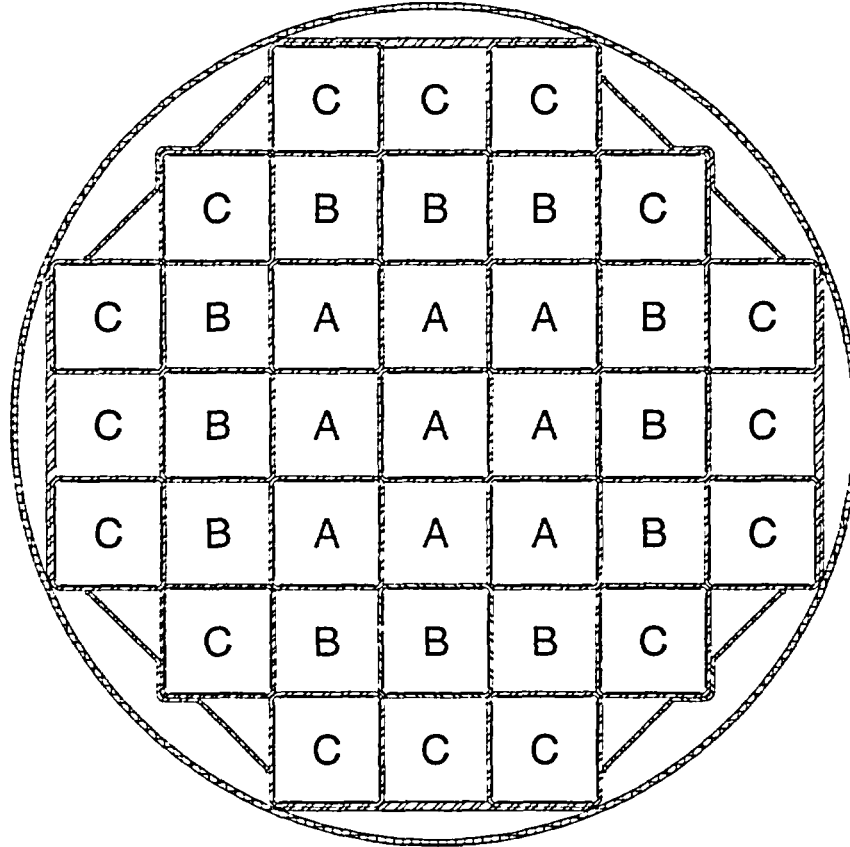
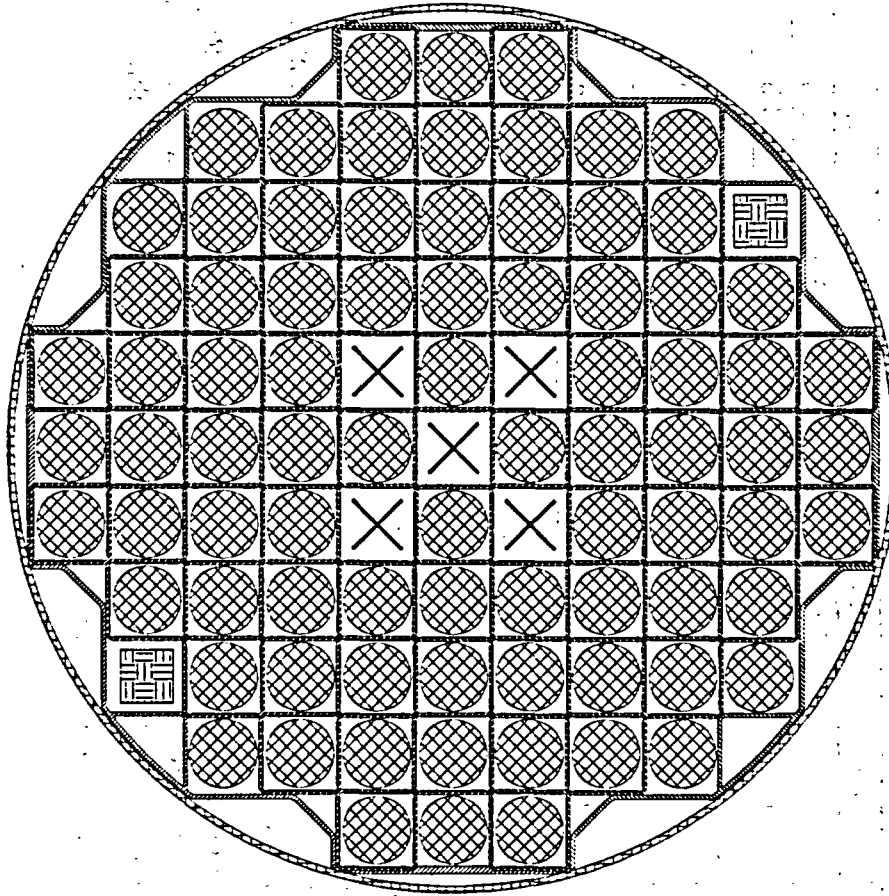


Figure 2.2-2 82-Assembly-BWR Basket Pattern



-  = Fuel Assembly Locations
-  = Vent/Drain Port Locations
-  = Designated Nonfuel Locations

Table 2.2-1 PWR Fuel Assembly Characteristics

Characteristic	Fuel Class					
	14x14	14x14	15x15	15x15	16x16	17x17
Max Initial Enrichment (wt% ²³⁵ U)	5.0	5.0	5.0	5.0	5.0	5.0
Min Initial Enrichment (wt% ²³⁵ U)	1.3	1.3	1.3	1.3	1.3	1.3
Number of Fuel Rods	176	179	204	208	236	264
Max Assembly Average Burnup (MWd/MTU)	70,000	70,000	70,000	70,000	70,000	70,000
Min Cool Time (years)	4	4	4	4	4	4
Max Weight (lb) per Storage Location	1,680	1,680	1,680	1,680	1,680	1,680
Max Decay Heat (Watts) per Storage Location	1,350	1,350	1,350	1,350	1,350	1,350

- Fuel cladding is a zirconium-based alloy.
- All reported enrichment values are nominal preirradiation fabrication values.
- Weight includes the weight of nonfuel-bearing components.
- Assemblies may contain a flow mixer (thimble plug), a burnable poison rod assembly, a control element assembly, and/or solid stainless steel or zirconium-based alloy filler rods.
- Maximum initial enrichment is based on a minimum soluble boron concentration in the spent fuel pool water. Required soluble boron content is fuel type and enrichment specific. Minimum soluble boron content varies between 1,500 and 2,500 ppm. Maximum initial enrichment represents the peak fuel rod enrichment for variably-enriched fuel assemblies.
- Spacers may be used to axially position fuel assemblies to facilitate handling.

Table 2.2-2 BWR Fuel Assembly Characteristics

Characteristic	Fuel Class			
	7x7	8x8	9x9	10x10
Max Initial Enrichment (wt% ²³⁵ U)	4.5	4.5	4.5	4.5
Number of Fuel Rods	48/49	59/60/61/ 62/63/64	72/74 ^a /76/ 79/80	91 ^a /92 ^a / 96 ^a /100
Max Assembly Average Burnup (MWd/MTU)	60,000	60,000	60,000	60,000
Min Cool Time (years)	4	4	4	4
Min Average Enrichment (wt% ²³⁵ U)	1.3	1.3	1.3	1.3
Max Weight (lb) per Storage Location	704	704	704	704
Max Decay Heat (Watts) per Storage Location	437	437	437	437

- Each BWR fuel assembly may have a zirconium-based alloy channel up to 120 mil thick.
- Assembly weight includes the weight of the channel.
- Maximum initial enrichment is the peak planar-average enrichment.
- Water rods may occupy more than one fuel lattice location. Fuel assembly to contain nominal number of water rods for the specific assembly design.
- All enrichment values are nominal preirradiation fabrication values.
- Spacers may be used to axially position fuel assemblies to facilitate handling.

^a Assemblies may contain partial-length fuel rods.

2.3 Design Criteria for Environmental Conditions and Natural Phenomena

This section presents the design criteria for site environmental conditions and natural phenomena applied in the design basis analyses of MAGNASTOR. Analyses to demonstrate that the design basis system meets the design criteria defined in this section are presented in the appropriate chapters.

The use of MAGNASTOR at a specific site requires that the site either meet the design criteria of this section or be separately evaluated against the site-specific conditions to ensure the acceptable performance of the system.

2.3.1 Tornado Missiles and Wind Loadings

The concrete casks are typically placed outdoors on an unsheltered reinforced concrete storage pad at an ISFSI site. This storage condition exposes the casks to tornado and wind loading.

2.3.1.1 Applicable Design Parameters

The design basis tornado and wind loading is defined based on Regulatory Guide 1.76 [11], Region 1, and NUREG-0800 [12]. The tornado and wind loading criteria are as follows.

Tornado and Wind Condition	Limit
Rotational Wind Speed, mph	290
Translational Wind Speed, mph	70
Maximum Wind Speed, mph	360
Radius of Maximum Wind Speed, ft	150
Pressure Drop, psi	3.0
Rate of Pressure Drop, psi/sec	2.0

2.3.1.2 Determination of Forces on Structures

Tornado wind forces on the concrete cask are calculated by multiplying the dynamic wind pressure by the frontal area of the cask normal to the wind direction. Wind forces are applied to the cask in the wind direction. No streamlining is assumed. The cask is demonstrated to remain stable under design basis tornado wind loading in conjunction with impact from a high-energy tornado missile.

2.3.1.3 Tornado Missiles

The design basis tornado missile impacts are defined in Paragraph 4, Subsection III, Section 3.5.1.4 of NUREG-0800 [12]. The design basis tornado is considered to generate three types of missiles that impact the cask at normal incidence.

Massive Missile – (deformable w/high kinetic energy)	Weight = 4,000 lb Frontal Area = 20 sq ft
Penetration Missile – (rigid hardened steel)	Weight = 280 lb Diameter = 8.0 in
Protective Barrier Missile – (solid steel sphere)	Weight = 0.15 lb Diameter = 1.0 in

Each missile is assumed to impact the concrete cask at a velocity of 126 miles per hour, horizontal to the ground, which is 35% of the maximum wind speed of 360 miles per hour. For missile impacts in the vertical direction, the assumed missile velocity is $(0.7)(126) = 88.2$ miles per hour.

The analysis of the loaded concrete cask for missile impacts applies the laws of conservation of momentum and conservation of energy to determine the rigid body response of the concrete cask. Each missile impact is evaluated, and all missiles are assumed to impact in a manner that produces the maximum damage to the cask.

2.3.2 Water Level (Flood) Design

The loaded concrete cask may be exposed to a flood during storage on an unsheltered concrete storage pad at an ISFSI site. The source and magnitude of the probable maximum flood depend on specific site characteristics.

2.3.2.1 Flood Elevations

The concrete cask design basis is a maximum floodwater depth of 50 feet above the base of the cask and a floodwater velocity of 15 ft per second. Under design basis flood conditions, the cask does not float or tip on the storage pad and the confinement function is maintained.

2.3.2.2 Phenomena Considered in Design Load Calculations

The occurrence of flooding at an ISFSI site is dependent upon the specific site location and the surrounding natural and man-made geographical features. Some possible sources of a flood at an ISFSI site are: overflow from a river or stream due to unusually heavy rain, snow-melt runoff, or a dam or major water supply line break caused by a seismic event (earthquake); high tides

produced by a hurricane; and a tsunami (tidal wave) caused by an underwater earthquake or volcanic eruption.

Flooding at an ISFSI site is highly improbable because of the extensive environmental impact studies that are performed during the selection of a site for a nuclear facility.

2.3.2.3 Flood Force Application

The evaluation of the concrete cask for a flood condition determines a maximum permissible floodwater current velocity and a maximum permissible floodwater depth. The criteria employed in the determination of the maximum permissible values are that a cask tip-over will not occur, and that the TSC material yield strength is not exceeded.

The force of the floodwater current on the concrete cask is calculated as a function of the velocity by multiplying the dynamic water pressure by the frontal area of the cask that is normal to the direction of the current. The dynamic water pressure is calculated using Bernoulli's equation relating fluid velocity and pressure. The maximum permissible force of the floodwater current is determined such that the overturning moment on the cask will be less than that required to tip the cask over.

During a flood condition, the force of the floodwater exerts a hydrostatic pressure on the canister shell. This pressure is based on the design basis flood: floodwater depth of 50 ft and floodwater velocity of 15 ft per second. Therefore, the force exerted on the canister shell is 22 psi. The analysis of the canister shell will demonstrate that there is no containment malfunction or impairment of the ability to retrieve fuel from the canister.

2.3.2.4 Flood Protection

The inherent strength of the reinforced concrete cask provides a substantial margin of safety against any permanent deformation of the cask for a credible flood event at an ISFSI site. Therefore, no special flood protection measures for the cask are necessary. For the design basis flood, the allowable stresses in the TSC are not exceeded.

2.3.3 Seismic Design

An ISFSI site may be subject to seismic events (earthquakes) during its lifetime. The seismic response spectra experienced by the concrete cask depends upon the geographical location of the specific site and the distance from the epicenter of the earthquake. The possible significant effect of a beyond-design-basis seismic event on the concrete cask would be a tip-over; however, the

loaded concrete cask does not tip over during the design-basis seismic event. Although it is a nonmechanistic event, the loaded concrete cask design basis includes consideration of the consequences of a hypothetical cask tip-over event.

The TSC is analyzed for loads induced by the application of a 0.37g seismic acceleration to the concrete cask at the top surface of the ISFSI pad.

2.3.4 Snow and Ice Loadings

The criterion for determining design snow loads is based on ANSI/ASCE 7-93 [13], Section 7.0. Flat roof snow loads apply and the design basis snow and ice load are calculated from the following formula.

$$\begin{aligned} p_f &= 0.7C_e C_t I p_g \\ &= 100.8 \text{ psf} \end{aligned}$$

where:

$$\begin{aligned} p_f &= \text{flat roof snow load (psf)} \\ C_e &= \text{exposure factor} = 1.0 \\ C_t &= \text{thermal factor} = 1.2 \\ I &= \text{importance factor} = 1.2 \\ p_g &= \text{ground snow load, (psf)} = 100 \end{aligned}$$

The numerical values of C_e , C_t , I , and p_g are obtained from Tables 1, 18, 19, and 20 and Figure 7, respectively, of ANSI/ASCE 7-93.

The exposure factor, C_e , accounts for wind effects. The exposure factor of the concrete cask is assumed to be Category C, which is defined to be "locations in which snow removal by wind cannot be relied on to reduce roof loads because of terrain, higher structures, or several trees nearby." The thermal factor, C_t , accounts for the importance of buildings and structures in relation to public health and safety. The concrete cask is conservatively classified as a Category III building or other structure. Ground snow loads for the contiguous United States are given in Figures 5, 6, and 7 of ANSI/ASCE 7-93. A worst-case value of 100 lb per square ft is assumed.

The design basis snow and ice load is bounded by the weight of the loaded transfer cask on the top of the concrete cask shell and by the tornado missile loading on the concrete cask lid. The snow load is considered in the load combinations evaluations of the concrete cask.

2.3.5 Combined Load Criteria

Each normal condition and off-normal and accident event has a combination of load cases that defines the total combined loading for that condition/event. The individual load cases considered include thermal, seismic, external and internal pressure, missile impacts, drops, snow and ice loads, and/or flood water forces. The load conditions to be evaluated for storage casks are identified in 10 CFR 72 [10] and ANSI/ANS-57.9 [14].

2.3.5.1 Load Combinations and Design Strength - Concrete Cask

Refer to Table 2.3-1 for the load combinations for the concrete cask. The live loads are considered to vary from 0% to 100% to ensure that the worst-case condition is evaluated. In each case, use of 100% of the live load produces the maximum load condition. The steel liner of the concrete cask is a stay-in-place form that also provides radiation shielding. The concrete cask is designed to the requirements of ACI 349 [4].

In calculating the design strength of concrete in the concrete cask body, nominal strength values are multiplied by a strength reduction factor in accordance with Section 9.3 of ACI 349.

2.3.5.2 Load Combinations and Design Strength – TSC and Fuel Basket

The TSC is designed in accordance with the ASME Code, Section III, Subsection NB [1]. The basket is designed in accordance with the ASME Code, Section III, Subsection NG [2]. Structural buckling of the basket is evaluated in accordance with NUREG/CR-6322 [3].

Refer to Table 2.3-2 for the load combinations for all normal conditions and off-normal or accident events and the corresponding ASME service levels. Levels A and D service limits represent normal conditions and accident events, respectively. Levels B and C service limits are used for off-normal events. The analysis criteria of the ASME Code, Section III, Subsection NB are employed. Stress intensities produced by pressure, temperature, and mechanical loads are combined before comparison to the ASME Code allowable criteria. For components used in the TSC, refer to the allowable criteria in Table 2.3-3.

The load combinations considered for the fuel basket for normal conditions and off-normal or accident events are the same as those identified for the TSC in Table 2.3-2, except that there are

no internal pressure loads. The analysis criteria of the ASME Code, Section III, Subsection NG are employed. For the fuel basket components, refer to the allowable criteria in Table 2.3-3.

2.3.5.3 Design Strength - Transfer Cask

The transfer cask is a special lifting device. It is designed, fabricated, and load tested to meet the requirements of ANSI N14.6 [6] for the handling of vertical loads defined in NUREG 0612 [15]. The design criteria are as follows.

- The combined shear stress or maximum tensile stress during the lift (with 10% dynamic load factor) shall be $\leq S_y/6$ and $S_u/10$.
- For off-normal (Level C) conditions, membrane stresses shall be less than $1.2S_m$ and membrane plus bending stresses shall be the lesser of $1.8S_m$ and $1.5S_y$.
- The ferritic steel material used for the load-bearing members of the transfer cask shall satisfy the material toughness requirements of ANSI N14.6, paragraph 4.2.6.

Refer to Chapter 10 for information on load testing of the transfer cask.

2.3.6 Environmental Temperatures

A temperature of 100°F is selected to establish a conservative boundary for the annual average temperature for MAGNASTOR in storage. This temperature conservatively bounds the maximum average annual temperature in the 48 contiguous United States, specifically, Miami, FL, at 75.6°F [16], and is, therefore, used so as to bound existing and potential ISFSI sites. Refer to Chapter 4 for the evaluation of this environmental condition along with the thermal analysis models. Refer to Chapter 3 for the thermal stress evaluation for the normal operating conditions. Normal temperature fluctuations are bounded by the severe ambient temperature cases that are evaluated as off-normal and accident events.

Off-normal, severe environmental events are defined as -40°F with no solar loads and 106°F with solar loads. An extreme environmental condition of 133°F with maximum solar loads is evaluated as an accident case to show compliance with the maximum heat load case required by ANSI/ANS-57.9. Thermal performance is also evaluated assuming both the half blockage of the concrete cask air inlets and the complete blockage of the air inlets.

The design basis temperatures used in the concrete cask analysis follow. Solar insolation is as specified in 10 CFR 71.71 [17] and Regulatory Guide 7.8 [18].

Condition	Ambient Temperature	Solar Insolation
Normal	100°F	yes
Off-Normal - Severe Heat	106°F	yes
Off-Normal - Severe Cold	-40°F	no
Accident - Extreme Heat	133°F	yes

Table 2.3-1 Load Combinations for the Concrete Cask

Load Combination	Condition	Dead	Live	Wind	Thermal	Seismic	Tornado/ Missile	Drop/ Impact	Flood
1	Normal	1.4D	1.7L						
2	Normal	1.05D	1.275L		1.275T _o				
3	Normal	1.05D	1.275L	1.275W	1.275T _o				
4	Off-Normal and Accident	D	L		T _a				
5	Accident	D	L		T _o	E _{ss}			
6	Accident	D	L		T _o			A	
7	Accident	D	L		T _o				F
8	Accident	D	L		T _o		W _t		

Load Combinations are from ANSI/ANS-57.9 [14] and ACI 349 [4]. Where:

- | | |
|-------------------------------------|---|
| D = Dead Load | T _a = Off-Normal or Accident Temperature |
| L = Live Load | E _{ss} = Design Basis Earthquake |
| W = Wind | W _t = Tornado/Tornado Missile |
| T _o = Normal Temperature | A = Drop/Impact |
| F = Flood | |

Table 2.3-2 Load Combinations for the TSC

LOAD		NORMAL			OFF-NORMAL					ACCIDENT					
ASME Service Level Load Combinations		A			B			C		D					
		1	2	3	1	2	3	4	5	1	2	3	4	5	6
Dead Weight	TSC w/ fuel	X	X	X	X	X	X	X	X	X	X	X	X	X	X
Thermal	Inside concrete cask: 100°F ambient	X		X				X		X	X	X	X	X	
	Inside transfer cask: 100°F ambient		X		X		X								X
	Inside concrete cask: -40°F or 106°F ambient					X			X						
Internal Pressure	Normal	X	X	X			X	X	X	X	X	X	X		
	Off-Normal				X	X									
	Accident (fire)													X	X
Handling Load	Normal (1.1g)		X	X	X										
	Off-Normal						X	X	X						
Drop/Impact	24-in drop, < 60g									X					
Seismic	Tip-over and complete burial										X				
Flood	50-ft water head											X			
Tornado	Pressure drop of 3.0 psi												X		

Table 2.3-3 Structural Design Criteria for Components Used in the TSC

Component	Criteria
1. Normal Operations: Service Level A TSC: ASME Section III, Subsection NB [1] Basket: ASME Section III, Subsection NG [2]	$P_m \leq S_m$ $P_L + P_b \leq 1.5 S_m$ $P_L + P_b + Q \leq 3S_m$
2. Off-Normal Operations: Service Level B TSC: ASME Section III, Subsection NB	$P_m < 1.1 S_m$ $P_L + P_b < 1.65 S_m$
3. Off-Normal Operations: Service Level C TSC: ASME Section III, Subsection NB Basket: ASME Section III, Subsection NG	Subsection NB Criteria: $P_m < 1.2 S_m$ or S_y (whichever is greater) $P_L + P_b < 1.8 S_m$ or $1.5 S_y$ (whichever is lesser) Subsection NG Criteria: $P_m < 1.5S_m$ $P_L + P_b < 2.25S_m$
4. Accident Conditions, Service Level D TSC: ASME Section III, Subsection NB Basket: ASME Section III, Appendix F Basket: ASME Section III, Subsection NG	$P_m \leq 2.4 S_m$ or $0.7 S_u$ (whichever is lesser) $P_L + P_b \leq 3.6 S_m$ or $1.0 S_u$ (whichever is lesser) Plastic Analysis (Basket): $P_m \leq 0.7S_u$ $P_{int} \leq 0.9S_u$
5. Basket Structural Buckling	NUREG/CR-6322 [3]

Symbols:

S_m = material design stress intensity
 S_u = material ultimate strength
 S_y = material yield strength

P_L = primary local membrane stress
 P_m = primary general membrane stress
 P_b = primary bending stress
 P_{int} = primary stress intensity

2.4 Safety Protection Systems

MAGNASTOR relies upon passive systems to ensure the protection of public health and safety, except in the case of fire or explosion. As previously discussed, fire and explosion events are effectively precluded by site administrative controls that prevent the introduction of flammable and explosive materials. The use of passive systems provides protection from mechanical or equipment failure.

2.4.1 General

MAGNASTOR is designed for safe, long-term storage of spent fuel. The system will withstand all of the evaluated normal conditions and off-normal and postulated accident events without release of radioactive material or excessive radiation exposure to workers or the general public. The major design considerations used to assure safe, long-term fuel storage are as follows.

- Continued radioactive material confinement in postulated accidents.
- Thick steel and concrete biological shield.
- Passive systems that ensure reliability.
- Pressurized inert helium atmosphere to provide corrosion protection for fuel cladding and enhanced heat transfer for the stored fuel.

Each major component of the system is classified with respect to its function and corresponding potential effect on public safety. In accordance with Regulatory Guide 7.10 [19], each major system component is assigned a safety classification (see Table 2.4-1). The safety classification is based on review of the component's function and the assessment of the consequences of its failure following the guidelines of NUREG/CR-6407 [20]. The safety classification categories are defined in the following list.

- Category A - Components critical to safe operations whose failure or malfunction could directly result in conditions adverse to safe operations, integrity of spent fuel, or public health and safety.
- Category B - Components with major impact on safe operations whose failure or malfunction could indirectly result in conditions adverse to safe operations, integrity of spent fuel, or public health and safety.
- Category C - Components whose failure would not significantly reduce the packaging effectiveness and would not likely result in conditions adverse to safe operations, integrity of spent fuel, or public health and safety.

As discussed in the following sections, the MAGNASTOR design incorporates features addressing the design considerations described previously to assure safe operation during loading, handling, and storage of spent nuclear fuel.

2.4.2 Confinement Barriers and Systems

The radioactive materials that MAGNASTOR must confine during storage originate from the stored fuel assemblies and residual contamination inside the TSC. The system is designed to safely confine this radioactive material under all storage conditions.

The stainless steel TSC is assembled and closed by welding. All of the field-installed welds are liquid penetrant examined as detailed in Chapter 10 and on the License Drawings. The longitudinal and girth shop welds of the TSC shell are full penetration welds that are radiographically and liquid penetrant examined during fabrication. The TSC bottom-plate-to-shell shop weld joint is ultrasonically and liquid penetrant examined during fabrication.

The TSC vessel provides a leaktight boundary precluding the release of solid, volatile, and gaseous radioactive material. There are no evaluated normal condition or off-normal or accident events that result in the breach of the TSC and the subsequent release of radioactive materials. The TSC is designed to withstand a postulated drop accident without precluding the subsequent removal of the fuel (i.e., the fuel tubes do not deform such that they bind the fuel assemblies).

Operator radiation exposure during handling and closure of the TSC is minimized by the following.

- Minimizing the number of operations required to complete the TSC loading and sealing process.
- Placing the closure lid on the TSC while the transfer cask and TSC are under water in the fuel pool.
- Using temporary shielding, including a weld shield plate as the mounting component of the weld machine.
- Using retaining blocks on the transfer cask to ensure that the TSC is not raised out of the transfer cask.

2.4.3 Concrete Cask Cooling

The loaded concrete cask is passively cooled. Ambient air enters at the bottom of the concrete cask through four air inlets and heated air exits through the four air outlets at the top of the cask due to natural convection heat transfer. Radiant heat transfer also occurs from the TSC to the concrete cask liner. Consequently, the liner also heats the convective airflow. This natural

circulation of air inside the concrete cask, in conjunction with radiation from the TSC surface, maintains the fuel cladding and concrete cask component temperatures below their design limits. Conduction does not play a substantial role in heat removal from the TSC surface. Refer to Chapter 4 for details on the concrete cask thermal analyses.

2.4.4 Protection by Equipment

There is no important-to-safety equipment required for the safe storage operation of MAGNASTOR. The important-to-safety equipment employed in the handling of MAGNASTOR is the lifting yoke used to lift the transfer cask. The lifting yoke is designed, fabricated, and tested in accordance with ANSI N14.6 as a special lifting device as defined as NUREG 0612. The lifting yoke is proof load tested to 300% of its design load when fabricated. Following the load test, the bolted connections are disassembled, and the components are inspected for deformation. Permanent deformation of components is not acceptable. Engagement pins are examined by dye penetrant examination. The TFR and lifting yoke are inspected for visible defects prior to each use. Transfer cask annual inspection requirements are defined in Chapter 10.

2.4.5 Protection by Instrumentation

No instrumentation is required for the safe storage operations of MAGNASTOR.

A remote temperature-monitoring system may be used to measure the outlet air temperature of the concrete casks in long-term storage. The outlet temperature can be monitored daily as a check of the continuing thermal performance of the concrete cask. Alternately, a daily visual inspection for blockage of the air inlet and air outlet screens of all concrete casks may be performed. Following any natural phenomena event, such as an earthquake or tornado, the concrete casks shall be inspected for damage and air inlet and air outlet blockage.

2.4.6 Nuclear Criticality Safety

MAGNASTOR design includes features to ensure that nuclear criticality safety is maintained (i.e., the cask remains subcritical under normal conditions and off-normal and accident events). The design of the TSC and fuel basket is such that, under all conditions, the highest neutron multiplication factor (k_{eff}) is less than 0.95.

2.4.6.1 Control Methods for Prevention of Criticality

The principal design criterion is that k_{eff} remain less than 0.95 for all conditions. Criticality control for PWR spent fuel is achieved using neutron absorber material fixed in the basket and by maintaining a minimum boron concentration in the TSC during fuel loading. The fixed neutron absorber attracts thermal neutrons that are moderated in the water surrounding the fuel. Fast, high-energy neutrons escape the system. The minimum effective loading for neutron absorber sheets for PWR baskets is $0.036 \text{ g }^{10}\text{B}/\text{cm}^2$. As manufactured, boron concentrations depend on the effectiveness of the sheet, typically 75% or 90%. Neutron absorber sheets are mechanically attached to the fuel tube structure to ensure that the neutron absorber remains in place during the design basis normal conditions and off-normal and accident events.

Similarly, the BWR basket design uses neutron absorber material fixed in the basket. Minimum effective loading of neutron absorber sheets for BWR baskets is $0.027 \text{ g }^{10}\text{B}/\text{cm}^2$. Neutron absorber sheets are mechanically attached to the fuel tube to ensure that the sheets remain in place during the design basis normal conditions and off-normal and accident events.

The basket designs ensure that there is sufficient absorption of moderated neutrons by the neutron absorber (and by boron in the cavity water in some cases) to maintain criticality control in the basket ($k_{eff} < 0.95$). See Chapter 6 for the detailed criticality analyses.

2.4.6.2 Error Contingency Criteria

The standards and regulations of criticality safety require that k_{eff} , including uncertainties, be less than 0.95. The bias and 95/95 uncertainty are applied to the calculation using an upper safety limit (USL) approach [22]. The $k_{eff} + 2\sigma$ value must be less than the USL. Based on MCNP critical benchmarks, the USL as a function of fission neutron lethargy (eV) is shown as:

$$\text{USL} = 0.9364 + 8.4409 \times 10^{-3} \times x$$

where:

$$x = \text{energy of average neutron lethargy causing fission}$$

2.4.6.3 Verification Analyses

The MCNP criticality analysis code is benchmarked through a series of calculations based on critical experiments. These experiments span a range of fuel enrichments, fuel rod pitches, poison sheet characteristics, shielding materials, and geometries that are typical of light water

reactor fuel in a cask. To achieve accurate results, three-dimensional models, as close to the actual experiment as possible, are used to evaluate the experiments.

2.4.7 Radiological Protection

MAGNASTOR is designed to minimize operator radiological exposure in keeping with the As Low As Reasonably Achievable (ALARA) philosophy.

2.4.7.1 Access Control

Access to MAGNASTOR at an ISFSI site will be controlled by a fence with lockable truck and personnel access gates to meet the requirements of 10 CFR 72, 10 CFR 73, and 10 CFR 20 [21]. Access to the storage area, and its designation as to the level of radiation protection required, will be established by site procedures by the licensee.

2.4.7.2 Shielding

MAGNASTOR is designed to limit the dose rates in accordance with 10 CFR 72.104 and 72.106, which set whole body dose limits for an individual located beyond the controlled area at ≤ 25 mrem per year (whole body) during normal operations and ≤ 5 rem (5,000 mrem) from any design basis accident.

2.4.7.3 Ventilation Off-Gas

MAGNASTOR is passively cooled by radiation and natural convection heat transfer at the outer surface of the concrete cask and in the TSC-concrete cask annulus. In the TSC-concrete cask annulus, air enters the air inlets, flows up between the TSC and concrete cask liner in the annulus, and exits the air outlets. If the exterior surface of the TSC is excessively contaminated, the possibility exists that contamination could be carried aloft by the airflow. Therefore, during fuel loading, the spent fuel pool water is minimized in the transfer cask/TSC annulus by supplying the annulus with clean water. Clean water is injected into the annulus during the entire time the transfer cask is submerged. The use of the annulus clean water system minimizes the potential for contamination of the TSC.

Once the transfer cask is removed from the pool, smear surveys are taken on the exterior surfaces of the TSC. If TSC decontamination is required, clean water can be used to flush the annulus. To facilitate decontamination, the TSC exterior surfaces are smooth.

MAGNASTOR has no radioactive releases during normal conditions or off-normal or accident events of storage. Hence, there are no off-gas system requirements for MAGNASTOR.

2.4.7.4 Radiological Alarm Systems

No radiological alarms are required on MAGNASTOR. Typically, total radiation exposure due to the ISFSI installation is monitored by the use of the licensee's boundary dose monitoring program.

2.4.8 Fire Protection

A major ISFSI fire is not considered credible, since there is very little material near the concrete casks that could contribute to a fire. The concrete cask is largely impervious to incidental thermal events. Administrative controls will be established by the licensee to ensure that the presence of combustibles at the ISFSI is minimized. A hypothetical 1,475°F fire engulfing the cask for eight minutes is evaluated as an accident condition. This condition is considered to be highly conservative.

2.4.9 Explosion Protection

MAGNASTOR is analyzed to ensure its proper function under an over-pressure event. The TSC is protected from direct over-pressure conditions by the concrete cask. For the same reasons as for the fire condition, a severe explosion on an ISFSI site is not considered credible. The evaluated 20 psig over-pressure condition is considered to bound any explosive over-pressure resulting from an industrial explosion at the boundary of the owner-controlled area.

2.4.10 Auxiliary Structures

The loading, welding, drying, transfer, and transport of MAGNASTOR requires the use of auxiliary equipment as described in Chapter 9. External transfer of a TSC may require the use of a structure, referred to as a "TSC Handling and Transfer Facility." The TSC Handling and Transfer Facility is a specially designed and engineered structure independent of the 10 CFR 50 facilities at the site.

The design of the TSC Handling and Transfer Facility would meet the requirements for MAGNASTOR described in the Design Features presented in Appendix A of the Technical Specifications, in addition to those requirements established by the licensee.

The design, analysis, fabrication, operation, and maintenance of the TSC Handling and Transfer Facility would be performed in accordance with the quality assurance program requirements of the licensee. The components of the TSC Handling and Transfer Facility would be classified as Important-to-Safety or Not-Important-to-Safety in accordance with the guidelines of NUREG-6407.

Table 2.4-1 Safety Classification of MAGNASTOR Components

Component Description	Reference Drawings	Safety Function	Safety Classification
TSC Assembly Shell and Base Plate Closure Lid Port Covers	71160-581 71160-584 71160-585	Structural and Confinement	A
Fuel Basket Assembly Basket Support Weldments Fuel Tube Assemblies Neutron Absorbers	71160-551 71160-571 71160-572 71160-574 71160-575 71160-591 71160-598 71160-599	Criticality, Structural, and Thermal	A
Transfer Cask Assembly Trunnions Inner and Outer Shells Shield Doors and Rails Lead Gamma Shield Neutron Shield	71160-560	Structural, Shielding and Operations	B
Adapter Plate Assembly Base Plate Door Rails Hydraulic Operating System Side Shields	None	Operations and Shielding	NQ
Concrete Cask Assembly Structural Weldments and Base Plate Lid Weldment Lifting Lugs Reinforcing Bars Concrete	71160-561 71160-562 71160-590	Structural, Shielding, Operations, and Thermal	B

2.5 Decommissioning Considerations

The principal components of MAGNASTOR are the concrete cask and the TSC. Refer to Chapter 15 for information on decommissioning MAGNASTOR.

Decommissioning of MAGNASTOR involves removing the TSC by offsite transport and disassembling the concrete cask. It is expected that the concrete will be broken up and the steel components segmented to reduce volume. The concrete and carbon steel are not expected to be surface-contaminated and no significant activation is expected.

The TSC is designed and fabricated for use as a component of the waste package for permanent disposal at the Mined Geological Disposal System. Consequently, decommissioning may not be required. If necessary, the TSC could be decommissioned following unloading by decontaminating the inside and segmenting the shell and closure plates. Since the neutron flux rate from the stored fuel is low, only minimal activation of the TSC is expected. The resulting stainless steel could be disposed of, or recycled, in accordance with the appropriate regulatory requirements.

The storage pad, fence, and supporting utility fixtures are not expected to require decontamination as a result of use of MAGNASTOR. Consequently, these items may be reused or disposed of as locally generated clean waste.

2.6 References

1. ASME Boiler and Pressure Vessel Code, Section III, Subsection NB, "Class 1 Components," American Society of Mechanical Engineers, New York, NY, 2001 Edition with 2003 Addenda.
2. ASME Boiler and Pressure Vessel Code, Section III, Subsection NG, "Core Support Structures," American Society of Mechanical Engineers, New York, NY, 2001 Edition with 2003 Addenda.
3. NUREG/CR-6322, "Buckling Analysis of Spent Fuel Basket," US Nuclear Regulatory Commission, Washington, DC, May 1995.
4. "Code Requirements for Nuclear Safety Related Concrete Structures (ACI 349) and Commentary (ACI 349R)," American Concrete Institute, Farmington Hills, MI.
5. "Building Code Requirements for Structural Concrete (ACI 318) and Commentary (ACI 318R)," American Concrete Institute, Farmington Hills, MI.
6. ANSI N14.6-1993, "American National Standard for Radioactive Materials - Special Lifting Devices for Shipping Containers Weighing 10,000 Pounds (4,500 kg) or More," American National Standards Institute, Inc., Washington, DC, June 1993.
7. ISG-11, "Cladding Considerations for the Transport and Storage of Spent Fuel," US Nuclear Regulatory Commission, Washington, DC, Revision 3, November 17, 2003.
8. PNL-4835, "Technical Basis for Storage of Zircaloy-Clad Spent Fuel in Inert Gases," Johnson, A.B., and Gilbert, E.R., Pacific Northwest Laboratory, Richland, WA, September, 1983.
9. NUREG-1536, "Standard Review Plan for Dry Cask Storage Systems," US Nuclear Regulatory Commission, Washington, DC, January 1997.
10. 10 CFR 72, Code of Federal Regulations, "Licensing Requirements for the Independent Storage of Spent Nuclear Fuel, High-Level Radioactive Waste and Reactor-Related Greater Than Class C Waste," US Government, Washington, DC.
11. Regulatory Guide 1.76, "Design Basis Tornado for Nuclear Power Plants," US Nuclear Regulatory Commission, Washington, DC, April 1974.
12. NUREG-0800, "Standard Review Plan," US Nuclear Regulatory Commission, Washington, DC, April 1996.

13. ANSI/ASCE 7-93 (formerly ANSI A58.1), "Minimum Design Loads for Buildings and Other Structures," American Society of Civil Engineers, New York, NY, May 1994.
14. ANSI/ANS-57.9-1992, "Design Criteria for an Independent Spent Fuel Storage Installation (Dry Type)," American Nuclear Society, La Grange Park, IL, May 1992.
15. NUREG-0612, "Control of Heavy Loads at Nuclear Power Plants," US Nuclear Regulatory Commission, Washington, DC, July 1980.
16. ASHRAE Handbook, "Fundamentals," American Society of Heating, Refrigeration, and Air Conditioning Engineers, Atlanta, GA, 1993.
17. 10 CFR 71, "Packaging and Transportation of Radioactive Materials," Code of Federal Regulations, US Government, Washington, DC.
18. Regulatory Guide 7.8, "Load Combinations for the Structural Analysis of Shipping Casks for Radioactive Material," US Nuclear Regulatory Commission, Washington, DC, March 1989.
19. Regulatory Guide 7.10, "Establishing Quality Assurance Programs for Packaging Used in the Transport of Radioactive Material," US Nuclear Regulatory Commission, Washington, DC.
20. NUREG/CR-6407, "Classification of Transportation Packaging and Dry Spent Fuel Storage System Components According to Importance to Safety," US Nuclear Regulatory Commission, Washington, DC, February 1996.
21. 10 CFR 20, "Standards for Protection Against Radiation," Code of Federal Regulations, US Government, Washington, DC.
22. NUREG/CR-6361, "Criticality Benchmark Guide for Light-Water-Reactor Fuel in Transportation and Storage Packages", US Nuclear Regulatory Commission, Washington, DC, December 1997.
23. ASME Boiler and Pressure Vessel Code Case 595-4, "Requirements for Spent Fuel Storage Canisters, Section III."

Chapter 3 Structural Evaluation

Table of Contents

3	STRUCTURAL EVALUATION.....	3-1
3.1	MAGNASTOR Structural Design	3.1-1
3.1.1	Major Components.....	3.1-1
3.1.2	Discussion of MAGNASTOR	3.1-1
3.1.3	Design Criteria Summary.....	3.1-4
3.2	Weights and Centers of Gravity.....	3.2-1
3.3	Materials	3.3-1
3.4	General Standards for Casks	3.4-1
3.4.1	Chemical and Galvanic Reactions	3.4-1
3.4.2	Positive Closure	3.4-1
3.4.3	Lifting Devices.....	3.4-2
3.5	Normal Operating Conditions.....	3.5-1
3.5.1	TSC Evaluation for Normal Operating Conditions	3.5-1
3.5.2	Fuel Basket Evaluation for Normal Operating Conditions.....	3.5-5
3.5.3	Concrete Cask Evaluations for Normal Operating Conditions.....	3.5-23
3.6	Off-normal Operating Events.....	3.6-1
3.6.1	TSC Evaluations for Off-normal Operating Events.....	3.6-1
3.6.2	Fuel Basket Evaluation for Off-normal Events.....	3.6-2
3.6.3	Concrete Cask Evaluation for Off-normal Events	3.6-8
3.7	Storage Accident Events	3.7-1
3.7.1	TSC Evaluations for Storage Accident Conditions	3.7-1
3.7.2	Fuel Baskets Evaluation for Storage Accident Events.....	3.7-4
3.7.3	Concrete Cask Evaluation for Accident Events.....	3.7-37
3.8	Fuel Rods	3.8-1
3.9	References.....	3.9-1

Appendices

Table of Contents.....	3.A-i
List of Figures	3.A-ii

List of Figures

Figure 3.1-1	Principal Components of MAGNASTOR.....	3.1-5
Figure 3.4-1	Top Ring Section Cuts	3.4-26
Figure 3.7-1	PWR Fuel Tube Array – 0° Basket Orientation	3.7-57
Figure 3.7-2	PWR Fuel Tube Section Cuts – 0° Basket Orientation.....	3.7-58
Figure 3.7-3	PWR Fuel Tube Array – 45° Basket Orientation	3.7-59
Figure 3.7-4	PWR Fuel Tube Section Cuts – 45° Basket Orientation.....	3.7-60
Figure 3.7-5	PWR Corner Support Weldment Section Cuts – 0° Basket Orientation....	3.7-61
Figure 3.7-6	PWR Corner Support Weldment Section Cuts – 45° Basket Orientation..	3.7-62
Figure 3.7-7	PWR Side Support Weldment Section Cuts – 0° Basket Orientation.....	3.7-63
Figure 3.7-8	PWR Side Support Weldment Section Cuts – 45° Basket Orientation.....	3.7-64
Figure 3.7-9	PWR Fuel Tube Model for Buckling Evaluation	3.7-65
Figure 3.7-10	BWR Fuel Tube Array – 0° Basket Orientation	3.7-66
Figure 3.7-11	BWR Fuel Tube Section Cuts – 0° Basket Orientation	3.7-67
Figure 3.7-12	BWR Fuel Tube Array – 45° Basket Orientation	3.7-68
Figure 3.7-13	BWR Fuel Tube Section Cuts – 45° Basket Orientation	3.7-69
Figure 3.7-14	BWR Corner Support Weldment Section Cuts – 0° Basket Orientation....	3.7-70
Figure 3.7-15	BWR Corner Support Weldment Section Cuts – 45° Basket Orientation..	3.7-71
Figure 3.7-16	BWR Side Support Weldment Section Cuts – 0° Basket Orientation.....	3.7-72
Figure 3.7-17	BWR Side Support Weldment Section Cuts – 45° Basket Orientation.....	3.7-73
Figure 3.7-18	BWR Fuel Tube Model for Buckling Evaluation	3.7-74
Figure 3.7-19	PWR Neutron Absorber and Retainer Finite Element Model.....	3.7-75
Figure 3.7-20	Permanent Strain Contour Plot for the PWR Basket Retainer Strip – Cask Tip-over.....	3.7-76
Figure 3.7-21	Acceleration Time History of the Upper-bound weight TSC – 24-inch Concrete Cask Drop.....	3.7-77
Figure 3.7-22	Acceleration Time History of the Lower-bound Weight TSC – 24-inch Concrete Cask Drop.....	3.7-78
Figure 3.7-23	Acceleration Time History for Concrete Cask Tip-over Condition - Standard Pad	3.7-79
Figure 3.7-24	Acceleration Time History of Oversized Pad	3.7-80

List of Tables

Table 3.2-1	MAGNASTOR Storage Weight and Center of Gravity Summary.....	3.2-2
Table 3.4-1	Stresses for Trunnions and Top Ring	3.4-27
Table 3.4-2	Stresses for Transfer Cask Shells and Bottom Ring.....	3.4-27
Table 3.5-1	TSC Thermal Stress, Q.....	3.5-26
Table 3.5-2	TSC Normal Conditions, P_m Stresses.....	3.5-26
Table 3.5-3	TSC Normal Conditions, $P_m + P_b$ Stresses.....	3.5-26
Table 3.5-4	TSC Normal Conditions, $P + Q$ Stresses.....	3.5-26
Table 3.5-5	Concrete Cask Vertical Stress Summary – Outer Surface, psi.....	3.5-27
Table 3.5-6	Concrete Cask Vertical Stress Summary – Inner Surface, psi.....	3.5-27
Table 3.5-7	Concrete Cask Circumferential Stress Summary – Inner Surface, psi	3.5-27
Table 3.6-1	TSC Off-Normal Events, P_m Stresses.....	3.6-9
Table 3.6-2	TSC Off-Normal Events, $P_m + P_b$ Stresses.....	3.6-9
Table 3.6-3	TSC Off-Normal Events, $P + Q$ Stresses	3.6-9
Table 3.7-1	TSC Accident Events, P_m Stresses	3.7-81
Table 3.7-2	TSC Accident Events, $P_m + P_b$ Stresses	3.7-81
Table 3.7-3	PWR Fuel Tube Nodal Stresses – Concrete Cask Tip-over Accident.....	3.7-81
Table 3.7-4	PWR Corner Mounting Plate P_m Stresses – Concrete Cask Tip-over Accident.....	3.7-82
Table 3.7-5	PWR Corner Mounting Plate $P_m + P_b$ Stresses – Concrete Cask Tip-over Accident.....	3.7-82
Table 3.7-6	PWR Side Weldment P_m Stresses – Concrete Cask Tip-over Accident.....	3.7-82
Table 3.7-7	PWR Side Weldment $P_m + P_b$ Stresses – Concrete Cask Tip-over Accident.....	3.7-82
Table 3.7-8	BWR Fuel Tube Stresses – Concrete Cask Tip-over Accident	3.7-83
Table 3.7-9	BWR Corner Mounting Plate P_m Stresses – Concrete Cask Tip-over Accident.....	3.7-83
Table 3.7-10	BWR Corner Mounting Plate $P_m + P_b$ Stresses – Concrete Cask Tip-over Accident	3.7-83
Table 3.7-11	BWR Side Weldment P_m Stresses – Concrete Cask Tip-over Accident.....	3.7-83
Table 3.7-12	BWR Side Weldment $P_m + P_b$ Stresses – Concrete Cask Tip-over Accident	3.7-84
Table 3.7-13	Concrete Cask Vertical Stress Summary – Outer Surface, psi	3.7-84
Table 3.7-14	Concrete Cask Vertical Stress Summary – Inner Surface, psi	3.7-84
Table 3.7-15	Concrete Cask Circumferential Stress Summary – Inner Surface, psi.....	3.7-84
Table 3.7-16	Basket Modal Frequency for Concrete Cask Tip-over.....	3.7-85
Table 3.7-17	DLF and Amplified Accelerations for Concrete Cask Tip-over.....	3.7-85

3 STRUCTURAL EVALUATION

This chapter describes the design and analysis of the principal structural components of MAGNASTOR. It demonstrates that MAGNASTOR meets the structural requirements for confinement of contents, criticality control, heat dissipation, radiological shielding, and contents retrievability required by 10 CFR 72 [1] for the design basis normal conditions, and off-normal and accident events.

3.1 MAGNASTOR Structural Design

3.1.1 Major Components

The three principal components of MAGNASTOR are the concrete cask, TSC, and the transfer cask; refer to Figure 3.1-1. The following table shows the principal structural components of the three major MAGNASTOR components.

Concrete Cask	TSC	Transfer Cask
Reinforced concrete shell	Closure lid	Trunnions
Liner weldment	Shell	Inner and outer steel shells
Bottom Weldment	Bottom plate	Shield doors
Lid Assembly	Fuel basket assembly (PWR or BWR)	Door support rails
		Lead and NS-4-FR shielding

3.1.2 Discussion of MAGNASTOR

MAGNASTOR has four basic configurations to accommodate all PWR and BWR fuel assemblies. The type (PWR or BWR) and overall length of the fuel assembly determine the basic storage configuration, or group. The allocation of a fuel design to the MAGNASTOR grouping is shown in Table 1.3-2. The TSC is designed in two different lengths to accommodate the four groupings of PWR (2) and BWR (2) fuel assemblies. The concrete cask and transfer cask are one length that accommodates the two TSC lengths. The bounding weights and center of gravity of a loaded concrete cask are presented in Table 3.2-1.

The evaluations presented in this chapter are based on the bounding, or limiting, configuration of the components for the condition being evaluated. In most cases, the bounding condition evaluates the heaviest configuration, with either a total weight or bounding weight used as specified in the analysis. Factors of safety greater than ten are generally stated in the analyses as "Large." Numerical values are shown for factors of safety that are less than ten.

Concrete Cask

The concrete cask is a reinforced concrete cylinder with an outside diameter of 136 inches and an overall height of approximately 225 inches. The internal cavity of the concrete cask is lined by a 1.75-inch thick carbon steel shell having an inside diameter of 79.5 inches. There are 24 standoffs (3 × 7½ S-Beam) welded to the inner diameter of the liner. The overall cavity opening in the concrete cask is 73.5 inches. The liner thickness is designed primarily on radiation shielding requirements, but is also related to the need to establish a practical limit for the

diameter of the concrete shell. The concrete shell, constructed using Type II Portland Cement, has a nominal density of 145 lb/ft³ and a nominal compressive strength of 4,000 psi. Vertical hook bars and horizontal hoop bars form the inner and outer rebar assemblies.

A ventilation airflow path is formed by inlets at the bottom of the concrete cask, the annular space between the concrete cask inner shell and the TSC, and outlets in the concrete cask lid assembly. The passive ventilation system operates by natural convection as cool air enters the bottom inlets, is heated by the TSC, and exits from the outlets. Both the air inlets and air outlets are formed with carbon steel in the concrete cask body.

The lid assembly is composed of carbon steel and concrete and forms the concrete cask closure. The lid assembly is 6.75-inches thick and 88 inches in diameter.

TSC

The TSC consists of a cylindrical shell closed at its top end by a closure lid. The bottom of the TSC is a 2.75-inch thick stainless steel plate that is welded to the TSC shell. The TSC forms the confinement boundary for the PWR or BWR spent fuel that is contained in the fuel basket assembly. The TSC is designed to accommodate both PWR and BWR classes of spent fuel assemblies. The TSC is fabricated from dual certified SA240 Type 304/304L stainless steel. SA182 Type 304 stainless steel may be substituted for the SA240 Type 304 stainless steel used in the closure lid assembly provided that the SA182 material yield and ultimate strengths are equal to or greater than those of the SA240 material. The TSC shell is a 0.5-inch thick plate formed into a 72-inch outer diameter cylinder. The TSC closure lid consists of a 9-inch thick stainless steel plate. The closure lid is welded to the TSC shell to seal the TSC with a partial penetration groove weld. Prior to welding, the closure lid assembly is supported by four lift lugs attached to the inside diameter of the TSC at equally spaced angular intervals. Handling of the TSC is accomplished by the use of six hoist rings threaded into the closure lid providing redundancy for heavy lifts.

The fuel basket assembly is provided in two configurations – one for up to 37 PWR fuel assemblies and one for up to 87 BWR fuel assemblies. The baskets are manufactured from SA537 Class 1 Carbon Steel. For both the PWR basket and BWR basket, the basic components are the same. The baskets are assembled from three major components – fuel tube assemblies, corner support weldments, and side support weldments. The fuel tube assemblies are equipped with neutron absorbers and stainless steel covers on up to four interior surfaces of the fuel tubes. The geometric integrity of the fuel tube array (21 fuel tubes – PWR, 45 fuel tubes – BWR) is maintained by the corner and side support weldments, which are bolted to the fuel tube array.

The nominal inner dimension of the PWR fuel tubes is 8.86-inch square. The nominal inner dimension of the BWR fuel tubes is 5.86-inch square.

Transfer Cask

The transfer cask, with its lifting yoke, is primarily a shielded lifting device used to handle the TSC. It provides biological shielding for a loaded TSC. The transfer cask is used for the vertical transfer of the TSC between workstations and the concrete cask, or transport cask. The shielding of the cask incorporates a multiwall (steel/lead/NS-4-FR/steel) design. The transfer cask is provided in one configuration capable of handling both the PWR and BWR configurations. The transfer cask can handle a loaded TSC weighing up to 118,000 pounds. The transfer cask is a heavy lifting device that is designed, fabricated, and load-tested to the requirements of ANSI-N14.6 [2] and NUREG-0612 [3]. The transfer cask design incorporates three retainer assemblies attached to the top of the transfer cask to prevent a loaded TSC from being inadvertently lifted through the top of the transfer cask. The transfer cask has retractable bottom shield doors. During loading operations, the doors are closed and secured by bolts/pins, so they cannot inadvertently open. During unloading, the doors are retracted using hydraulic cylinders to allow the TSC to be lowered into the concrete cask or transport cask.

Component Evaluation

The following components are evaluated in this chapter.

- TSC lifting devices
- TSC shell, bottom plate, and closure lid
- Fuel basket assembly
- Transfer cask trunnions, shells, retainer assemblies, shield doors, and support rails
- Concrete cask body
- Concrete cask steel components (reinforcement, inner shell, lid assembly, bottom weldment, etc.)

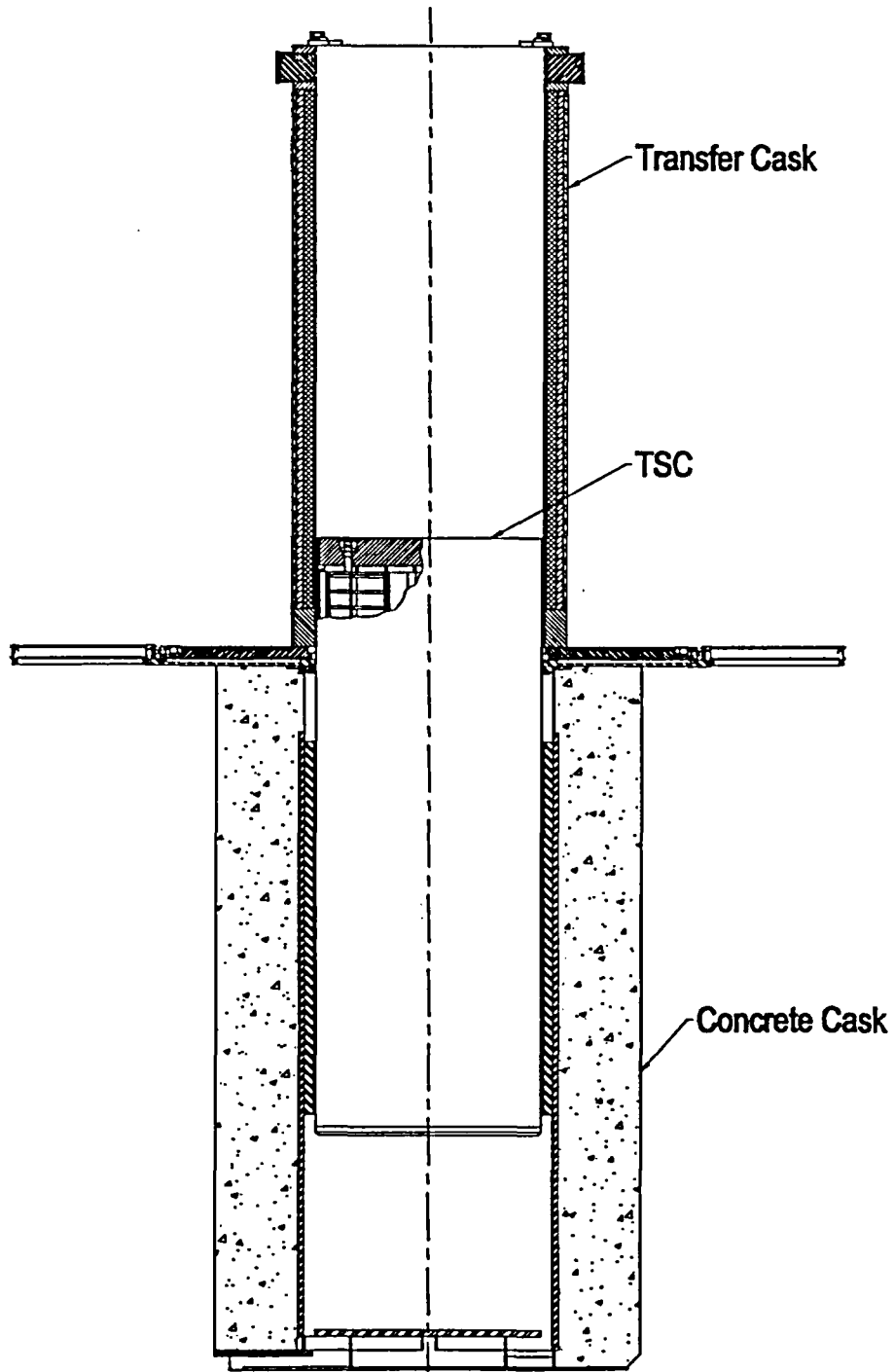
Other MAGNASTOR components shown on the license drawings in Chapter 1 are included as loads in these component evaluations.

The structural evaluations in this chapter demonstrate that MAGNASTOR components meet their respective structural design criteria and are capable of safely storing the design basis PWR or BWR spent fuel assemblies.

3.1.3 Design Criteria Summary

MAGNASTOR structural design criteria are described in Chapter 2. Load combinations for normal, off-normal, and accident loads are evaluated in accordance with ANSI/ANS-57.9 [4] and ACI-349 [5]. The TSC is evaluated in accordance with ASME Code, Section III, Subsection NB for Class 1 components [6]. The basket is evaluated in accordance with ASME Code, Section III Subsection NG [7] and ASME Code, Section III, Appendix F [8]. The buckling evaluation of the TSC shell is performed in accordance with NUREG/CR-6322 [9]. The transfer cask and lifting yoke are lifting devices that are designed to NUREG-0612 [3] and ANSI N14.6 [2].

Figure 3.1-1 Principal Components of MAGNASTOR



3.2 Weights and Centers of Gravity

The maximum calculated weights and centers of gravity (CGs) for MAGNASTOR PWR and BWR configurations are presented in Table 3.2-1. The weights and CGs presented in this section are calculated based on nominal design dimensions.

Table 3.2-1 MAGNASTOR Storage Weight and Center of Gravity Summary

Description	PWR		BWR	
	Weight (lb)	CG (in)	Weight (lb)	CG (in)
Fuel (rod insert weight included for PWR fuel)	62,500	-	61,500	-
Basket	20,000	-	22,000	-
TSC w/o lid	9,500	-	9,500	-
Closure Lid	10,500	-	10,500	-
Water in TSC	17,000	-	16,000	-
Transfer Cask (does not include lifting yoke or transfer adapter)	108,500	-	108,500	-
Concrete Cask (does not include Lid)	214,000	-	214,000	-
Lifting Yoke (not included in transfer cask weight)	3,000	-	3,000	-
Concrete Cask Lid	5,000	-	5,000	-
Loaded TSC (TSC, lid, basket, and fuel)	101,500	96	102,500	98
Storage Cask Loaded (concrete cask, TSC, basket, fuel, concrete cask lid)	320,000	103	321,000	104
Transfer Cask, TSC, Basket, Lifting yoke - Empty	151,000	-	152,500	-
Under Hook Wet Weight (Transfer Cask, TSC, Basket, Lifting Yoke, Closure Lid, Fuel, and Water)	229,500	-	229,500	-
Under Hook Dry Weight (Transfer Cask, TSC, Basket, Transfer Yoke, Closure Lid, Fuel)	212,000		213,000	

- Weights and CGs are maximum calculated values based on nominal component dimensions.
- All weights rounded to the nearest 500 pounds. Component weights are rounded individually, so total assembly weights may not equal the sum of the component weights.
- CG is measured from the bottom of each component.
- Average concrete density is considered to be 148 pcf.
- Transfer cask lifting yoke weight for specific sites may vary from listed weight. The site-specific yoke weight should be used for site-specific applications.
- Concrete cask weight bounds alternate segmented body.

3.3 Materials

Refer to Chapter 8 for the information on Materials.

3.4 General Standards for Casks

MAGNASTOR is designed for safe, long-term storage of spent fuel. The system will withstand all of the evaluated normal conditions, and off-normal and postulated accident events without release of radioactive material or excessive radiation exposure to workers or to the general public.

3.4.1 Chemical and Galvanic Reactions

The materials used in the fabrication and operation of MAGNASTOR are evaluated in Section 8.10.

3.4.2 Positive Closure

A stainless steel closure lid closes the top end of the TSC. Prior to being welded to the TSC shell, the closure lid is supported by lugs welded on the inside surface of the TSC shell at an elevation that allows for thermal expansion of the canister and fuel basket without contact with the closure lid. The lugs also serve as the handling points for the empty TSC shipping/receiving and placement in the transfer cask. The closure lid includes locations for installing load-tested hoist rings or lifting points that are used to lift and lower the loaded TSC after the closure lid is welded to the TSC shell. The closure lid and its weld to the TSC shell can support the weight of the TSC with a load factor of six on material yield strength and ten on material ultimate strength (ANSI N14.6/NUREG 0612). The TSC lifting attachments can support the weight of the TSC with a load factor of three on material yield strength and five on material ultimate strength (ANSI N14.6/NUREG 0612) when used in a redundant lifting arrangement. The TSC has a single 0.5-inch full penetration J-weld attaching the closure lid to the TSC shell. Two port penetrations through the closure lid are used for water removal/TSC drying/helium backfill. Both have a single welded port cover over them to provide the confinement boundary. The port cover welds are field welds and the final weld surfaces are liquid penetrant (PT) examined. The TSC closure lid weld is a field weld with the root, midplane, and final weld surfaces liquid penetrant (PT) examined. The critical flaw evaluation defines the progressive inspection requirements and considers the following criteria.

- Weld is a partial penetration groove weld with an effective throat of 0.5 inch
- Weld Filler material is E308L
- Weld Process is Gas Tungsten Arc Welding (GTAW)
- Inner diameter of the TSC is 71.0 inch

3.4.3 Lifting Devices

To provide more efficient handling of MAGNASTOR, different methods of lifting are designed for each of the components. The transfer cask, the TSC, and the concrete cask, are handled using trunnions, hoist rings, and lift lugs, respectively.

The design of the MAGNASTOR addresses the concerns identified in NRC Bulletin 96-02, "Movement of Heavy Loads Over Spent Fuel, Over Fuel in the Reactor Core, or Over Safety-Related Equipment" (April 11, 1996) listed as follows.

- The MAGNASTOR lifting and handling components satisfy the requirements of NUREG-0612 and ANSI N14.6 for safety factors on redundant and non-redundant load paths as described in this chapter.
- Transfer cask lifting in the spent fuel pool or cask loading pit or transfer cask lifting and movement above the spent fuel pool operating floor will be addressed on a plant-specific basis.

3.4.3.1 Concrete Cask Lift

The concrete cask is lifted by means of embedded lug assemblies located in the top of the concrete cask body or by air pads beneath the cask. The concrete cask lift is analyzed in accordance with ANSI N14.6 and ACI-349. The concrete cask lid assembly is evaluated for lift conditions related to installation on the concrete cask body.

Lift Lug

A weight of 322,000 lb is conservatively used for the evaluation of the lift lugs, which bounds the maximum weight of a loaded concrete cask. Assuming a 10% dynamic load factor, the design load (P) on each lug is as follows.

$$P = \frac{322,000 \times 1.1}{4} = 88,550 \text{ lb}$$

The lugs are evaluated for adequate strength using this bounding load. The bearing stresses and loads for lug failure involving bearing, shear-tear-out, or hoop tension are determined using an allowable load coefficient (K). Actual lug failures may involve more than one failure mode, but such interaction effects are accounted for in the values of K [10].

The allowable ultimate bearing load (P_{bruL}) for lug failure in bearing, shear-out, or hoop tension is determined to be as in the following.

$$P_{bruL} = 445.8 \text{ kip}$$

where the lug materials are:

$$F_{tu} = 80.0 \text{ ksi} \text{ ----- Ultimate strength, A537 CL2, at } 100^{\circ}\text{F}$$
$$F_{ty} = 60.0 \text{ ksi} \text{ ----- Yield strength, A537 CL2, at } 100^{\circ}\text{F}$$

The allowable yield bearing load (P_{bryL}) is calculated as follows.

$$P_{bryL} = 341.9 \text{ kip}$$

Using the criteria of minimum factors of safety of 5 on ultimate strength and 3 on yield strength, the factors of safety (FS) for the lugs are shown as follows.

Ultimate Bearing:

$$FS = \frac{P_{bryL}}{P} = \frac{445.8}{88.55} = 5.03 > 5$$

Yield Bearing:

$$FS = \frac{P_{bryL}}{P} = \frac{341.9}{88.55} = 3.86 > 3$$

The tensile stress (σ) in the net cross sectional area of the lug is calculated to be as follows.

$$\sigma = \frac{P}{A} = \frac{88.55}{7.08} = 12.5 \text{ ksi}$$

The factors of safety (FS) are listed as follows.

Ultimate:

$$FS = \frac{80.0}{12.5} = 6.4 > 5$$

Yield:

$$FS = \frac{60.0}{12.5} = 4.8 > 3$$

Lift Anchor

From the previous lug analysis, the maximum load on each embedment plate is 88.55 kip. The ultimate strength (σ) in the plate is calculated as follows.

$$\sigma = \frac{P}{A} = \frac{88.55}{15.2} = 5.8 \text{ ksi}$$

The factors of safety (FS) are as follows.

Ultimate Tensile:

$$FS = \frac{80.0}{5.8} = 13.8 > 5$$

Yield Tensile:

$$FS = \frac{53.0}{5.8} = 9.1 > 3$$

Where the embedment plate material strengths are listed as follows.

$$F_{tu} = 80.0 \text{ ksi} \text{ ----- Ultimate strength, A537 CL2, at } 200^{\circ}\text{F}$$
$$F_{ty} = 53.0 \text{ ksi} \text{ ----- Yield strength, A537 CL2, at } 200^{\circ}\text{F}$$

Concrete Anchor

The concrete shear area is conservatively assumed to be the perimeter of the bottom plate of the lift anchor. The shear cone in the concrete is ignored. The required anchor depth, D, is determined to be as follows.

$$D = \frac{W}{\phi 2P \sqrt{f_c}} = \frac{177,100}{0.85 \times 2 \times 39.6 \times \sqrt{3800}} = 42.7 \text{ inch} \quad [15]$$

where:

$$W = 2 \times 88.55 \text{ kip} = 177,100 \text{ lb} \text{ ----- Anchor load}$$
$$\phi = 0.85 \text{ ----- Shear factor}$$
$$f_c = 3800 \text{ psi} \text{ ----- Concrete Strength, } 300^{\circ}\text{F}$$
$$P = 39.6 \text{ inch} \text{ ----- Perimeter of bottom plate}$$

Excluding the bottom anchor plate, the length of the anchor is 65.5 inch; therefore, the factor of safety (FS) is as follows.

$$FS = \frac{65.5}{42.7} = 1.53$$

Lift Pin

The lift pin allowable ultimate shear load (P_{usp}) for the symmetrical joint is the double shear strength of the pin.

$$P_{usp} = 1.571 D_p^2 F_{sup} = 678.6 \text{ kip} \quad [10]$$

where:

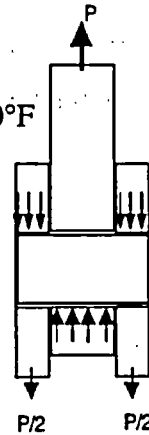
$$D_p = 4.0 \text{ inch} \text{ ----- Pin diameter}$$

$$F_{sup} = 0.6S_m = 0.6 \times 45.0 \text{ ksi} = 27 \text{ ksi}$$

$$S_m = 45.0 \text{ ksi} \text{ ----- 17-4PH stainless steel, at } 200^\circ\text{F}$$

The load on the pin is twice the lift lug load (P); therefore, the factor of safety (FS) for the pin is as follows.

$$FS = \frac{P_{usp}}{2 \times P} = \frac{678.6}{2 \times 88.55} = 3.83 > 3.0$$



Lift Lug Bolt

The eight bolts that attach each set of the lift lugs to the embedded anchor are in tension. The tensile load is the combination of axial loads and the prying action of the lug fitting. The load per bolt (P_t) is as follows.

$$P_t = \frac{W_1}{8} = \frac{177.1}{8} = 22.1 \text{ kip}$$

where:

$$W_1 = 2 \times 88.55 = 177.1 \text{ kip} \text{ ----- Anchor Load}$$

The tensile load (Q) on the bolt due to prying is calculated to be 2.4 kip [11]

The total load on the bolt (T) is as follows.

$$T = P_t + Q = 22.1 + 2.4 = 24.5 \text{ kip}$$

The allowable bolt tensile load is as follows.

$$T_{all} = \frac{\pi D^2 F_y}{4} = \frac{\pi \times 1.25^2 \times 144.0}{4} = 176.7 \text{ kip}$$

where:

$$F_y = 144.0 \text{ ksi} \text{ ----- Yield Strength, SB637 Grade N07718 Nickel alloy steel, at } 200^\circ\text{F}$$

The factor of safety (FS) is as follows.

$$FS = \frac{176.7}{24.5} = 7.2$$

The bolts are threaded into the top plate of the lift anchor. The plate material is A537 Class 2 carbon steel. The bolt material is SB637 Grade N07718 nickel alloy steel. Bolt threads are 1 1/4-7 UNC 2A. For mating internal and external threads of materials having equal tensile strength, the length of engagement (L_e) is calculated as shown in the following.

$$L_e = \frac{2A_t}{3.1416(K_{n_{max}}) \left[\frac{1}{2} + 0.57735(n)(E_{s_{min}} - K_{n_{max}}) \right]} = 0.90 \text{ inch [12]}$$

where:

$$A_t = \pi \left(\frac{E_{s_{min}}}{2} - \frac{0.16238}{n} \right)^2 = 0.952 \text{ inch}^2 \text{ ---Tensile area of 1 1/4-7 UNC 2A}$$

Since the bolt and plate materials are different, the required length of engagement (Q) is calculated to be as follows.

$$Q = L_e J = 0.9 \times 1.59 = 1.43$$

where:

$$J = \frac{A_s \times S_{u \text{ bolt}}}{A_n \times S_{u \text{ plate}}} = 1.59 > 1.0$$

Su bolt = 177.6 ksi -----Ultimate Strength, SB-637 Grade N07718 nickel alloy steel, at 200°F

Su plate = 80.0 ksi -----Ultimate Strength, A-537 Class 2 carbon steel, at 200°F

The bolt thread length is 2.0 inch; therefore, the factor of safety (FS) is as follows.

$$FS = \frac{2.0}{1.43} = 1.40$$

Concrete Cask Lid Assembly Lift

The lid assembly of the concrete cask is lifted using three 3/4-10 UNC 2A threaded bolts with a 3/4-inch thread engagement in the A36 carbon steel lid. A weight of 5,000 lb is conservatively used for the evaluation of the cask lid assembly lift, which bounds the maximum weight of the lid assembly. The load per bolt (P), including dynamic load factor of 10%, is as follows.

$$P = \frac{5,000 \times 1.1}{3} = 1,834 \text{ lb}$$

The required length of engagement is calculated to be as shown in the following.

$$L_e = \frac{2A_t}{3.1416(K_{n\max}) \left[\frac{1}{2} + 0.57735(n)(E_{s\min} - K_{n\max}) \right]} = 0.54 \text{ inch [12]}$$

The factor of safety (FS) is as follows.

$$FS = \frac{0.75}{0.54} = 1.39$$

Pedestal Structural Evaluation

This section presents the structural evaluation of the pedestal during a concrete cask top-end lift. The ANSYS finite element model, presented in Appendix 3.D, is used to evaluate the concrete cask pedestal. The critical loading is during the concrete cask lift operations using the concrete cask lift anchors mounted on top of the concrete cask body.

Component Stresses:

From the finite element model, the maximum stresses in the pedestal stand occur in the support rails. The critical section is the unsupported region between the pedestal stand and the inlet top. The maximum membrane stress is 16.7 ksi. The maximum membrane plus bending stress is 25.3 ksi. The factors of safety are shown as follows.

Membrane

$$FS = \frac{S_m}{\sigma_m} = \frac{19.3}{16.7} = 1.16$$

Membrane plus Bending

$$FS = \frac{1.5S_m}{\sigma_{m+b}} = \frac{28.95}{25.3} = 1.14$$

where:

$$S_m = 19.3 \text{ ksi} \text{ ----- Design Stress Intensity, A-36 Carbon Steel, at 300°F}$$

Pedestal Welds

The pedestal is a welded assembly. The structural welds in the pedestal are evaluated using an allowable stress of $0.6S_m$. The weld forces (F_x , F_y , and F_z) are obtained from the pedestal finite element analysis results. The total weld load (F_w) is obtained by using the square root of the sum of the squares method of the weld forces.

Support Rail to Inlet Top Weld

The support rails are welded to the inlet top with a $\frac{5}{8}$ -inch fillet weld. The stress in the weld (σ) is as follows.

$$\sigma = \frac{F_w}{A} = 9.1 \text{ ksi}$$

where:

- $F_w = 36,077 \text{ lb}$ -----Total weld load
- $F_x = 3,248 \text{ lb}$ -----Weld force, X-direction
- $F_y = 32,351 \text{ lb}$ -----Weld force, Y-direction
- $F_z = -15,633 \text{ lb}$ -----Weld force, Z-direction
- $A = 3.95 \text{ inch}^2$ -----Area
- $l_w = 8.95 \text{ inch}$ -----Weld length
- $t_w = \frac{5}{8}\text{-inch}$ -----Weld size

The factor of Safety (FS) is as follows.

$$FS = \frac{0.6S_m}{\sigma} = 1.27$$

where:

- $S_m = 19.3 \text{ ksi}$ -----Design Stress Intensity, A-36 Carbon Steel, 300°F

Inlet Top to Inlet Side Weld

The inlet top is welded to the inlet side with a $\frac{1}{8}$ -inch fillet weld plus a $\frac{1}{4}$ -inch groove weld. The stress in the weld is as follows.

$$\sigma = \frac{F_w}{A} = \frac{34,099}{8.03} = 4.2 \text{ ksi}$$

where:

$$\begin{aligned}
 F_w &= 34,099 \text{ lb} \text{-----Total weld load} \\
 F_x &= 10,437 \text{ lb} \text{-----Weld force, X-direction} \\
 F_y &= -32,351 \text{ lb} \text{-----Weld force, Y-direction} \\
 F_z &= -2,685 \text{ lb} \text{-----Weld force, Z-direction} \\
 A &= l_w \times t_w = 8.03 \text{ inch}^2 \text{-----Area} \\
 l_w &= 30.9 \text{ inch} \text{-----Weld length} \\
 t_w &= ((0.125 + 0.25) \times .707) = 0.26 \text{ inch} \text{-----Weld size}
 \end{aligned}$$

The factor of Safety (FS) is as follows.

$$FS = \frac{0.6S_m}{\sigma} = \frac{0.6 \times 19.3}{4.2} = 2.76$$

where:

$$S_m = 19.3 \text{ ksi} \text{-----Design Stress Intensity, A-36 Carbon Steel, at } 300^\circ\text{F}$$

Inlet Side to Base Plate Weld

The critical section of the inlet side to base plate weld is the 8.25-inch segment at the inner end of the inlet. The weld is a 1/4-inch groove weld. The stress in the weld is as follows.

$$\sigma = \frac{F_w}{A} = 9.9 \text{ ksi}$$

where:

$$\begin{aligned}
 F_w &= \sqrt{F_x^2 + F_y^2 + F_z^2} = 20,484 \text{ lb} \\
 F_x &= 270 \text{ lb} \text{-----Weld force, X-direction} \\
 F_y &= 20,459 \text{ lb} \text{-----Weld force, Y-direction} \\
 F_z &= -971 \text{ lb} \text{-----Weld force, Z-direction} \\
 A &= l_w \times t_w = 2.06 \text{ inch}^2 \\
 l_w &= 8.25 \text{ inch} \text{-----Weld length} \\
 t_w &= 0.25 \text{ inch} \text{-----Weld size}
 \end{aligned}$$

The factor of safety (FS) is as follows.

$$FS = \frac{0.6S_m}{\sigma} = \frac{0.6 \times 19.3}{9.9} = 1.17$$

where:

$$S_m = 19.3 \text{ ksi} \text{-----Design Stress Intensity, A-36 Carbon Steel, at 300°F}$$

Support Rail Gusset to Support Rail Weld

The rail gusset weld is a 3/8-inch fillet weld. The stress in the weld is as follows.

$$\sigma = \frac{F_w}{A} = 2.5 \text{ ksi}$$

where:

$$F_w = \sqrt{F_x^2 + F_y^2 + F_z^2} = 4,915 \text{ lb}$$

$$F_x = 2,224 \text{ lb} \text{-----Weld force, X-direction}$$

$$F_y = -1,636 \text{ lb} \text{-----Weld force, Y-direction}$$

$$F_z = -4,066 \text{ lb} \text{-----Weld force, Z-direction}$$

$$A = l_w \times (t_w \times 0.707) = 1.97 \text{ inch}^2$$

$$l_w = 4.45 \text{ inch} \text{-----Weld length}$$

$$t_w = 3/8\text{-inch} \text{-----Weld size}$$

The factor of safety (FS) is as follows.

$$FS = \frac{0.6S_m}{\sigma} = 4.63$$

where:

$$S_m = 19.3 \text{ ksi} \text{-----Design Stress Intensity, A-36 Carbon Steel, at 300°F}$$

Nelson Studs

During a top-end concrete cask lift, the Nelson studs transmit the weight of a loaded TSC to the concrete cask. The liner is not directly attached to the pedestal. The ability of the Nelson studs to transfer load to the concrete cask is based upon the compressive strength of the concrete.

Using ACI-349-85 [15], the maximum pullout strength of the concrete is defined by the equation

$$P_d = 4 \times \phi \times \sqrt{f'_c} \times A_{cd}$$

where:

$$\begin{aligned}\phi &= 0.85 \text{-----Strength reduction factor} \\ f_c &= 3,800 \text{ psi -----Concrete compression strength, } 300^\circ\text{F} \\ A_{cd} &= \text{Projected cone area of Nelson stud less head area}\end{aligned}$$

The projected area of a single Nelson stud is calculated by creating a cone that projects 45° from the head of the Nelson stud and omits the projected area of the Nelson stud head.

For a 0.75-inch diameter, 6.0-inch long Nelson stud, the projected area is as follows.

$$A_{cd} = \pi(l_c(l_c + d_h)) = 116.6 \text{ inch}^2$$

where:

$$\begin{aligned}l_c &= 5.5 \text{ inch -----Bolt length} \\ d_h &= 1.25 \text{ inch -----Head diameter}\end{aligned}$$

For a single Nelson stud the allowable concrete pullout strength is as follows.

$$P_d = 4 \times 0.85 \times \sqrt{3800} \times 116.6 = 24,438 \text{ lb}$$

The maximum load on a Nelson stud is 17,145 lb; therefore, the factor of safety (FS) is as follows.

$$FS = \frac{P_d}{F} = \frac{24,438}{17,145} = 1.43$$

The geometry of the four Nelson studs on the inlet top plate is such that the projected cones intersect each other. The combined projected area (A_{cd}) is 332 inch^2 . The total load on the four Nelson studs is 18,817 pounds. The allowable concrete pullout strength (P_{cd}) is as follows.

$$P_{cd} = 4 \times 0.85 \times \sqrt{3800} \times 332.0 = 69,584 \text{ lb}$$

The factor of safety (FS) is as follows.

$$FS = \frac{P_{cd}}{F} = \frac{69,584}{18,817} = 3.70$$

The maximum stress in a Nelson stud is as follows.

$$\sigma = \frac{F}{A_s} = 39.0 \text{ ksi}$$

where:

$$A_s = \frac{\pi}{4} D^2 = 0.44 \text{ inch}^2$$

The factor of safety (FS) is as follows.

$$FS = \frac{S_u}{\sigma} = \frac{58.0}{39.0} = 1.49$$

where:

$$S_u = 58.0 \text{ ksi} \text{ ----- Ultimate Strength, A-36 Carbon Steel, at } 300^\circ\text{F}$$

3.4.3.2 TSC Lift

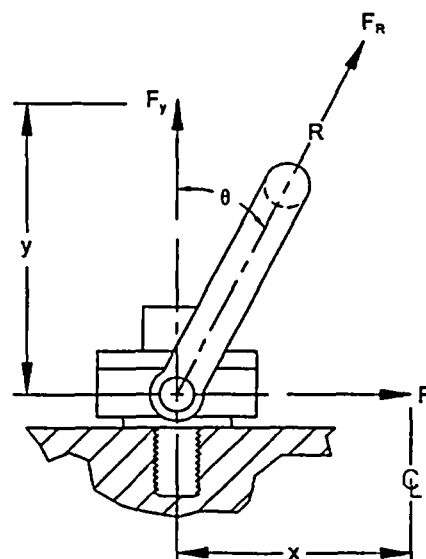
The adequacy of the TSC lifting components is demonstrated by evaluating the hoist rings, the TSC closure lid, and the weld that joins the closure lid to the TSC shell against the criteria in NUREG-0612 [3] and ANSI N14.6 [2]. The lifting configuration for the TSC consists of six hoist rings threaded into the closure lid assembly at equally spaced angular intervals. The hoist rings are analyzed as a redundant system with two three-legged lifting slings. For redundant lifting systems, ANSI N14.6 requires that load-bearing members be capable of lifting three times the load without exceeding the yield strength of the material and five times the load without exceeding the ultimate strength of the material. The closure lid is evaluated for lift conditions as a redundant system that demonstrates a factor of safety greater than three based on yield strength and a factor of safety greater than five based on ultimate strength. The TSC lift analysis is based on a load of 120,000 lb, which bounds the weight of the heaviest loaded TSC configuration. A dynamic load factor of 10% is considered in the analysis.

Hoist Ring and Sling Evaluation

The TSC lift configuration is shown in the accompanying sketch. The vertical component force on the hoist ring, assuming a 10% dynamic load factor, is as follows.

$$F_y = \frac{120,000 \text{ lb} \times 1.1}{3 \text{ lift points}} = 44,000 \text{ lb}$$

As shown in the sketch, x is the distance from the TSC centerline to the hoist ring centerline (20.5 inch); F_x is the



horizontal component of force on the hoist ring; R is the sling length; F_R is the maximum allowable force on the hoist ring; and, the angle θ is the angle from vertical to the sling.

The hoist rings are rated at 50,000 lb with a safety factor of five on ultimate strength. Calculating the maximum angle (θ) that will limit F_R to 50,000 pounds.

$$\theta = \cos^{-1}\left(\frac{F_y}{F_R}\right) = \cos^{-1}\left(\frac{44,000}{50,000}\right) = 28.4^\circ$$

The minimum sling length, R , is as follows.

$$R = \frac{x}{\sin \theta} = \frac{20.5}{\sin 28.4} = 43.1 \text{ inch}$$

A 50-inch sling places the lift hook about 44 inch above the top of the TSC ($y = R \cos \theta = 50 \cos 28.4^\circ = 44$ inch).

Bolt Shear

From the Machinery's Handbook [12], the shear stress (τ) in the hoist ring hole threads (2½-4-UNC) in the closure lid is calculated as follows.

$$\tau = \frac{F_y}{A_n} = \frac{44,000 \text{ lb}}{12.148 \text{ in}^2} = 3,622 \text{ psi}$$

where:

$$A_n = 12.148 \text{ inch}^2 \text{-----Shear area of the closure lid assembly threads based on a length of engagement of 2.0 inches.}$$

The TSC closure lid is constructed of SA240, Type 304 stainless steel. Using shear allowables of $0.6 S_y$ and $0.5 S_u$ at a temperature of 300°F, the shear stress factors of safety are as follows.

Yield:

$$FS_y = \frac{0.6 \times 22,400 \text{ psi}}{3,622 \text{ psi}} = 3.7 > 3$$

Ultimate:

$$FS_u = \frac{0.5 \times 66,200 \text{ psi}}{3,622 \text{ psi}} = 9.1 > 5$$

The criteria of NUREG-0612 and ANSI N14.6 for redundant systems are met and the minimum thread engagement length of 2.0-inch is adequate.

The weight of the heaviest loaded transfer cask is less than 230,000 pounds. Three times the bounding weight of the loaded TSC is (3 × 120,000) 360,000 lb, which is greater than the weight of the heaviest transfer cask plus the weight of the loaded TSC (108,500 + 102,500 lb). Consequently, the preceding analysis bounds the inadvertent lift of the transfer cask during the handling of the TSC.

TSC Lift Evaluation

The structural adequacy of the TSC closure lid assembly and weld is evaluated using a finite element model described in Appendix 3.C. During a TSC lift, the acceleration due to gravity, with a dynamic load factor of 10%, is applied to the fully loaded TSC in the vertical direction. The maximum nodal stress intensity experienced by the various TSC components during a three-point lift is as follows.

Component Description	Nodal Stress (psi)
TSC Shell (inner surface of shell below closure lid weld)	2,198
Closure Lid Weld	1,980

The TSC shell and closure lid are constructed of SA240, Type 304 stainless steel. The yield strength is 18,000 psi and the ultimate strength is 63,400 psi. These are conservatively evaluated at a temperature of 650°F. The strength of the weld joint is taken as the same as the strength of the base material. Thus, when compared to the yield and ultimate strengths, the maximum nodal stress intensity of 2,198 psi produces the following factors of safety for a three-point lift.

Yield:

$$FS_y = \frac{\text{yield strength}}{\text{maximum nodal stress intensity}} = \frac{18,000 \text{ psi}}{2,198 \text{ psi}} = 8.2 > 3$$

Ultimate:

$$FS_u = \frac{\text{ultimate strength}}{\text{maximum nodal stress intensity}} = \frac{63,400 \text{ psi}}{2,198 \text{ psi}} = 28.8 > 5$$

The criteria of NUREG-0612 and ANSI N14.6 for nonredundant systems are met. Thus, the TSC shell and closure lid are adequate.

3.4.3.3 Transfer Cask Lift

The MAGNASTOR transfer cask is analyzed for loads associated with the heavy lift requirements specified in ANSI N14.6 [2] and NUREG-0612 [3]. All load path components of the cask are evaluated for structural adequacy. The transfer cask is analyzed for loads associated with the vertical lift of the transfer cask. The transfer cask is not designed for redundant lifting; therefore, factors of safety of six on material yield strength and ten on material ultimate strength are required for the lifting trunnions.

The analysis of the fully loaded transfer cask consists of a finite element analysis using the ANSYS program to calculate the stress in the transfer cask forgings, shells, and the trunnion region for the operational vertical lift condition. Details of the ANSYS finite element model are presented in Appendix 3.E. The structural evaluations of the rail, the shield door, and the rail welds are performed using standard engineering equations. The design weight of the transfer cask is 230,000 pounds. A bounding weight of the transfer cask of 240,000 lb is considered in the evaluation. A conservative load of 264,000 lb ($240,000 \times 1.1$ dynamic load factor) is used in the finite element analysis.

Transfer Cask Body

Table 3.4-1 provides the summaries of the stress intensities for the seven cross-sectional locations of the trunnion and top ring. Table 3.4-2 provides the stress summaries for the inner and outer shells and bottom ring. The maximum primary membrane, P_m , and the maximum primary membrane plus bending stress, $P_m + P_b$, is compared with the allowable stress criteria.

The cross-section of the trunnion is circular. Two cross-sectional areas are examined as shown in Figure 3.4-1. The maximum bending stress occurs at the cross-section ($x = 43.9$ inch) at the intersection of the trunnions with the outer diameter of the top-forging ring. The maximum stress occurs at the trunnion surface. The maximum stress in the trunnion is 3.8 ksi. Comparing the stress to the material (A350 Grade LF 2) allowable yield and ultimate strength, the factors of safety are 8.1(>6) for material yield strength and 18.5 (>10) for material ultimate strength.

For the top ring, the five cross-sectional areas selected for stress examination are shown in Figure 3.4-1. The maximum bending plus membrane stress occurs at the radial cross-section (topring-A1) above the trunnion. The bending stress through this cross-sectional area is 4.9 ksi. Comparing the stress to the material (A516 Gr 70) allowable yield and ultimate strength, the factors of safety are 6.6 (>6) and 14.2 (>10) for yield and ultimate material strengths, respectively.

For the inner shell, the maximum stress intensity occurs at the location of " $\theta = 10^\circ$, $z = -7.0$ inch", which is outside the inter-section just below the trunnion. The maximum bending plus membrane stress is through the shell is 2.3 ksi. Comparing the stress to the material (A588) allowable yield and ultimate strengths, the factors of safety are 18.6 (>6) and 30.2 (>10), respectively.

For the outer shell, the maximum stress intensity occurs at the location of " $\theta = 10^\circ$, $z = -7.0$ inch", which is outside the intersection just below the trunnion. The maximum bending plus membrane stress is the shell thickness is 3.5 ksi. Comparing the stress to the material (A588) allowable yield and ultimate strengths, the factors of safety are 12.3 (>6) and 20 (>10), respectively.

For the bottom ring the maximum stress intensity occurs at the nodal location of " $\theta = 90^\circ$, $z = -173.5$ inch", which is just below the inner and outer shells. The maximum bending plus membrane stress is the ring thickness is 0.7 ksi. Comparing the stress to the material (A588) allowable yield and ultimate strengths, the factors of safety are 58 (>6) and 94 (>10) for yield and ultimate strength, respectively.

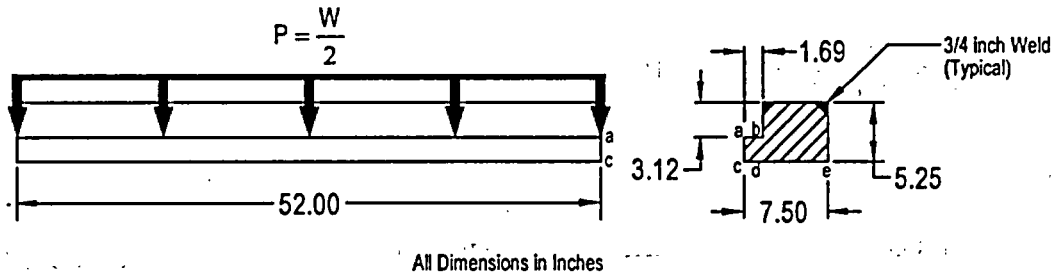
Transfer Cask Shield Door Rails and Welds

This section demonstrates the adequacy of the transfer cask shield doors, door rails, and welds in accordance with NUREG-0612 and ANSI N14.6, which require safety factors of six and ten on material yield strength and ultimate strength, respectively, for nonredundant lift systems. The transfer cask shield doors and door rails are designed to retain and support the maximum loaded TSC weight of 118,000 lb, which includes the weight of basket, fuel, and water. The shield doors are 5-inch thick plates that slide on the door rails. The rails are 7.50 inch wide \times 52 inch long and are welded to the bottom ring of the transfer cask. The doors and the rails are constructed of A-588 and SA-350 Grade LF 2 low alloy steel, respectively.

A weight of 143,000 pounds ($>118,000 \times 1.1$) is conservatively used for the evaluation of the rails. This weight bounds the weight of the heaviest loaded TSC, the weight of the water in the TSC, and the weight of the shield doors and rails. The 10% dynamic load factor is included to ensure that the evaluation bounds all normal operating conditions. Allowable stresses for the component materials are taken at 400°F, which bounds the maximum temperature at the bottom of the transfer cask under normal conditions.

Stress Evaluation for Door Rail

Each rail is assumed to carry one half of the load.



The shear stress (τ) in each door rail bottom plate (section b-d) due to the applied load is as follows.

$$\tau = \frac{P}{A} = \frac{143.0/2}{110.8} = 0.65 \text{ ksi}$$

where:

$$A = (5.25 - 3.12) \times 52 = 110.8 \text{ inch}^2 \text{ -----Shear area}$$

The bending stress (σ_b) in each rail bottom section b-d due to the applied load, P, is as follows.

$$\sigma_b = \frac{6M}{L t_{a-c}^2} = 3.1 \text{ ksi}$$

where:

- $M = P \times L_{a-b} = 120.8 \text{ inch-kip}$
- $L_{a-b} = 1.69 \text{ inch}$ -----Applied load moment arm
- $L = 52 \text{ inch}$ -----Length of the rail
- $t_{a-c} = 2.13 \text{ inch}$ -----Thickness of the rail

The maximum stress (σ) intensity in the bottom section of the rail is as follows.

$$\sigma = \sqrt{(\sigma_b)^2 + 4\tau^2} = 3.4 \text{ ksi}$$

The factor of safety (FS) based on the material yield strength is as follows.

$$FS = \frac{S_y}{\sigma} = \frac{30.8 \text{ ksi}}{3.4 \text{ ksi}} = 9.1 > 6$$

where:

$$S_y = 30.8 \text{ ksi} \text{-----Yield strength for A350 Grade LF 2, at } 400^\circ\text{F}$$

The factor of safety (FS) based on the material ultimate strength is as follows.

$$FS = \frac{S_u}{\sigma} = \frac{70 \text{ ksi}}{3.4 \text{ ksi}} = 20.6 > 10$$

where:

$$S_u = 70.0 \text{ ksi} \text{-----Ultimate strength A-350 Grade LF 2, at } 400^\circ\text{F}$$

Stress Evaluation for the Shield Doors

The shield doors are 5 inch thick at the center and step down to 2.94 inch thick at the edges, where they rest on the rails. The stepped edges of the two door leaves are designed to interlock at the center. Therefore, the doors are analyzed as single simply supported plates. The engagement length of the door with the rail is 52 inches. The shear stress (τ) at the edge of the shield door where the door contacts the rail is as follows.

$$\tau = \frac{P}{A_s} = 0.94 \text{ ksi}$$

where:

$$A_s = t_d \times L = 152.9 \text{ inch}^2 \text{-----Total shear area}$$

$$t_d = 5.0 - 2.06 = 2.94 \text{ inch} \text{-----Thickness of the door at edge}$$

$$L = 52 \text{ inch} \text{-----Length of door and rail engagement}$$

The maximum bending stress (σ_b) at the center of the doors, is as follows.

$$\sigma_b = \frac{Mc}{I} = 4.0 \text{ ksi}$$

where:

$$M = \frac{WL}{8} = 1.36 \times 10^6 \text{ inch-lb}$$

$$W = 143,000 \text{ lb} \text{-----Total weight}$$

$$c = \frac{h}{2} = 2.5 \text{-----Distance to surface}$$

$$I = \frac{bh^3}{12} = 855 \text{ inch}^4 \text{-----Cross-sectional moment of inertia}$$

$$L = 76 \text{ inch} \text{-----Span length}$$

The maximum stress intensity (σ) in the door is as follows.

$$\sigma = \sqrt{(\sigma_b)^2 + 4\tau^2} = 4.1 \text{ ksi}$$

The factor of safety (FS) based on the yield strength is as follows.

$$FS = \frac{S_y}{\sigma} = \frac{43 \text{ ksi}}{4.1 \text{ ksi}} = 10.5 > 6$$

where:

$$S_y = 43 \text{ ksi} \text{-----Yield strength for A-588, at } 400^\circ\text{F}$$

The factor of safety (FS) based on the ultimate strength is as follows.

$$FS = \frac{S_u}{\sigma} = \frac{70 \text{ ksi}}{4.1 \text{ ksi}} = 17.1 > 10$$

where:

$$S_u = 70.0 \text{ ksi} \text{-----Ultimate strength for A-588, at } 400^\circ\text{F}$$

Door Rail Weld Evaluation

The door rails are attached to the bottom forging of the transfer cask by 0.75-inch partial penetration bevel groove welds that extend the full length of the inside and outside of each rail. The loaded TSC weight is conservatively assumed to act at a point on the inside edge of the rail. Since the base metal is the limiting strength of the welded section, the ultimate strength on the inner weld is evaluated. Summing moments about the edge of outer weld are as follows.

$$\Sigma M = 0 = P \times L_{c-c} - F_w \times \left(L_{d-e} - \frac{L_w}{2} \right) \Rightarrow F_w = 91 \text{ kip}$$

where:

$$P = \frac{W}{2} = 71.5 \text{ kip} \text{-----Load on a single rail}$$

$$L_w = 0.75 \text{ inch} \text{-----Weld length}$$

$$L_{d-e} = 7.5 - 1.69 = 5.81 \text{-----Distance from edge of inner weld to edge of outer weld}$$

$$L_{c-c} = 7.5 \text{ inch} \text{-----Width of the rail}$$

The maximum stress (σ) in the base metal attached by the inner weld is as follows.

$$\sigma = \frac{F_w}{A_w} = 2.3 \text{ ksi}$$

where:

$$A_w = 0.75 \times 52 = 39 \text{ inch}^2 \text{ -----Area on the base metal supporting inner weld}$$

The factor of safety (FS) based on the yield strength is as follows.

$$FS = \frac{43 \text{ ksi}}{2.3 \text{ ksi}} = 18.7 > 6$$

The factor of safety (FS) based on the ultimate strength is as follows.

$$FS = \frac{70 \text{ ksi}}{2.3 \text{ ksi}} = 30.4 > 10$$

Trunnion Bearing Stress Evaluation

During a vertical lifting load case, the transfer cask is being lifted by the trunnions.

The load on each trunnion is 132 kips ($240 \times 1.1/2$). The minimum trunnion bearing engagement depth is 7.5-inch, but only 50% of this is used in the evaluation. The diameter of the trunnion is 9-inch. The bearing stress on the trunnion (σ_b) is as follows.

$$\sigma_{brg} = \frac{W_{vt}}{A_{brg}} = \frac{132}{33.75} = 3.92 \text{ ksi}$$

The factor of safety (FS) is as follows.

$$FS = \frac{S_y}{\sigma} = \frac{30.8}{3.92} = 7.85$$

where:

$$S_y = 30.8 \text{ ksi -----Yield strength, SA-350 LF2, at 400°F}$$

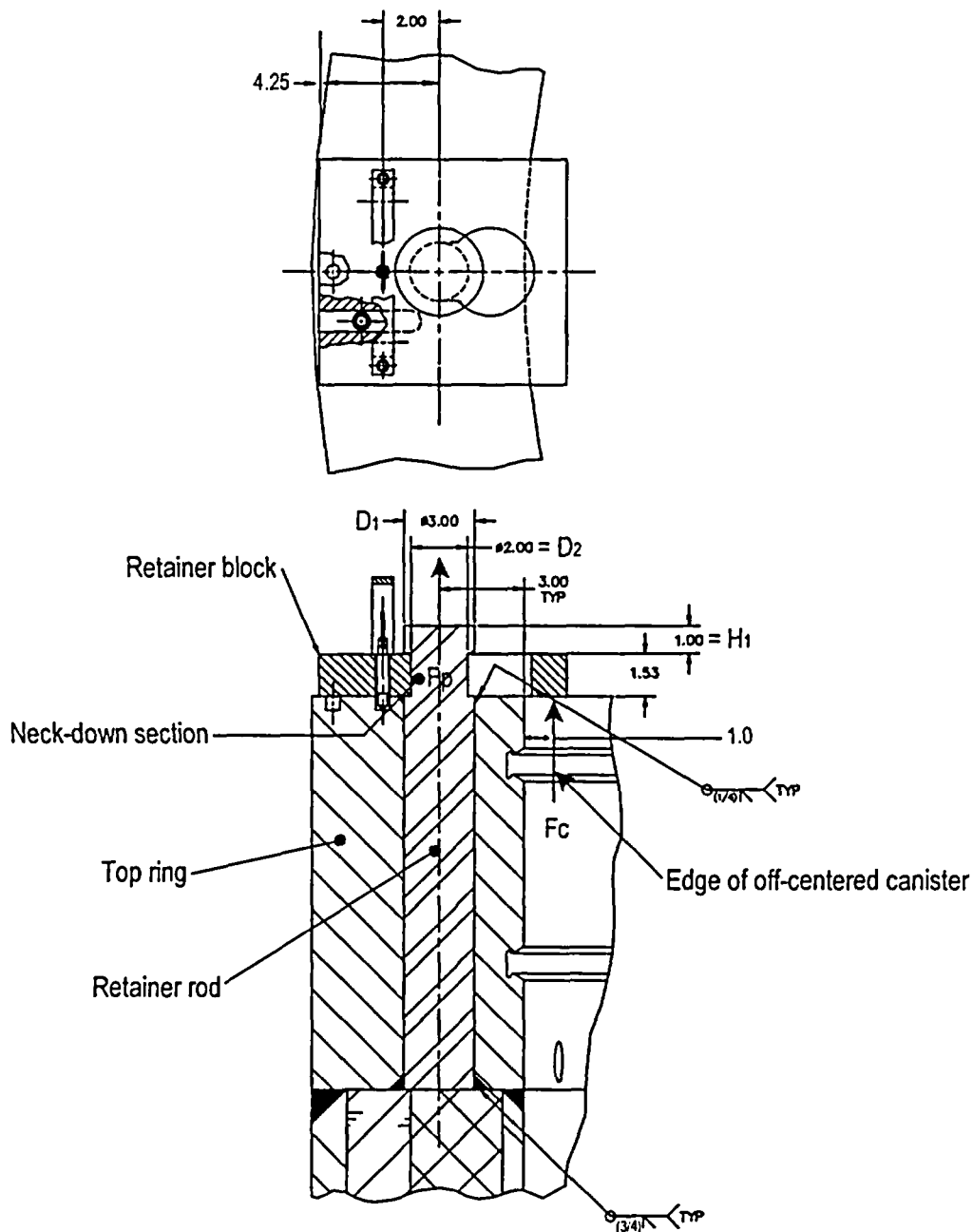
Inadvertent Lift of Transfer Cask by TSC

The inadvertent lift of the transfer cask by the TSC is considered an off-normal event. The stresses associated with this condition are required to satisfy allowable stress limits for ASME Boiler and Pressure Vessel Code, Service Level C condition. The temperature of the cask at the top is assumed to be 300°F.

In the event the transfer cask is lifted by the TSC during handling operations, instead of by the transfer cask trunnions, the weight of the transfer cask is supported by the three retaining blocks mounted on top of the transfer cask top ring. In this case, the retaining blocks must have sufficient strength to support the weight of the transfer cask. The three retaining blocks on the top-forging ring are spaced 120° apart.

Retainer Rod Evaluation

During an inadvertent lift of the transfer cask, the retainer rod is subjected to a tensile load, F_P , due to the prying action of the retaining block. The top view and the side view of the retaining block are shown in the following sketches.



A conservative weight of 110,000 lb is used for this evaluation. This weight bounds the maximum weight of the transfer cask. The dynamic load factor, DLF, is 1.1. The maximum uplifting force applied by the TSC to the retainer block, F_c , is 110 kip $(1.1)/3 = 40.3$ kip. When the TSC is off-center, the maximum distance between the TSC outer edge and the inner edge of the transfer cask is one inch. The prying force applied to the retainer rod (F_p) is as follows.

$$F_p = \frac{40.3 \times (1 + 3 + 4.25)}{4.25} = 78.2 \text{ kip}$$

Effective Stress Areas of Retainer Rod

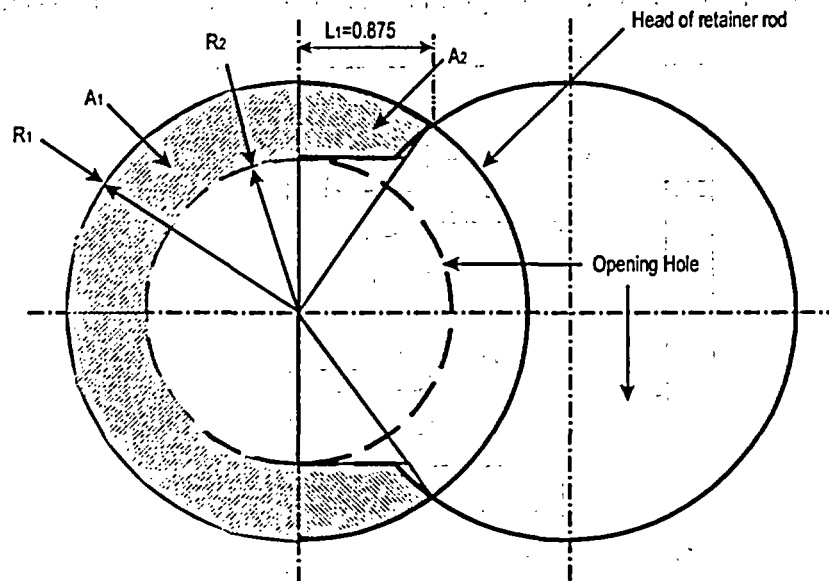
Referring to the previous sketch, the cross-sectional areas for the retainer rod evaluation is as follows.

$$A_t = \frac{\pi}{4} D_2^2 = 3.14 \text{ inch}^2 \text{-----Tensile area (neck down area)}$$

$$A_{ws} = \pi D_1 H_w = 7.07 \text{ inch}^2 \text{-----Weld shear area}$$

$$A_{sh} = \pi D_2 H_1 = 6.28 \text{ inch}^2 \text{-----Head shear area (through head thickness)}$$

The bearing area in the retainer rod just above the neck-down area is the hatched area as shown in the following.



The total bearing area (A_{brg}) is as follows.

$$A_{brg} = 2(A_1 + A_2) = 2(0.982 + 0.342) = 2.648 \text{ inch}^2$$

Retainer Rod Load Capacity:

The load capabilities of the retainer rod are calculated in the following.

- $F_{tensile} = (A_t)(SM) = (3.14)(26.9) = 84.4 \text{ kip}$ -----Load capability at D2
- $F_{ws} = (A_{ws})(S_s) = (7.07)(13.4) = 94.7 \text{ kip}$ -----Shear capability of weld
- $F_{brg} = (A_{brg})(S_{brg}) = (2.648)(33.6) = 88.9 \text{ kip}$ -----Bearing capability of rod head
- $F_{sh} = (A_{sh})(S_s) = (6.28)(13.4) = 84.2 \text{ kip}$ -----Shear capability under rod head

where:

$$S_M = 1.2 S_m = 1.2 (22.4) = 26.9 \text{ ksi}$$

$$S_S = 0.6 S_m = 0.6 (22.4) = 13.4 \text{ ksi}$$

$$S_{brg} = S_y = 33.6 \text{ ksi}$$

$$S_y = 33.6 \text{ ksi} \text{ ----- Yield Strength, SA-516 Grade 70 at } 300^\circ\text{F}$$

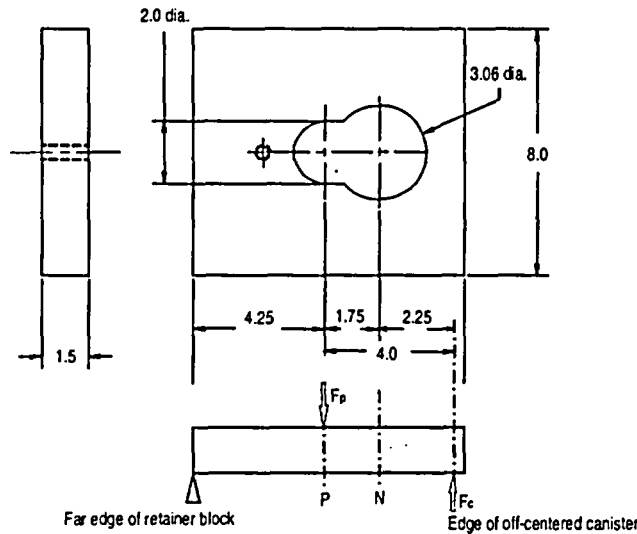
$$S_m = 22.4 \text{ ksi} \text{ ----- Design Stress Intensity, SA-516 Grade 70 at } 300^\circ\text{F}$$

The minimum factor of safety (FS) is as follows.

$$FS = \frac{F_{sh}}{F_p} = \frac{84.2}{78.2} = 1.08$$

Retainer Block Evaluation

The retainer block and the force-loading diagram are shown in the following sketch.



Point P is where the headed retainer rod is loaded under prying force F_p . The maximum bending stress (σ_b) in the retainer block is as follows.

$$\sigma_b = \frac{Mc}{I} = 71.6 \text{ ksi}$$

where:

$$M = F_c(4) = 161.2 \text{ kip-inch}$$

$$F_c = 40.3 \text{ kip}$$

$$I = \frac{bh^3}{12} = 1.688 \text{ inch}^4$$

$$C = 0.75 \text{ inch}$$

The factor of safety (FS) is as follows.

$$FS = \frac{1.8S_m}{\sigma_b} = 1.13$$

where:

$$S_m = 45.0 \text{ ksi} \text{ ----- Yield Strength, 17-4 PH at } 300^\circ\text{F}$$

Figure 3.4-1 Top Ring Section Cuts

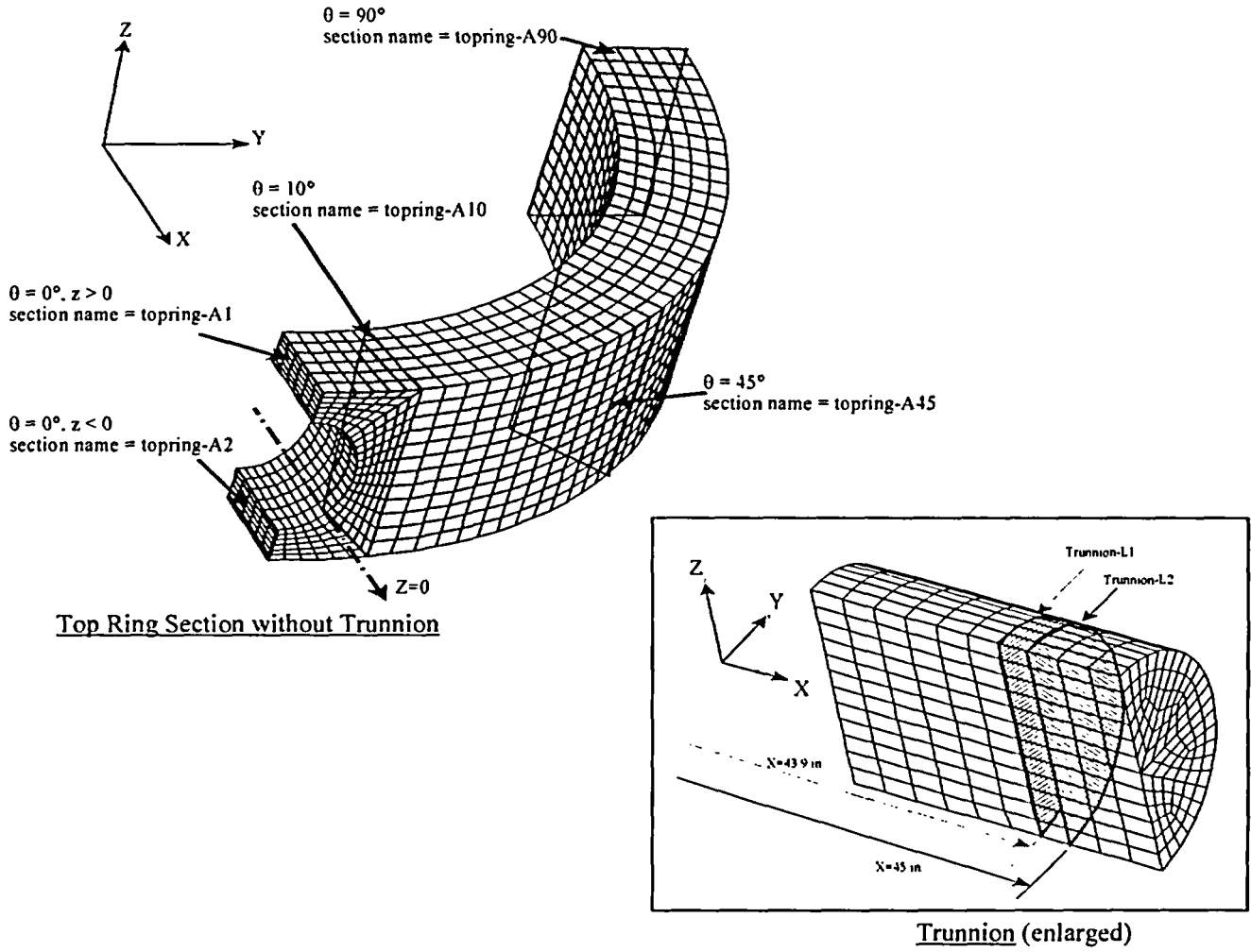


Table 3.4-1 Stresses for Trunnions and Top Ring

Location ^{a)}	Position ^{a)}	P_m ^{b)} ksi	P_b ^{b)} ksi	$P_m + P_b$ ^{b)} ksi	Material	S_{yield} ksi	$S_{ultimate}$ ksi	FS_{Yield}	$FS_{Ultimate}$
Trunnion-L1	$x = 43.9$ inch	0.04	3.75	3.79	SA350	30.8	70.0	8.1	Large
Trunnion-L2	$x = 45$ inch	0.00	2.05	2.05	SA350	30.8	70.0	Large	Large
TopRing-A1	$\theta = 0^\circ, z > 0$	2.37	2.57	4.93	SA516	32.5	70.0	6.6	Large
TopRing-A2	$\theta = 0^\circ, z < 0$	0.33	1.29	1.63	SA516	32.5	70.0	Large	Large
TopRing-A10	$\theta = 10^\circ$	0.07	1.02	1.09	SA516	32.5	70.0	Large	Large
TopRing-A45	$\theta = 45^\circ$	0.11	0.84	0.95	SA516	32.5	70.0	Large	Large
TopRing-A90	$\theta = 90^\circ$	0.11	0.75	0.86	SA516	32.5	70.0	Large	Large

Table 3.4-2 Stresses for Transfer Cask Shells and Bottom Ring

Location ^{c)}	Position ^{c)}	$P_m + P_b$ ^{d)} ksi	Material	S_{yield} ksi	$S_{ultimate}$ ksi	FS_{Yield}	$FS_{Ultimate}$
Inner Shell	$\theta = 10^\circ, z = -7$ inch	2.32	A588	43.0	70.0	Large	Large
Outer Shell	$\theta = 10^\circ, z = -7$ inch	3.50	A588	43.0	70.0	Large	Large
Botm Ring	$\theta = 90^\circ, z = -173.5$	0.74	A588	43.0	70.0	Large	Large

^{a)} The locations and positions are defined in Figure 3.4-1.

^{b)} P_m = primary membrane stress; P_b = primary bending stress; $P_m + P_b$ = primary membrane + bending stress

^{c)} The locations and positions correspond to the axis shown in Figure 3.E-1 Appendix 3.E.

^{d)} $P_m + P_b$ = primary membrane + bending stress

3.5 Normal Operating Conditions

This section presents the analyses of the major structural components of MAGNASTOR for normal conditions of storage. The TSC, fuel baskets, and concrete cask are evaluated using finite element models and classical hand calculations.

3.5.1 TSC Evaluation for Normal Operating Conditions

For normal conditions of storage, the TSC is evaluated using ASME Code, Section III, Subsection NB 'Service Level A' allowable stresses.

3.5.1.1 TSC Thermal Stress Analysis

The thermal stresses in the TSC during normal conditions of storage are evaluated using a finite element model described in Appendix 3.C. The thermal gradient applied to the TSC model bounds all conditions of storage; therefore, the results presented are conservative. The resulting maximum (secondary) thermal stresses in the TSC are shown in Table 3.5-1. The locations of the stress sections are shown in Figure 3.C-2 in Appendix 3.C.

3.5.1.2 TSC Dead Load

The TSC is analyzed for dead load using the finite element model described in Appendix 3.C. The normal handling plus normal pressure conditions presented in Section 3.5.1.5 bound the resulting maximum TSC dead load stresses; therefore, results for the dead load analysis are not presented separately.

3.5.1.3 TSC Maximum Internal Pressure

The TSC is analyzed for a maximum internal pressure load using the finite element model described in Appendix 3.C. A maximum internal pressure of 110 psig is applied as a surface load to the elements along the internal surface of the TSC shell, bottom plate, and closure lid. This pressure bounds the maximum calculated pressure for PWR and BWR fuel under normal conditions.

The resulting maximum internal pressure load stresses for the TSC are summarized in Table 3.5-2 and Table 3.5-3 for primary membrane and primary membrane plus primary bending stress categories, respectively. The locations for the stress sections are shown in Figure 3.C-2 in Appendix 3.C.

3.5.1.4 TSC Handling Loads

The TSC is analyzed for handling loads using the finite element model described in Appendix 3.C. Normal handling is simulated by constraining the model at nodes on the closure lid simulating three lift points. A 1.1g acceleration load, which corresponds to the dead weight with a 10% dynamic load factor, is applied to the model in the axial direction. Pressure is applied to the TSC bottom plate to simulate the weight of the basket and fuel with an acceleration of 1.1g.

The resulting maximum stresses in the TSC due to handling loads are bounded by the maximum stresses for the normal handling loads plus normal pressure condition presented in Section 3.5.1.5; therefore, the stress results for the handling condition are not presented separately.

The lift lugs are evaluated for dead weight using classical methods. The TSC lift lugs are welded to the inner surface of the TSC shell to accommodate handling of the empty TSC and to support the closure lid prior to completion of the weld to the shell. The total weight, W, imposed on the lift lugs conservatively considers the weight of the closure lid and supplemental support equipment. A 10% load factor is also applied to ensure all normal operating loads are bounded. The stresses evaluated for the lift lugs are bearing stress and shear stress through the weld. The bearing stress is as follows.

$$\sigma_{\text{bearing}} = \frac{W}{4A} = \frac{22,550 \text{ lb}}{21.6 \text{ in}^2} = 1,044 \text{ psi}$$

where:

$$W = (10,500 \text{ lb} + 10,000 \text{ lb}) \times 1.1 = 22,550 \text{ lb}$$
$$A = 5.4 \text{ inch}^2 \text{-----Area of lifting lug}$$

Using a conservative temperature of 650°F, the factor of safety (FS) is as follows.

$$FS = \frac{1.0 S_y}{\sigma_{\text{bearing}}} = \frac{19,400 \text{ psi}}{1,044 \text{ psi}} = \text{Large}$$

where:

$$S_y = 19,400 \text{ psi} \text{-----Yield strength of SA-240, Type 304 stainless steel}$$

The attachment weld for the lift lugs is a 1/8-inch double-bevel weld. The shear stress (τ_w) is as follows.

$$\tau_w = \frac{W}{4A_{eff}} = \frac{22,550 \text{ lb}}{5.40 \text{ in}^2} = 4,176 \text{ psi}$$

where:

$$A_{eff} = L_{eff} \times t_{eff} = 1.35 \text{ inch}^2 \text{ ----- Area of lifting lug weld}$$

$$L_{eff} = 5.4 \times = 10.8 \text{ ----- Length of lifting lug weld}$$

$$t_{eff} = 0.125 \text{ inch ----- Thickness of lifting lug weld}$$

Conservatively using the temperature of 650°F and material allowables of the base metal, the factor of safety (FS) is as follows.

$$FS = \frac{S_{allow}}{\tau_w} = \frac{0.6 S_m}{\tau_w} = \frac{9,720 \text{ psi}}{4,176 \text{ psi}} = 2.3$$

where:

$$S_{allow} = 0.6 S_m \text{ ----- Weld allowable}$$

$$S_m = 16,200 \text{ psi ----- Design stress intensity of SA-240, Type 304 stainless steel}$$

3.5.1.5 TSC Load Combinations

The TSC is structurally analyzed for combined thermal, dead, maximum internal pressure, and handling loads using the finite element model described in Appendix 3.C.

The resulting maximum stresses in the TSC for combined loads are summarized in Table 3.5-2, Table 3.5-3, and Table 3.5-4 for primary membrane, primary membrane plus primary bending, and primary plus secondary stresses, respectively. The sectional stresses at 12 locations are evaluated for each angular division of the model (a total of 19 angular locations for each axial location). The locations for the stress sections are shown in Figure 3.C-2, Appendix 3.C.

As shown in Table 3.5-2 through Table 3.5-4, the TSC maintains factors of safety greater than one for the combined load conditions. The minimum factor of safety of 1.37 occurs at Section 11 for the P_m+P_b stresses.

3.5.1.6 TSC Fatigue Evaluation

The purpose of this section is to evaluate whether an analysis for cyclic service is required for the TSC. For the TSC, the requirements for cyclic operation are presented in ASME Code, Section III, Subsection NB, Article NB-3222.4 [6]. The criteria for determining whether cyclic loading

analysis is required are comprised of six conditions, which, if met, preclude the requirement for further analysis.

1. Atmospheric to Service Pressure Cycle
2. Normal Service Pressure Fluctuation
3. Temperature Difference — Startup and Shutdown
4. Temperature Difference — Normal and Off-normal Service
5. Temperature Difference — Dissimilar Materials
6. Mechanical Loads

The evaluation of these conditions is as follows.

Condition 1 — Atmospheric to Service Pressure Cycle

This condition is not applicable. The ASME Code defines a cycle as an excursion from atmospheric pressure to service pressure and back to atmospheric pressure. Once sealed, the TSC remains closed throughout its operational life, and no atmospheric to service pressure cycles occur.

Condition 2 — Normal Service Pressure Fluctuation

This condition is not applicable. The condition establishes a maximum pressure fluctuation as a function of the number of significant pressure fluctuation cycles specified for the component, the design pressure, and the allowable stress intensity of the component material. Operation of the TSC is not cyclic, and no significant cyclic pressure fluctuations are anticipated.

Condition 3 — Temperature Difference — Startup and Shutdown

This condition is not applicable. MAGNASTOR is a passive, long-term storage system that does not experience cyclic startups and shutdowns.

Condition 4 — Temperature Difference — Normal and Off-Normal Service

The ASME Code specifies that temperature excursions are not significant if the change in ΔT between two adjacent points does not experience a cyclic change of more than the quantity:

$$\Delta T = \frac{S_a}{2E\alpha} = 57^\circ\text{F}$$

where: for Type 304 stainless steel,

$S_a = 28,200$ psi -----Value obtained from the fatigue curve for service cycles $< 10^6$

$E = 25.1 \times 10^6$ psi -----Modulus of elasticity at 650 °F

$$\alpha = 9.9 \times 10^{-6} \text{ inch/inch-}^\circ\text{F} \text{ -----Coefficient of thermal expansion at } 650^\circ\text{F}$$

Because of the large thermal mass of the TSC and the concrete cask and the relatively constant heat load produced by the TSC's contents, cyclic changes in ΔT greater than 57°F will not occur.

Condition 5 — Temperature Difference Between Dissimilar Materials

The TSC and its internal components contain several materials. However, the design of all components considers thermal expansion, thus precluding the development of unanalyzed thermal stress concentrations.

Condition 6 — Mechanical Loads

This condition does not apply. Cyclic mechanical loads are not applied to the concrete cask and TSC during storage conditions. Therefore, no further cyclic loading evaluation is required.

The criteria of ASME Code, Section III, Subsections NB, Articles NB-3222.4 and NG-3222.4 are met; therefore fatigue analysis is not required.

3.5.2 Fuel Basket Evaluation for Normal Operating Conditions

3.5.2.1 PWR Fuel Basket

This section evaluates the MAGNASTOR PWR fuel basket for normal operating conditions. Factors of safety for the PWR fuel basket are calculated based on the criteria for Service Level 'A' limits from ASME Code, Section III, Subsection NG [7].

Normal Handling Evaluation

The PWR fuel basket is analyzed using classical hand calculations for a 1.1g inertia loading in the basket axial direction to account for the dead load and handling load. During normal conditions, the PWR fuel assemblies do not apply loads to the basket, they rest on the TSC bottom. Using a bounding basket weight of 22,500 lb, the maximum stress in the fuel tube is calculated. There are 21 fuel tubes in the PWR fuel basket. Conservatively assuming the entire basket weight is carried through the fuel tubes, the stress in the tube (σ_{tube}) is as follows.

$$\sigma_{\text{tube}} = \frac{P_{\text{tube}}}{A} = \frac{1178}{11.4} = 0.1 \text{ ksi}$$

where:

$$P_{\text{tube}} = \frac{W \times a}{n} = 1,178 \text{ lb -----Load per tube}$$

$W = 22,500 \text{ lb}$ -----Bounding basket weight
 $a = 1.1g$ -----Inertia g-load
 $n = 21$ -----Number of fuel tubes
 $A = 11.4 \text{ inch}^2$ -----Tube cross-sectional area

The factor of safety (FS) is as follows.

$$FS = \frac{S_m}{\sigma_{\text{tube}}} = \frac{21.4}{0.1} = \text{Large}$$

where:

$S_m = 21.4 \text{ ksi}$ -----Design stress intensity, SA-537 Class 1, at 700°F

The weight of the fuel tubes is supported on connector pins. Referring to Figure 3.7-1, the interior tubes (Tube #4) are supported by four connector pins, the side fuel tubes (Tube #1) are supported by two connector pins and the side and corner weldments, and the corner fuel tubes (Tube #3) are supported by three connector pins. The bearing stress on the fuel tube (σ_{brg}) is as follows.

$$\sigma_{\text{brg}} = \frac{1.1 \times P_{\text{pin}}}{A_{\text{brg}}} = \frac{1.1 \times 394}{0.21} = 2.1 \text{ ksi}$$

where:

$A_{\text{brg}} = 0.21 \text{ inch}^2$ -----Bearing area
 $P_{\text{pin}} = \frac{1}{3} P_t + \frac{1}{4} P_t = 394 \text{ lb}$
 $P_t = 675 \text{ lb}$ -----Tube weight



Bearing Area of Fuel Tube and Connector Pin Intersection

The factor of safety (FS) for bearing is as follows.

$$FS = \frac{S_y}{\sigma_{\text{brg}}} = \frac{32.3}{2.1} = \text{Large}$$

where:

$S_y = 32.3 \text{ ksi}$ -----Yield strength, SA-537 Class 1, at 700°F

The bearing stress (σ_{brg}) in the connector pin at the TSC bottom plate, conservatively using P_{tube} , as previously determined is as follows.

$$\sigma_{brg} = \frac{P_{tube}}{A_{brg}} = \frac{1178}{0.41} = 2.9 \text{ ksi}$$

where:

$$A_{brg} = \frac{\pi}{4}(D_o^2 - D_i^2) = \frac{\pi}{4}(0.75^2 - 0.19^2) = 0.41 \text{ inch}^2$$

The factor of safety (FS) for bearing is as follows.

$$FS = \frac{S_y}{\sigma_{brg}} = \frac{24.7}{2.9} = 8.5$$

where:

$$S_y = 24.7 \text{ ksi} \text{ ----- Yield strength, SA-240 Type 304, at } 400^\circ\text{F}$$

The buckling evaluation of the connector pin is performed for the governing condition of the 24-inch concrete cask end-drop accident, as shown in Section 3.7.2.1. The accident condition buckling is bounding due to the 60g axial inertia loading.

The weight of the side and corner weldments is carried through to the TSC bottom plate by supports at the bottom of the basket. The bounding dimensions for the supports of the weldments are 5.0-inch length and 0.3125-inch thickness (corner weldment). The maximum weight of one weldment is 800 lb (bounding side weldment). The weldment supports one-quarter of the weight of two fuel tubes (675 lb per tube, bounding). The bearing stress (σ_{brg}) is as follows.

$$\sigma_{brg} = \frac{1.1 \times W_{sup}}{A_{sup}} = \frac{1.1 \times 1138}{1.56} = 0.8 \text{ ksi}$$

where:

$$W_{sup} = 800 + 2 \times (0.25 \times 675) = 1138 \text{ lb}$$

$$A_{sup} = 5.0 \times 0.3125 = 1.56 \text{ inch}^2$$

The factor of safety (FS) for bearing is as follows.

$$FS = \frac{S_y}{\sigma_{brg}} = \frac{32.3}{0.8} = \text{Large}$$

where:

$$S_y = 32.3 \text{ ksi} \text{ -----Yield strength, SA-537 Class 1, 700°F}$$

The side and corner weldments are attached to the fuel tube array with bolts. The maximum torque on the 5/8-inch bolt is 50.0 inch-lb (40 inch-lb ±10 inch-lb). The preload on the bolt (P) is as follows.

$$P = \frac{T}{0.2D} = \frac{50}{0.2 \times 0.625} = 400 \text{ lb} \quad [12]$$

where:

$$T = 50 \text{ inch-lb} \text{ -----Maximum bolt torque}$$

$$D = 0.625 \text{ inch} \text{ -----Bolt diameter}$$

The bolt thread is a 5/8-11 UNC and the length of engagement is 0.50 inch. From Machinery's Handbook [12], the ultimate strength (σ_t) in the bolt is as follows.

$$\sigma_t = \frac{P}{A_t} = \frac{400}{0.23} = 1.74 \text{ ksi}$$

where:

$$A_t = 0.7854 \left(D - \frac{0.9743}{n} \right)^2 = 0.23 \text{ inch}^2$$

$$D = 0.625 \text{ inch}$$

$$n = 11$$

The factor of safety (FS) is as follows.

$$FS = \frac{2(S_{mBM})}{\sigma_t} = \frac{2 \times 5.9}{1.74} = 6.78$$

where:

$$S_{mBM} = 5.9 \text{ ksi} \text{ -----Design stress intensity for SA 193, Gr B8 at 700°F}$$

The shear stress (τ_{bolt}) in the bolt thread is as follows.

$$\tau_{bolt} = \frac{P}{A_s} = \frac{400}{0.499} = 0.8 \text{ ksi}$$

where:

$$A_s = 3.1416nL_e K_{n \max} \left[\frac{1}{2n} + 0.57735(E_{s \min} - K_{n \max}) \right] = 0.499 \text{ inch}^2$$

The factor of safety (FS) is as follows.

$$FS = \frac{0.6S_m}{\tau_{\text{bolt}}} = \frac{0.6 \times 16.0}{0.8} = \text{Large}$$

where:

$$S_m = 16.0 \text{ ksi} \text{ ----- Design stress intensity, SA-193 Grade B8 at } 700^\circ\text{F}$$

The shear stress in the boss thread (τ_{boss}) is as follows.

$$\tau_{\text{boss}} = \frac{P}{A_n} = \frac{400}{0.713} = 0.6 \text{ ksi}$$

where:

$$A_n = 3.1416nL_e D_{s \min} \left[\frac{1}{2n} + 0.57735(D_{s \min} - E_{n \max}) \right] = 0.713 \text{ inch}^2$$

The factor of safety (FS) is as follows.

$$FS = \frac{0.6S_m}{\tau_{\text{bolt}}} = \frac{0.6 \times 19.2}{0.6} = \text{Large}$$

where:

$$S_m = 19.2 \text{ ksi} \text{ ----- Design stress intensity, SA-695 Type B, Gr } 40, \text{ at } 700^\circ\text{F}$$

The boss is welded into the fuel tube with a 1/8-inch groove weld. The shear stress in the boss weld (τ_{weld}), is as follows.

$$\tau_{\text{weld}} = \frac{P}{A_w} = \frac{400}{0.49} = 0.8 \text{ ksi}$$

where:

$$P = 400 \text{ lb}$$
$$A_w = \pi D t_{\text{weld}} = \pi \times 1.25 \times 0.125 = 0.49 \text{ inch}$$

$$D = 1.25 \text{ inch} \text{-----Boss diameter}$$

Using the lesser allowable, S_m , of SA537 Class 1 or SA695 Type B, Gr 40, the factor of safety (FS) is as follows.

$$FS = \frac{0.6S_m}{\tau_{\text{weld}}} = \frac{0.6 \times 19.2}{0.8} = \text{Large}$$

where:

$$S_m = 19.2 \text{ ksi} \text{-----Design stress intensity, SA-695 Type B, Gr 40, at } 700^\circ\text{F}$$

The washers under the bolts are subjected to a bending load due to the bolt preload. Using Roark's [13], Table 24-1a, the maximum stress in the washer is calculated. The maximum stress (σ) in the washer is as follows.

$$\sigma = \frac{6M_t}{t^2} = \frac{6 \times 55.3}{0.13^2} = 19.6 \text{ ksi}$$

where:

$$a = \frac{1.50}{2} = 0.75 \text{ inch} \text{-----Radius of the cut out in support weldments}$$

$$b = \frac{0.625}{2} = 0.31 \text{ inch} \text{-----Inner radius of the washer}$$

$$r_o = 0.50 \text{ inch} \text{-----Average radius of bolt head}$$

$$t = 0.13 \text{ inch} \text{-----Thickness of washer}$$

$$E = 30.0 \times 10^6 \text{ psi} \text{-----Modulus of elasticity (SA-240 Type 304)}$$

$$\nu = 0.3 \text{-----Poisson's ratio}$$

$$w = \frac{P}{\pi \times 2r_o} = \frac{400}{\pi \times 2 \times 0.5} = 127 \text{ inch-lb}$$

$$G = \frac{E}{2(1+\nu)} = \frac{30.0 \times 10^6}{2(1+0.3)} = 11.45 \times 10^6 \text{ psi}$$

$$D = \frac{Et^3}{12(1-\nu^2)} = \frac{30.0 \times 10^6 (0.13^3)}{12(1-0.3^2)} = 6035.7 \text{ inch-lb}$$

$$M_t = 55.3 \text{ inch-lb} \text{-----Calculated using formulas in Roark's [13]}$$

The factor of safety (FS) is as follows.

$$FS = \frac{1.5S_m}{\sigma} = \frac{1.5 \times 16.0}{19.6} = 1.22$$

where:

$$S_m = 16.0 \text{ ksi} \text{-----Design stress intensity, SA-240 Type 304, at } 700^\circ\text{F}$$

The evaluation of the neutron absorber for normal handling conditions is bounded by the evaluation for the 24-inch concrete cask end-drop accident (60g) as shown in Section 3.7.2.1. Therefore, no evaluation for normal handling is presented in this section.

Thermal Stress Evaluation

The thermal stresses for the PWR fuel basket are calculated using an ANSYS finite element model (Appendix 3.A). The 0° basket orientation model is used for the thermal stress evaluation. The model calculates the stresses in the basket based upon an applied temperature distribution. The thermal stresses are combined with the normal handling condition stress. Factors of safety are calculated based on Service Level 'A' limits from ASME Code, Section III, Subsection NG [7]. The maximum handling stress in the basket is 0.1 ksi. The following presents the combined normal handling plus thermal stress (P+Q) for the PWR basket.

Component	S _{therm} , ksi	S _{total} , ksi	S _{allow} , ksi	FS
Fuel Tube	48.3	48.4	64.2	1.33
Support Weldments	37.6	37.7	64.2	1.70

The total stress is the sum of the component thermal stress and the normal handling stress. The allowable stress is 3S_m (3 × 21.4 = 64.2 ksi for SA537 C1 at 700°F). The maximum nodal thermal stress (48.3 ksi) occurs at the nodes, which are coupled between the fuel tube and the support weldment. This is conservative because the single nodal coupling does not account for the load being distributed over the boss area.

The axial average temperature at the center of the basket is 469°F. The axial average temperature at the outer radius of the basket is 444°F. The relative thermal expansion of the basket in the axial direction between the center and outer edge of the basket is as follows.

$$\Delta x = \Delta x_{\text{inner}} - \Delta x_{\text{outer}} = 0.50 - 0.47 = 0.03 \text{ inch}$$

where:

$$\Delta x_{\text{inner}} = \Delta T \times L \times \alpha_1 = (469 - 70)(173.5)(7.24 \times 10^{-6}) = 0.50 \text{ inch}$$

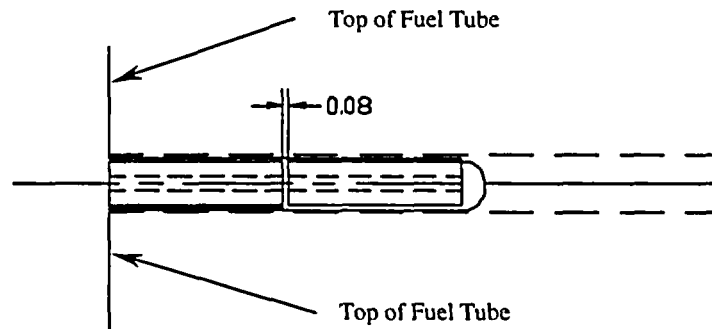
$$\Delta x_{\text{outer}} = \Delta T \times L \times \alpha_2 = (444 - 70)(173.5)(7.19 \times 10^{-6}) = 0.47 \text{ inch}$$

$$L = 173.5 \text{ inch} \text{-----Fuel tube length}$$

$$\alpha_1 = 7.24 \times 10^{-6} \text{ inch/inch/}^\circ\text{F} \text{-----Coefficient of thermal expansion, SA537 CL1, at } 469^\circ\text{F}$$

$$\alpha_2 = 7.19 \times 10^{-6} \text{ inch/inch/}^\circ\text{F} \text{ -----Coefficient of thermal expansion, SA537 CL1, at } 444^\circ\text{F}$$

Connector pins at the top and bottom of the basket are used to maintain the geometry of the fuel tube array during manufacturing. A pin is inserted into the connector pin to maintain geometry between adjacent fuel tubes. Adjacent fuel tube connector pins have a 0.08-inch gap between the connector pins; see the following sketch. Since the relative thermal expansion of the basket between the center and outer edge of the basket is less than the pin gap, no axial thermal stresses are produced by the axial expansion of the basket.



The maximum shear load calculated by ANSYS in the basket attachment bosses is 3.2 kip due to the radial thermal expansion of the basket. The shear stress in the boss (τ_{boss}) is as follows.

$$\tau_{\text{boss}} = \frac{P}{A} = \frac{3.2}{0.92} = 3.5 \text{ ksi}$$

where:

$$A = \frac{\pi}{4} (D_o^2 - D_i^2) = 0.92 \text{ inch}^2$$

$$D_o = 1.25 \text{ inch}$$

$$D_i = 0.63 \text{ inch}$$

The factor of safety (FS) is as follows.

$$\text{FS} = \frac{0.6S_m}{\tau_{\text{boss}}} = \frac{0.6 \times 19.2}{3.5} = 3.29$$

where:

$$S_m = 19.2 \text{ ksi} \text{ -----Design stress intensity SA-695 Type B, Gr 40 at } 700^\circ\text{F}$$

From the finite element model, the bolt tensile load due to thermal expansion is ten pounds. The maximum bolt load for normal handling conditions is 400 pounds. The minimum factor of safety for normal conditions is 1.22 (washer bending). For normal handling plus thermal loads the maximum bolt load is 410 pounds, a 2.5% increase in load. Therefore, the minimum factor of safety for the attachment bolts is 1.19.

Neutron Absorber Retainer Thermal Stress Evaluation

The stainless steel corner clips are attached to the fuel tubes using plug welds spaced every five inches. The stainless steel retainer strips are fastened to the carbon steel fuel tube using weld posts spaced every ten inches along the length of the tube. Because of the dissimilar material properties, differential expansion of the components creates thermal stresses in some of the components.

Corner Clip

The equation used to calculate the difference in expansion between carbon and stainless steel, Δ , is as follows.

$$\Delta = (\alpha_{ss} \times \Delta T \times L) - (\alpha_{cs} \times \Delta T \times L) \quad (1)$$

The standard formula to calculate the deflection of a beam or plate is as follows.

$$\Delta = \frac{PL}{AE} = \frac{\sigma L}{E} \quad (2)$$

Substituting equation (1) into equation (2) and solving, the corner clip thermal stress, σ , is as follows.

$$\sigma = \frac{E\Delta}{L} = E(\alpha_{ss} - \alpha_{cs})(\Delta T) = 34,700 \text{ psi} \quad (3)$$

where:

- $\alpha_{ss} = 9.9 \times 10^{-6} \text{ inch/inch/}^\circ\text{F}$ -----Coefficient of thermal expansion, SA-240 Type 304, at 667°F
- $\alpha_{cs} = 7.6 \times 10^{-6} \text{ inch/inch/}^\circ\text{F}$ -----Coefficient of thermal expansion, SA-537 Class 1, at 667°F
- $\Delta T = 672^\circ\text{F} - 70^\circ\text{F} = 602^\circ\text{F}$ -----Difference between maximum PWR temperature and ambient conditions
- $T_{\text{max}} = 672^\circ\text{F}$ -----Maximum basket temperature

$$E = 25 \times 10^6 \text{ psi} \text{ ----- Modulus of elasticity, SA-240 Type 304, at } 672^\circ\text{F}$$

The factor of safety (FS) is as follows.

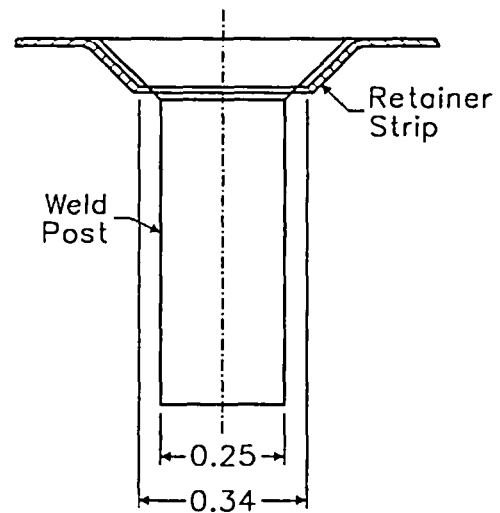
$$FS = \frac{3S_m}{\sigma} = \frac{48,300}{34,328} = 1.4$$

where:

$$S_m = 16,100 \text{ psi} \text{ ----- Design stress intensity, SA-240 Type 304, at } 667^\circ\text{F}$$

Retainer Strip

The attachments of the retainer strip and neutron absorber to the fuel tube using weld posts and corner clips allows each component to move independently during thermal growth. In the case of the stainless steel retainer strip, the expansion of the neutron shield material, which is composed primarily of aluminum, and carbon steel fuel tube tends to tighten the joint created by the weld post. Thermal stresses may develop between the weld posts because the carbon steel fuel tube expands at a different rate than the retainer strip.



From equation (3) previously listed, it is observed that thermal stress developed between dissimilar materials is independent of the length. Assuming the same boundary conditions as the corner clip, the stresses in the retainer strip are the same as the corner clip. Therefore, no further evaluation is required.

3.5.2.2 BWR Basket

This section evaluates the MAGNASTOR BWR basket for normal operating conditions. Factors of safety for the BWR basket are calculated based on the criteria for Service Level 'A' limits from ASME Code, Section III, Subsection NG [7].

Normal Handling Evaluation

The BWR basket is analyzed using classical hand calculations for a 1.1g inertia loading in the basket axial direction to account for the dead load and handling load. During normal conditions, the BWR fuel assemblies do not apply loads to the basket; they rest on the TSC bottom. Using a bounding weight of 24,000 pounds, the maximum stress in the fuel tube is calculated. There are 45 fuel tubes in the BWR basket. Conservatively assuming the entire basket weight is carried through the fuel tubes, the stress in the tube (σ_{tube}) is as follows.

$$\sigma_{tube} = \frac{P_{tube}}{A} = \frac{587}{6.1} = 0.1 \text{ ksi}$$

where:

$$P_{tube} = \frac{W \times a}{n} = 587 \text{ lb} \text{ ----- Load per tube}$$

$$W = 24,000 \text{ lb} \text{ ----- Bounding basket weight}$$

$$a = 1.1g \text{ ----- Inertia g-load}$$

$$n = 45 \text{ ----- Number of fuel tubes}$$

$$A = 6.1 \text{ inch}^2 \text{ ----- Tube cross-sectional area}$$

The factor of safety (FS) is as follows.

$$FS = \frac{S_m}{\sigma_{tube}} = \frac{21.4}{0.1} = \text{Large}$$

where:

$$S_m = 21.4 \text{ ksi} \text{ ----- Design stress intensity, SA-537 Class 1, at } 700^\circ\text{F}$$

The weight of the fuel tubes is supported on connector pins. For tube locations presented in Figure 3.7-10, the interior tubes (Tube #4) are supported by four connector pins, the side fuel tubes (Tube #1) are supported by two connector pins and the side and corner weldments, and the corner fuel tubes (Tube #5) are supported by three connector pins. The bearing stress (σ_{brg}) on the fuel tube is as follows.

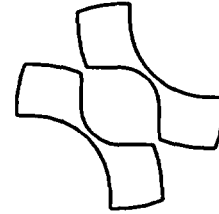
$$\sigma_{brg} = \frac{1.1 \times P_{pin}}{A_{brg}} = \frac{1.1 \times 233}{0.34} = 0.8 \text{ ksi}$$

where:

$$A_{brg} = 0.34 \text{ inch}^2 \text{-----Bearing area}$$

$$P_{pin} = \frac{1}{3} P_t + \frac{1}{4} P_t = 233 \text{ lb}$$

$$P_t = 400 \text{ lb} \text{-----Tube weight}$$



Bearing area of Fuel Tube and Connector Pin Intersection

The factor of safety (FS) for bearing is as follows.

$$FS = \frac{S_y}{\sigma_{brg}} = \frac{32.3}{0.8} = \text{Large}$$

where:

$$S_y = 32.3 \text{ ksi} \text{-----Yield strength, SA-537 Class 1, at } 700^\circ\text{F}$$

The bearing stress (σ_{brg}) in the connector pin at the TSC bottom plate, conservatively using P_{tube} as previously determined is as follows.

$$\sigma_{brg} = \frac{P_{tube}}{A_{brg}} = \frac{587}{0.75} = 0.8 \text{ ksi}$$

where:

$$A_{brg} = \frac{\pi}{4} (D_o^2 - D_i^2) = \frac{\pi}{4} (1.0^2 - 0.19^2) = 0.75 \text{ inch}^2$$

The factor of safety (FS) for bearing is as follows.

$$FS = \frac{S_y}{\sigma_{brg}} = \frac{24.7}{0.8} = \text{Large}$$

where:

$$S_y = 24.7 \text{ ksi} \text{ -----Yield strength, SA-240 Type 304, at } 700^\circ\text{F}$$

The buckling evaluation of the connector pin is performed for the governing condition of the 24-inch concrete cask end-drop accident, as prescribed in Section 3.7.2.2. The accident event buckling evaluation is bounding due to the 60g axial inertia loading.

The weight of the side and corner weldments is carried through to the TSC bottom plate by supports at the bottom of the basket. The corner weldment is bounding for the top and bottom supports. The dimensions for the corner support weldment are 8.0-inch length and 0.375-inch thickness. The bounding weight of the corner weldment is 1,100 pounds. The corner weldment also supports one-quarter of the weight of four fuel tubes (400 lb per tube, bounding). The bearing stress (σ_{brg}) is as follows.

$$\sigma_{brg} = \frac{W_{sup}}{A_{sup}} = \frac{1650}{3.0} = 0.6 \text{ ksi}$$

where:

$$W_{sup} = 1.1 \times (1,100 + 4 \times (0.25 \times 400)) = 1650 \text{ lb}$$

$$A_{sup} = 8.0 \times 0.375 = 3.0 \text{ inch}^2$$

The factor of safety (FS) for bearing is as follows.

$$FS = \frac{S_y}{\sigma_{brg}} = \frac{32.3}{0.6} = \text{Large}$$

where:

$$S_y = 32.3 \text{ ksi} \text{ -----Yield strength, SA-537 Class 1, } 700^\circ\text{F}$$

The side and corner weldments are attached to the fuel tube array with bolts. The maximum torque on the 5/8-inch bolt is 50 inch-lb (40 ±10 inch-lb). The preload on the bolt (P) is as follows.

$$P = \frac{T}{0.2D} = \frac{50}{0.2 \times 0.625} = 400 \text{ lb} \quad [12]$$

where:

$$T = 50 \text{ inch-lb} \text{ -----Maximum bolt torque}$$

$$D = 0.625 \text{ inch} \text{ -----Bolt diameter}$$

The bolt thread is a 3/8-11 UNC and the length of engagement is 0.50 inch. From Machinery's Handbook [12], the ultimate strength (σ_t) in the bolt is as follows.

$$\sigma_t = \frac{P}{A_t} = \frac{400}{0.23} = 1.74 \text{ ksi}$$

where:

$$A_t = 0.7854 \left(D - \frac{0.9743}{n} \right)^2 = 0.23 \text{ inch}^2$$

$$D = 0.625 \text{ inch}$$

$$n = 11$$

The factor of safety (FS) is as follows.

$$FS = \frac{2(S_{mBM})}{\sigma_t} = \frac{2 \times 5.9}{1.74} = 6.78$$

where:

$$S_{mBM} = 5.9 \text{ ksi} \text{-----Design stress intensity for SA-193, Gr B8, at } 700^\circ\text{F}$$

The shear stress in the bolt thread (τ_{bolt}) is as follows.

$$\tau_{bolt} = \frac{P}{A_s} = \frac{400}{0.379} = 1.1 \text{ ksi}$$

where:

$$A_s = 3.1416nL_c K_{n \max} \left[\frac{1}{2n} + 0.57735(E_{s \min} - K_{n \max}) \right] = 0.379 \text{ inch}^2$$

$$n = 11$$

The factor of safety (FS) is as follows.

$$FS = \frac{0.6S_m}{\tau_{bolt}} = \frac{0.6 \times 16.0}{1.1} = 8.73$$

where:

$$S_m = 16.0 \text{ ksi} \text{-----Design stress intensity, SA-193 Grade B8, at } 700^\circ\text{F}$$

The shear stress in the boss thread (τ_{boss}) is as follows.

$$\tau_{boss} = \frac{P}{A_n} = \frac{400}{0.542} = 0.7 \text{ ksi}$$

where:

$$A_n = 3.1416nL_c D_{s \min} \left[\frac{1}{2n} + 0.57735(D_{s \min} - E_{n \max}) \right] = 0.542 \text{ inch}^2$$

$$\begin{aligned} L_c &= 0.38 \text{ inch} \\ E_{n \max} &= 0.5732 \\ D_{s \min} &= 0.6113 \\ n &= 11 \end{aligned}$$

The factor of safety (FS) is as follows.

$$FS = \frac{0.6S_m}{\tau_{bolt}} = \frac{0.6 \times 19.2}{0.7} = \text{Large}$$

where:

$$S_m = 19.2 \text{ ksi} \text{ ----- Design stress intensity, SA-695, Type B, Gr 40, at } 700^\circ\text{F}$$

The boss is welded into the fuel tube with a 1/8-inch groove weld. The shear stress in the boss weld (τ_{weld}) is as follows.

$$\tau_{weld} = \frac{P}{A_w} = \frac{400}{0.49} = 0.8 \text{ ksi}$$

where:

$$\begin{aligned} P &= 400 \text{ lb} \\ A_w &= \pi D t_{weld} = \pi \times 1.00 \times 0.156 = 0.49 \text{ inch} \\ D &= 1.00 \text{ inch} \text{ ----- Smallest boss diameter} \end{aligned}$$

Using the lesser allowable, S_m , of SA-537 Class 1 or SA-695 Type B, Gr 40, the factor of safety (FS) is as follows.

$$FS = \frac{0.6S_m}{\tau_{weld}} = \frac{0.6 \times 19.2}{0.8} = \text{Large}$$

where:

$$S_m = 19.2 \text{ ksi} \text{ -----Design stress intensity, SA-695 Type B Grade 40, at } 700^\circ\text{F}$$

The washers under the bolts are subjected to a bending load to the torque of the bolts. Using "Roark's Formulas for Stress and Strain" Table 24-1a [13], the maximum stress in the washer is calculated. The maximum stress (σ) in the washer is as follows.

$$\sigma = \frac{6M_t}{t^2} = \frac{6 \times 55.3}{0.13^2} = 19.6 \text{ ksi}$$

where:

$$a = \frac{1.50}{2} = 0.75 \text{ inch} \text{ -----Radius of cut out in support weldments}$$

$$b = \frac{0.625}{2} = 0.31 \text{ inch} \text{ -----Inner radius of the washer}$$

$$r_o = 0.50 \text{ inch} \text{ -----Average radius of bolt head}$$

$$t = 0.13 \text{ inch} \text{ -----Thickness of washer}$$

$$E = 30.0 \times 10^6 \text{ psi} \text{ -----Modulus of elasticity (SA240 Type 304)}$$

$$\nu = 0.3 \text{ -----Poisson's ratio}$$

$$w = \frac{P}{\pi \times 2r_o} = \frac{400}{\pi \times 2 \times 0.5} = 127 \text{ inch-lb}$$

$$G = \frac{E}{2(1+\nu)} = \frac{30.0 \times 10^6}{2(1+0.3)} = 11.45 \text{e}6 \text{ psi}$$

$$D = \frac{Et^3}{12(1-\nu^2)} = \frac{30.0 \times 10^6 (0.13^3)}{12(1-0.3^2)} = 6035.7 \text{ inch-lb}$$

$$M_t = 55.3 \text{ inch-lb} \text{ -----Calculated using the formula in Roark's [13]}$$

The factor of safety (FS) is as follows.

$$FS = \frac{1.5S_m}{\sigma} = \frac{1.5 \times 16.0}{19.6} = 1.22$$

where:

$$S_m = 16.0 \text{ ksi} \text{ -----Design stress intensity, SA-240 Type 304, at } 700^\circ\text{F}$$

The evaluation of the neutron absorber for normal handling conditions is bounded by the evaluation for the 24-inch concrete cask end-drop accident (60g) as shown in Section 3.7.2.2. Therefore, no evaluation for normal handling is presented in this section.

Thermal Stress Evaluation

The thermal stresses for the BWR fuel basket are calculated using an ANSYS finite element model (Appendix 3.B). The 0° basket orientation model is used for the thermal stress evaluation. The model calculates the stresses in the basket based upon an applied temperature distribution. The thermal stresses are combined with the normal handling condition stress. Factors of safety are calculated based on Service Level 'A' limits from ASME Code, Section III, Subsection NG [7]. The maximum handling stress in the basket is 0.1 ksi. The following presents the combined normal handling plus thermal stress (P+Q) for the BWR fuel basket:

Component	S _{therm} , ksi	S _{total} , ksi	S _{allow} , ksi	FS
Fuel Tube	22.3	22.4	64.2	2.87
Support Weldments	21.1	21.2	64.2	3.03

The total stress is the sum of the component thermal stress and the normal condition stress. The allowable stress is 3S_m (3 × 21.4 = 64.2 ksi for SA-537 Class 1 steel at 700°F). The maximum nodal thermal stress (22.3 ksi) occurs at the nodes, which are coupled between the fuel tube and the support weldment. This is conservative because the nodal coupling does not account for the load being distributed over the boss area.

The average temperature at the center of the basket is 465°F. The average temperature at the outer radius of the basket is 430°F. The relative thermal expansion of the basket in the axial direction between the center and outer edge of the basket is as follows.

$$\Delta x = \Delta x_{inner} - \Delta x_{outer} = 0.48 - 0.43 = 0.05 \text{ inch}$$

where:

$$\Delta x_{inner} = \Delta T \times L \times \alpha_1 = (465 - 70)(166.5)(7.3 \times 10^{-6}) = 0.48 \text{ inch}$$

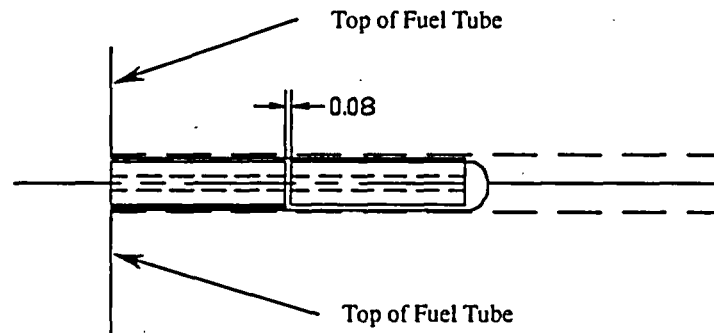
$$\Delta x_{outer} = \Delta T \times L \times \alpha_2 = (430 - 70)(166.5)(7.2 \times 10^{-6}) = 0.43 \text{ inch}$$

L = 166.5 inch ----- Fuel tube length

α₁ = 7.3 × 10⁻⁶ inch/inch/°F ----- Coefficient of thermal expansion, SA537 CL1, at 500°F

α₂ = 7.2 × 10⁻⁶ inch/inch/°F ----- Coefficient of thermal expansion, SA537 CL1, at 450°F

Connector pins at the top and bottom of the basket are used to maintain the geometry of the fuel tube array. A pin is inserted into the connector pin to maintain geometry between adjacent fuel tubes. Adjacent fuel tube connector pins have a 0.08-inch gap between the connector pins; see the following sketch. Since the relative thermal expansion of the basket between the center and outer edge of the basket is less than the pin gap, no axial thermal stresses are produced by the axial expansion of the basket.



The maximum shear load calculated by ANSYS in the basket attachment bosses is 1,379 lb (1.4 kip) due to the radial thermal expansion of the basket. The shear stress in the boss (τ_{boss}) is as follows.

$$\tau_{boss} = \frac{P}{A} = \frac{1.4 \text{ kip}}{0.47} = 2.98 \text{ ksi}$$

where:

$$A = \frac{\pi}{4}(D_o^2 - D_i^2) = 0.47 \text{ inch}^2$$

$$D_o = 1.00 \text{ inch}$$

$$D_i = 0.63 \text{ inch}$$

The factor of safety (FS) is as follows.

$$FS = \frac{0.6S_m}{\tau_{boss}} = \frac{0.6 \times 19.2}{2.98} = 3.87$$

where:

$$S_m = 19.2 \text{ ksi} \text{ ----- Design stress intensity, SA-695 Type B, Gr 40, at } 700^\circ\text{F}$$

The thermal expansion of the basket does not add significant additional tensile loads to the bolts; therefore, no additional bolt analysis for thermal loads is required.

Neutron Absorber Retainer Thermal Stress Evaluation

The stainless steel corner clips are attached to the fuel tubes using plug welds. Similarly, the stainless steel retainer strips are fastened to the carbon steel fuel tube using fixed weld posts spaced along the length of the tube. Because of the dissimilar material properties, differential thermal expansion of the components results in thermal stresses in some of the components. However, the PWR basket thermal gradient is greater than that of the BWR basket. Therefore, the evaluation provided in Section 3.5.2.1 bounds the BWR basket.

3.5.3 Concrete Cask Evaluations for Normal Operating Conditions

The structural evaluation of the concrete cask for normal conditions considers the combination of thermal stresses, dead and live loads, and wind loads (see Chapter 2 for load combinations). The analysis results are presented in Section 3.5.3.3. The conservative stress due to wind loads is obtained from Section 3.7.3.2.

3.5.3.1 Concrete Cask Thermal Stresses

Using the finite element model presented in Appendix 3.D, a structural evaluation of the concrete cask for normal conditions thermal loads was performed. The analysis conservatively considered a bounding temperature profile corresponding to the off-normal thermal event (106°F ambient). The following summarizes the critical thermal stresses for normal conditions.

Component	Stress (ksi)
Circumferential Rebar	15.6
Vertical Rebar	19.1
Concrete, Compression	1.0
Concrete, Tension	0.1

3.5.3.2 Dead and Live Loads

Dead Loads

The concrete cask dead load consists primarily of the weight of the concrete. Assuming all dead loads are reacted by the lower concrete surface only, stress levels can be determined. Under these conditions, the only stress component is the vertical axial compression stress. The maximum stress (σ_{cask}) at the base of the concrete cask in the concrete is as follows.

$$\sigma_{\text{cask}} = \frac{W_{\text{cask}}}{A} = \frac{210,000}{9,119} = 23.0 \text{ psi}$$

where:

$$W_{\text{cask}} = 210,000 \text{ lb} \text{-----Bounding weight for empty concrete cask}$$

$$D_o = 136.0 \text{ inch}$$

$$D_i = 82.98 \text{ inch}$$

$$A = \pi (D_o^2 - D_i^2) / 4 = 9,119 \text{ inch}^2$$

The concrete bearing strength (f_b) is much larger than the applied load.

$$f_b = \phi(0.85f'_c A) = 0.85(0.85 \times 3800 \times 9119) = 25.0 \times 10^6 \text{ lb} > 210,000 \text{ lb}$$

where:

$$f'_c = 3,800 \text{ psi} \text{-----Compressive strength, concrete, at } 300^\circ\text{F}$$

Live Loads

The live load calculation considers the loaded transfer cask positioned on top of the concrete cask for transfer of the TSC for development of the peak live load bounding condition. Assuming live loads are reacted by concrete sections (no credit taken for steel liner), stress levels are conservatively determined. Under these conditions, the only stress component is the vertical axial compression stress ($\sigma_{\text{concrete cask}}$).

$$\sigma_{\text{concrete cask}} = \frac{W_{\text{TFR}}}{A} = \frac{230,000}{9,119} = 25.2 \text{ psi}$$

where:

$$W_{\text{TFR}} = 230,000 \text{ lb} \text{-----Loaded transfer cask}$$

$$D_o = 136.0 \text{ inch}$$

$$D_i = 82.98 \text{ inch}$$

$$A = \pi (D_o^2 - D_i^2) / 4 = 9,119 \text{ inch}^2$$

3.5.3.3 Concrete Cask Combined Stresses

The load combinations described in Chapter 2 are used to evaluate the concrete cask for normal conditions of storage (Load Conditions 1, 2, and 3). Concrete cask stresses are summarized in Table 3.5-5, Table 3.5-6, and Table 3.5-7 for the various loading conditions on the concrete cask.

The allowable compressive stress for concrete (S_{con}) is as follows.

$$S_{\text{con}} = \phi f'_c = 2,660 \text{ psi}$$

where:

$$\begin{aligned}\phi &= 0.7 \text{ -----Strength reduction factor [15]} \\ f_c &= 3800 \text{ psi -----Compressive strength, concrete, at } 300^\circ\text{F}\end{aligned}$$

The concrete ultimate strength allowable is 8% to 15% of the compressive stress [14]; therefore, the allowable ultimate strength (S_{tc}) is as follows:

$$S_{tc} = 0.08 \times S_{con} = 0.08 \times 2660 = 213 \text{ psi or } 0.21 \text{ ksi}$$

The maximum concrete compressive stress is 1,332 psi (see Table 3.5-6); therefore, the minimum factor of safety (FS) for normal conditions is as follows.

$$FS = \frac{2,660}{1,332} = 2.00$$

From Section 3.5.3.1, the maximum concrete ultimate strength due to thermal load is 0.1 ksi. Multiplying the stress by 1.275 factor for normal conditions thermal stresses (see Chapter 2) the factor of safety (FS) for concrete ultimate strengths is as follows.

$$FS = \frac{S_{tc}}{S_t \times 1.275} = \frac{0.21}{0.1 \times 1.275} = 1.62$$

The allowable stress for rebar (S_{rebar}) is as follows.

$$S_{rebar} = \phi F_r = 54.0 \text{ ksi}$$

where:

$$\begin{aligned}\phi &= 0.9 \text{ -----Strength reduction factor [15]} \\ F_r &= 60.0 \text{ ksi -----Yield strength, rebar}\end{aligned}$$

From Section 3.5.3.1, the maximum rebar stress due to thermal load is 19.1 ksi. The stresses due to other loadings are negligible for normal conditions. Compressive loads are carried by the concrete. Multiplying the stress by 1.275 factor for normal conditions thermal stresses (see Chapter 2) the factor of safety (FS) for the rebar is as follows.

$$FS = \frac{S_{rebar}}{S_t \times 1.275} = \frac{54.0}{19.1 \times 1.275} = 2.21$$

Table 3.5-1 TSC Thermal Stress, Q

Load Case	Service Level	Section ^{a)}	Component Stresses (ksi) ^{b)}						S _{int}
			S _x	S _y	S _z	S _{xy}	S _{yz}	S _{xz}	
Thermal	A	12	-37.06	-34.16	-22.33	0.26	2.82	0.14	15.40

Table 3.5-2 TSC Normal Conditions, P_m Stresses

Load Case	Service Level	Section ^{a)}	Component Stresses (ksi) ^{b)}						S _{int}	S _{allow}	FS
			S _x	S _y	S _z	S _{xy}	S _{yz}	S _{xz}			
Pressure	A	2	2.42	-7.21	-1.98	0.32	-0.01	-0.39	9.68	N/A	N/A
Pressure + Handling	A	3	0.00	-7.39	4.92	-0.24	-0.03	0.78	12.43	20.00	1.61

Table 3.5-3 TSC Normal Conditions, P_m + P_b Stresses

Load Case	Service Level	Section ^{a)}	Component Stresses (ksi) ^{b)}						S _{int}	S _{allow}	FS
			S _x	S _y	S _z	S _{xy}	S _{yz}	S _{xz}			
Pressure	A	1	1.80	-2.46	14.94	0.11	0.03	0.21	17.41	N/A	N/A
Pressure + Handling	A	11	25.58	25.57	5.14	0.08	3.81	0.66	21.88	30.00	1.37

Table 3.5-4 TSC Normal Conditions, P + Q Stresses

Load Case	Service Level	Section ^{a)}	Component Stresses (ksi) ^{b)}						S _{int}	S _{allow}	FS
			S _x	S _y	S _z	S _{xy}	S _{yz}	S _{xz}			
Pressure + Handling + Thermal	A	11	-40.76	-39.22	-7.89	0.11	2.42	0.60	33.07	60.00	1.81

^{a)} See Figure 3.C-2 for section locations.

^{b)} The x,y,z component of stress are to be interpreted radial, circumferential, and axial directions, respectively.

Table 3.5-5 Concrete Cask Vertical Stress Summary – Outer Surface, psi

Condition	Dead	Live	Wind	Thermal	Seismic	Flood	Tornado	Total
1	-32	-43	0	0	0	0	0	-75
2	-24	-32	0	0	0	0	0	-56
3	-24	-32	-24	0	0	0	0	-80

Table 3.5-6 Concrete Cask Vertical Stress Summary – Inner Surface, psi

Condition	Dead	Live	Wind	Thermal	Seismic	Flood	Tornado	Total
1	-32	-43	0	0	0	0	0	-75
2	-24	-32	0	-1261	0	0	0	-1317
3	-24	-32	-15	-1261	0	0	0	-1332

Table 3.5-7 Concrete Cask Circumferential Stress Summary – Inner Surface, psi

Condition	Dead	Live	Wind	Thermal	Seismic	Flood	Tornado	Total
1	0	0	0	0	0	0	0	0
2	0	0	0	-566	0	0	0	-566
3	0	0	0	-566	0	0	0	-566

3.6 Off-normal Operating Events

This section presents the analyses of the major structural components of MAGNASTOR for off-normal events of storage. MAGNASTOR is evaluated using finite element models and classical hand calculations for the fuel baskets and TSC. Off-normal environmental events are defined as -40°F with no solar load, 106°F with solar load, and half-blockage of the concrete cask air inlets.

3.6.1 TSC Evaluations for Off-normal Operating Events

3.6.1.1 Thermal Stresses for Off-normal Events

The thermal stresses of the TSC are calculated using the ANSYS finite element model described in Appendix 3.C. As discussed in Section 3.5.1.1, the temperature gradient applied to the TSC bounds the temperature gradient for all conditions of storage. Therefore, the maximum thermal stresses for the off-normal severe ambient temperature event are bounded by those presented in Table 3.5-1.

3.6.1.2 Off-Normal TSC Load Analyses

Based on the load combinations specified in Table 2.3-2, the following two off-normal load events are evaluated.

- Off-normal internal pressure + normal handling + thermal (ASME Code, Level B)
- Normal internal pressure + off-normal handling (ASME Code, Level C)

Off-Normal Internal Pressure with Normal Handling

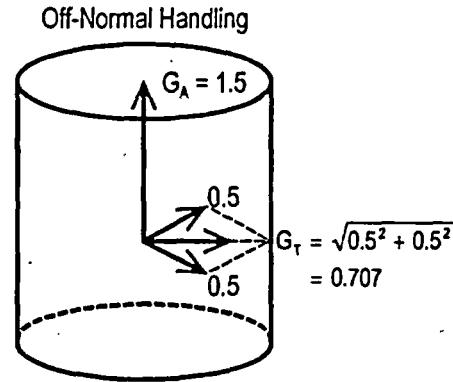
The TSC is analyzed for off-normal pressurization and normal handling loads using the finite element model described in Appendix 3.C. Applying a 1.1g acceleration load in the axial direction to a loaded TSC simulates normal handling. To represent the off-normal pressure, an internal pressure of 130 psig is applied to all internal surfaces. A bounding temperature profile is considered for the thermal stress calculation as discussed in Appendix 3.C.

The resulting maximum stresses in the TSC for Service Level B off-normal loads are summarized in Table 3.6-1 for primary membrane, Table 3.6-2 for primary membrane plus primary bending, and Table 3.6-3 for primary plus secondary stress categories. The minimum factor of safety of 1.32 ($P_m + P_b$) occurs at Section 11 (center of bottom plate). The locations for the stress sections are shown in Appendix 3.C.

Off-Normal Handling with Normal Internal Pressure

An evaluation is performed for the off-normal handling loads on the TSC during the installation of the TSC in the concrete cask, removal of the TSC from the concrete cask, and removal from the transfer cask. The TSC is handled vertically in both the concrete and transfer casks.

The TSC is analyzed for handling loads using the finite element model described in Appendix 3.C. The off-normal TSC handling loads are defined as 0.5g applied in all directions (i.e., in the global x, y, and z directions) in addition to a 1g lifting load applied in the finite element model. The resulting off-normal handling accelerations are 0.707g in the lateral direction and 1.5g (0.5g + 1.0g) in the vertical direction. To represent the normal pressure, an internal pressure of 110 psig is applied to all internal surfaces.



The resulting maximum stresses in the TSC for Service Level C off-normal loads are summarized in Table 3.6-1 for primary membrane, Table 3.6-2 for primary membrane plus primary bending, and Table 3.6-3 for primary plus secondary stress categories. The minimum factor of safety of 1.45 ($P_m + P_b$) occurs at Section 1 (bottom plate / shell). The locations for the stress sections are shown in Appendix 3.C.

3.6.2 Fuel Basket Evaluation for Off-normal Events

3.6.2.1 PWR Fuel Basket

This section evaluates the MAGNASTOR PWR basket for off-normal events using both classical hand calculations and finite element analysis methods. Factors of safety for the PWR basket are calculated based on the criteria for Service Level 'C' limits from ASME Code, Section III, Subsection NG [7].

The inertia loading for off-normal handling events is a 1.5g vertical acceleration and a 0.707g (0.5g inch each transverse direction) transverse acceleration. The basket stresses due to the transverse loading are calculated using the three-dimensional periodic finite element models described in Appendix 3.A. Both half-symmetry models for the 0° and 45° basket orientations are used. Using a bounding weight of 22,500 pounds for the PWR basket, the maximum stress in the fuel tube in the axial direction is calculated. Conservatively assuming the entire basket weight is carried through the fuel tubes, the stress in the tube due to the axial acceleration is as follows.

$$\sigma_{tube} = \frac{P_{tube}}{A} = \frac{1607}{11.4} = 0.14 \text{ ksi}$$

where:

$$P_{tube} = \frac{W \times a}{n} = \frac{22500 \times 1.5}{21} = 1,607 \text{ lb}$$

- W = 22,500 lb ----- Bounding basket weight
- n = 21 ----- Number of fuel tubes
- a = 1.5g ----- Inertia g-load
- A = 11.4 inch² ----- Tube cross-sectional area

The maximum stresses due to transverse loading (S_{tran}), from the finite element analysis results, are shown in the following table. The combined maximum stress intensity (S_{tot}) is conservatively obtained by adding the maximum stresses due to axial load (σ_{tube}) to the maximum stresses due to transverse load (S_{tran}). The combined stresses and factors of safety are presented in the following. The allowable stresses for the off-normal events (Level C) are $1.5S_m$ for membrane stresses and $2.25S_m$ for membrane plus bending stresses.

Component	S_{tran} , ksi	S_{tot} , ksi	S_{allow} , ksi	FS
Fuel Tube, P_m	7.0	7.1	32.10	4.52
Fuel Tube, $P_m + P_b$	16.2	16.3	48.15	2.95
Support Weldments, P_m	0.7	0.8	32.10	Large
Support Weldments, $P_m + P_b$	6.4	6.5	48.15	7.41

The weight of the fuel tubes is supported on connector pins. Referring to Figure 3.7-1, the interior tubes (Tube #4) are supported by four connector pins, the side fuel tubes (Tube #1) are supported by two connector pins and the side and corner weldments, and the corner fuel tubes (Tube #3) are supported by three connector pins. The bearing stress on the fuel tube (σ_{brg}) is as follows.

$$\sigma_{brg} = \frac{1.5 \times P_{pin}}{A_{brg}} = \frac{1.5 \times 394}{0.21} = 2.8 \text{ ksi}$$

where:

- A_{brg} = 0.21 inch² ----- Bearing area
- P_{pin} = $\frac{1}{3}P_1 + \frac{1}{4}P_2 = 394 \text{ lb}$ ----- Combined loading on one support pin
- P_1 = 675 lb ----- Tube weight



Bearing Area of Fuel Tube and Connector Pin Intersection

The factor of safety (FS) for bearing is as follows.

$$FS = \frac{S_y}{\sigma_{brg}} = \frac{32.3}{2.8} = \text{Large}$$

where:

$S_y = 32.3$ ksi -----Yield strength, SA-537 Class 1, at 700°F

The bearing stress (σ_{brg}) in the connector pin at the TSC bottom plate, conservatively using P_{tube} as previously determined is as follows.

$$\sigma_{brg} = \frac{P_{tube}}{A_{brg}} = \frac{1607}{0.41} = 3.9 \text{ ksi}$$

where:

$$A_{brg} = \frac{\pi}{4}(D_o^2 - D_i^2) = \frac{\pi}{4}(0.75^2 - 0.19^2) = 0.41 \text{ inch}^2$$

$$D_o = 0.75 \text{ inch}$$

$$D_i = 0.19 \text{ inch}$$

The factor of safety (FS) for bearing is as follows.

$$FS = \frac{S_y}{\sigma_{brg}} = \frac{24.7}{3.9} = 6.3$$

where:

$S_y = 24.7$ ksi -----Yield strength, SA-240 Type 304, at 700°F

The weight of the side and corner weldments is carried through to the TSC bottom plate by supports at the bottom of the basket. The bounding dimensions for the supports of the weldments are 5.0-inch length and 0.3125-inch thickness (corner weldment). The maximum weight of one weldment is 800 lb (bounding, side weldment). The weldment supports one-quarter of the weight of two fuel tubes (675 lb per tube, bounding). The bearing stress is as follows.

$$\sigma_{brg} = \frac{1.5 \times W_{sup}}{A_{sup}} = 1.1 \text{ ksi}$$

where:

$$W_{sup} = 800 + 2 \times (0.25 \times 675) = 1138 \text{ lb}$$

$$A_{sup} = 5.0 \times 0.3125 = 1.56 \text{ inch}^2$$

The factor of safety (FS) for bearing is as follows.

$$FS = \frac{S_y}{\sigma_{brg}} = \frac{32.3}{1.1} = \text{Large}$$

where:

$$S_y = 32.3 \text{ ksi} \text{ ----- Yield strength, SA-537 Class 1, at } 700^\circ\text{F}$$

The buckling evaluation of the connector pin is performed in Section 3.7.2.1. The accident condition buckling evaluation is bounding due to the conservative 60g axial inertia loading.

During off-normal storage events, the only load on the attachment bolts is due to preload. The analysis presented in Section 3.5.2.1 is bounding. Therefore, additional bolt analysis is not required.

From the finite element analysis results for off-normal handling, the maximum shear load in the basket attachment bosses is 883 pounds. The attachment bosses are evaluated in Section 3.5.2.1 (normal condition) for a shear load of 1,379 lb, which bounds the maximum load of 883 lb for off-normal events; therefore, no additional analysis is required.

The analysis presented in Section 3.7.2.1 bounds the off-normal analysis of the neutron absorber and retainer strip; therefore, no additional analysis is required.

3.6.2.2 BWR Fuel Basket

The analysis of the BWR basket for off-normal events uses both classical hand calculations and finite element analysis methods. The ANSYS finite element model and boundary conditions are presented in Appendix 3.B for the 0° and 45° basket orientations. Factors of safety for the BWR basket are calculated based on the criteria for Service Level 'C' limits from ASME Code, Section III, Subsection NG [7]. The inertia loading for off-normal events is a 1.5g vertical acceleration and a 0.707g (0.5g in each transverse direction) transverse acceleration

For off-normal events of storage, a 1.5g acceleration (a) is applied to the basket in the axial direction. Using a bounding weight of 24,000 lb for the BWR basket, the maximum stress in the fuel tube in the axial direction is calculated. Conservatively assuming the entire basket weight is carried through the fuel tubes, the stress in the tube due to the axial acceleration is as follows.

$$\sigma_{tube} = \frac{P_{tube}}{A} = \frac{800}{6.1} = 0.13 \text{ ksi}$$

where:

$$P_{tube} = \frac{W \times a}{n} = \frac{24,000 \times 1.5}{45} = 800 \text{ lb}$$

W = 24,000 lb -----Bounding basket weight

N = 45 -----Number of fuel tubes

a = 1.5g -----Inertia g-load

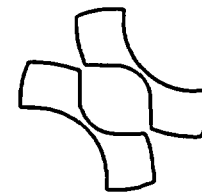
A = 6.1 inch² -----Tube cross-sectional area

The maximum stresses due to transverse loading (S_{tran}), from the finite element analysis results, are as follows. The combined maximum stress intensity (S_{tot}) is conservatively obtained by adding the maximum stresses due to axial load (σ_{tube}) to the maximum stresses due to transverse load (S_{tran}). The combined stresses and factors of safety are presented in the following table. The allowable stresses for the off-normal events (Level C) are $1.5S_m$ for membrane stresses and $2.25S_m$ for membrane plus bending stresses.

Component	S_{tran} , ksi	S_{tot} , ksi	S_{allow} , ksi	FS
Fuel Tube, P_m	7.8	7.9	32.10	4.06
Fuel Tube, $P_m + P_b$	10.9	11.0	48.15	4.38
Support Weldment, P_m	0.5	0.7	32.10	Large
Support Weldment, $P_m + P_b$	7.3	7.5	48.15	6.42

The weight of the fuel tubes is supported on connector pins. Referring to Figure 3.7-10, the interior tubes (Tube #4, typical) are supported by four connector pins, the side fuel tubes (Tube #1, typical) are supported by two connector pins and the side and corner weldments, and the corner fuel tubes (Tube #5, typical) are supported by three connector pins. The bearing stress (σ_{brg}) on the fuel tube is as follows.

$$\sigma_{brg} = \frac{1.5 \times P_{pin}}{A_{brg}} = \frac{1.5 \times 233}{0.34} = 1.0 \text{ ksi}$$



Bearing area of Fuel Tube and Connector Pin Intersection

where:

$A_{brg} = 0.34 \text{ inch}^2$ -----Bearing area

$P_{pin} = \frac{1}{3}P_t + \frac{1}{4}P_t = 233 \text{ lb}$ -----Combined loading on one pin

$P_t = 400 \text{ lb}$ -----Fuel tube weight

The factor of safety (FS) for bearing is as follows.

$$FS = \frac{S_y}{\sigma_{brg}} = \frac{32.3}{1.0} = \text{Large}$$

where:

$$S_y = 32.3 \text{ ksi} \text{ -----Yield strength, SA-537 Class 1, at } 700^\circ\text{F}$$

The bearing stress (σ_{brg}) in the connector pin at the TSC bottom plate, conservatively using P_{tube} as previously determined, is as shown.

$$\sigma_{brg} = \frac{P_{tube}}{A_{brg}} = \frac{800}{0.75} = 1.1 \text{ ksi}$$

where:

$$A_{brg} = \frac{\pi}{4}(D_o^2 - D_i^2) = \frac{\pi}{4}(1.0^2 - 0.19^2) = 0.75 \text{ inch}^2$$

$$D_o = 1.00 \text{ inch}$$

$$D_i = 0.19 \text{ inch}$$

The factor of safety (FS) for bearing is as follows.

$$FS = \frac{S_y}{\sigma_{brg}} = \frac{24.7}{1.1} = \text{Large}$$

where:

$$S_y = 24.7 \text{ ksi} \text{ -----Yield strength, SA-240 Type 304, at } 700^\circ\text{F}$$

The weight of the side and corner weldments is carried through to the TSC bottom plate by supports at the bottom of the basket. The corner weldment is bounding for the top and bottom supports. The dimensions for the corner support weldment are 8.0-inch length and 0.375-inch thickness. The bounding weight of the corner weldment is 1,100 pounds. The corner weldment also supports one-quarter of the weight of four fuel tubes (conservatively 400 lb per tube). The bearing stress is as follows.

$$\sigma_{brg} = \frac{W_{sup}}{A_{sup}} = 0.8 \text{ ksi}$$

where:

$$W_{sup} = 1.5 \times (1,100 + 4 \times (0.25 \times 400)) = 2,250 \text{ lb}$$

$$A_{sup} = 8.0 \times 0.375 = 3.0 \text{ inch}^2$$

The factor of safety (FS) for bearing is as follows.

$$FS = \frac{S_y}{\sigma_{brg}} = \frac{32.3}{0.8} = \text{Large}$$

where:

$$S_y = 32.3 \text{ ksi} \text{ -----Yield strength, SA-537 Class 1, at } 700^\circ\text{F}$$

The buckling evaluation of the connector pin is performed in Section 3.7.2.1. The accident condition buckling evaluation is bounding due to the 60g axial inertia loading.

During off-normal events of storage, the only load on the attachment bolts is due to preload. The analysis presented in Section 3.5.2.2 is bounding; therefore, no additional bolt analysis is required.

From the finite element results for off-normal handling, the maximum shear load in the basket attachment bosses is 1,370 pounds. The attachment bosses have been evaluated in Section 3.5.2.2 (normal conditions) for a shear load of 1,379 lb, which bounds the maximum shear load of 1,370 lb for off-normal events. Therefore, no additional analysis is required.

The analysis presented in Section 3.7.2.2 bounds the off-normal analysis of the neutron absorber and retainer strip; therefore, no additional analysis is required.

3.6.3 Concrete Cask Evaluation for Off-normal Events

Section 3.5.3.1 presents the thermal stress evaluation for normal conditions for the concrete cask. The analysis used the 106°F ambient condition thermal gradient, which is the off-normal event; therefore, the analysis is conservative. The analysis bounds both the normal and off-normal events; therefore, no thermal stress evaluation is presented in this section. All analyses of the concrete cask are bounded by the analyses presented in the normal and accident sections

Table 3.6-1 TSC Off-Normal Events, P_m Stresses

Load Case	Service Level	Section ^{a)}	Component Stresses (ksi) ^{b)}						S_{int}	S_{allow}	FS
			S_x	S_y	S_z	S_{xy}	S_{yz}	S_{xz}			
Off-Normal Pressure + Normal Handling	B	3	0.00	-8.29	5.63	-0.27	-0.04	0.89	14.07	22.00	1.56
Normal Pressure + Off-Normal Handling	C	3	0.05	-8.50	5.59	0.03	-0.14	0.87	14.23	24.50	1.72

Table 3.6-2 TSC Off-Normal Events, $P_m + P_b$ Stresses

Load Case	Service Level	Section ^{a)}	Component Stresses (ksi) ^{b)}						S_{int}	S_{allow}	FS
			S_x	S_y	S_z	S_{xy}	S_{yz}	S_{xz}			
Off-Normal Pressure + Handling	B	11	29.25	29.23	5.87	0.09	4.36	0.75	25.02	33.00	1.32
Normal Pressure + Off-Normal Handling	C	1	2.47	-4.01	20.32	-0.09	-0.19	0.28	24.34	35.40	1.45

Table 3.6-3 TSC Off-Normal Events, $P + Q$ Stresses

Load Case	Service Level	Section ^{a)}	Component Stresses (ksi) ^{b)}						S_{int}	S_{allow}	FS
			S_x	S_y	S_z	S_{xy}	S_{yz}	S_{xz}			
Off-Normal Pressure + Normal Handling + Thermal	B	2	1.32	-18.21	-35.37	0.00	0.00	-1.80	36.86	60.00	1.63

^{a)} See Figure 3.C-2 for section cut locations.

^{b)} The x,y,z component of stress are to be interpreted radial, circumferential, and axial directions, respectively.

3.7 Storage Accident Events

This section presents the analyses of the structural components of MAGNASTOR for storage accident events. MAGNASTOR is evaluated using finite element models and classical hand calculations for the TSC, fuel baskets, and concrete cask.

3.7.1 TSC Evaluations for Storage Accident Conditions

The TSC is analyzed for an accident pressurization of 250 psig, a 24-inch end drop of the concrete cask, and the hypothetical concrete cask tip-over accident.

3.7.1.1 Accident Pressurization

Accident pressurization is a hypothetical event that assumes the failure of all of the fuel rods contained within the TSC. No postulated storage condition is expected to lead to the rupture of all fuel rods. The TSC is analyzed for accident pressurization and dead weight loads using the finite element model and conditions described in Appendix 3.C. Dead weight is simulated by applying a 1.0g acceleration load in the axial direction in conjunction with pressure being applied to the TSC bottom plate to simulate the weight of the basket and fuel. To represent the accident pressure, an internal pressure of 250 psig is applied to all inner surfaces of the TSC. The canister bottom plate, which is resting on the pedestal plate is conservatively subjected to the 250 psig pressure and the dead weight of the fuel and basket.

The resulting TSC stresses for the accident pressurization condition are summarized in Table 3.7-1 and Table 3.7-2 for primary membrane and primary membrane plus primary bending stress categories, respectively. The minimum factor of safety of 1.75 occurs at Section 11 for the P_m+P_b stresses. The locations for the stress sections are shown in Appendix 3.C.

Results of analysis of this event demonstrate that the TSC is not significantly affected by the increase in internal pressure that results from the hypothetical rupture of all PWR or BWR fuel rods in the TSC.

3.7.1.2 Concrete Cask 24-inch End-Drop

This section addresses the TSC stresses and potential TSC shell buckling associated with the postulated 24-inch end-drop accident of the concrete cask. The evaluation of the TSC during the end impact is performed using an inertial load of 60g. This inertial load conservatively bounds the maximum calculated acceleration including dynamic load factor (DLF).

3.7.1.2.1 TSC End Impact Stress Evaluation

The TSC is analyzed for the concrete cask 24-inch drop accident condition using the finite element model described in Appendix 3.C. The 24-inch drop is simulated by applying a 60g acceleration load in the axial direction with pressure applied to the TSC bottom plate to simulate the inertial load of the basket and fuel. To represent the normal pressure, an internal pressure of 110 psig is applied to all inner surfaces of the TSC. The canister bottom plate, which is resting on the pedestal plate is conservatively subjected to the pressure due to the 60g inertia of the basket and fuel, as well as the 110 psig internal pressure.

The resulting maximum stresses in the TSC for the 24-inch drop accident events are summarized in Table 3.7-1 and Table 3.7-2 for primary membrane, and primary membrane plus primary bending stress categories, respectively. The minimum factor of safety of 3.61 occurs at section 4 (lower TSC shell) for the P_m stresses. The locations for the stress sections are shown in Appendix 3.C.

3.7.1.2.2 TSC Buckling Evaluation

During the 24-inch bottom-end drop of the concrete cask, the 60g inertial load conservatively applied to the closure lid assembly generates longitudinal compressive stresses in the TSC shell. The critical buckling stress (S_{CR}) in the TSC shell based on the TSC geometry and material properties is as follows.

$$S_{CR} = E \frac{0.605 - 10^{-7} m^2}{m(1 + 0.004\phi)} = 34.5 \text{ ksi} \quad [16]$$

where:

$E = 25.8 \times 10^3 \text{ ksi}$ ----- Modulus of elasticity of SA-240, Type 304, at 500°F

$\phi = \frac{E}{S_y} = 1,330$ ----- Inverse strain parameter

$S_y = 19.4 \text{ ksi}$ ----- Yield strength of SA-240, Type 304, at 500°F

$m = \frac{r_m}{t} = 71.5$ ----- Mean radius to thickness ratio

$r_m = 35.75 \text{ inch}$ ----- Mean radius TSC shell

$t = 0.5 \text{ inch}$ ----- Thickness of TSC shell

The results from the 24-inch end-drop analysis are screened for the maximum longitudinal compressive stress. The maximum longitudinal compressive stress, S_z , of 9.2 ksi occurs at the

intersection of the TSC shell and bottom plate (See Appendix 3.C). The factor of safety (FS) is as follows.

$$FS = \frac{S_{CR}}{S_z} = \frac{34.5 \text{ ksi}}{9.2 \text{ ksi}} = 3.8$$

Therefore, buckling of the TSC does not occur.

3.7.1.3 Concrete Cask Tip-Over

The TSC is analyzed for the concrete cask tip-over using the finite element model described in Appendix 3.C. A 40g inertial load is conservatively used in the evaluation of the loaded TSC. This value bounds the calculated maximum g-load for the TSC during the concrete cask tip-over event including the dynamic load factor (Section 3.7.3.7).

The resulting maximum stresses in the TSC for tip-over conditions are summarized in Table 3.7-1 and Table 3.7-2 for primary membrane and primary membrane plus primary bending stress categories, respectively. The minimum factor of safety of 1.85 occurs at Section 1 for the P_m stresses. The locations for the stress sections are shown in Appendix 3.C. Note that the maximum stresses occur at the section cut at the 0-degree location.

3.7.1.4 Flood

This evaluation considers design basis flood conditions of a 50-foot depth of water having a velocity of 15 feet per second. The hydrostatic pressure (P_h) exerted on the TSC during a 50-foot flood event is as follows.

$$P_h = \rho \times h = \left(62.4 \frac{\text{lb}}{\text{ft}^3}\right) \left(\frac{1 \text{ ft}^3}{1728 \text{ in}^3}\right) \times (50 \text{ ft}) \left(\frac{12 \text{ in}}{1 \text{ ft}}\right) = 22 \text{ psi}$$

where:

$$\begin{aligned} \rho &= 62.4 \text{ lb/ft}^3 \text{-----Density of water} \\ h &= 50 \text{ ft} \text{-----Immersion depth} \end{aligned}$$

During normal conditions, the TSC is evaluated for an internal pressure of 110 psig. Because the pressure differential is reduced during flood conditions ($110 - 22 = 88$ psig), stresses in the TSC shell are reduced. Therefore, the hydrostatic pressure exerted by the 50-foot depth of water actually reduces the stress in the TSC. MAGNASTOR is therefore, not adversely affected by the design basis flood.

3.7.1.5 Tornado and Tornado-driven Missiles

The postulated tornado wind loading and tornado missile impacts are not capable of overturning the concrete cask, or penetrating the boundary established by the concrete cask. Consequently, there is no effect on the TSC. Stresses resulting from the decreased external pressure due to a tornado are bounded by the stresses due to the accident internal pressure condition evaluated in Section 3.7.1.1.

3.7.2 Fuel Baskets Evaluation for Storage Accident Events

3.7.2.1 PWR Basket

3.7.2.1.1 24-inch Concrete Cask End Drop

For the 24-inch concrete cask drop, a 60g acceleration (a) is conservatively applied to the PWR basket in the axial direction. The basket is evaluated using classical hand calculations. Using a bounding weight of 22,500 lb for the PWR basket, the maximum stress in the fuel tube is calculated. Factors of safety for the PWR basket are calculated based on the criteria for Service Level 'D' limits from ASME Code, Section III, Subsection NG [7] and Appendix F [8]. Conservatively assuming the entire basket weight is carried through the fuel tubes, the stress in the tube is as follows.

$$\sigma_{\text{tube}} = \frac{P_{\text{tube}}}{A} = \frac{64286}{11.4} = 5.6 \text{ ksi}$$

where:

$$P_{\text{tube}} = \frac{W \times a}{n} = \frac{22,500 \times 60}{21} = 64,286 \text{ lb}$$

W = 22,500 lb -----Bounding basket weight
n = 21 -----Number of fuel tubes
A = 11.4 inch²-----Tube cross-sectional area

The factor of safety (FS) is as follows.

$$FS = \frac{0.7 \times S_u}{\sigma_{\text{tube}}} = \frac{0.7 \times 68.4}{5.6} = 8.6$$

where:

S_u = 68.4 ksi -----Ultimate strength, SA-537 Class 1, at 700°F

The weight of the fuel tubes is supported by connector pins. Referring to Figure 3.7-1 the interior tubes (Tube #4, typical) are supported by four connector pins, the side fuel tubes (Tube #1, typical) are supported by two connector pins and the side and corner weldments, and three connector pins support the corner fuel tubes (Tube #3, typical). The load is transferred by shear through the connector pin welds (four welds on two connector pins, which attaches them to the fuel tube at bottom of basket) and by axial compression through the area of the end of the fuel tube in contact with the connector pin assembly which rests on the bottom canister plate.

The load capability (P_{joint}) of the weld and the common area is determined by the sum of the loads, which each load path can sustain. A conservative evaluation is performed in which the stresses are evaluated against allowables associated with an elastic evaluation as opposed to the plastic evaluation permitted in Appendix F [8].



Common Area of Fuel
 Tube
 and Connector Pin

$$P_{joint} = A_m (0.7S_u) + A_w (wf \times 0.42S_u) = 25.3 \text{ kips}$$

where:

- $A_m = 0.21 \text{ inch}^2$ ----- Common area for compression
- $A_w = 4(l_w t_w) = 1.52 \text{ inch}^2$ ----- Weld area for shear
- $l_w = 2.0 \text{ inch}$ ----- Connector pin length
- $t_w = 3/16 \text{ inch}$ ----- Weld size
- $wf = 0.35$ ----- Weld quality factor visual inspection
 (ASME Code Section III, Subsection NG, Article NG-3352)
- $S_u = 68.4 \text{ ksi}$ ----- Tensile strength, SA-537 Class 1, at 700°F

The load in the tube joint (P) is as follows.

$$P = 60 \times P_{pin} = 60 \times 394 = 23.6 \text{ ksi}$$

where:

- $P_{pin} = \frac{1}{3}P_t + \frac{1}{4}P_t = 394 \text{ lb}$
- $P_t = 675 \text{ lb}$ ----- Tube weight

The factor of safety (FS) is as follows.

$$FS = \frac{P_{joint}}{P} = \frac{25.3}{23.6} = 1.07$$

The weight of the side and corner weldments is carried through to the TSC base plate by supports at the bottom of the weldments. The bounding dimensions for the supports of the weldments are 5.0-inch length and 0.3125-inch thickness (corner weldment). The maximum weight of one

weldment is 800 lb (bounding, side weldment). The weldment supports one-quarter the weight of two fuel tubes (675 lb per tube, bounding). The membrane stress (σ_m) is as follows.

$$\sigma_m = \frac{60 \times W_{sup}}{A_{sup}} = \frac{60 \times 1,138}{1.56} = 43.8 \text{ ksi}$$

where:

$$W_{sup} = 800 + 2 \times (0.25 \times 675) = 1138 \text{ lb}$$

$$A_{sup} = 5.0 \times 0.3125 = 1.56 \text{ inch}^2$$

The factor of safety (FS) is as follows.

$$FS = \frac{0.7S_u}{\sigma_m} = \frac{0.7 \times 68.4}{43.8} = 1.09$$

where:

$$S_u = 68.4 \text{ ksi} \text{ ----- Ultimate strength, SA-537 Class 1, at } 700^\circ\text{F}$$

The thirty-two basket connector pins support the PWR basket during a 60g bottom-end drop accident. The bounding temperature at the bottom of the basket is 500°F. The pins are subjected to compressive loads; therefore, a buckling evaluation of the pins is presented as follows. The load on one connector pin (P_{pin}) is as follows.

$$P_{pin} = \frac{W \times 60}{n} = \frac{22500 \times 60}{32} = 42.2 \text{ kips}$$

where:

$$W = 22,500 \text{ lb} \text{ ----- Bounding basket weight}$$

$$n = 32 \text{ ----- Number of pins}$$

Using the Euler buckling theory, the critical buckling load (P_{cr}) is as follows.

$$P_{cr} = \frac{\pi^2 EI}{(KL)^2} = \frac{\pi^2 \times (25.8 \times 10^6) \times 0.015}{(2 \times 3.0)^2} = 106.0 \text{ kip [9]}$$

where:

$$A_{pin} = 0.44 \text{ inch}^2$$

$$D = 0.75 \text{ inch} \text{ ----- Pin diameter}$$

$$L = 3.0 \text{ inch} \text{ ----- Pin length}$$

$$I = \frac{\pi r^4}{4} = 0.015 \text{ inch}^4$$

$$K = 2.0 \text{-----Buckling constant, clamped-free}$$
$$E = 25.8 \times 10^6 \text{ psi-----SA-240 Type 304, at } 500^\circ\text{F}$$

The factor of safety (FS) for buckling of the connector pins is as follows.

$$FS = \frac{P_{cr}}{P_{pin}} = \frac{106.0 \text{ kip}}{42.2 \text{ kip}} = 2.51$$

PWR Neutron Absorber Evaluation

For the end-drop impact, the governing stress is the shearing stress in the BWR fuel tube neutron absorber presented in Section 3.7.2.2.1. Therefore, no evaluation of the PWR neutron absorber is presented for an end impact.

3.7.2.1.2 Concrete Cask Tip-over

The analysis results for the PWR basket subjected to a hypothetical concrete cask tip-over accident are presented in this section. Factors of safety for the PWR basket are calculated based on the criteria for Service Level 'D' limits from ASME Code, Section III, Subsection NG [7] and Appendix F [8].

PWR Fuel Tube Evaluation

The PWR basket fuel tubes are analyzed for a tip-over accident using the two-dimensional plane strain plastic finite element models described in Appendix 3.A. The fuel tube is conservatively evaluated for 40g side impact load.

Plastic stress intensities are calculated for the PWR fuel tubes for the bounding basket orientations of 0° and 45° (see Figure 3.7-1 through Figure 3.7-4 for tube ID and locations for stress evaluations.) The maximum membrane and membrane plus bending nodal stress intensities for each fuel tube are reported in Table 3.7-3. Note that for a plastic analysis, ANSYS reports stresses in the elastic region as the yield strength (31.7 ksi at 500°F) for the stress-strain curve.

The ANSYS plastic finite element model follows the material stress strain curve and allows for nonlinear behavior above the yield strength point. The stress allowables for plastic analysis are based on ASME Code, Section III, Appendix F. The allowable membrane stress is $0.7S_u$. The allowable primary stress intensity is $0.9S_u$. The minimum factors of safety (45° basket orientation) for the fuel tubes are 1.28 for membrane stresses and 1.48 for primary stress intensity. The critical stress locations occur in the fuel tube corners.

The fuel tubes are constructed by welding two tube halves together using a full penetration weld for the length of the fuel tube. A surface MT weld examination per ASME Code, Section III,

Subsection NG, Article NG-5232 is used, which has a 0.65 weld quality factor (wf). From the plastic analysis of the PWR basket, the maximum membrane and membrane plus bending stress intensity at a tube weld is 10.3 ksi and 31.72 ksi respectively. The factors of safety (FS) for the weld are as follows.

Membrane:

$$FS = \frac{0.7S_u \times wf}{\sigma} = 3.02$$

Membrane plus bending:

$$FS = \frac{0.9S_u \times wf}{\sigma} = 1.26$$

where:

$$S_u = 68.4 \text{ ksi} \text{-----Ultimate strength, SA-537 Class 1, at } 700^\circ\text{F}$$

ASME Code, Appendix F-1336 [8] provides guidelines for a bearing stress analysis of pinned joints. Bearing on the pin only occurs for the 0° basket orientation. For the 45° basket orientation, the load between adjacent fuel tubes is reacted out in bearing on the tube corner flats. Using the 0° basket orientation, the maximum bearing stress (σ_{brg}) is as follows.

$$\sigma_{brg} = \frac{P}{l_{brg} l_{pin}} = 82.4 \text{ ksi}$$

where:

$$P = \left(\frac{n_f}{2} \times W_f + \frac{n_t}{2} \times W_t \right) \times a = 56,000 \text{ lb}$$

$$a = 40\text{g}$$

$$n_f = 11 \text{-----Number of fuel assemblies contributing to maximum bearing load on pin (2 pins per tube react load)}$$

$$n_t = 6 \text{-----Number of fuel tubes contributing to maximum bearing load on pin (2 pins per tube react load)}$$

$$l_{brg} = 0.34 \text{ inch-----Effective bearing arc length (25\% of pin circumference)}$$

$$l_{pin} = 2.0 \text{ inch-----Length of pin}$$

$$W_t = W_{tube} \frac{L_{pin}}{L_{tube}} = 78 \text{ lb}$$

$$W_{tube} = 675 \text{ lb-----Fuel tube weight}$$

$$L_{pin} = 20 \text{ inch} \text{ ----- Length of periodic section (center to center distance between pins)}$$

$$L_{tube} = 173.5 \text{ inch} \text{ ----- Length of fuel tube}$$

$$W_f = W_{fuel} \frac{L_{pin}}{L_{fuel}} = 212 \text{ lb}$$

$$W_{fuel} = 1,680 \text{ lb} \text{ ----- Maximum PWR fuel weight}$$

$$L_{pin} = 20 \text{ inch} \text{ ----- Length of periodic section}$$

$$L_{fuel} = 158.6 \text{ inch} \text{ ----- Shortest fuel assembly length}$$

The factor of safety (FS) is as follows.

$$FS = \frac{2.1S_u}{\sigma_{brg}} = 1.74$$

where:

$$S_u = 68.4 \text{ ksi} \text{ ----- Ultimate strength, SA-537 Class 1, at } 700^\circ\text{F}$$

The 45° basket orientation does not produce shear loads in the pins, the load between adjacent fuel tubes is reacted out directly in bearing in the corner flats; therefore, the maximum shear loads on the pins occurs in the 0° basket orientation. The pins react shear loads between adjacent tubes. The maximum shear stress (τ_{pin}) in the pin during a tip-over accident is as follows.

$$\tau_{pin} = \frac{P}{Dl_{pin}} = 11.4 \text{ ksi}$$

where:

$$P = 10,000 \text{ lb} \text{ ----- Bounding maximum shear load on pin}$$

$$D = 0.44 \text{ inch} \text{ ----- Pin diameter}$$

$$l_{pin} = 2.0 \text{ inch} \text{ ----- Length of pin}$$

The factor of safety (FS) is as follows.

$$FS = \frac{0.42S_u}{\tau_{pin}} = 2.58$$

where:

$$S_u = 70.0 \text{ ksi} \text{ ----- Ultimate strength, SA-695 Type B Gr 40, at } 700^\circ\text{F}$$

PWR Neutron Absorber and Retainer

The PWR neutron absorber and retainer are conservatively evaluated for a 60g side-impact load and for the concrete cask tip-over event. The retainer strip assembly consists of a retainer strip and corner clips, both are made of 304 stainless steel. The strip is supported by a single row of weld posts placed every ten inches along the inside of the fuel tube.

The neutron absorber is supported by the retainer strip at the inside surface of the fuel tube. The pitches of the slotted holes in the neutron absorber are the same as the holes in the retainer strip. The slotted holes are used to prevent interference during differential thermal expansion. Two corner clips support the edges of the neutron absorber. The head of the weld posts supporting the retainer strip are engaged in the recessed conical pockets of the retainer. The corner clip restrains the edge of the retaining strip against the fuel tube.

As shown in Figure 3.7-19, a quarter symmetry finite element model is generated to represent a quarter of the ten-inch periodic section for the PWR design. The model is comprised of the retainer strip with the conical slot, the neutron absorber, and the weld post. Inelastic properties are employed for the stainless steel retainer strip and the neutron absorber at 700°F to adequately represent the stiffness at the maximum temperature condition. To provide a bounding minimal stiffness for the neutron absorber, properties for 1100 series aluminum were used. The weld post was modeled as being rigid to maximize deformation of the conical shaped section of the retainer by the weld post. Symmetry conditions were imposed along the planes of symmetry, and the effect of the corner clip was represented by constraining the edge in contact with the corner clip. The parts are modeled independently and the automatic contact surface option in LS-DYNA was used between the parts to transfer load between the neutron absorber, the retainer, the weld post, and the edge restraints. The evaluation of the side impact was performed using LS-DYNA and the impact was simulated by imposing the acceleration time history whose maximum acceleration was 60g's. This conservatively envelops the maximum tip over acceleration of 40g's.

Since the function of the retainer is to maintain the neutron absorber in its position, the criteria for the retainer is to limit the motion of the neutron poison during and after the impact. This is confirmed by considering the permanent strains and the permanent set of the retainer. Figure 3.7-20 shows the strain after the impact, which is the permanent set in the retainer. The strain of 0.02%, which is minimal, is observed to be localized to the conical shape hole. Since inelastic strains are not recovered, this indicates that maximum inelastic strain during the impact is also limited to 0.02%. Such a minimal strain level indicates that the conical pocket retains its configuration for the weld post to restrain the retainer. The final displacement of the retainer strip is computed to be 0.01 inch, which is consistent with the minimal plastic strain in the retainer.

This also confirms that the retainer remains engaged with the weld post during and after the impact. The maximum permanent set of 0.01 inch, which is less than the thickness of the retainer, and only 10% of the thickness of the neutron absorber indicates that the neutron absorber remains in its original configuration.

The peak force on the weld post determined from the analysis is 35 pounds. The shear area governs the capacity of the weld. The depth of the weld (h) is 0.13 inch. The diameter of the weld post (D) is 0.25 inch. The governing stress is the shear stress in the base material. The allowable shear stress for the accident condition is $0.42\Phi_u$. The ultimate strength (Φ_u) of the base material (SA240, Type 304) is 63,200 psi. The weld capacity, F_{cap} , is calculated as shown in the following.

$$\begin{aligned} F_{cap} &= 0.42 \times n \times \Phi_u \times h \times BD \\ &= 0.42 \times 0.3 \times 63,200 \times 0.13 \times (3.1416 \times 0.25) \\ &= 813 \text{ lb} \end{aligned}$$

where:

$n = 0.3$ ----- The design factor per ASME Code, Section III, Subsection NG, Table NG-3352-1 for the intermittent plug weld employing a surface visual examination method per NG-5260.

The factor of safety (FS) is as follows.

$$FS = \frac{813}{35} = 23$$

For the corner clip weld the peak force on the edge support is 58 pounds. The length of the edge support is ten inches per periodic section. The plug welds supporting the corner clip are installed along every five inches of the fuel tube corner. Two plug welds support each periodic section of the corner clip. The peak force on each plug weld is 29 pounds. The shear capacity of the base metal in the corner clip governs the weld capacity. The allowable shear stress for the accident condition is $0.42\Phi_u$. The ultimate strength (Φ_u) of the base material (SA240, Type 304) is 63,200 psi. The thickness of the corner clip is 0.048 inch. The diameter of the plug weld is 0.13 inch. The weld capacity, F_{cap} , is calculated as shown in the following.

$$\begin{aligned} F_{cap} &= 0.42 \times n \times \Phi_u \times t \times (BD) \\ &= 0.42 \times 0.3 \times 63,200 \times 0.048 \times (3.1416 \times 0.13) \end{aligned}$$

$$= 156 \text{ lb}$$

where:

$$n = 0.3 \text{-----The design factor per ASME Code, Section III, Subsection NG, Table NG-3352-1 for the intermittent plug weld employing a surface visual examination method per NG-5260.}$$

The factor of safety (FS) is as follows.

$$FS = \frac{156}{29} = 5.4$$

PWR Corner Support Weldment Evaluation

The PWR basket corner support weldment is analyzed for the tip-over accident using the three-dimensional periodic finite element model and boundary conditions described in Appendix 3.A. The corner support weldment is comprised of two major components: the mounting plate (vertical plate) and the side support bars, which are located on five-inch centers.

The analysis results for the mounting plate are presented in Table 3.7-4 and Table 3.7-5. Figure 3.7-5 and Figure 3.7-6 show the location of the section cuts for the 0° and 45° basket orientations. The minimum factors of safety for the corner support weldment mounting plates are 3.74 for membrane stresses and 1.71 for membrane plus bending stresses.

For the support bars, the beam forces and moments are extracted from the finite element model from which the membrane and bending stresses are calculated. At the welded joint of the support bar and mounting plate, the bar is evaluated using a plastic analysis in accordance with ASME Code, Section III, Appendix F. At the midpoint of the support bars, the bars are analyzed using elastic stress equations. The stresses in the bar are calculated using the following classical formulas.

$$\sigma_m = \frac{F_x}{A} = \frac{F_x}{bt}$$

$$\tau_{yz} = \frac{F_{yz}}{A} = \frac{F_{yz}}{bt}$$

$$\sigma_{b, \text{elastic}} = \frac{Mc}{I} = \frac{6M}{bt^2}$$

$$\sigma_{b, plastic} = \frac{Mc}{KI} = \frac{6M}{Kbt^2}$$

where:

$$K = 1.5 \text{ ----- Shape factor for plastic bending [13 and 10]}$$

The maximum load at the welded joints between the support bar and corner mounting plate occurs in the 45° basket orientation. The axial load (F_x) in the bar is -2,676 lb, the shear load (F_{yz}) is 980 lb, and the bending moment (M) is 7,375 inch-lb. The stress intensity (σ_{int}) in the bar at the welded joint is as follows.

$$\sigma_{int} = \sqrt{\sigma_b^2 + 4\tau_{yz}^2} = 47.6 \text{ ksi}$$

where:

$$\sigma_b = \frac{F_x}{A} \pm \frac{6M}{Kbt^2} = 47.5 \text{ ksi}$$

$$\tau_{yz} = \frac{F_{yz}}{A} = \frac{980}{0.875^2} = 1.3 \text{ ksi}$$

$$K = 1.5$$

$$b = 0.875 \text{ inch}$$

$$t = 0.875 \text{ inch}$$

The factor of safety (FS) is as follows.

$$FS = \frac{0.9S_u}{\sigma_{int}} = \frac{0.9 \times 70.0}{47.6} = 1.32$$

where:

$$S_u = 70.0 \text{ ksi ----- Ultimate strength, SA-695, Type B, Gr 40, at 700°F}$$

The maximum load at the center of the support bar span occurs in the 0° basket orientation. The axial load (F_x) in the bar is -3,296 lb, the shear load (F_{yz}) is 952 lb, and the bending moment (M) is 1,749 inch-lb. The stress intensity in the bar is as follows.

$$\sigma_{int} = \sqrt{\sigma_b^2 + 4\tau_{yz}^2} = 14.9 \text{ ksi}$$

where:

$$\sigma_b = \frac{F_x}{A} \pm \frac{6M}{bt^2} = 14.7 \text{ ksi}$$

$$\tau_{yz} = \frac{F_{yz}}{A} = 1.3 \text{ psi}$$

The factor of safety (FS) is as follows.

$$FS = \frac{S_u}{\sigma_{int}} = 4.7$$

where:

$$S_u = 70.0 \text{ ksi} \text{ ----- Ultimate strength, SA-695, Type B, Gr 40, at } 700^\circ\text{F}$$

The support bar is a continuous bar that is bent at the ridge gusset. The support bars are welded to the corner mounting plate where cutouts in the corner mounting plate accept the end of the bars. The bars are welded to the wall on the backside with a minimum 1/4-inch groove weld using the visual inspection criteria per ASME Code, Section III, Subsection NG, Article NG-5260. A weld quality factor of 0.35 is applied based on visual inspection of the weld per ASME Code, Section III, Subsection NG, Article NG-3352.

The welds only carry the axial load in the bar. Bending and shear loads are carried in the corner assembly mounting plate directly. The maximum axial load in the support bar is -5,554 lb, for the 0° basket orientation. The weld stress intensity (σ_{weld}) is as follows.

$$\sigma_{weld} = \frac{P}{A} = \frac{5554}{0.875^2} = 7.3 \text{ ksi}$$

The factor of safety (FS) for the weld is as follows.

$$FS = \frac{0.35(0.42S_u)}{\sigma_{weld}} = 1.38$$

where:

$$S_u = 68.4 \text{ ksi} \text{ ----- Ultimate strength, SA-537 Class 1, at } 700^\circ\text{F}$$

The ridge gusset is welded to the corner mounting plate with 1/8-inch flair bevel welds on both sides of the plate. The weld uses the visual inspection criteria per ASME Code, Section III, Subsection NG, Article NG-5260 and quality factor of 0.35, as defined previously. The support bar intersects the ridge gusset at 11° and generates a load that is reacted out by the ridge gusset and ridge gusset/mounting plate weld. A compressive load in the support bar produces a load (P_{kick}) that results in the ridge gusset/mounting plate weld being in tension. Additionally, the moment (M_z) acting on the ridge gusset will also have to be reacted out by the weld. The total tensile load acting on the weld is the sum of these two loads.

From the finite element analysis results, the compressive forces (P) in the support bars at the ridge gusset are 2041 lb, 5024 lb, 5470 lb and 3324 lb. The bending moment (M_z) in the ridge gusset at the mounting plate is 2574 inch-lb. The stress in the weld (σ_{weld}) is as follows.

$$\sigma_{weld} = \frac{P_{weld}}{A_{wg}} = 8.2 \text{ ksi}$$

where:

$$P_{weld} = P_c + P_{kick} = 5148 + 3026 = 8,174 \text{ lb}$$

$$P_c = \frac{M_z}{t_{plate}} = \frac{2574}{0.5} = 5148 \text{ lb}$$

$$P_{kick} = (\sum P)(\sin\theta) = (5470 + 3324 + 2041 + 5024)\sin 11^\circ = 3026 \text{ lb.}$$

$$A_{wg} = t_{weld} \times l_{weld} = 0.125 \times 8.0 = 1.0 \text{ inch}^2$$

$$t_{weld} = \frac{1}{8}\text{-inch}$$

$$t_{plate} = 0.5 \text{ inch}$$

$$l_{weld} = 10.0 \text{ inch} - 2.0 \text{ inch} = 8.0 \text{ inch}$$

The factor of safety (FS) in the weld is as follows.

$$FS = \frac{0.35 \times S_u}{\sigma_{weld}} = 2.92$$

where:

$$S_u = 68.4 \text{ ksi} \text{ ----- Ultimate strength, SA-537 Class 1, at } 700^\circ\text{F}$$

PWR Side Support Weldment Evaluation

The PWR basket side support weldment is analyzed for the tip-over accident using the three-dimensional periodic finite element model and boundary conditions described in Appendix 3.A. The analysis results for the side support weldment are presented in Table 3.7-6 and Table 3.7-7. Figure 3.7-7 and Figure 3.7-8 show the location of the section cuts for the 0° and 45° basket orientations. The minimum factors of safety for the corner support weldment mounting plates are 3.42 for membrane stresses and 1.43 for membrane plus bending stresses.

PWR Side and Corner Weldment / Fuel Tube Attachment Evaluation

The corner and side support weldments are the primary structure that maintains the geometry of the fuel tube array during a hypothetical tip-over accident. The support weldments are bolted to the fuel tubes at sixteen circumferential locations. The boss and bolt connection is designed so

that the bolts are only loaded in tension, including preload. Otherwise, the support weldments apply a bearing load on the fuel tube array.

A review of the modeled attachment locations in the 0° and 45° basket orientation finite element models show that the concrete cask tip-over accident does not apply additional tensile loads to the attachment, because the gap elements between weldments and fuel tubes are closed at boss locations. The bolt and washer evaluation is bounded by the normal conditions analysis presented in Section 3.5.2.1. The bosses transfer shear loads between the support weldments and fuel tube array. The maximum shear load on a boss is 24.4 kip. The outer diameter of the boss is 1.25 inch and the inner diameter is 0.625 inch. The shear stress on the boss is as follows.

$$\tau_{\text{boss}} = \frac{P}{A} = \frac{24.4}{0.92} = 26.5 \text{ ksi}$$

The factor of safety (FS) is as follows.

$$FS = \frac{0.42S_u}{\tau_{\text{boss}}} = \frac{0.42 \times 70.0}{26.5} = 1.11$$

where:

$$S_u = 70.0 \text{ ksi} \text{----- Ultimate strength, SA-695, Type B, Gr 40, at } 700^\circ\text{F}$$

Loads between the fuel tube array and the corner and side weldments are reacted out in shear and bearing in the support weldments. Bearing stresses are not considered for accident events. Due to the geometry of the basket, the cutout in the corner support weldments has an edge distance less than two times the diameter of the cutout. The shear stress in the corner weldment mounting plate is as follows.

$$\tau = \frac{P}{A_{\text{shear}}} = \frac{24.4}{1.14} = 21.4 \text{ ksi}$$

where:

$$A_{\text{shear}} = 2 \left[\frac{L_{\text{ed}}}{\sin 45^\circ} t_{\text{plate}} \right] = 1.14 \text{ inch}^2$$

$$L_{\text{ed}} = 1.30 \text{ inch} \text{-----Boss cutout edge distance in corner weldment}$$

$$t_{\text{plate}} = 0.31 \text{ inch} \text{-----Mounting plate thickness}$$

The factor of safety (FS) is as follows.

$$FS = \frac{0.42S_u}{\tau} = \frac{0.42 \times 68.4}{21.4} = 1.34$$

where:

$$S_u = 68.4 \text{ ksi} \text{ ----- Ultimate strength, SA-537 Class 1, at } 700^\circ\text{F}$$

PWR Fuel Basket Buckling Evaluation

For the hypothetical concrete cask tip-over accident, a buckling evaluation of the basket is performed. Due to the multiple components and load paths in the PWR basket, the buckling evaluation of the PWR basket used three different methodologies. All three buckling evaluations are conservative because they employ a constant acceleration along the length of the basket as opposed to a uniformly varying acceleration.

The first method is a buckling evaluation of the entire basket. It uses the ANSYS buckling solution and the three-dimensional periodic finite element models for the 0° and 45° basket orientations. The factor of safety against buckling for the PWR basket is 6.8 for the 0° basket orientation and 7.4 for the 45° basket orientation.

The second method is a buckling evaluation of a single fuel tube in the 0° basket orientation using a two-dimensional finite element model, as shown in Figure 3.7-9. Loads are applied to the fuel tube to represent a fuel tube at the bottom of the tube array during a tip-over accident for the 0° basket orientation (maximum stress on tube sidewalls). Figure 3.7-9 shows the boundary conditions and applied loads to the model. Similar to the basket buckling evaluation for the entire basket (first method), the tube buckling evaluation, conservatively neglects the tapered inertia loading of a tip-over accident. The factor of safety for fuel tube buckling is 1.90.

The final buckling evaluation of the PWR basket is a buckling evaluation of a side wall of the fuel tube per NUREG/CR-6322 [9]. Using the plane strain plastic finite element model the critical buckling of a fuel tube occurs in the 0° basket orientation (Tube 12, Figure 3.7-1). The applied loads on a side of the fuel tube are 3.21 kip/inch axial compression and 534 inch-lb/inch bending. The factor of safety is calculated based on the interaction Equations 31 and 32 inch NUREG/CR-6322. These two equations adopt the "Limit Analysis Design" approach for structural members subjected to stresses beyond the yield limit of the material. Methodology and equations for the buckling evaluation are summarized as follows.

Symbols and Units:

$$P = \text{Applied axial compressive loads, kips}$$

- M = Applied bending moment, kips-inch
P_a = Allowable axial compressive load, kips
P_{cr} = Critical axial compression load, kips
P_e = Euler buckling loads, kips
P_y = Average yield load, equal to profile area times specified yield strength, kips
C_c = Column slenderness ratio separating elastic and inelastic buckling
C_m = Coefficient applied to bending term in interaction equation
M_m = Critical moment that can be resisted in the absence of axial load, kip-inch
M_p = Plastic moment, kip-inch.
F_a = Axial compressive stress permitted in the absence of bending moment, ksi
F_e = Euler stress for a prismatic member divided by factor of safety, ksi
K = Ratio of effective column length to actual unsupported length
l = Unsupported length of member, inch
r = Radius of gyration, inch
S_y = Yield strength, ksi
A = Cross sectional area of member, inch²
Z_x = Plastic section modulus, inch³
λ = Allowable reduction factor, dimensionless.

From NUREG/CR-6322, the following interaction equations (Eqn. 31 and 32) are used for the evaluation of accident events.

$$\frac{P}{P_{cr}} + \frac{C_m M}{M_m \left[1 - \frac{P}{P_e} \right]} \leq 1.0$$

$$\frac{P}{P_y} + \frac{M}{1.18M_p} \leq 1.0$$

where:

$$P_{cr} = 1.7 \times A \times F_a$$

$$F_a = \frac{P_a}{A} \text{ for } P_a = P_y \left[\frac{1 - \frac{\lambda^2}{4}}{1.11 + 0.5\lambda + 0.17\lambda^2 - 0.28\lambda^3} \right]$$

and

$$\lambda = \frac{1}{\pi} \left(\frac{KI}{r} \right) \sqrt{\frac{S_y}{E}}$$

$$F_c = \frac{\pi^2 E}{1.30 \left(\frac{kl}{r} \right)^2}$$

$$P_c = 1.92 \times A \times F_c$$

$$P_y = S_y \times A$$

$$C_m = 0.85 \text{ for members with joint translation (sideways)}$$

$$M_p = S_y \times Z_x$$

$$M_m = M_p \left(1.07 - \frac{\left(\frac{1}{r} \right) \sqrt{S_y}}{3160} \right) \leq M_p$$

From NUREG/CR-6322 the factors of safety are calculated using the following equations.

$$P_1 = \frac{P}{P_{cr}}$$

$$M_1 = \frac{C_m M}{\left(1 - \frac{P}{P_c} \right) M_m}$$

$$P_2 = \frac{P}{P_y}$$

$$M_2 = \frac{M}{1.18} M_p$$

$$FS_1 = \frac{1}{P_1 + M_1}$$

$$FS_2 = \frac{1}{P_2 + M_2}$$

For the PWR basket fuel tube the following parameters are used in the buckling evaluation.

- $t = 0.31$ inch-----Tube thickness
 $b = 1.00$ inch-----Unit width
 $l = 8.20$ inch-----Sidewall length
 $K = 0.80$ -----Effective length factor
 $E = 27.3 \times 10^6$ psi-----Modulus of elasticity, SA-537 Class 1, at 700°F
 $S_y = 35.4$ ksi-----Yield strength, SA-537 Class 1, at 700°F

For $P = 3.21$ kip/inch and $M = 534$ inch-lb/inch (Tube 12, 0° basket orientation):

$$P_1 = \frac{P}{P_{cr}} = 0.19$$

$$M_1 = \frac{C_m M}{\left(1 - \frac{P}{P_c}\right) M_m} = 0.58$$

$$P_2 = \frac{P}{P_y} = 0.29$$

$$M_2 = \frac{M}{1.18} M_p = 0.52$$

The factors of safety are listed as follows.

$$FS_1 = \frac{1}{P_1 + M_1} = \frac{1}{0.19 + 0.58} = 1.30$$

$$FS_2 = \frac{1}{P_2 + M_2} = \frac{1}{0.29 + 0.52} = 1.23$$

3.7.2.2 BWR Fuel Basket

3.7.2.2.1 24-inch Concrete Cask End-Drop

For the 24-inch concrete cask drop, a 60g acceleration (a) is conservatively applied to the BWR basket in the axial direction. The basket is evaluated using classical hand calculations. Factors of safety for the BWR basket are calculated based on the criteria for Service Level 'D' limits from ASME Code, Section III Subsection NG [7] and Appendix F [8]. Using a bounding weight of 24,000 pounds for the BWR basket, the maximum stress in the fuel tube is calculated. Conservatively assuming the entire basket weight is carried through the fuel tubes, the stress in the tube is as follows.

$$\sigma_{\text{tube}} = \frac{P_{\text{tube}}}{A} \approx 5.3 \text{ ksi}$$

where:

$$P_{\text{tube}} = \frac{W \times 60}{n} = \frac{24,000 \times 60}{45} = 32,000 \text{ lb}$$

W = 24,000 lb -----Bounding basket weight

n = 45 -----Number of fuel tubes

A = 6.1 inch² -----Tube cross-sectional area

The factor of safety (FS) is as follows.

$$FS = \frac{0.7 \times S_u}{\sigma_{\text{tube}}} = \frac{0.7 \times 68.4}{5.3} = 9.03$$

where:

S_u = 68.4 ksi -----Ultimate strength, SA-537 Class 1, at 700°F

The weight of the fuel tubes is supported on connector pins. Referring to Figure 3.7-10, the interior tubes (Tube #4) are supported by four connector pins, the side fuel tubes (Tube #1) are supported by two connector pins and the side and corner weldments, and the corner fuel tubes (Tube #5) are supported by three connector pins. The stress (σ) on the fuel tube is as follows.

$$\sigma = \frac{60 \times P_{\text{pin}}}{A_m} = \frac{60 \times 233}{0.34} = 41.1 \text{ ksi}$$

where:

A_m = 0.34 inch² -----Common area

$$P_{\text{pin}} = \frac{1}{3}P_t + \frac{1}{4}P_t = 233 \text{ lb}$$

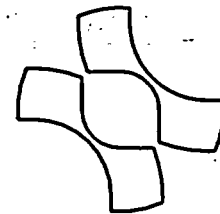
$$P_t = 400 \text{ lb}$$

The factor of safety (FS) is as follows.

$$FS = \frac{0.7 \times S_u}{\sigma_{\text{brg}}} = \frac{0.7 \times 68.4}{41.1} = 1.17$$

where:

S_u = 68.4 ksi -----Ultimate strength, SA-537 Class 1, at 700°F



Common area of Fuel Tube and Connector Pin Intersection

The weight of the side and corner weldments is carried through to the TSC base plate by supports at the bottom of the weldments. The corner weldment is bounding for the supports. The dimensions for the corner support weldment are 8.0-inch length and 0.375-inch thickness. The bounding weight of the corner weldment is 1,100 pounds. The corner weldment also supports one-quarter of the weight of four fuel tubes (400 lb per tube, bounding). The membrane stress (σ_m) is as follows.

$$\sigma_m = \frac{W_{sup}}{A_{sup}} = \frac{90,000}{3.0} = 30.0 \text{ ksi}$$

where:

$$W_{sup} = 60 \times (1,100 + 4 \times (0.25 \times 400)) = 90,000 \text{ lb}$$

$$A_{sup} = 8.0 \times 0.375 = 3.0 \text{ inch}^2$$

The factor of safety (FS) is as follows.

$$FS = \frac{0.7S_u}{\sigma_m} = \frac{0.7 \times 68.4}{30.0} = 1.60$$

where:

$$S_u = 68.4 \text{ ksi} \text{ ----- Ultimate strength, SA-537 Class 1, at } 700^\circ\text{F}$$

The seventy-six basket connector pins support the BWR basket during a 60g bottom-end drop accident. The bounding temperature at the bottom of the basket is 500°F. The pins are subjected to compressive loads; therefore, a buckling evaluation of the pins is presented as follows. The load on one connector pin (P_{pin}) is as follows.

$$P_{pin} = \frac{W \times 60}{n} = \frac{24,000 \times 60}{76} = 18.9 \text{ kips}$$

where:

$$W = 24,000 \text{ lb} \text{ ----- Bounding basket weight}$$

$$n = 76 \text{ ----- Number of pins}$$

Using the Euler buckling theory, the critical buckling load (P_{cr})

$$P_{cr} = \frac{\pi^2 EI}{(KL)^2} = \frac{\pi^2 \times (25.8 \times 10^6) \times 0.049}{(2 \times 3.0)^2} = 346.6 \text{ kip} \quad [9]$$

where:

$$A_{pin} = \frac{\pi}{4} D^2 = 0.78 \text{ inch}^2$$

$$D = 1.0 \text{ inch} \text{-----Pin Diameter}$$

$$L = 3.0 \text{ inch} \text{-----Pin Length}$$

$$I = \frac{\pi r^4}{4} = 0.049 \text{ inch}^4$$

$$K = 2.0 \text{-----Buckling constant, clamped-free}$$

$$E = 25.8 \times 10^6 \text{ psi} \text{-----Modulus of elasticity of SA-240 Type 304, at } 500^\circ\text{F}$$

The factor of safety (FS) for buckling of the hinge pins is as follows.

$$FS = \frac{P_{cr}}{P_{pin}} = \frac{346.6}{18.9} = \text{Large}$$

BWR Neutron Absorber Evaluation

The neutron absorber evaluation assumes an acceleration of 60g, which bounds the end impact acceleration. During a 60g end impact, the BWR neutron absorber is subject to shearing force parallel to its longitudinal axis. There are four weld-posts installed in each neutron absorber sheet. The force due to the weight of the neutron absorber during the end impact is as follows.

$$F = L_{absorber} \times L \times t \times \Delta \times a = 487 \text{ lb}$$

where:

$$\Delta = 0.098 \frac{\text{lb}}{\text{in}^3} \text{-----Density of the neutron absorber plate}$$

$$a = 60g \text{-----End drop acceleration}$$

$$t = 0.1 \text{ inch} \text{-----Thickness of neutron absorber}$$

$$L = 5.25 \text{ inch} \text{-----Cross section length}$$

$$L_{absorber} = 157.8 \text{ inch} \text{-----Length of neutron absorber in axial direction}$$

The shearing capacity of the neutron absorber is as follows.

$$F_{shear} = A_s \times S_a = 10.56 \times 882 = 9,314 \text{ lb}$$

where:

$$A_s = 2 \times (L_{pitch} - L_{hole}) \times t = 10.56 \text{ inch} \text{-----Shear area that withstands the shear force acting on each weld-post}$$

$$L_{pitch} = 54.03 \text{ inch} \text{-----Pitch length between slotted holes in the BWR neutron absorber}$$

$L_{hole} = 1.25$ inch-----Length in the longitudinal direction of the
BWR neutron absorber
 $S_a = 0.42 S_u = 882$ psi -----Allowable shear stress
 $S_u = 2,100$ psi-----Ultimate strength, aluminum 1100, at 700°F

The factor of safety (FS) is as follows.

$$FS = \frac{F_{shear}}{F} = \frac{9,314}{487} = \text{Large}$$

The BWR neutron absorber is adequate to withstand a 60g end drop impact. Since the PWR neutron absorber has more weld-posts and smaller pitch spacing than the BWR, the PWR neutron absorber is bounded by the BWR neutron absorber evaluation.

The strength of the weld posts is significantly higher than that of the neutron absorber. Therefore, no evaluation is required for the weld posts for the concrete cask 24-inch end-drop evaluation.

3.7.2.2.2 Concrete Cask Tip-over

The analysis results for the BWR basket subjected to a hypothetical concrete cask tip-over accident are presented in this section. Each basket component is evaluated in the following sections. Factors of safety for the BWR basket are calculated based on the criteria for Service Level 'D' limits from ASME Code, Section III, Subsection NG [7] and Appendix F [8].

BWR Fuel Tube Evaluation

The BWR basket fuel tubes are analyzed for a tip-over accident using the two-dimensional plastic finite element models described in Appendix 3.B. The fuel tube is conservatively evaluated for a 40g side impact load.

Plastic stress intensities are calculated for the BWR fuel tubes for the 0° and 45° basket orientations. The maximum membrane and membrane plus bending nodal stress intensities for each fuel tube are reported in Table 3.7-8. Note that for a plastic analysis, ANSYS reports stresses in the elastic region as the yield strength (31.7 ksi at 500°F) for the stress-strain curve.

The ANSYS plastic finite element model employs the material stress strain curve and accounts for the inelastic behavior of the material. The stress allowables for plastic analysis are based on ASME Code, Section III, Appendix F. The allowable membrane stress is $0.7S_u$. The allowable primary stress intensity is $0.9S_u$. Figure 3.7-10 through Figure 3.7-13 show the tube ID numbers and section cut locations for the 0° and 45° basket orientations. The minimum factors of safety (45° basket orientation) for the fuel tubes are 1.28 for membrane stresses and 1.40 for primary stress intensities. The critical stress locations occur in the fuel tube corners.

The fuel tubes are constructed by welding two tube halves together using a full penetration weld the length of the fuel tube. A root and final MT weld examination per ASME Code, Section III, Subsection NG-5232 is used, which has a 0.75 weld quality factor (wf). From the plastic analysis of the BWR basket, the maximum membrane and primary stress intensity at the tube weld is 12.1 ksi and 31.9 ksi respectively. The factors of safety for the weld are as follows.

Membrane:

$$FS = \frac{0.7S_u \times wf}{\sigma} = \frac{0.7 \times 68.4 \times 0.75}{12.1} = 2.97$$

Membrane plus bending:

$$FS = \frac{0.9S_u \times wf}{\sigma} = \frac{0.9 \times 68.4 \times 0.75}{31.9} = 1.45$$

where:

$S_u = 68.4$ ksi ----- Ultimate strength, SA-537 Class 1, at 700°F

ASME Code, Appendix F-1336 [8] provides guidelines for a bearing stress analysis of pinned joints. Bearing on the pin only occurs for the 0° basket orientation. For the 45° basket orientation, the load between adjacent fuel tubes is reacted out in bearing on the tube corner flats. Using the 0° basket orientation, the maximum bearing stress (σ_{brg}) is as follows.

$$\sigma_{brg} = \frac{P}{l_{brg} l_{pin}} = 61.0 \text{ ksi}$$

where:

$$P = \left(\frac{n_f}{2} \times W_f + \frac{n_t}{2} \times W_t \right) \times a = 35,400 \text{ lb}$$

$a = 40$ g

$n_f = 19$ -----Number of fuel assemblies contributing to maximum bearing load on pin (2 pins per tube react load)

$n_t = 10$ -----Number of fuel tubes contributing to maximum bearing load on pin (2 pins per tube react load)

$l_{brg} = 0.29$ inch-----Effective bearing arc length (25% of pin circumference)

$l_{pin} = 2.0$ inch-----Length of pin

$$W_t = W_{\text{tube}} \frac{L_{\text{pin}}}{L_{\text{tube}}} = 50 \text{ lb}$$

$$W_{\text{tube}} = 400 \text{ lb} \text{ -----Fuel tube weight}$$

$$L_{\text{pin}} = 20 \text{ inch} \text{ -----Length of periodic section}$$

$$L_{\text{tube}} = 159.1 \text{ inch} \text{ -----Length of fuel tube}$$

$$W_f = W_{\text{fuel}} \frac{L_{\text{pin}}}{L_{\text{fuel}}} = 82 \text{ lb}$$

$$W_{\text{fuel}} = 704 \text{ lb} \text{ -----Maximum BWR fuel weight}$$

$$L_{\text{pin}} = 20 \text{ inch} \text{ -----Length of periodic section}$$

$$L_{\text{fuel}} = 171.2 \text{ inch} \text{ -----Shortest fuel assembly length}$$

The factor of safety (FS) is as follows.

$$FS = \frac{2.1S_u}{\sigma_{\text{brg}}} = 2.35$$

where:

$$S_u = 68.4 \text{ ksi} \text{ -----Ultimate strength, SA-537 Class 1, at } 700^\circ\text{F}$$

The 45° basket orientation does not produce shear loads in the pins, the load between adjacent fuel tubes is reacted out directly in bearing in the corner flats; therefore, the maximum shear loads on the pins occurs in the 0° basket orientation. The pins react shear loads between adjacent tubes. The maximum shear stress (τ_{pin}) in the pin during a tip-over accident is as follows.

$$\tau_{\text{pin}} = \frac{P}{D l_{\text{pin}}} = \frac{5000}{0.38 \times 2.0} = 6.6 \text{ ksi}$$

where:

$$P = 5000 \text{ lb} \text{ -----Maximum shear load on pin, bounding}$$

$$D = 0.38 \text{ inch} \text{ -----Pin diameter}$$

$$l_{\text{pin}} = 2.0 \text{ inch} \text{ -----Length of pin}$$

The factor of safety (FS) is as follows.

$$FS = \frac{0.42S_u}{\tau_{\text{pin}}} = \frac{0.42 \times 70.0}{6.4} = 4.59$$

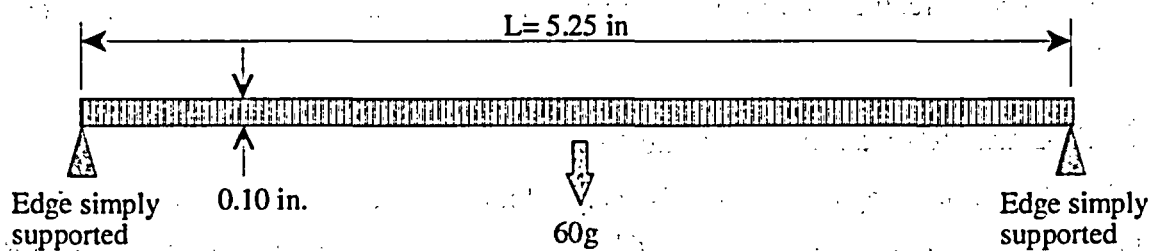
where:

$$S_u = 70.0 \text{ ksi} \text{----- Ultimate strength, SA695 Type B Gr 40, at } 700^\circ\text{F}$$

BWR Neutron Absorber and Retainer

The neutron absorber and retainer are conservatively evaluated for a 60g side-impact load for the concrete cask tip-over accident event. The neutron absorber for the BWR fuel tube is 0.10-inch thick. Retainer strips are used to fasten the neutron absorber to the BWR fuel tubes similar to the PWR fuel tube. For conservatism, the neutron absorber is analyzed as a simply supported beam without the support of the retainer strip or weld posts. Additionally, the properties for the neutron absorber material are taken to be 1100 series aluminum, which is annealed, and would provide bounding minimum values for strength for the neutron absorber material.

The neutron absorber is a continuous sheet along the longitudinal axis of the fuel tube. The simple beam model shown in the following represents a typical cross-section of the neutron absorber plate with unit length along the longitudinal axis of the fuel tube.



From the classical beam formula of Equation 2E, Table 3 in Roark [13], the maximum moment in the center span of the beam is as follows.

$$M = \frac{(wg)L^2}{8} = \frac{(0.0098)(60)(5.25)^2}{8} = 2.026 \text{ inch-lb}$$

where:

$$w = \Delta \times t = (0.098)(0.1) = 0.0098 \frac{\text{lb}}{\text{in}} \text{----- Unit weight of the beam}$$

$$\Delta = 0.098 \frac{\text{lb}}{\text{in}^3} \text{----- Density of the neutron absorber}$$

$$t = 0.1 \text{ inch} \text{----- Thickness of the neutron absorber plate}$$

$$g = 60g \text{----- Acceleration}$$

The maximum tensile stress at the center span of the beam is as follows.

$$\sigma_t = \frac{M}{S} = \frac{2.026}{0.001667} = 1,215 \text{ psi}$$

where:

$$S = \frac{t^2}{6} = 0.001667 \text{ inch}^3 \text{ -----Section modulus of the beam per unit length}$$

The factor of safety (FS) is as follows.

$$FS = \frac{S_y}{\sigma_t} = \frac{1,600}{1,215} = 1.3$$

where:

$$S_y = 1,600 \text{ psi -----Yield strength, Aluminum alloy 1100, at } 700^\circ\text{F}$$

The neutron absorber remains elastic during the impact without the support of the retainer strip or weld posts. Therefore, the neutron absorber retainer design is adequate to withstand the 60g side impact.

BWR Corner Support Weldment Evaluation

The BWR basket corner support weldment is analyzed for the tip-over accident using the three-dimensional periodic finite element model and boundary conditions described in Appendix 3.B. The corner support weldment is comprised of two major components: the mounting plate, which is the vertical plate and the side support plate, which are located on ten-inch centers.

The analysis results for the mounting plate are presented in Table 3.7-9 and Table 3.7-10. Figure 3.7-14 and Figure 3.7-15 show the location of the section cuts for the 0° and 45° basket orientations. The minimum factors of safety for the corner support weldment mounting plates are 7.62 for membrane stresses and 1.22 for membrane plus bending stresses.

The side support plate acts as a stiffener to provide rigidity to the corner weldment assembly. A rectangular opening is cut into the plate, which forms two 0.75-inch × 0.75-inch bars. For the bars, the beam forces and moments are extracted from the finite element model. Using the forces and bending moment from the finite element model, the membrane and bending stresses are calculated. At the welded joint of the support plate and mounting plate, the bar is evaluated using a plastic analysis in accordance with ASME Code, Section III, Appendix F. The cross-section at the mounting plate is 0.75 inch × 2.00 inches because of the large radii in the corners of

the cutout. At the midpoint of the support plate, an elastic evaluation is conservatively performed. The bar stress is calculated using the following classical formulas.

$$\sigma_m = \frac{F_x}{A} = \frac{F_x}{bt}$$

$$\tau_{yz} = \frac{F_{yz}}{A} = \frac{F_{yz}}{bt}$$

$$\sigma_{b, \text{elas}} = \frac{Mc}{I} = \frac{6M}{bt^2}$$

$$\sigma_{b, \text{plas}} = \frac{Mc}{KI} = \frac{6M}{Kbt^2}$$

where:

$$K = 1.5 \text{ ----- Shape factor for plastic bending [13]}$$

The maximum load at the welded joints between the support bar and corner-mounting plate occurs in the 45° basket orientation. The axial load (F_x) in the bar is -14,388 lb, the shear load (F_{yz}) is 622 lb, and the bending moment (M) is 4,039 inch-lb. The stress intensity in the bar at the welded joint is as follows.

$$\sigma_{\text{int}} = \sqrt{\sigma_b^2 + 4\tau_{yz}^2} = 24.0 \text{ ksi}$$

where:

$$\sigma_b = \frac{F_x}{A} \pm \frac{6M}{Kbt^2} = 24.0 \text{ ksi}$$

$$\tau_{yz} = \frac{F_{yz}}{A} = \frac{622}{2.0 \times 0.75} = 0.4 \text{ ksi}$$

$$K = 1.5$$

$$b = 2.0 \text{ inch}$$

$$t = 0.875 \text{ inch}$$

The factor of safety (FS) is as follows.

$$FS = \frac{0.9S_u}{\sigma_{\text{int}}} = 2.57$$

where:

$$S_u = 70.0 \text{ ksi} \text{ ----- Tensile strength, SA-695, Type B, Gr 40, at } 700^\circ\text{F}$$

The maximum load at the center of the span occurs in the 0° basket orientation. The axial load (F_x) in the bar is -14,375 lb, the shear load (F_{yz}) is 595 lb, and the bending moment (M) is 1,019 inch-lb. The stress intensity in the bar is as follows.

$$\sigma_{int} = \sqrt{\sigma_b^2 + 4\tau_{yz}^2} = 40.1 \text{ ksi}$$

where:

$$\sigma_b = \frac{F_x}{A} \pm \frac{6M}{bt^2} = 40.0 \text{ ksi}$$

$$\tau_{yz} = \frac{F_{yz}}{A} = 1.1 \text{ ksi}$$

The factor of safety (FS) is as follows.

$$FS = \frac{S_u}{\sigma_{int}} = 1.71$$

where:

$$S_u = 70.0 \text{ ksi} \text{ ----- Ultimate strength, SA-695 Type B, Gr 40, at } 700^\circ\text{F}$$

The support plate is welded to the corner mounting plate. The plate is welded to the wall on the backside with a minimum $5/16$ -inch groove weld using the visual inspection criteria per ASME Code, Section III, Subsection NG-5260. Visual inspection of the weld has a weld quality factor of 0.35, per ASME Code, Section III, Subsection NG-3352.

The welds only carry the axial load in the plate. Bending and shear loads are carried out in the corner assembly mounting plate directly. The maximum axial load in the plate is 28,200 lb, 0° basket orientation. The weld stress intensity is as follows.

$$\sigma_{weld} = \frac{P}{A} = \frac{28200}{3.59} = 7.9 \text{ ksi}$$

where:

$$A = 2 \times h \times t_w = 2 \times 5.75 \times 0.3125 = 3.59 \text{ inch}^2$$

$$h = 5.75 \text{ inch} \text{ ----- Height of plate}$$

$$t_w = 5/16 \text{ inch} \text{ ----- Weld size}$$

The factor of safety (FS) for the weld is as follows.

$$FS = \frac{0.35(0.42S_u)}{\sigma_{weld}} = \frac{0.35 \times 0.42 \times 68.4}{7.9} = 1.27$$

where:

$$S_u = 68.4 \text{ ksi} \text{ ----- Tensile strength, SA-537 Class 1, at } 700^\circ\text{F}$$

BWR Side Support Weldment Evaluation

The BWR basket side support weldment is analyzed for the tip-over accident using the three-dimensional periodic finite element model and boundary conditions described in Appendix 3.B. The analysis results for the side support weldment are presented in Table 3.7-11 and Table 3.7-12. Figure 3.7-16 and Figure 3.7-17 show the location of the section cuts for the 0° and 45° basket orientations. The minimum factors of safety for the side support weldment are 8.58 for membrane stresses and 1.82 for membrane plus bending stresses.

BWR Side and Corner Weldment / Fuel Tube Attachment Evaluation

The corner and side support weldments are the primary structure that maintains the geometry of the fuel tube array during a hypothetical tip-over accident. The support weldments are bolted to the fuel tubes at 16 circumferential locations. The boss and bolt connection is designed so that the bolts are only loaded in tension, including preload. Otherwise, the support weldments apply a bearing load on the fuel tube array.

During a hypothetical concrete cask tip-over accident, the maximum tensile load on a bolt is 271 lb (0° basket model). Combining this load with the bolt preload (400 lb), the tensile load on the bolt is 671 pounds. The attachment joint analysis uses a bounding bolt load (P) of 1,000 pounds.

The bolt thread is a 3/8-11 UNC and the length of engagement is a minimum of 0.38 inch. The bolt material is SA-193 Grade B8 stainless steel. From Machinery's Handbook [12], the ultimate strength in the bolt (σ_t) is as follows.

$$\sigma_t = \frac{P}{A_t} = \frac{1000}{0.23} = 4.3 \text{ ksi}$$

where:

$$A_t = 0.7854 \left(D - \frac{0.9743}{n} \right)^2 = 0.23 \text{ inch}^2 \quad [12]$$

$$D = 0.625 \text{ inch}$$

$$n = 11$$

The factor of safety (FS) is as follows.

$$FS = \frac{S_y}{\sigma_t} = 4.09$$

where:

$$S_y = 17.6 \text{ ksi} \text{ -----Yield strength for SA 193, Gr B8, at } 700^\circ\text{F}$$

The shear stress in the bolt thread (τ_{bolt}) is as follows.

$$\tau_{\text{bolt}} = \frac{P}{A_s} = \frac{1000}{0.370} = 2.6 \text{ ksi}$$

where:

$$A_s = 3.1416nL_eK_{n \text{ max}} \left[\frac{1}{2n} + 0.57735(E_{s \text{ min}} - K_{n \text{ max}}) \right] = 0.379 \text{ inch}^2 [12]$$

$$L_e = 0.38 \text{ inch}$$

$$K_{n \text{ max}} = 0.546$$

$$E_{s \text{ min}} = 0.5589$$

$$n = 11$$

The factor of safety (FS) is as follows.

$$FS = \frac{0.6S_y}{\tau_{\text{bolt}}} = 4.06$$

where:

$$S_y = 17.6 \text{ ksi} \text{ -----Yield strength for SA 193, Gr B8, at } 700^\circ\text{F}$$

The shear stress in the boss thread (τ_{boss}) is as follows.

$$\tau_{\text{boss}} = \frac{P}{A_n} = \frac{1000}{0.541} = 1.9 \text{ ksi}$$

where:

$$A_n = 3.1416nL_eD_{s \text{ min}} \left[\frac{1}{2n} + 0.57735(D_{s \text{ min}} - E_{n \text{ max}}) \right] = 0.541 \text{ inch}^2 [12]$$

$$L_e = 0.38 \text{ inch}$$

$$E_{n \text{ max}} = 0.5732$$

$$D_{s \text{ min}} = 0.6113$$

$$n = 11$$

The factor of safety (FS) is as follows.

$$FS = \frac{0.42S_u}{\tau_{bolt}} = \text{Large}$$

where:

$$S_u = 70.0 \text{ ksi} \text{-----Ultimate strength, SA-695 Type B, Gr 40, at } 700^\circ\text{F}$$

The boss is welded into the fuel tube with a 1/8-inch groove weld. The shear stress in the boss (τ_{weld}), using the lesser of SA-537 Class 1 and SA-695 Type B, Gr 40 S_u allowable, is as follows.

$$\tau_{weld} = \frac{P}{A_w} = \frac{1000}{0.49} = 2.0 \text{ ksi}$$

where:

$$P = 1,000 \text{ lb}$$

$$A_w = \pi D t_{weld} = \pi \times 1.00 \times 0.156 = 0.49 \text{ inch}$$

$$D = 1.00 \text{ inch} \text{-----Smallest boss diameter}$$

The factor of safety (FS) is as follows.

$$FS = \frac{0.42S_u}{\tau_{weld}} = \text{Large}$$

where:

$$S_u = 68.4 \text{ ksi} \text{-----Ultimate strength, SA-537 Class 1, at } 700^\circ\text{F}$$

The washers under the bolts are subjected to a bending load due to the preload. Using "Roark's Formulas for Stress and Strain" Table 24-1a [13], the maximum bending moment (M_t) is calculated to be 138.4 inch-lb and the maximum stress (σ) in the washer is as follows.

$$\sigma = \frac{6M_t}{t^2} = \frac{6 \times 138.4}{0.13^2} = 49.1 \text{ ksi}$$

where:

$$t = 0.13 \text{ inch} \text{-----Thickness of washer}$$

The factor of safety (FS) is as follows.

$$FS = \frac{S_u}{\sigma} = \frac{63.2}{49.1} = 1.29$$

where:

$$S_u = 63.2 \text{ ksi} \text{ ----- Ultimate Strength, SA-240 Type 304, at } 700^\circ\text{F}$$

The maximum shear load in the side support weldment attachment (P_1) is 4,700 lb (45° basket orientation). The maximum shear loads in the corner support weldments are 9,737 lb (P_2) for the bosses with a mounting bolt and 36,202 lb (P_3) for the bosses without the attachment bolts (45° basket orientation). For the side weldment boss, the shear stress in the boss (τ_{boss}) is as follows.

$$\tau_{\text{boss}} = \frac{P_1}{A} = \frac{4,700}{0.47} = 10.0 \text{ ksi}$$

where:

$$A = \frac{\pi}{4}(D_o^2 - D_i^2) = 0.47 \text{ inch}^2$$

$$D_o = 1.00 \text{ inch}$$

$$D_i = 0.63 \text{ inch}$$

The factor of safety (FS) is as follows.

$$FS = \frac{0.42S_u}{\tau_{\text{boss}}} = 2.94$$

where:

$$S_u = 70.0 \text{ ksi} \text{ ----- Ultimate strength, SA-695 Type B, Gr 40, at } 700^\circ\text{F}$$

The corner weldments have two attachment joints. One joint can react both shear and tensile loads with the addition of a bolt. The other joint can only react shear loads parallel to the face of a fuel tube because the boss is solid. For the corner weldment boss with a bolt, the shear stress in the boss (τ_{boss}) is as follows.

$$\tau_{\text{boss}} = \frac{P_2}{A} = \frac{9737}{1.17} = 8.3 \text{ ksi}$$

where:

$$A = \frac{\pi}{4}(D_o^2 - D_i^2) = 1.17 \text{ inch}^2$$

$$D_o = 1.375 \text{ inch}$$

$$D_i = 0.63 \text{ inch}$$

The factor of safety (FS) is as follows.

$$FS = \frac{0.42S_u}{\tau_{\text{boss}}} = 3.54$$

where:

$$S_u = 70.0 \text{ ksi} \text{ ----- Ultimate strength, SA-695 Type B, Gr 40, at } 700^\circ\text{F}$$

For the corner weldment boss without a bolt, the shear stress in the boss (τ_{boss}) is as follows.

$$\tau_{\text{boss}} = \frac{P_3}{A} = \frac{36,202}{1.48} = 24.5 \text{ ksi}$$

where:

$$A = \frac{\pi}{4}(D^2) = 1.48 \text{ inch}^2$$

$$D = 1.375 \text{ inch}$$

The factor of safety (FS) is as follows.

$$FS = \frac{0.42S_u}{\tau_{\text{boss}}} = 1.20$$

where:

$$S_u = 70.0 \text{ ksi} \text{ ----- Ultimate strength, SA-695 Type B, Gr 40, at } 700^\circ\text{F}$$

Loads between the fuel tube array and the corner and side weldments are reacted out in shear and bearing in the support weldments. Bearing stresses are not considered for accident events. Due to the geometry of the basket, the cutout in the corner support weldments has an edge distance less than two times the diameter of the cutout. The shear stress in the corner weldment mounting plate is as follows.

$$\tau = \frac{P}{A_{\text{shear}}} = \frac{9737}{1.14} = 8.5 \text{ ksi}$$

where:

$$A_{\text{shear}} = 2 \left[\frac{L_{\text{ed}}}{\sin 45^\circ} t_{\text{plate}} \right] = 1.14 \text{ inch}^2$$

$L_{\text{ed}} = 1.30 \text{ inch}$ -----Boss edge distance

$t_{\text{plate}} = 0.31 \text{ inch}$ -----Mounting plate thickness

The factor of safety (FS) is as follows.

$$FS = \frac{0.42S_u}{\tau} = 3.38$$

where:

$S_u = 68.4 \text{ ksi}$ -----Ultimate strength, SA-537 Class 1, at 700°F

BWR Basket Buckling Evaluation

For the hypothetical concrete cask tip-over accident, a buckling evaluation of the basket is required. Due to the multiple components and load paths in the BWR basket, the buckling evaluation of the BWR basket used three different methodologies. All three buckling evaluations are conservative because they employ a constant acceleration along the length of the basket as opposed to a uniformly varying acceleration.

The first method is a buckling evaluation of the entire basket using the ANSYS buckling solution and the three-dimensional periodic finite element models for the 0° and 45° basket orientations. The factor of safety against buckling for the BWR basket is 10.7 for the 0° basket orientation and 11.4 for the 45° basket orientation.

The second method is a buckling evaluation of a single fuel tube in the 0° basket orientation using a two-dimensional finite element model, as shown in Figure 3.7-18. Loads are applied to the fuel tube to represent a fuel tube at the bottom of the tube array during a tip-over accident for the 0° basket orientation (maximum stress on tube sidewalls). Figure 3.7-18 shows the boundary conditions and applied loads to the model. Similar to the previous basket buckling evaluation, the tube buckling evaluation, conservatively neglects the tapered inertia loading of a tip-over accident. The factor of safety for fuel tube buckling is 2.64.

The final buckling evaluation of the BWR basket is a buckling evaluation of a side of the fuel tube per NUREG/CR-6322 [9]. Using the plane strain plastic finite element model, the critical buckling of a fuel tube occurs in the 0° basket orientation (Tube 25, Figure 3.7-10). The applied loads on a side of the fuel tube are 2.75 kip/inch axial compression and 325 inch-lb/inch bending.

The factor of safety is calculated based on the interaction Equations 31 and 32 in NUREG/CR-6322. These two equations adopt the "Limit Analysis Design" approach for structural members subjected to stresses beyond the yield limit of the material. Methodology and equations for the buckling evaluation are the same as those presented in Section 3.7.2.1.2 for the PWR basket.

For the BWR basket fuel tube the following parameters are used in the buckling evaluation.

- t = 0.25 inch-----Tube thickness
- b = 1.00 inch-----Unit Thickness
- l = 5.34 inch-----Sidewall length
- K = 0.80-----Effective length factor
- E = 27.3 × 10⁶ psi-----SA-537 Class 1, at 700°F
- S_y = 35.4 ksi -----Yield strength, SA-537 Class 1, at 700°F

For P = 2.75 kip/inch and M = 325 inch-lb/inch (Tube 25, 0° basket orientation)

$$P_1 = \frac{P}{P_{cr}} = 0.20$$

$$M_1 = \frac{C_m M}{\left(1 - \frac{P}{P_e}\right) M_m} = 0.54$$

$$P_2 = \frac{P}{P_y} = 0.31$$

$$M_2 = \frac{M}{1.18 M_p} = 0.51$$

The factors of safety are as follows.

$$FS_1 = \frac{1}{P_1 + M_1} = \frac{1}{0.20 + 0.54} = 1.3$$

$$FS_2 = \frac{1}{P_2 + M_2} = \frac{1}{0.31 + 0.51} = 1.22$$

3.7.3 Concrete Cask Evaluation for Accident Events

Structural evaluation of the concrete is performed for accident events including the extreme temperature events (133°F ambient), tornado and tornado-driven missiles, flood, earthquake, concrete cask 24-inch drop and the tip-over accident.

3.7.3.1 Concrete Cask Thermal Stresses

Using the finite element model presented in Appendix 3.D, a structural evaluation of the concrete cask for accident thermal loads was performed. The analysis considered a temperature profile corresponding to the accident thermal condition (133°F ambient). The following summarizes the critical thermal stresses for accident events.

Component	Stress (ksi)
Circumferential Rebar	16.6
Vertical Rebar	20.2
Concrete, Compression	1.0
Concrete, Tension	0.1

3.7.3.2 Tornado and Tornado-Driven Missiles

This section evaluates the strength and stability of the concrete cask for a maximum tornado wind loading and for the impacts of tornado-driven missiles. It also demonstrates that the concrete cask remains stable in tornado wind loading in conjunction with an impact from a high-energy tornado missile.

Concrete cask stability analysis for the maximum tornado wind loading is based on NUREG-0800, Section 3.3.1, "Wind Loadings," and Section 3.3.2, "Tornado Loadings," [17]. Loads due to tornado-driven missiles are based on NUREG-0800, Section 3.5.1.4, "Missiles Generated by Natural Phenomena."

The concrete cask stability in a maximum tornado wind is evaluated based on the design wind pressure calculated in accordance with ANSI/ASCE 7-93, [18] and using classical free body stability analysis methods.

Local damage to the concrete shell is assessed using a formula developed in NSS 5-940.1 [19]. This formula predicts the depth of missile penetration and minimum concrete thickness requirements to prevent scabbing of the concrete.

The local shear strength of the concrete shell is evaluated on the basis of ACI 349-85 Section 11.11.2.1 [15], without considering the reinforcing steel and the steel liner. The concrete shell shear capacity is also evaluated for missile loading using ACI 349-85, Section 11.7.

Tornado Wind Loading

The tornado wind velocity is transformed into an effective pressure applied to the concrete cask using procedures in ANSI/ASCE 7-93 "Building Code Requirements for Minimum Design

Loads in Buildings and Other Structures” [18]. The maximum pressure (q) is determined from the maximum tornado wind velocity as follows:

$$q = (0.00256)(K \times I \times V)^2 \text{ lb/ft}^2 = (0.00256)(360)^2 \times 180 = 331.8 \text{ psf}$$

where:

$$\begin{aligned} V &= 360 \text{ mph} \text{-----Maximum tornado wind speed} \\ K &= 1.0 \text{-----Terrain effect} \\ I &= 1.0 \text{-----Importance Factor} \end{aligned}$$

Considering that the concrete cask is small with respect to the tornado radius, the velocity pressure is assumed uniform over the projected area of the concrete cask. Because the concrete cask is vented, the tornado-induced pressure drop is equalized from inside to outside and has no effect on the concrete cask structure. The total wind loading (F_w) on the projected area of the concrete cask, is computed as follows.

$$F_w = q \times G \times C_f \times A_p = 36,003 \text{ lb} \cong 36,100 \text{ lb}$$

where:

$$\begin{aligned} q &= 331.8 \text{ lb/ft}^2 \text{-----Maximum pressure} \\ C_f &= 0.51 \text{-----Force coefficient (ASCE 7-93)} \\ A &= H \times D_o = 30,637 \text{ inch}^2 = 212.7 \text{ ft}^2 \text{----Projected area} \\ H &= 225.27 \text{ inch-----Concrete cask height} \\ D_o &= 136.0 \text{ inch-----Concrete cask outer diameter} \\ G &= 1.0 \text{-----Gust factor} \end{aligned}$$

The wind overturning moment (M_w) is as follows.

$$M_w = F_w \times \frac{H}{2} = 4,066,123 \text{ inch-lb} = 3.38 \times 10^5 \text{ ft-lb}$$

The stability moment (M_s) of the concrete cask (with the TSC, basket and no fuel load) about an edge of the base is as follows.

$$M_s = W_{cc} \times \frac{D_o}{2} = 14.72 \times 10^6 \text{ inch-lb} = 1.23 \times 10^6 \text{ ft-lb}$$

where:

$$\begin{aligned} D_o &= 128.0 \text{ inch-----Concrete cask base plate diameter} \\ W_{cc} &= 230,000 \text{ lb-----Minimum concrete cask loaded weight} \end{aligned}$$

ASCE 7-93 requires that the overturning moment due to wind load shall not exceed two-thirds of the dead load stabilizing moment unless the structure is anchored. Therefore, the factor of safety (FS) against overturning is as follows.

$$FS = \frac{0.67M_s}{M_w} = 2.44$$

The stresses in the concrete due to the tornado wind load are conservatively calculated. The concrete cask is considered to be fixed at its base. The stresses in the concrete are as follows.

$$\sigma_{outer} = \frac{M_{max} c_{outer}}{I} = 19.1 \text{ psi (tension or compression)}$$

$$\sigma_{inner} = \frac{M_{max} c_{inner}}{I} = 11.7 \text{ psi (tension or compression)}$$

where:

$$D_o = 136.0 \text{ inch}$$

$$D_i = 82.98 \text{ inch}$$

$$H = 225.27 \text{ inch}$$

$$A = \frac{\pi(D_o^2 - D_i^2)}{4} = 9,119 \text{ inch}^2$$

$$I = \frac{\pi(D_o^4 - D_i^4)}{64} = 14.47 \times 10^6 \text{ inch}^4$$

$$M_{max} = \frac{F_w \times H}{2} = 4.07 \times 10^6 \text{ lb-inch}$$

$$c_{outer} = 136.0/2 = 68.0 \text{ inch}$$

$$c_{inner} = 82.98/2 = 41.49 \text{ inch}$$

Tornado Missiles

The concrete cask is designed to withstand the effects of impacts associated with postulated tornado-driven missiles identified in NUREG-0800 [17] Section 3.5.1.4.III.4, Spectrum I missiles. These missiles are listed as follows.

- A massive high kinetic energy missile (4,000 lb automobile, with a frontal area of 20 square feet that deforms on impact).
- A 280 lb, 8.0-inch-diameter armor piercing artillery shell.
- A 1.0-inch-diameter solid steel sphere.

All of these missiles are assumed to impact in a manner that produces the maximum damage at a velocity of 126 mph (35% of the maximum tornado wind speed of 360 mph). The concrete cask is evaluated for impact effects associated with each of the previously listed missiles.

The concrete cask has no openings except for the four air outlets at the top and four air inlets at the bottom. The outlets are configured such that a one-inch diameter solid steel missile cannot directly enter the concrete cask interior. Additionally, the basket is protected by the TSC closure lid. The TSC is protected from small missiles entering the inlets by the pedestal plate; therefore, a detailed analysis of the impact of a one-inch diameter steel missile is not required.

Concrete Shell Local Damage (Penetration Missile)

Local damage to the concrete cask body is assessed by using the methodology presented by NSS 5-940.1 [19]. This method predicts the depth of penetration and minimum concrete thickness requirements to prevent scabbing. Penetration depths calculated by using this formula have been shown to provide reasonable correlation with test results. The penetration depth is as follows.

$$x = \left[4KNW(d^{-0.8} \left(\frac{V}{1000} \right)^{1.8} \right)^{0.5} = 5.82 \text{ inch}$$

where:

- d = 8.0 inch ----- Missile diameter
- K = $180/(f_c')^{1/2} = 2.92$ ----- Coeff. depending on concrete strength
- N = 1.14 ----- Shape factor for sharp nosed missiles
- W = 280 lb ----- Missile weight
- V = 126 mph = 185 ft/sec ----- Missile velocity
- f_c' = 3,800 psi ----- Concrete compressive strength

The minimum concrete shell thickness to prevent scabbing is three times the penetration depth (17.46 inch). The thickness of the concrete shell is 26.51 inches. The factor of safety (FS) is as follows.

$$FS = \frac{26.51}{17.46} = 1.52$$

Note that the steel liner and rebar of the concrete cask is conservatively ignored in the previously listed evaluation.

Closure Plate Local Damage (Penetration Missile)

The concrete cask is closed with a 6.75-inch deep lid assembly. The top plate is 3/4-inch carbon steel with a carbon steel clad disk of concrete 5.75-inches deep. In this evaluation, only the steel plate is considered to withstand the impact of the 280-lb armor-piercing missile, impacting at 126 mph. The perforation thickness (T) of the closure steel plate is calculated by using the methodology presented in BC-TOP-9A [20].

$$T = \frac{\left(\frac{m_m V_s^2}{2} \right)^{2/3}}{672D} = 0.52 \text{ inch}$$

where:

- $m_m = 280 \text{ lb}/32.174 \text{ ft}/\text{sec}^2$ -----8.70 slugs (lb-sec²/ft) missile mass
- $V_s = 185 \text{ ft}/\text{sec}$ -----Missile velocity
- $D = 8 \text{ inch}$ -----Missile diameter

The report recommends that the plate thickness be 25% greater than the calculated perforation thickness (T) to prevent perforation. The recommended plate thickness is as follows.

$$T = 1.25 \times 0.52 = 0.65 \text{ inch}$$

The factor of safety (FS) is as follows.

$$FS = \frac{0.75}{0.65} = 1.15$$

High Energy Missile Impact Damage Prediction

The concrete cask is a freestanding structure. Therefore, the principal consideration in overall damage response is the potential for overturning the concrete cask as a result of the high-energy missile impact. From the principle of conservation of momentum, the impulse of the force from the missile impact on the concrete cask must equal the change in angular momentum of the concrete cask. Also, the impulse force due to the impact of the missile must equal the change in linear momentum of the missile. These relationships may be expressed as follows:

Change in momentum of the missile, during the deformation phase

$$\int_{t_1}^{t_2} (F)(dt) = m_m (v_2 - v_1)$$

where:

- F -----Impact impulse force on missile
- $m_m = 4,000 \text{ lb}/g = 124 \text{ slugs}/12 = 10.4 \text{ (lb sec}^2 \text{ /inch)}$
-----Missile mass
- t_1 -----Time at missile impact
- t_2 -----Time at conclusion of deformation phase
- $v_1 = 126 \text{ mph} = 185 \text{ ft}/\text{sec}$ -----Missile velocity at impact
- v_2 -----Velocity of missile at time t_2

The change in angular momentum of the concrete cask, about the bottom outside edge/rim, opposite the side of impact is as follows.

$$\int_1^2 M_c (dt) = \int_1^2 (H)(F)(dt) = I_m (\omega_1 - \omega_2)$$

Substituting,

$$\int (F)(dt) = m_m (v_2 - v_1) = \frac{I_m (\omega_1 - \omega_2)}{H}$$

where:

- M_c -----Moment of the impact force on the concrete cask
- I_m -----Concrete cask mass moment of inertia, about point of rotation on the bottom rim
- ω_1 -----Angular velocity at time t_1
- ω_2 -----Angular velocity at time t_2
- $m_c = 230,000/32.174 = 7,149 \text{ slugs}/12 = 596 \text{ lb sec}^2/\text{inch}$
-----Mass of concrete cask
- $I_{mx} = 1/12(m_c)(3r^2 + H^2) = 3.21 \times 10^6 \text{ lb-sec}^2\text{-inch}$
- $I_m = I_{mx} + (m_c)(d_{CG})^2 = 13.9 \times 10^6 \text{ lb-sec}^2\text{-inch}$
- $r = 68.0 \text{ inch}$ -----Concrete cask radius
- $H = 225.27$ -----Concrete cask height
- $d_{CG} = \sqrt{118.0^2 + 64.0^2} = 134.2 \text{ inch}$ -----Distance from CG to rotation point

Based on conservation of momentum, the impulse of the impact force on the missile is equated to the impulse of the force on the concrete cask.

$$m_m(v_2 - v_1) = I_m (\omega_1 - \omega_2)/H$$

at time t_1 , $v_1 = 185 \text{ ft/sec}$ and $\omega_1 = 0 \text{ rad/sec}$
 at time t_2 , $v_2 = 0 \text{ ft/sec}$

During the restitution phase, the final velocity of the missile depends upon the coefficient of restitution of the missile, the geometry of the missile and target, the angle of incidence, and on the amount of energy dissipated in deforming the missile and target. On the basis of tests conducted by EPRI, the final velocity (v_f) of the missile following the impact is assumed to be zero. This conservatively assumes that all of the missile energy is transferred to the concrete cask. Then, equating the impact force on the missile to the impulse force on the concrete cask.

$$(10.4)(v_2 - 185(12)) = 13.9 \times 10^6 (0 - \omega_2)/225.27$$

Setting $v_2 = 0$ and solving for ω_2

$$\omega_2 = 0.374 \text{ rad/sec}$$

The distance (Z) from the point of missile impact to the point of concrete cask rotation is as follows.

$$Z = \sqrt{132.0^2 + 225.27^2} = 261.1 \text{ inch}$$

And the impulse velocity is as follows.

$$v_2 = Z \times \omega_2 = (261.1)(0.374) = 97.7 \text{ inch/sec}$$

The line of missile impact is conservatively assumed normal to the concrete cask. Equating the force on the missile during restitution to the impulse of the force on the concrete cask yields the following.

$$-[m_m(v_f - v_2)] = I_m (\omega_f - \omega_2)/Z$$

$$-[10.4(0 - 97.7)] = 13.9 \times 10^6 (\omega_f - 0.374)/261.1$$

$$\omega_f = 0.393 \text{ rad/sec}$$

where:

$$v_f = 0$$

$$v_2 = 97.7 \text{ inch/sec}$$

$$\omega_2 = 0.374 \text{ rad/sec}$$

Thus, the final energy (E_k) of the concrete cask following the impact is as follows.

$$E_k = (I_m)(\omega_f)^2 / (2) = 10.73 \times 10^5 \text{ inch-lb}$$

The change in potential energy (E_p) of the concrete cask due to rotating it until its center of gravity is above the point of rotation is calculated. The height of the center of gravity has increased by the distance, $h_{PE} = d_{cg} - h_{cg}$.

$$E_p = (W_{cc})(h_{PE})$$

$$E_p = 230,000 \text{ lb} \times 16.2 \text{ inch}$$

$$E_p = 3.73 \times 10^6 \text{ inch-lb}$$

The massive high kinetic energy tornado-driven missile imparts less kinetic energy to the concrete cask than the change in potential energy of the concrete cask to reach the tip-over point. Therefore, concrete cask overturning from missile impact will not occur. The factor of safety (FS) against overturning is as follows.

$$FS = \frac{3.73 \times 10^6}{10.73 \times 10^5} = 3.48$$

Combined Tornado Wind and Missile Loading (High Energy Missile)

The concrete cask rotation due to the heavy missile impact is as follows.

$$h_{KE} = \frac{E_k}{W_{cc}} = \frac{10.73 \times 10^5}{230,000} = 4.67 \text{ inch}$$

The rotation after impact is as follows.

$$\theta = \alpha - \beta = 28.4 - 23.9 = 4.5^\circ$$

where:

$$\cos \beta = \frac{h_{cg} + h_{KE}}{d_{cg}} = \frac{118.0 + 4.67}{134.2} = 0.9141$$

$$\beta = 23.9^\circ$$

$$\cos \alpha = \frac{h_{cg}}{d_{cg}} = \frac{118.0}{134.2} = 0.8793$$

$$\alpha = 28.4^\circ$$

$$e = d_{cg} \sin \beta = 134.2 \times \sin(23.9) = 54.4 \text{ inch}$$

The available gravity restoration moment after missile impact is as follows.

$$M_{rst} = W_{cc}e = 230,000 \times 54.4 = 12.5 \times 10^6 \text{ inch-lb} = 1.04 \times 10^6 \text{ ft-lb}$$

The tornado wind moment is 3.38×10^5 ft-lb; therefore, the factor of safety (FS) is as follows.

$$FS = \frac{0.67(1.04 \times 10^6)}{3.38 \times 10^5} = 2.06$$

Therefore, the concrete cask will not overturn due to the combined effect of tornado wind loading and high-energy missile impact.

Local Shear Strength Capacity of Concrete Shell (High Energy Missile)

This section evaluates the punching shear strength of the concrete shell when impacted by a high-energy missile. Where the high-energy missile is equivalent to a 20-ft² cross-sectional area object moving at 185 ft/sec weighing 4,000 lb having proportions of 2 horizontal to 1 vertical. The missile is assumed to impact flush with the top of the concrete shell. The concrete area required to resist the high-energy missile impact is as follows.

$$A = 2b \times b = 2(9.64)^2 = 185.9 \text{ inch}^2 = 1.3 \text{ ft}^2 < 20 \text{ ft}^2$$

where:

Setting the factored shear force, V_u , equal to the force of the high kinetic energy missile, F_u , the leg dimension, b , of the equivalent impacting area is as follows.

$$V_u = F_u \Rightarrow \phi V_c = F_u \Rightarrow \phi 4\sqrt{f'_c} b_o d = F_u \Rightarrow \phi 4\sqrt{f'_c} (4b + 53)d \Rightarrow b = 9.64 \text{ inch}$$

and

$$V_c = \left(2 + \frac{4}{\beta_c} \right) \sqrt{f'_c} (b_o d) = 4\sqrt{f'_c} (b_o d) \text{ ----- Concrete punching shear strength capacity}$$

[15 Eq. 11-36]

$$\beta_c = 2/1 = 2 \text{ ----- Ratio of long side to short side}$$

$$d = 26.51 \text{ inch ----- Concrete thickness}$$

$$f'_c = 3,800 \text{ psi ----- Concrete strength, } 300^\circ\text{F}$$

$$b_o = (2b + 26.51) + 2(b + 13.26) = 4b + 53 \text{ -- Perimeter of punching shear area at approximately } d/2 \text{ from the missile contact area}$$

$$\phi = 0.85 \text{ ----- Strength reduction factor [15]}$$

$$F_u = LF \times F = 508.8 \text{ kip ----- Force of high kinetic energy missile with load factor [20]}$$

$$F = 0.625(v)(W_m) = 462.5 \text{ kip ----- Force of high-energy missile [20]}$$

$$v = 185 \text{ ft/sec ----- Velocity of the missile}$$

$$W_m = 4,000 \text{ lb ----- Weight of high-energy missile}$$

$$LF = 1.1 \text{ ----- 10\% load factor}$$

Therefore, the concrete shell alone has sufficient capacity to resist the high-energy missile impact force.

3.7.3.3 Flood

This section will verify the stability of the concrete cask against overturning during a design basis flood accident, and ensure that the design is adequate to withstand stresses induced by the flood.

Overturning of the concrete cask due to the drag force of the flood water flow is resisted by the weight of the loaded cask. Assuming a full submersion and steady-state flow conditions, the drag force (F_D) on the concrete cask is calculated using classical fluid mechanics for turbulent flow conditions. The resultant drag force acts horizontally through the CG of the cask. The effective weight of the concrete cask acts vertically downward through the CG. The tendency of the concrete cask to overturn is determined by comparing the moment of the drag force about a point on the bottom edge of the concrete cask to the moment of effective concrete cask weight about the same point.

The effective weight of the fully submerged concrete cask is the actual weight minus the buoyancy force due to the displaced water. The bounding condition for buoyancy occurs for the concrete cask configuration with the greatest volume to weight ratio. Thus, for conservatism, the concrete cask is assumed to be empty.

The capacity of the concrete cask to react the stresses induced by the flood water flow drag forces is evaluated using the methodology described in ACI-349-85 [15]. For conservatism, only the concrete shell is considered.

Assuming a hollow cylinder, the volume of the concrete cask (V_{cc}) is as follows.

$$V_{cc} = \frac{\pi}{4}(D_o^2 - D_i^2)h = \frac{\pi}{4}(136.0^2 - 79.48^2)225.27 = 2,154,777 \text{ inch}^3$$

where:

- $D_o = 136.0 \text{ inch}$ -----Concrete cask outer diameter
- $D_i = 79.48 \text{ inch}$ -----Concrete cask inner diameter
- $H = 225.27 \text{ inch}$ -----Concrete cask height

The buoyancy force (F_b) is equal to the weight of water (62.4 lb/ft^3) displaced by the fully submerged concrete cask.

$$F_b = \frac{V_{cc}}{12^3} W_{h20} = \frac{2,154,777}{12^3} 62.4 \approx 77,800 \text{ lb}$$

Assuming complete submersion and steady-state flow for a rigid cylinder, the drag force (F_{D15}) of the water on the concrete cask is as follows.

$$F_{D15} = C_D \rho V^2 \left(\frac{A}{2} \right) = 0.7 \times 1.94 \times 15.0^2 \left(\frac{212.7}{2} \right) \approx 32,500 \text{ lb} \quad [21]$$

where:

- $C_D = 0.7$ -----Drag coefficient [21]
- $\rho = 1.94 \text{ slugs/ft}^3$ -----Density of water
- $V = 15 \text{ ft/sec}$ -----Flow velocity
- $A = H \times D_o = 30,637 \text{ inch}^2 = 212.7 \text{ ft}^2$ ----Projected area
- $H = 225.27 \text{ inch}$ -----Concrete cask height
- $D_o = 136.0 \text{ inch}$ -----Concrete cask outer diameter

The force (F_D) required to overturn the concrete cask is determined by summing the moments of the drag force and the submerged concrete cask about a point on the bottom of the concrete cask.

Assuming an empty concrete cask, the minimum required overturning force is as follows.

$$F_D = \frac{(W_{cc} - F_b)D_r}{h} = \frac{(200,000 - 77,800)128}{225.27} = 69,435 \text{ lb}$$

where:

$$\begin{aligned} W_{cc} &= 200,000 \text{ lb} \text{-----Minimum empty concrete cask weight} \\ D_r &= 128.0 \text{ inch} \text{-----Concrete cask base diameter} \\ h &= 225.27 \text{ -----Concrete cask height} \end{aligned}$$

The water velocity (V) required to overturn the concrete cask is as follows.

$$V = \sqrt{\frac{2F_D}{C_D \rho A}} = \sqrt{\frac{2 \times 69,435}{0.7 \times 1.94 \times 212.7}} = 21.9 \text{ ft/sec}$$

Therefore the factor of safety (FS) is as follows.

$$FS = \frac{21.9}{15.0} = 1.46$$

The stresses in the concrete due to the drag force (F_D) are conservatively calculated by considering the concrete cask to be fixed.

$$\sigma_{v \text{ outer}} = M / S_{\text{outer}} = 17.2 \text{ psi (tension or compression)}$$

$$\sigma_{v \text{ inner}} = M / S_{\text{inner}} = 10.5 \text{ psi (tension or compression)}$$

where:

$$\begin{aligned} D_o &= 136.0 \text{ inch} \\ D_i &= 82.98 \text{ inch} \\ h &= 225.27 \text{ inch} \\ A &= \pi (D_o^2 - D_i^2) / 4 = 9,119 \text{ inch}^2 \\ I &= \pi (D_o^4 - D_i^4) / 64 = 14.47 \times 10^6 \text{ inch}^4 \\ S_{\text{outer}} &= 2I/D_o = 212,794 \text{ inch}^3 \\ S_{\text{inner}} &= 2I/(D_i) = 348,759 \text{ inch}^3 \\ w &= F_{D15}/h = 144.3 \text{ lb/inch} \\ M &= w (h)^2 / 2 = 3.66 \times 10^6 \text{ inch-lb} \end{aligned}$$

3.7.3.4 Earthquake

The maximum horizontal acceleration at the surface of the concrete storage pad due to an earthquake is evaluated. Per 10 CFR 72.102 [1], the required minimum earthquake ground acceleration is 0.25g. This evaluation will show that MAGNASTOR is stable during a 0.37g

earthquake horizontal acceleration (including a 1.1 factor of safety). The vertical acceleration is defined as two-thirds of the horizontal acceleration in accordance with ASCE 4-86 [22].

This calculation determines the effects of ground accelerations (components a_x , a_y and a_z) on the concrete cask for tip-over. The peak ground acceleration is associated with a safe shutdown earthquake. For this evaluation, the maximum overturning moment is compared to the restoring moment required to keep the concrete cask in a stable upright position (i.e. concrete cask will not tip over due to the earthquake). The maximum ground accelerations and overturning/restoring forces and moment are calculated for both empty and fully loaded concrete cask configurations.

In the event of earthquake, there exists a base shear force or overturning force due to the horizontal ground acceleration and a restoring force due to the net force of vertical ground acceleration and gravity. This ground motion tends to rotate the concrete cask about its bottom corner at the point of rotation (at the chamfer). The horizontal moment arm is from the center of gravity (CG) toward the outer radius of the concrete cask. The vertical moment arm is from the CG to the bottom of the concrete cask. If the overturning moment is greater than the restoring moment, the concrete cask may tip over. Using the geometry of the concrete cask design, the maximum horizontal and vertical ground accelerations that the concrete cask can safely withstand without becoming unstable are identified.

The two orthogonal horizontal acceleration components (a_x and a_z) are combined for maximum horizontal acceleration magnitude. The result is applied simultaneously with the vertical component to statically evaluate the overturning force and moment. Upward ground acceleration reduces the vertical force that restores the cask to its undisturbed vertical position. Based upon the requirements presented in NUREG-0800 [17], the static analysis method is considered applicable if the natural frequency of the structure is greater than 33 cps. The natural frequency of the MAGNASTOR concrete cask is 138.3 Hz. During the design basis earthquake event a factor of safety of 1.1 against tip-over of the concrete cask must be maintained.

Tip-over Evaluation

To maintain the concrete cask in equilibrium, the restoring moment, M_R must be greater than, or equal to, the overturning moment, M_o . The combination of horizontal and vertical acceleration components is based on the 100-40-40 approach of ASCE 4-86 [22], which considers that when the maximum response from one component occurs, the response from the other two components are 40% of the maximum. The vertical component of acceleration can be obtained by scaling the corresponding ordinates of the horizontal components by two-thirds. The vertical component is conservatively considered to be the same as the horizontal component.

Let:

- $a_x = a_z = a$ -----Horizontal acceleration components
- $a_y = a$ -----Vertical acceleration component
- G_h -----Vector sum of two horizontal acceleration components
- G_v -----Vertical acceleration component

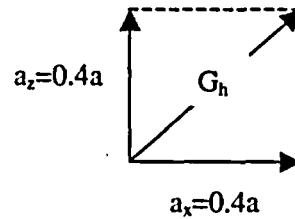
Two cases are analyzed:

Case 1) The vertical acceleration, a_y , is at its peak:

$$(a_y = 1.0a, a_x = 0.4a, \text{ and } a_z = 0.4a)$$

$$G_h = \sqrt{a_x^2 + a_z^2} = \sqrt{(0.4a)^2 + (0.4a)^2} = 0.566a$$

$$G_v = 1.0a_y = 1.0a$$

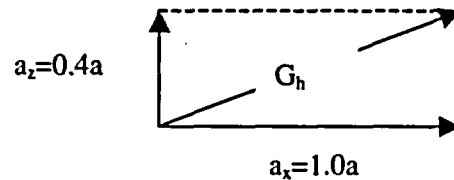


Case 2) One horizontal acceleration, a_x , is at its peak:

$$(a_y=0.4 \times a, a_x = a, \text{ and } a_z = 0.4a)$$

$$G_h = \sqrt{a_x^2 + a_z^2} = \sqrt{(1.0a)^2 + (0.4a)^2} = 1.077a$$

$$G_v = 0.4a_y = 0.4a$$



For the cask to resist overturning, the restoring moment (M_R) about the point of rotation, must be greater than the overturning moment (M_o).

$$M_R \geq M_o, \text{ or } F_r b \geq F_o d \Rightarrow (W \times 1 - W \times G_v) \times b \geq (W \times G_h) \times d$$

d -----Vertical distance measured from the base of the concrete cask to the center of gravity

b -----Horizontal distance measured from the point of rotation to the C.G.

W -----Weight of the concrete cask

F_o -----Overturning force

F_r -----Restoring force

Substituting for G_y and G_x gives:

Case 1

$$(1-a) \frac{b}{d} \geq 0.566a$$

$$a \leq \frac{b/d}{0.566 + b/d}$$

Case 2

$$(1-0.4a) \frac{b}{d} \geq 1.077a$$

$$a \leq \frac{b/d}{1.077 + 0.4 b/d}$$

Empty concrete cask:

Case 1

$$a \leq \frac{64.0/116.0}{0.566 + 64.0/116.0} = 0.49$$

Case 2

$$a \leq \frac{64.0/116.0}{1.077 + 0.4 \cdot 64.0/116.0} = 0.43$$

where:

- b = 64.0 inch
- d = 116.0 inch

Loaded concrete cask:

Case 1

$$a \leq \frac{63.77/118.0}{0.566 + 63.77/118.0} = 0.488$$

Case 2

$$a \leq \frac{63.77/118.0}{1.077 + 0.4 \cdot 63.77/118.0} = 0.41$$

where:

- d = 118.0 inch
- b = 64.0 - x = 64.0 - 0.23 = 63.77 inch
- e = $\frac{73.44 - 72.0}{2} = 0.72$ inch-----TSC CG shift
- x = $\frac{W_{can} \cdot e}{W_{cc}} = \frac{103,000 \times 0.72}{322,000} = 0.23$ inch---Loaded concrete cask CG shift

The minimum acceleration is 0.41g. A factor of safety of 1.1 is required for an earthquake evaluation; therefore, the maximum allowable horizontal acceleration (a_{max}) at the top of the concrete pad that will preclude a cask tip-over is as follows.

$$a_{max} = \frac{0.41}{1.1} = 0.37g$$

Concrete Cask Stress

To demonstrate the ability of the concrete cask to withstand earthquake loading conditions, the fully loaded cask is conservatively evaluated for seismic loads of 0.5g in the horizontal and 0.5g in the vertical direction. These accelerations reflect a more rigorous seismic loading, and therefore, bound the design basis earthquake. No credit is taken for the concrete cask steel liner. The maximum compressive stresses at the concrete shell outer and inner surfaces are

conservatively calculated by considering the cask as a cantilever beam with its bottom end fixed. The maximum compressive stresses are as follows.

$$\sigma_{v \text{ outer}} = \frac{M}{S_{\text{outer}}} + \frac{(1 + a_y)W_{\text{cc}}}{A} = 138 \text{ psi}$$

$$\sigma_{v \text{ inner}} = \frac{M}{S_{\text{inner}}} + \frac{(1 + a_y)W_{\text{cc}}}{A} = 105 \text{ psi}$$

where

$$\begin{aligned} a_x &= 0.50g \text{-----Horizontal direction} \\ a_y &= 0.50g \text{-----Vertical direction} \\ W_{\text{cc}} &= 322,000 \text{ lb-----Bounding weight of concrete cask} \\ D_o &= 136.0 \text{ inch} \\ D_i &= 82.98 \text{ inch} \\ A &= \pi (D_o^2 - D_i^2) / 4 = 9,119 \text{ inch}^2 \\ I &= \pi (D_o^4 - D_i^4) / 64 = 14.47 \times 10^6 \text{ inch}^4 \\ S_{\text{outer}} &= 2I/D_o = 212,794 \text{ inch}^3 \\ S_{\text{inner}} &= 2I/(D_i) = 348,759 \text{ inch}^3 \\ w &= (a_x \times W_{\text{cc}}) / 225.27 = 715 \text{ lb/inch} \\ M &= (w \times 225.27^2) / 2 = 1.81 \times 10^7 \text{ lb-inch} \end{aligned}$$

3.7.3.5 Concrete Cask Combined Stresses

The load combinations described in Table 2.3-1 are used to evaluate the concrete cask for accident events of storage. Concrete stresses are summarized in Table 3.7-13, Table 3.7-14, and Table 3.7-15 for the loading combination No. 4, 5, 7, and 8. Loading combination No. 6 corresponds to drop accidents, 24-inch end drop and tip-over, which are evaluated in Section 3.7.3.6 and Section 3.7.3.7, respectively.

As shown in Table 3.7-14, the maximum concrete compressive stress is 1,201 psi; therefore, the minimum compressive factor of safety (FS) for accident events is as follows.

$$FS = \frac{S_{\text{con}}}{S_c} = \frac{2,660}{1,201} = 2.21$$

where:

$$S_{\text{con}} = \phi F_c = 0.7 \times 3,800 = 2,660 \text{ psi -----Concrete compressive allowable}$$

From Section 3.7.3.1, the maximum concrete ultimate strength due to thermal load is 0.1 ksi. The factor of safety (FS) for concrete ultimate strengths is as follows.

$$FS = \frac{S_{tc}}{S_t} = \frac{0.21}{0.1} = 2.10$$

where:

$$S_{tc} = 0.08 \times S_{con} = 0.08 \times 2660 = 213 \text{ psi or } 0.21 \text{ ksi -----Concrete ultimate strength}$$

From Section 3.7.3.1, the maximum rebar stress (S_{rb}) is due to thermal load is 20.2 ksi. The factor of safety (FS) for the rebar is as follows.

$$FS = \frac{S_{rebar}}{S_{rb}} = \frac{54.0}{20.2} = 2.67$$

where:

$$S_{rebar} = \phi F_r = 0.9 \times 60.0 = 54.0 \text{ ksi -----Rebar stress allowable}$$

3.7.3.6 Concrete Cask 24-inch Drop

Evaluation of the Concrete Cask

During the 24-inch bottom-end drop of the concrete cask, the cylindrical portion of the concrete is in contact with the steel bottom plate that is a part of the base weldment. The plate is assumed to be part of an infinitely rigid storage pad. No credit is taken for the crush properties of the storage pad or the underlying soil layer. Therefore, energy absorbed by the crushing of the cylindrical concrete region of the concrete cask equals the product of the compressive strength of the concrete, the crush depth of the concrete, and the projected area of the concrete cylinder. Crushing of the concrete continues until the energy absorbed equals the potential energy of the cask at the initial drop height. The TSC is not rigidly attached to the concrete cask, so it is not considered to contribute to the concrete crushing. The energy balance equation is as follows.

$$w(h + \delta) = P_o A \delta$$

where:

- $h = 24.0 \text{ inch}$ -----Drop height
- δ -----The crush depth of the concrete cask
- $P_o = 3,800 \text{ psi}$ -----Compressive strength of the concrete, 300°F
- $A = \pi(R_2^2 - R_1^2) = 9,119 \text{ inch}^2$ -----Area of the concrete shield wall
- $R_1 = 41.49 \text{ inch}$ -----Inside radius of the concrete
- $R_2 = 68 \text{ inch}$ -----Outside radius of the concrete
- $w = 185,000 \text{ lb}$ -----Bounding weight of concrete, rebar, and lid assembly

It is assumed that the maximum force that can be exerted on the concrete cask is the compressive strength of the concrete multiplied by the area of the concrete being crushed. The concrete cask's steel shell will not experience any significant damage during a 24-inch drop. Therefore, its functionality will not be impaired due to the drop.

The crush distance computed from the energy balance equation is as follows.

$$\delta = \frac{hw}{P_o A - w} = \frac{(24)(185,000)}{(3800)(9,119) - (185,000)} = 0.13 \text{ inch}$$

Pedestal Crush Evaluation

Upon a bottom-end impact of the concrete cask, the TSC produces a force on the pedestal (base weldment) located near the bottom of the cask. The ring above the air inlets is expected to yield. To determine the resulting acceleration of the TSC and deformation of the pedestal, a LS-DYNA analysis is used. As described in Appendix 3.D, a quarter-symmetry finite element model of the pedestal is used for this evaluation. To ensure that maximum deformations and accelerations are determined, two analyses are performed. One analysis, which uses the upper-bound weight of 105 kips, envelops the maximum deformation of the pedestal. The second analysis employs the lower-bound weight of 60 kips to account for maximum acceleration.

The maximum accelerations of the TSC during the 24-inch bottom-end impact are calculated to be 14.5g and 25.2g for the upper-bound weight TSC and lower-bound weight TSC, respectively. The resulting acceleration time histories of the TSC, which correspond to a filter frequency of 200 Hz, are shown in Figure 3.7-21 for the analysis using the upper-bound weight model and Figure 3.7-22 for the lower-bound weight model. The dynamic load factor (DLF) for the TSC is calculated to be 1.35 for the upper-bound weight TSC and 0.95 (consider 1.0) for the lower-bound weight TSC, based on the response of one-degree systems subjected to a triangular load pulse [23]. Therefore, the accelerations for the upper-bound weight and lower-bound weight TSC are 19.6g and 25.2g, respectively.

The maximum strain in the pedestal is 15.4%. Since the ultimate strain of A36 steel is greater than 25%, the pedestal is not subject to failure. The maximum vertical displacement of the air inlet is calculated to be 1.46 inch for the upper-bound and lower-bound weight TSC. The original opening is 4.4 inches. Since the maximum displacement is 1.46 inch, the minimum air inlet opening is 2.9 inch (4.4 - 1.46), which is approximately 66% of the original air inlet opening. This condition is bounded by the consequences of the loss of one-half of the air inlets off-normal event.

3.7.3.7 Concrete Cask Tip-over

Tip-over of the concrete cask is a nonmechanistic, hypothetical accident condition that presents a bounding case for evaluation. Existing postulated design basis accidents do not result in the tip-over of the concrete cask. Functionally, the concrete cask does not suffer significant adverse consequences due to this event. The concrete cask, TSC, and basket maintain design basis shielding, geometry control of contents, and contents confinement performance requirements.

For a tip-over event to occur, the center of gravity of the concrete cask and loaded TSC must be displaced beyond its outer radius, i.e., the point of rotation. When the center of gravity passes beyond the point of rotation, the potential energy of the cask and TSC is converted to kinetic energy as the cask and TSC rotate toward a horizontal orientation on the ISFSI pad. The subsequent motion of the cask is governed by the structural characteristics of the cask, the ISFSI pad and the underlying soil.

The MAGNASTOR concrete cask tip-over analyses are performed using LS-DYNA. LS-DYNA is an explicit finite element program for the nonlinear dynamic analysis of structures in three dimensions. Details of the finite element model are presented in Appendix 3.D.

Two geometries are considered in this evaluation. The pad width of 30 ft in the models corresponds to the typical width of a concrete storage pad. One model considers a pad length of 30 ft while the second model, referred to as the “oversized pad” employs a length of 60 feet. The second model allows the effect of the pad length used in the analysis to be assessed.

The acceleration time histories for the TSC and basket for the standard and oversized pad cases are shown in Figure 3.7-23 and Figure 3.7-24. A cut-off frequency of 200 Hz is applied to filter the analysis results and measure the peak accelerations. The following is a summary of the peak accelerations.

Location	Position from base of concrete cask (in)	Acceleration Standard Pad (g)	Acceleration Oversized Pad (g)
Top of basket	177.7	26.4	26.6
Top of TSC Closure lid	197.6	29.5	29.6

Using two-dimensional models of the PWR and BWR basket (similar to the models described in Appendices 3.A and 3.B, meshing density modified for modal analysis), the modal frequencies for the basket are calculated. Table 3.7-16 summarized the frequencies for the first mode shape for the PWR and BWR baskets in the 0° and 45° basket orientations. The dynamic load factors are determined using the response of one-degree systems subjected to a triangular load pulse [23]. The dynamic load factors and the maximum accelerations at the top of the TSC and top of

the basket are summarized in Table 3.7-17. As the table and figures show, maximum accelerations are less than the specified design value of 40g. The acceleration results indicate that even with a 100% increase in the pad length the resulting change in the maximum accelerations is less than 1%. This demonstrates that the effect of the pad size employed in the analysis has an insignificant effect on the maximum accelerations.

Figure 3.7-1 PWR Fuel Tube Array – 0° Basket Orientation

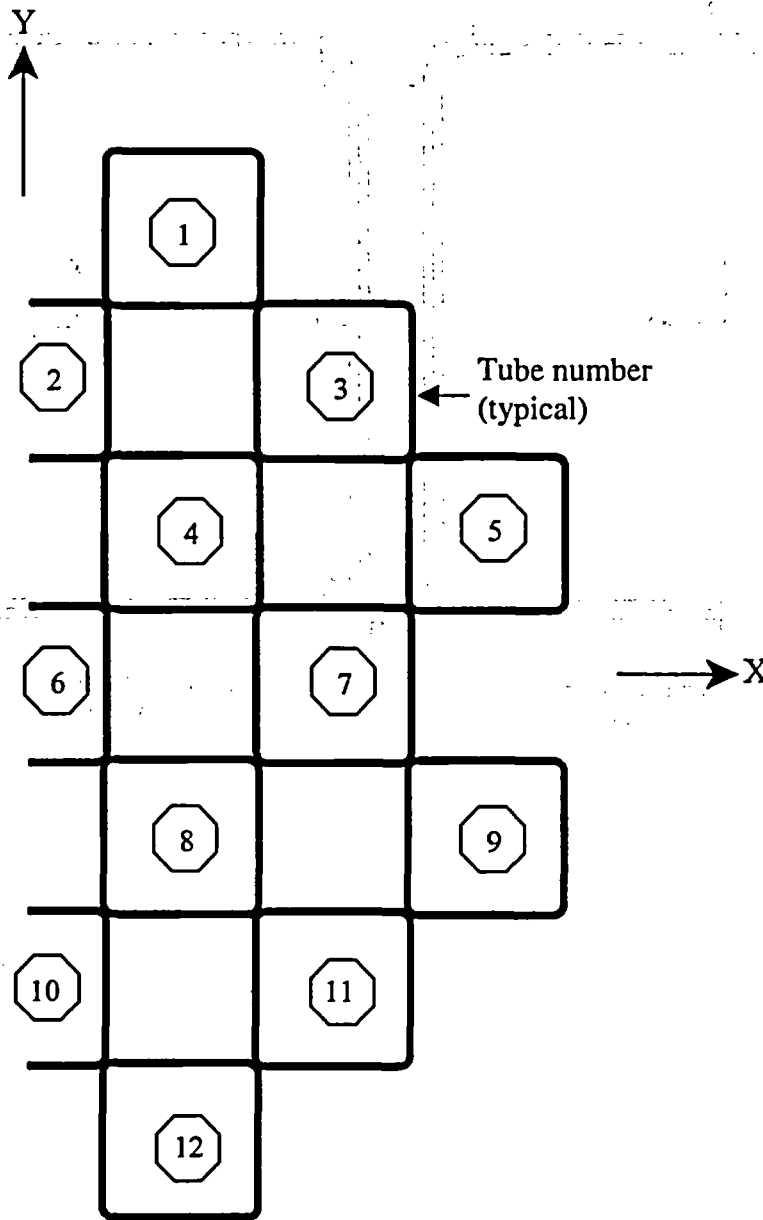


Figure 3.7-2 PWR Fuel Tube Section Cuts – 0° Basket Orientation

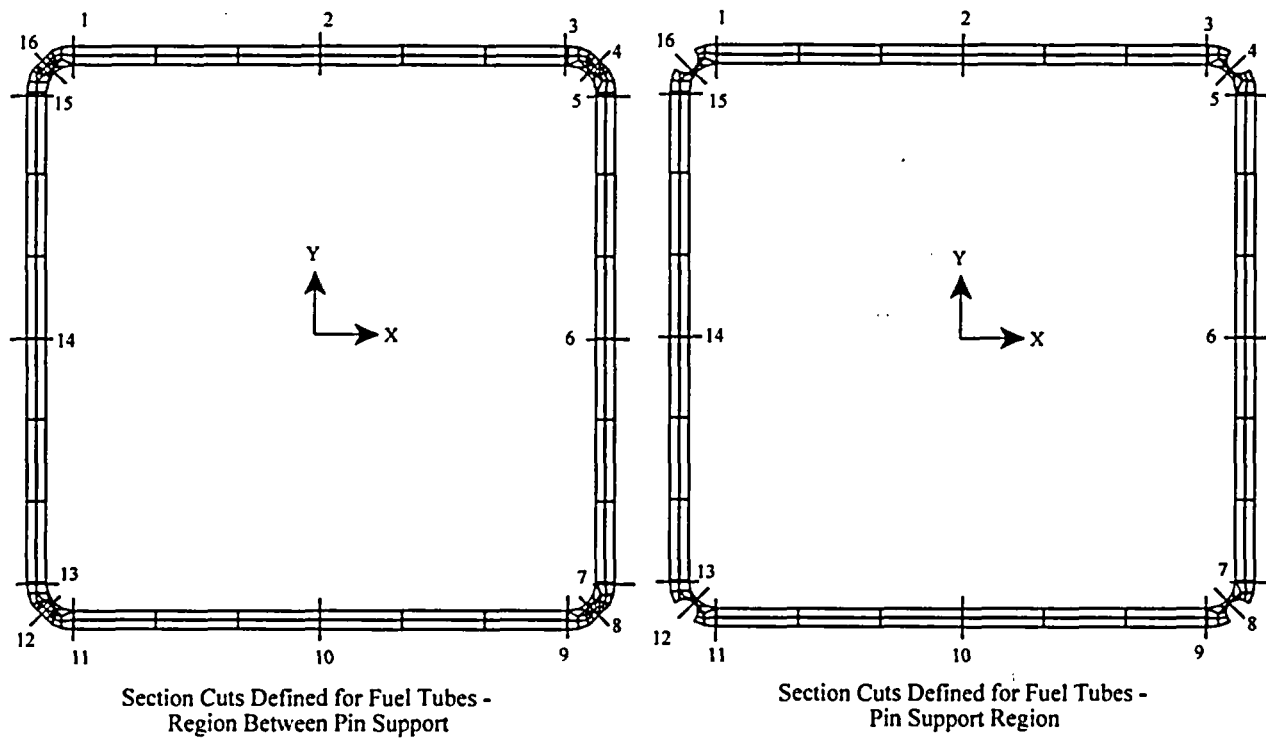


Figure 3.7-3 PWR Fuel Tube Array – 45° Basket Orientation

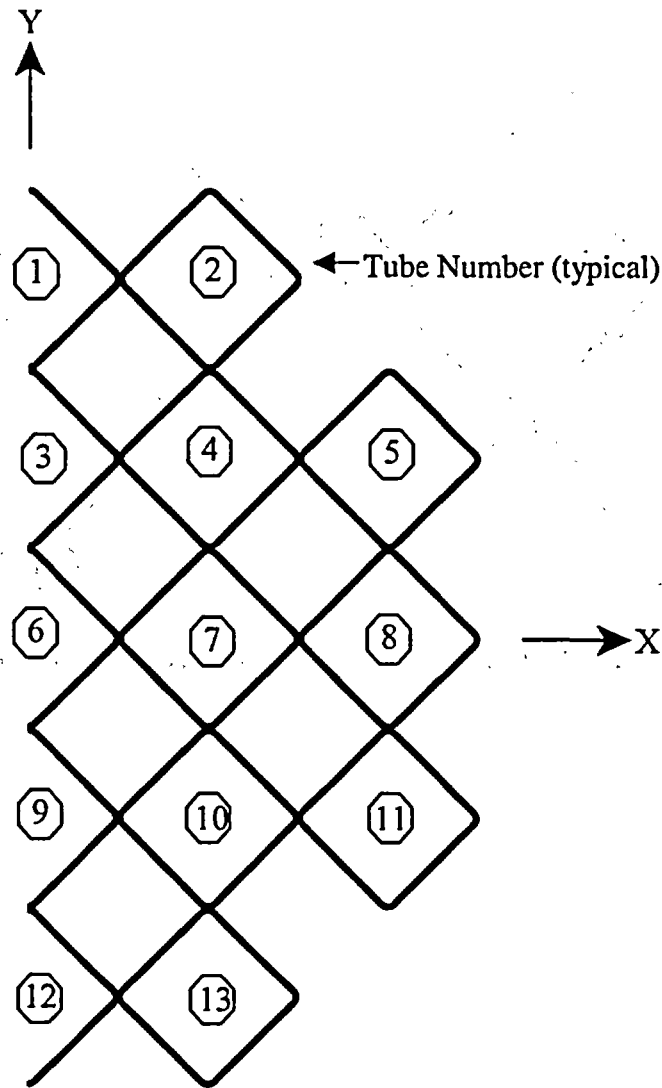


Figure 3.7-4 PWR Fuel Tube Section Cuts – 45° Basket Orientation

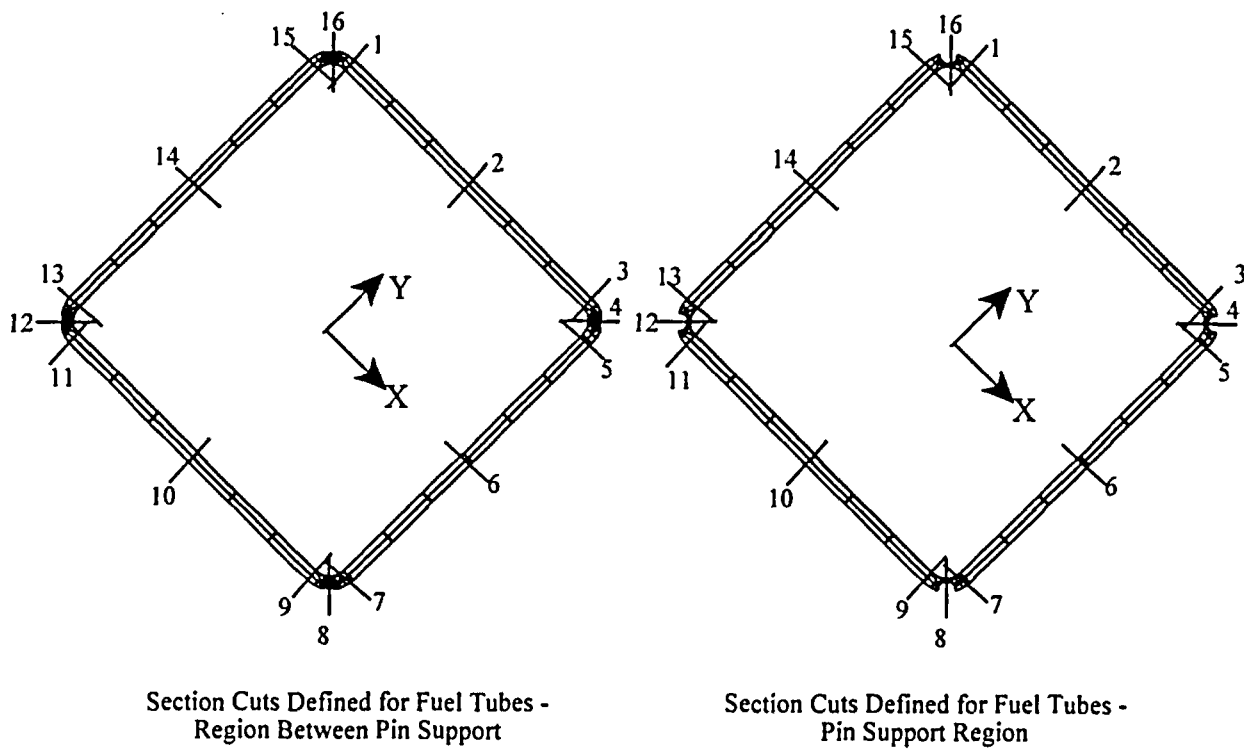


Figure 3.7-5 PWR Corner Support Weldment Section Cuts - 0° Basket Orientation

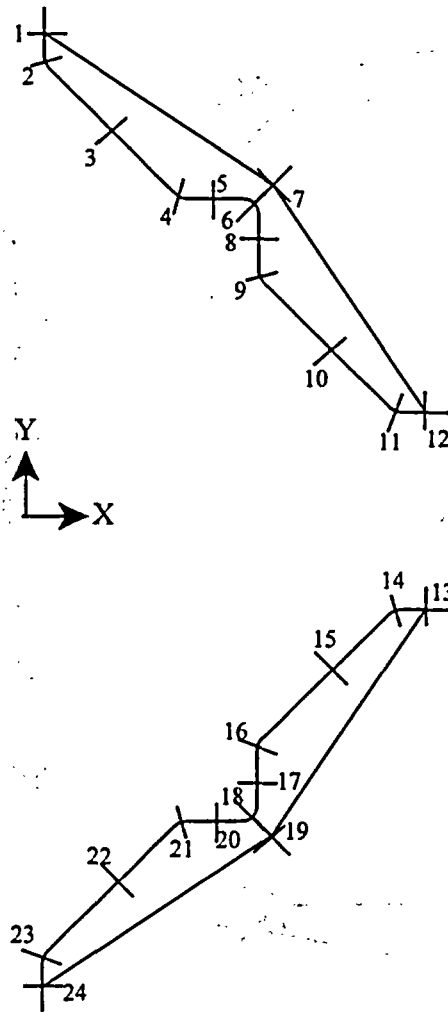


Figure 3.7-6 PWR Corner Support Weldment Section Cuts – 45° Basket Orientation

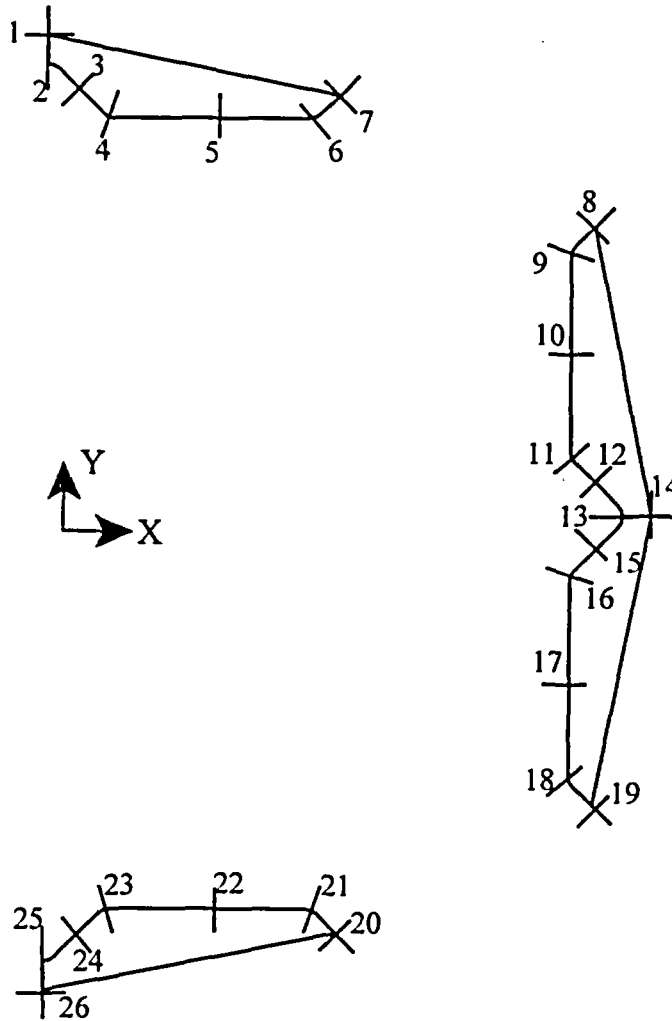


Figure 3.7-7 PWR Side Support Weldment Section Cuts - 0° Basket Orientation

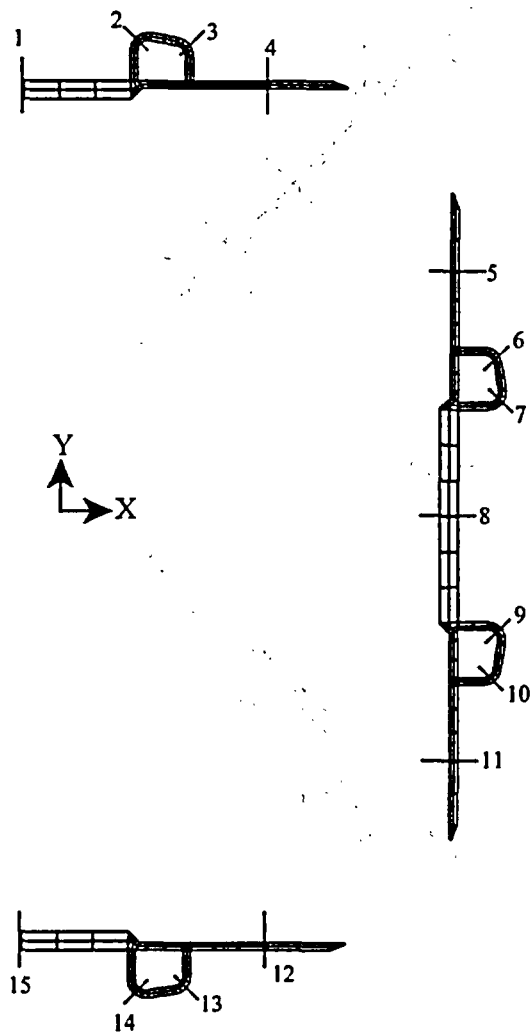


Figure 3.7-8 PWR Side Support Weldment Section Cuts – 45° Basket Orientation

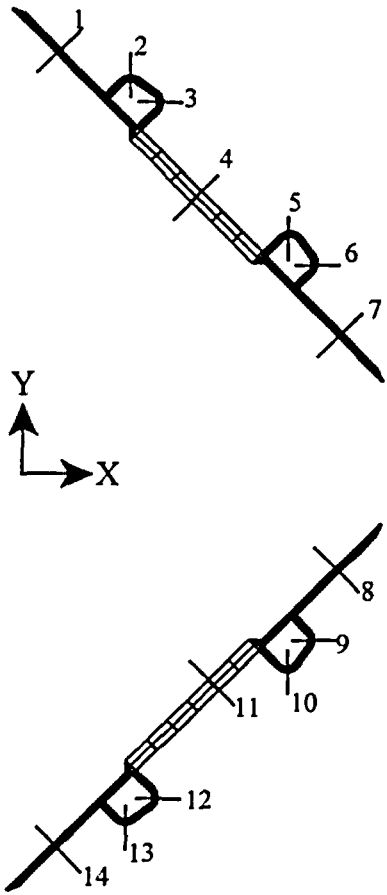
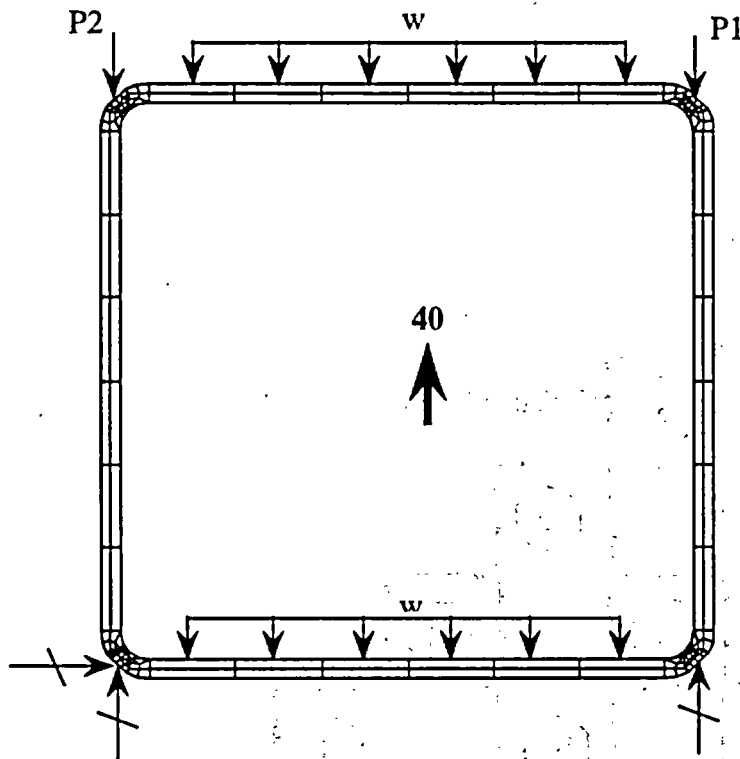


Figure 3.7-9 PWR Fuel Tube Model for Buckling Evaluation



Unit Thickness Loading (40g)

$$w = \frac{1.680}{165.5(8.202)} (40) = 49.5 \text{ psi}$$

$$P1 = \frac{6(665) + 10(1,680)}{2(165.5)} (40) = 2,520 \text{ lb/inch}$$

$$P2 = \frac{6(665) + 11(1,680)}{2(165.5)} (40) = 2,712 \text{ lb/inch}$$

Where:

PWR assembly weight = 1,680 lb

Fuel tube length = 165.5 inch

Inside tube width = 8.202 inch

Maximum acceleration = 40g

Tube weight = 675 lb

Figure 3.7-10 BWR Fuel Tube Array – 0° Basket Orientation

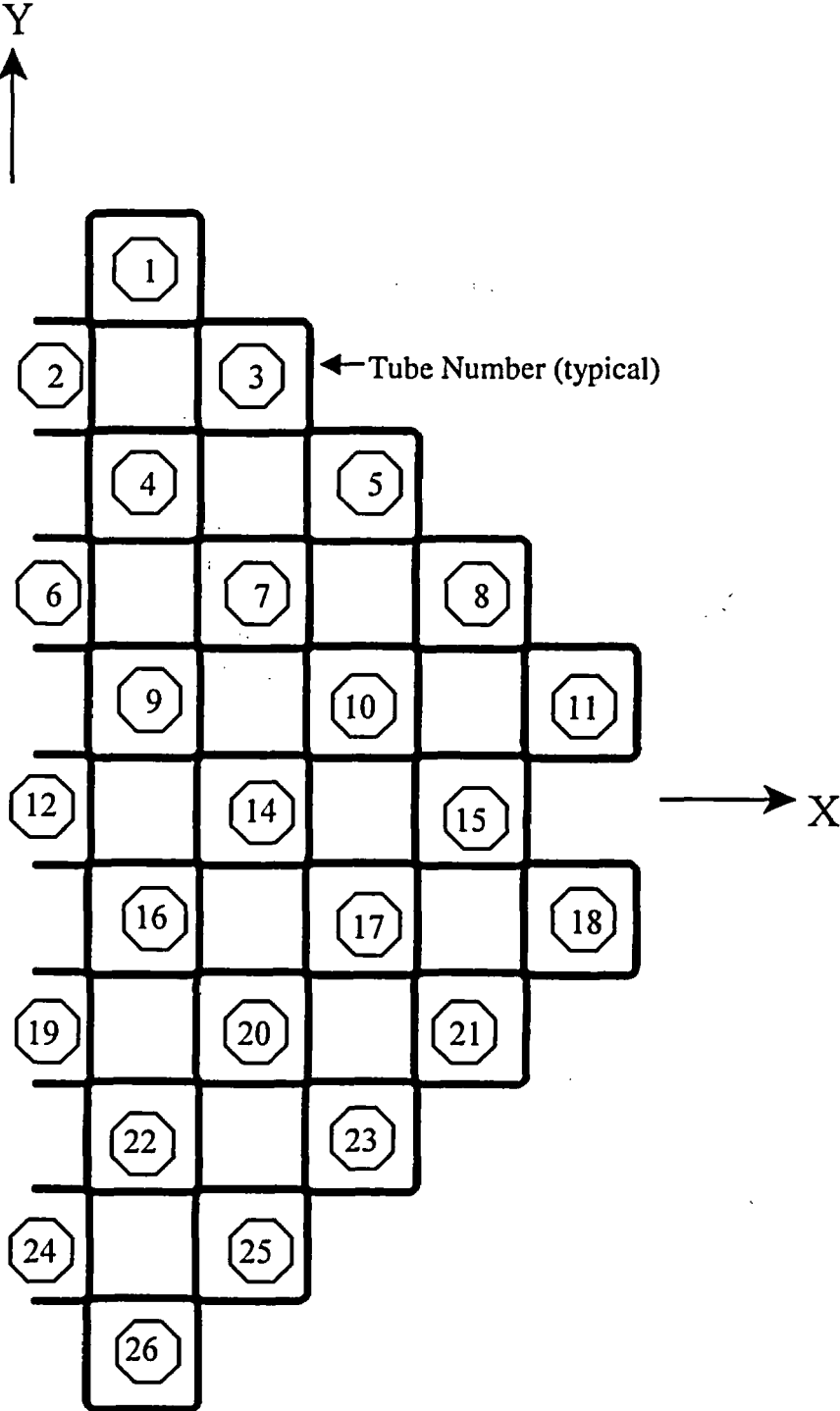


Figure 3.7-11 BWR Fuel Tube Section Cuts – 0° Basket Orientation

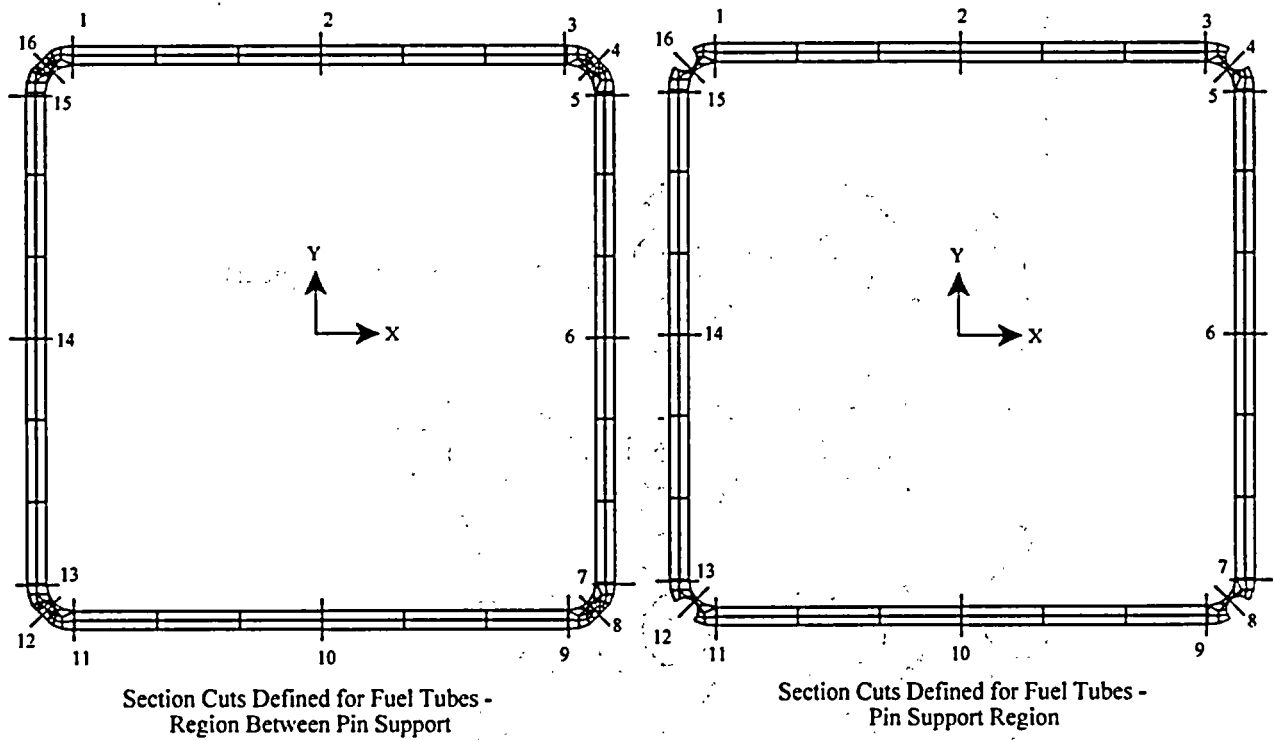


Figure 3.7-12 BWR Fuel Tube Array – 45° Basket Orientation

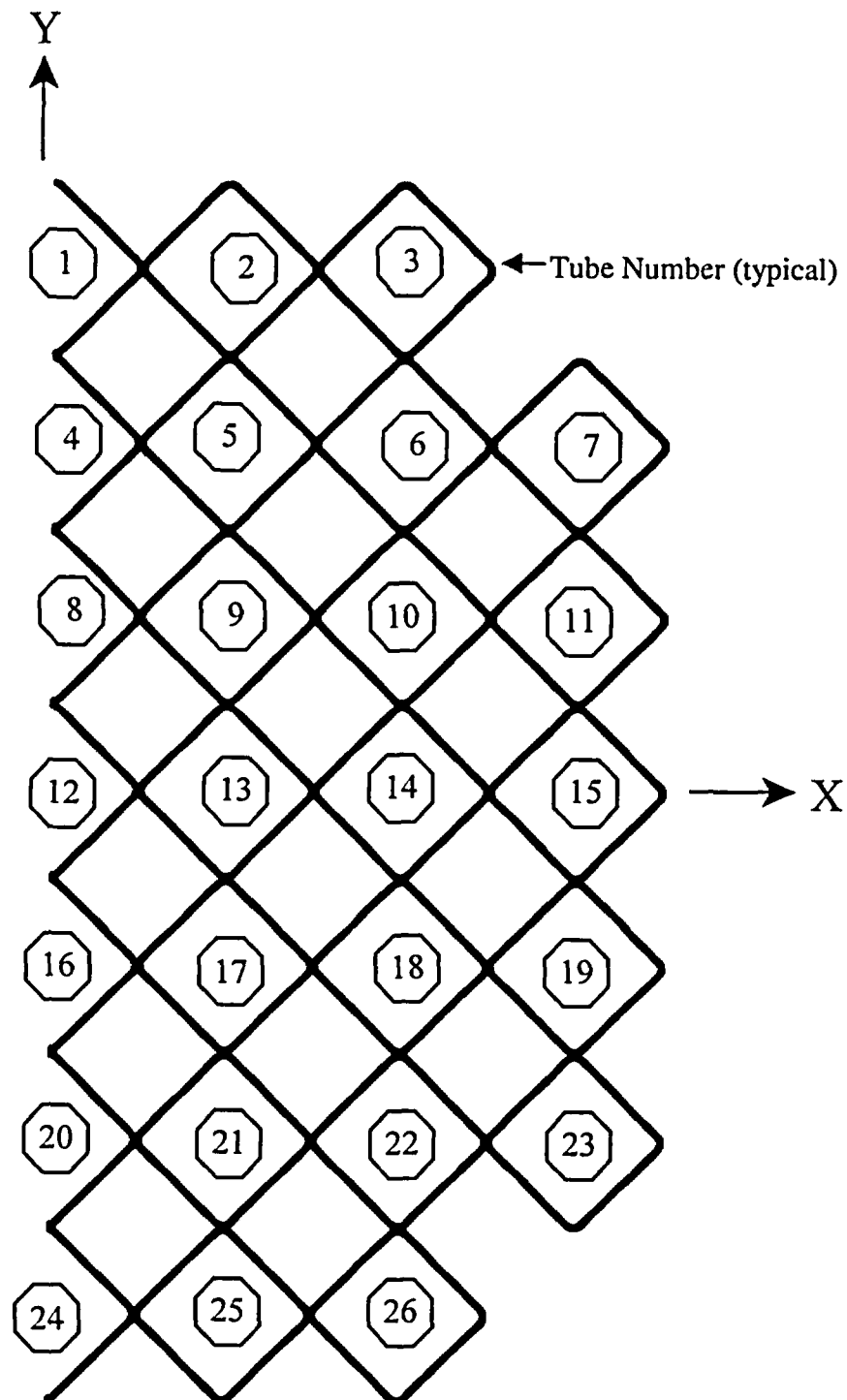


Figure 3.7-13 BWR Fuel Tube Section Cuts - 45° Basket Orientation

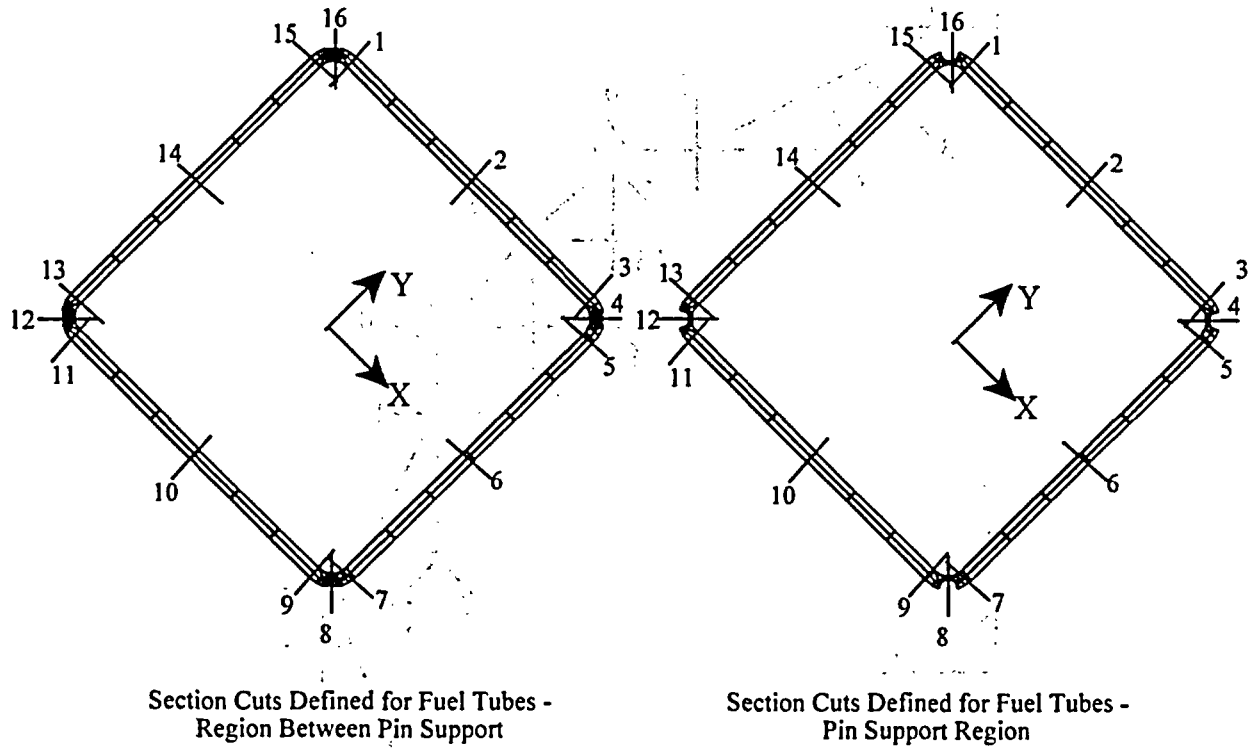


Figure 3.7-14 BWR Corner Support Weldment Section Cuts – 0° Basket Orientation

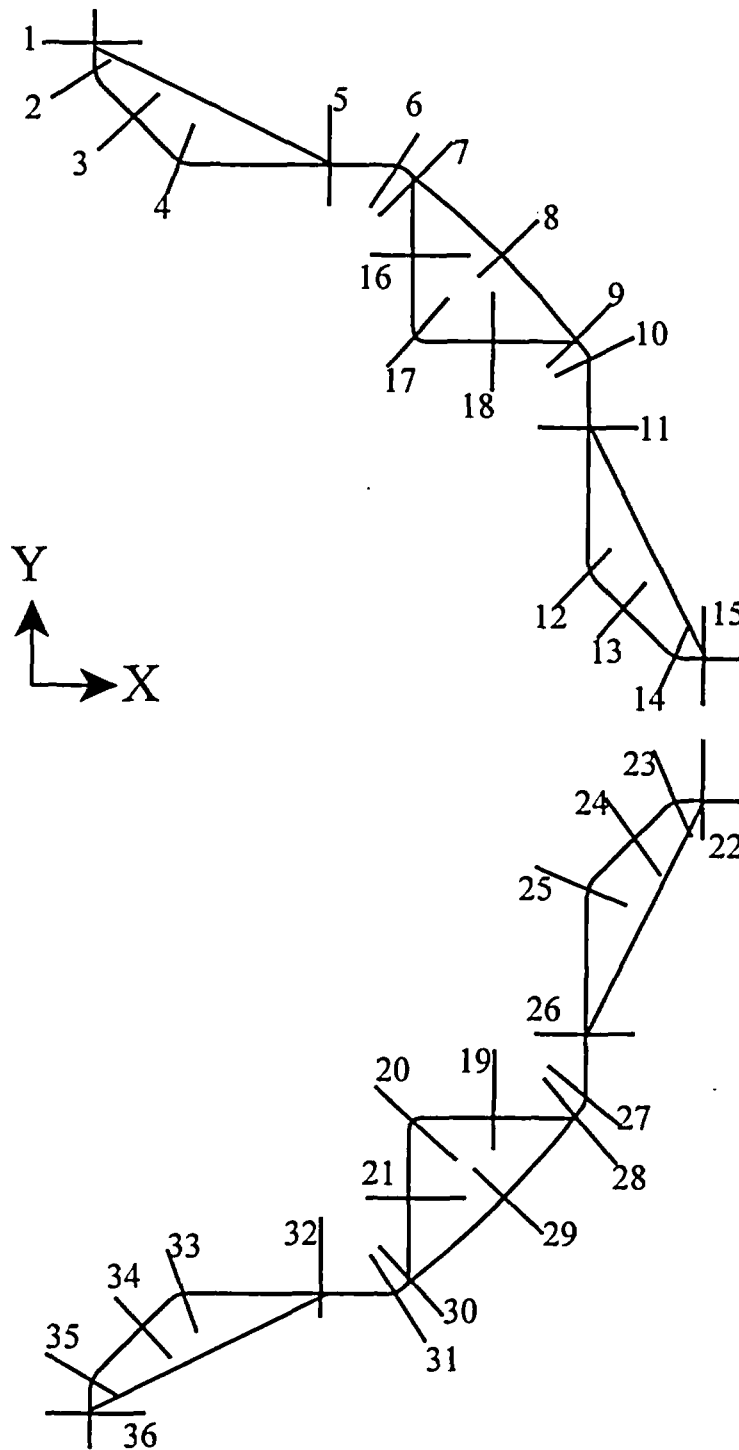


Figure 3.7-15 BWR Corner Support Weldment Section Cuts - 45° Basket Orientation

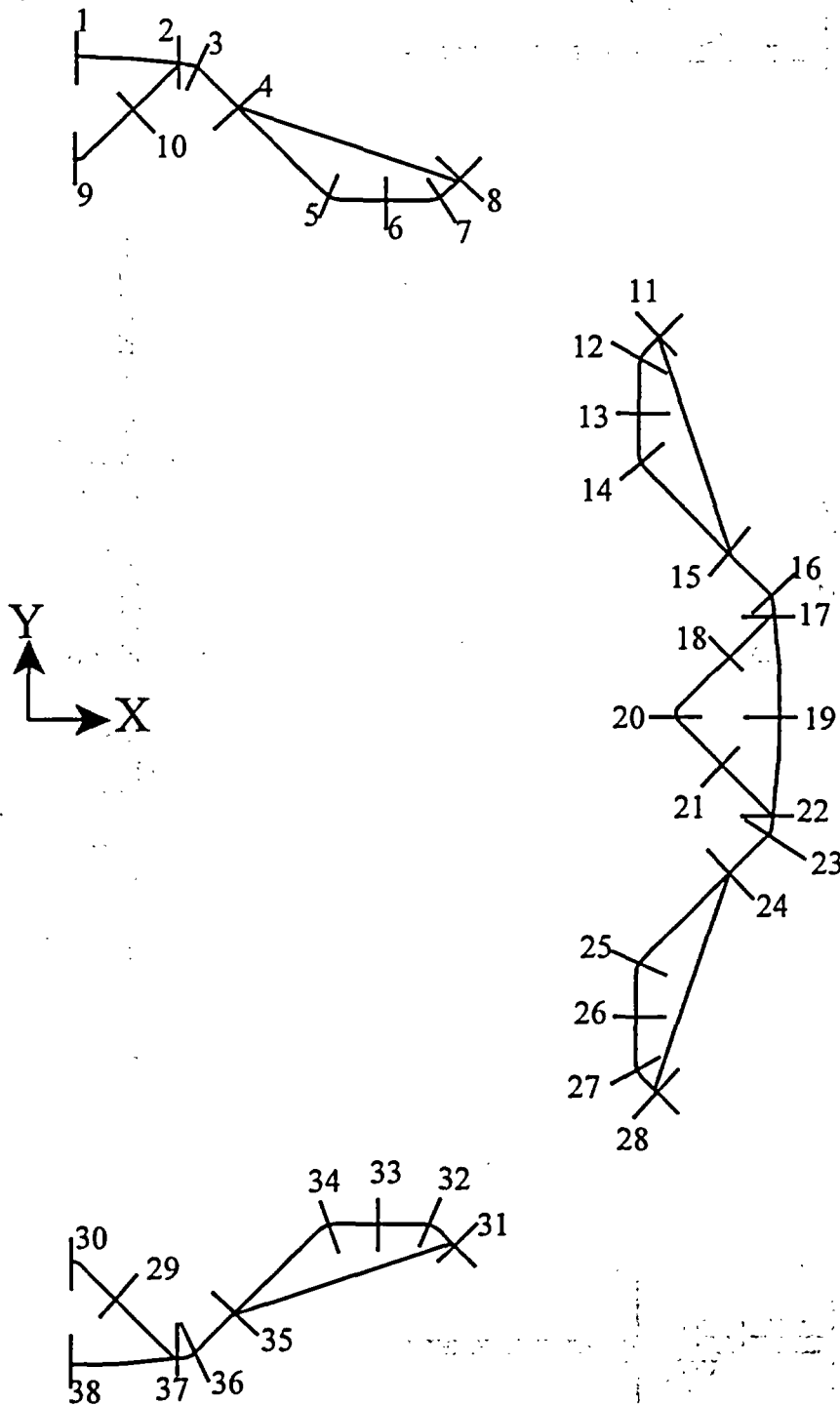


Figure 3.7-16 BWR Side Support Weldment Section Cuts – 0° Basket Orientation

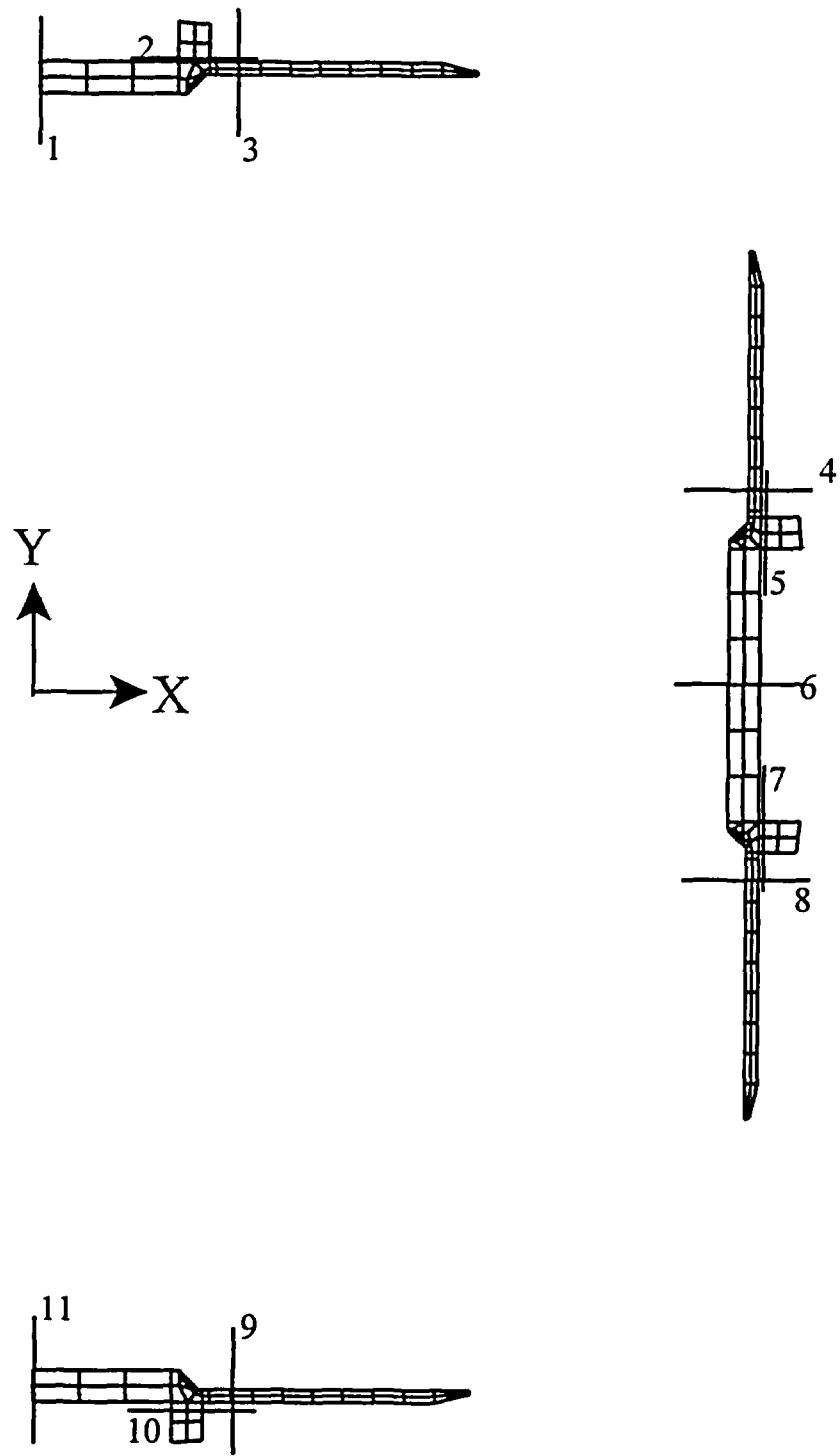


Figure 3.7-17 BWR Side Support Weldment Section Cuts – 45° Basket Orientation

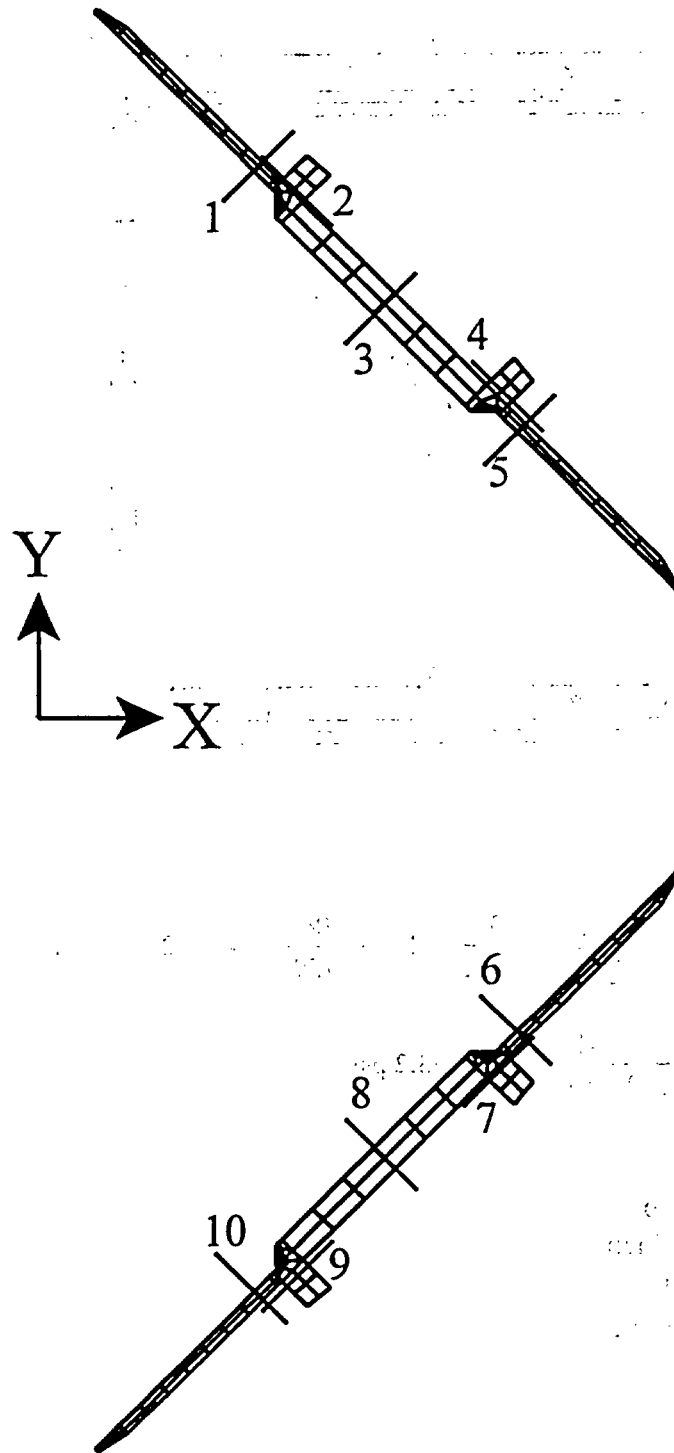
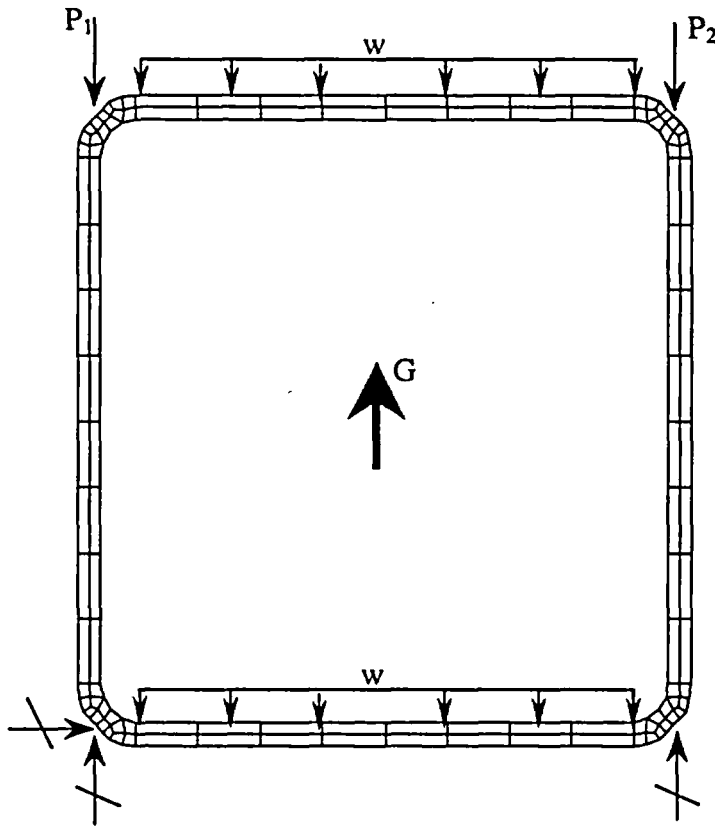


Figure 3.7-18 BWR Fuel Tube Model for Buckling Evaluation



$$P_1 = P_2 = \left[10 \left(\frac{400}{159.1 \times 2} \right) + 19 \left(\frac{704}{2 \times 159.1} \right) \right] 40 = 2185 \text{ lb/in}$$

$$w = \left(\frac{704}{159.1 \times 5.34} \right) 40 = 33.2 \text{ psi}$$

Where:

BWR fuel weight = 704 lb

Fuel tube length = 159.1 inch

Fuel tube weight = 400 lb

Maximum acceleration = 40g

Figure 3.7-19 PWR Neutron Absorber and Retainer Finite Element Model

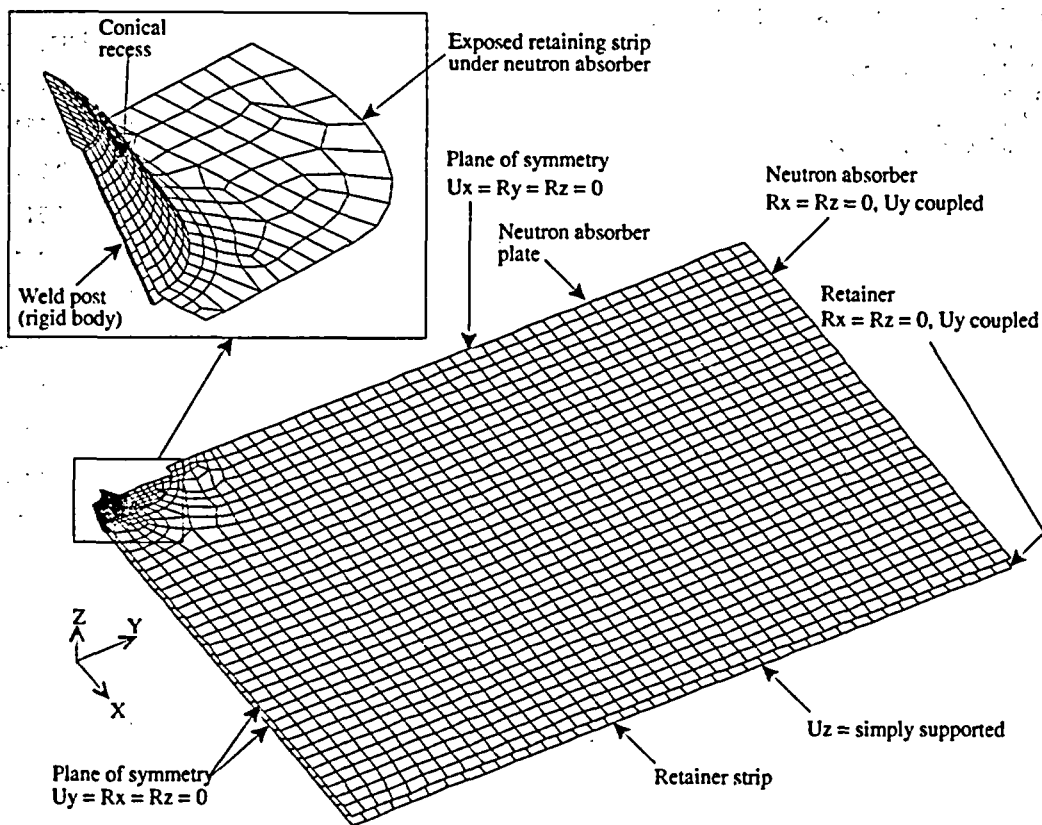


Figure 3.7-20 Permanent Strain Contour Plot for the PWR Basket Retainer Strip – Cask Tip-over

POISON PLATE, 8" WIDE W/SINGLE ROW RIVE
Time = 0.1
Isosurfaces of Effective Plastic Strain
max lpl. value
min=0, at elem# 490
max=0.00373435, at elem# 3177

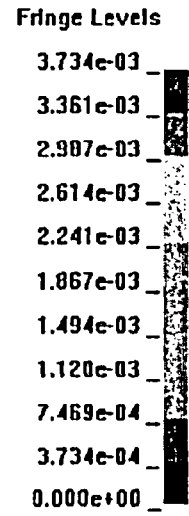
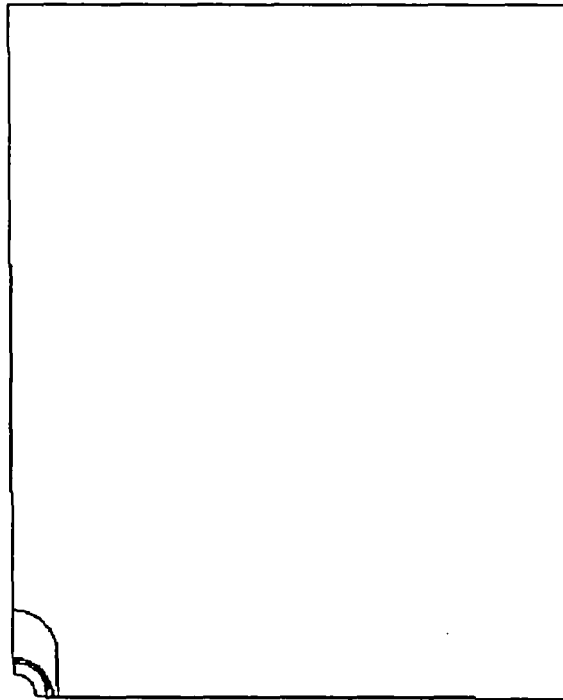


Figure 3.7-21 Acceleration Time History of the Upper-bound weight TSC – 24-inch Concrete Cask Drop

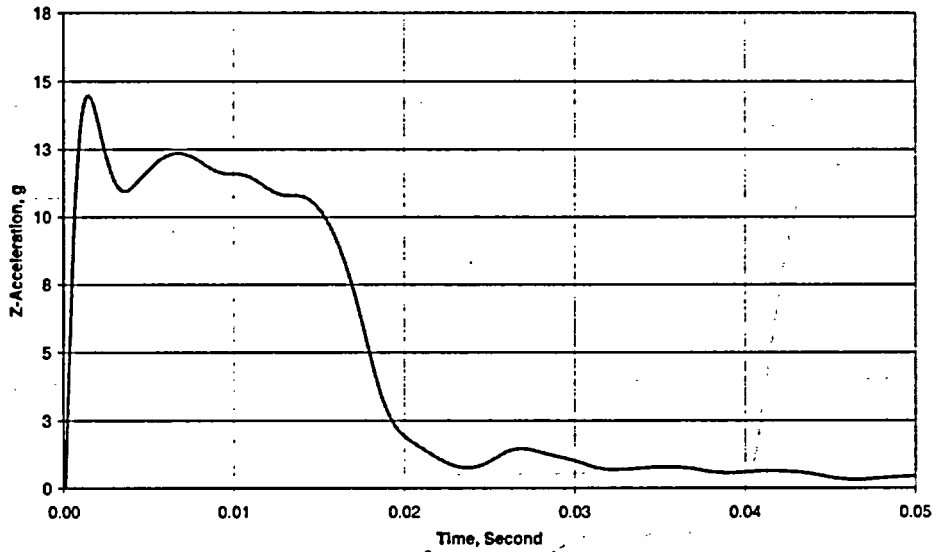


Figure 3.7-22 Acceleration Time History of the Lower-bound Weight TSC – 24-inch Concrete Cask Drop

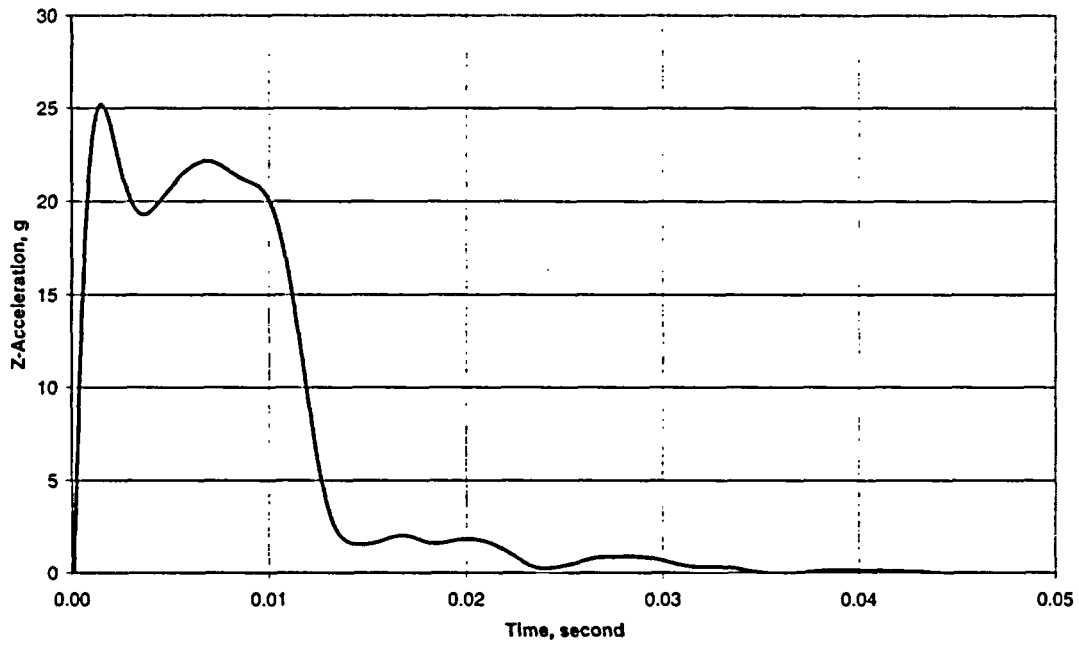


Figure 3.7-23 Acceleration Time History for Concrete Cask Tip-over Condition - Standard Pad

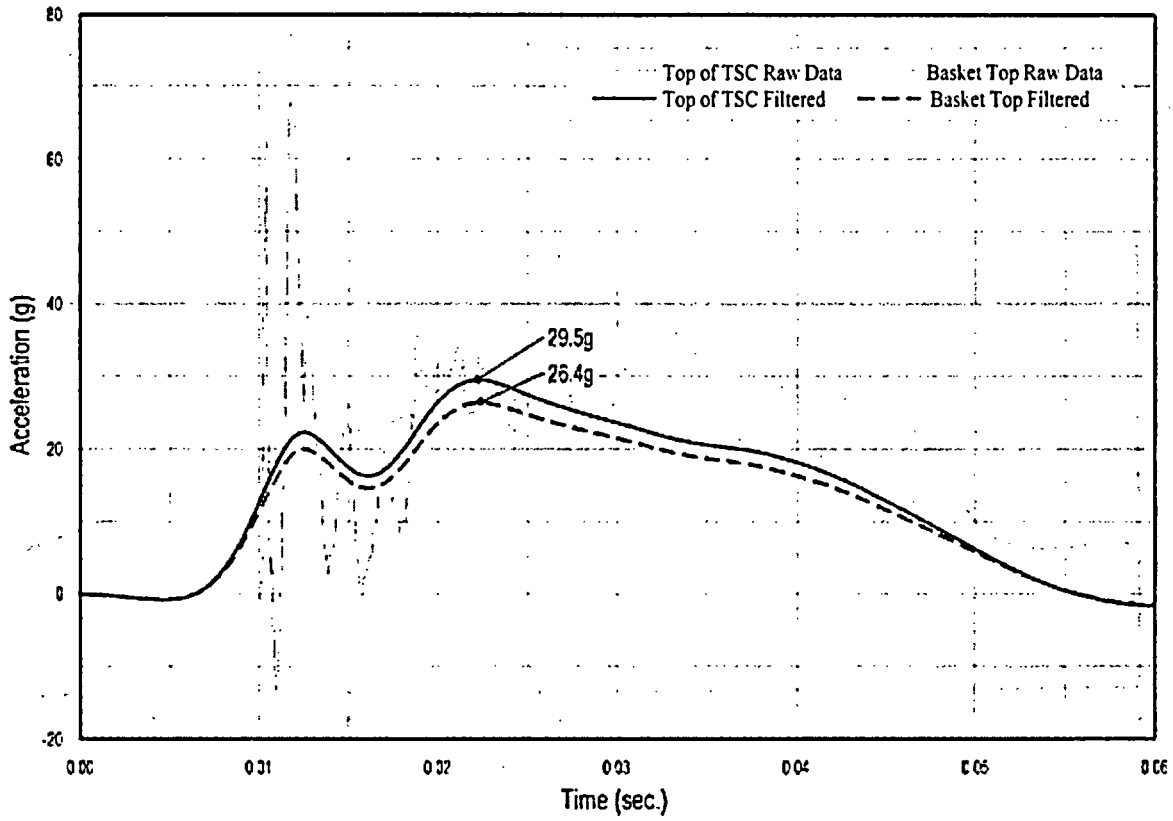


Figure 3.7-24 Acceleration Time History of Oversized Pad

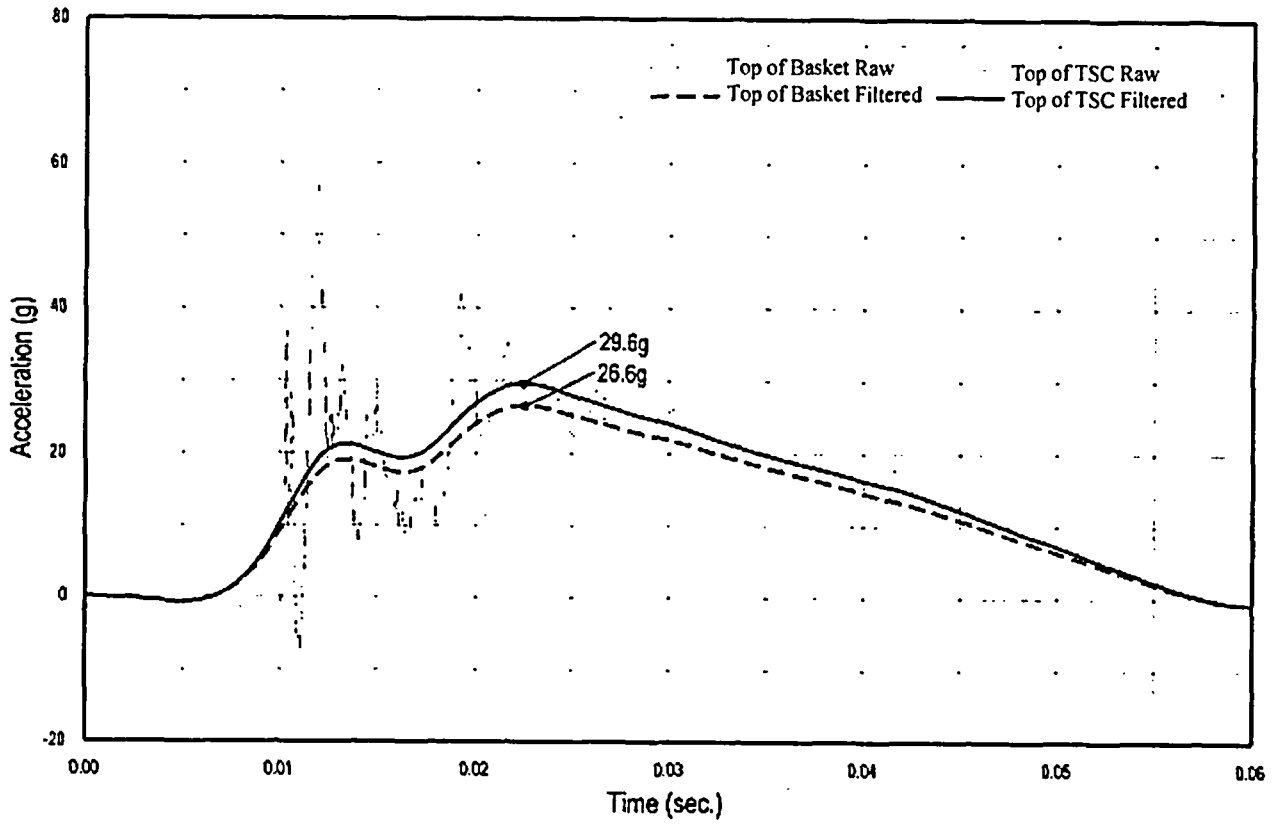


Table 3.7-1 TSC Accident Events, P_m Stresses

Load Case ^{a)}	Service Level	Section ^{b)}	Component Stresses (ksi)						S_{int}	S_{allow}	FS
			S_x	S_y	S_z	S_{xy}	S_{yz}	S_{xz}			
Accident Pressure	D	2	5.50	-16.40	-4.61	0.74	-0.01	-0.89	22.03	47.58	2.16
Normal Pressure + 24-inch Drop	D	4	-0.04	7.80	-4.20	-0.31	0.00	0.00	12.01	43.40	3.61
Normal Pressure + Tip-Over	D	1	-20.34	-9.69	5.01	1.88	0.14	-0.45	25.69	47.58	1.85

Table 3.7-2 TSC Accident Events, $P_m + P_b$ Stresses

Load Case ^{a)}	Service Level	Section ^{b)}	Component Stresses (ksi)						S_{int}	S_{allow}	FS
			S_x	S_y	S_z	S_{xy}	S_{yz}	S_{xz}			
Accident Pressure	D	11	45.86	45.84	9.17	0.14	6.83	1.18	39.26	68.60	1.75
Normal Pressure + 24-inch Drop	D	11	20.22	20.21	2.50	0.06	3.00	0.52	18.76	68.60	3.66
Normal Pressure + Tip-Over	D	1	-19.28	-12.82	13.90	1.72	0.25	-0.91	33.66	69.80	2.07

Table 3.7-3 PWR Fuel Tube Nodal Stresses – Concrete Cask Tip-over Accident

Tube ^{a)}	Basket (deg)	P_m (ksi)			$P_m + P_b$ (ksi)		
		S_{int}	S_{allow}	FS	S_{int}	S_{allow}	FS
10	45	36.6	47.88	1.31	41.6	61.56	1.48
7	45	36.6	47.88	1.31	41.5	61.56	1.48
3	45	37.5	47.88	1.28	40.7	61.56	1.51
12	0	36.7	47.88	1.30	39.4	61.56	1.56
10	0	36.6	47.88	1.31	38.7	61.56	1.59

^{a)} The x,y,z component of stress are to be interpreted radial, circumferential, and axial directions, respectively.

^{b)} See Figure 3.C-2 for section cut locations.

Table 3.7-4 PWR Corner Mounting Plate P_m Stresses – Concrete Cask Tip-over Accident

Basket	Section ^{a)}	S_{int} (ksi)	S_{allow} (ksi)	FS
0°	24	12.8	47.88	3.74
45°	19	12.1	47.88	3.96
0°	13	11.0	47.88	4.35
0°	23	10.9	47.88	4.39
45°	18	10.3	47.88	4.65

Table 3.7-5 PWR Corner Mounting Plate $P_m + P_b$ Stresses – Concrete Cask Tip-over Accident

Basket	Section ^{a)}	S_{int} (ksi)	S_{allow} (ksi)	FS
0°	20	39.9	68.40	1.71
45°	13	38.8	68.40	1.76
45°	15	36.2	68.40	1.89
45°	25	34.4	68.40	1.99
0°	13	26.7	68.40	2.56

Table 3.7-6 PWR Side Weldment P_m Stresses – Concrete Cask Tip-over Accident

Basket	Section ^{b)}	S_{int} (ksi)	S_{allow} (ksi)	FS
0°	13	14.0	47.88	3.42
45°	10	9.3	47.88	5.15
45°	12	7.3	47.88	6.56
0°	14	4.8	47.88	9.98
0°	15	4.0	47.88	Large

Table 3.7-7 PWR Side Weldment $P_m + P_b$ Stresses – Concrete Cask Tip-over Accident

Basket	Section ^{b)}	S_{int} (ksi)	S_{allow} (ksi)	FS
0°	15	47.8	68.40	1.43
45°	12	43.9	68.40	1.56
45°	9	39.3	68.40	1.74
0°	12	37.4	68.40	1.83
45°	10	21.6	68.40	3.17

^{a)} The locations of the sections for the 0° and 45° basket orientation are shown in Figure 3.7-5 and Figure 3.7-6, respectively.

^{b)} The locations of the sections for the 0° and 45° basket orientation are shown in Figure 3.7-7 and Figure 3.7-8, respectively.

Table 3.7-8 BWR Fuel Tube Stresses – Concrete Cask Tip-over Accident

Tube ^{a)}	Basket (deg)	P _m (ksi)			P _m + P _b (ksi)		
		S _{int}	S _{allow}	FS	S _{int}	S _{allow}	FS
23	45	36.8	47.88	1.30	43.9	61.56	1.40
8	45	37.5	47.88	1.28	40.9	61.56	1.51
5	45	37.0	47.88	1.29	39.1	61.56	1.57
4	45	36.8	47.88	1.30	38.5	61.56	1.60
18	45	36.8	47.88	1.30	38.3	61.56	1.61

Table 3.7-9 BWR Corner Mounting Plate P_m Stresses – Concrete Cask Tip-over Accident

Basket	Section ^{b)}	S _{int} (ksi)	S _{allow} (ksi)	FS
0°	21	6.3	47.88	7.62
0°	31	5.8	47.88	8.27
45°	30	5.7	47.88	8.39
0°	36	4.7	47.88	Large
45°	25	4.6	47.88	Large

Table 3.7-10 BWR Corner Mounting Plate P_m + P_b Stresses – Concrete Cask Tip-over Accident

Basket	Section ^{b)}	S _{int} (ksi)	S _{allow} (ksi)	FS
45°	28	56.0	68.40	1.22
0°	36	46.7	68.40	1.46
45°	27	41.0	68.40	1.67
0°	32	40.2	68.40	1.70
45°	23	38.7	68.40	1.77

Table 3.7-11 BWR Side Weldment P_m Stresses – Concrete Cask Tip-over Accident

Basket	Section ^{c)}	S _{int} (ksi)	S _{allow} (ksi)	FS
0°	11	5.6	47.88	8.58
45°	7	5.2	47.88	9.24
45°	6	4.0	47.88	Large
0°	10	3.7	47.88	Large
45°	9	3.5	47.88	Large

^{a)} See Figure 3.7-12 for tube locations.

^{b)} The locations of the sections for the 0° and 45° basket orientation are shown in Figure 3.7-14 and Figure 3.7-15, respectively.

^{c)} The locations of the sections for the 0° and 45° basket orientation are shown in Figure 3.7-16 and Figure 3.7-17, respectively.

Table 3.7-12 BWR Side Weldment $P_m + P_b$ Stresses – Concrete Cask Tip-over Accident

Basket	Section ^{a)}	S_{int} (ksi)	S_{allow} (ksi)	FS
45°	6	37.6	68.40	1.82
0°	3	12.9	68.40	5.31
0°	7	9.5	68.40	7.17
0°	11	9.5	68.40	7.17
45°	1	8.7	68.40	7.84

Table 3.7-13 Concrete Cask Vertical Stress Summary – Outer Surface, psi

Condition	Dead	Live	Wind	Thermal	Seismic	Flood	Tornado	Total
4	-23	-25	0	0	0	0	0	-48
5	-23	-25	0	0	-138	0	0	-186
7	-23	-25	0	0	0	-17	0	-65
8	-23	-25	0	0	0	0	-19	-67

Table 3.7-14 Concrete Cask Vertical Stress Summary – Inner Surface, psi

Condition	Dead	Live	Wind	Thermal	Seismic	Flood	Tornado	Total
4	-23	-25	0	-1048	0	0	0	-1096
5	-23	-25	0	-989	-105	0	0	-1201
7	-23	-25	0	-989	0	-11	0	-1107
8	-23	-25	0	-989	0	0	-12	-1108

Table 3.7-15 Concrete Cask Circumferential Stress Summary – Inner Surface, psi

Condition	Dead	Live	Wind	Thermal	Seismic	Flood	Tornado	Total
4	0	0	0	-217	0	0	0	-217
5	0	0	0	-211	0	0	0	-211
7	0	0	0	-211	0	0	0	-211
8	0	0	0	-211	0	0	0	-211

^{a)} The locations of the sections for the 0° and 45° basket orientation are shown in Figure 3.7-16 and Figure 3.7-17, respectively.

Table 3.7-16 Basket Modal Frequency for Concrete Cask Tip-over

Fuel Type and Basket Angle	Frequency (F), Hz
PWR-0	269
PWR-45	33
BWR-0	140
BWR-45	39

Table 3.7-17 DLF and Amplified Accelerations for Concrete Cask Tip-over

Fuel Type and Basket Angle	Top of TSC Lid			Top of Fuel Basket		
	Base Acceleration, g	DLF	Amplified Acceleration, g	Base Acceleration, g	DLF	Amplified Acceleration, g
PWR-0	29.6	1.0	29.6	26.6	1.01	26.9
PWR-45	29.6	1.0	29.6	26.6	1.21	32.2
BWR-0	29.6	1.0	29.6	26.6	1.02	27.1
BWR-45	29.6	1.0	29.6	26.6	1.07	28.5

3.8 Fuel Rods

MAGNASTOR limits normal storage condition fuel cladding temperatures to be $\leq 400^{\circ}\text{C}$ (752°F) in accordance with ISG-11, Rev 3. Zirconium alloy or stainless steel cladding degradation is not expected to occur below this temperature.

The fuel cladding temperature limit for short-term off-normal and accident events is 570°C ($1,058^{\circ}\text{F}$). Refer to Chapter 4, which demonstrates that the maximum fuel cladding temperatures are well below the temperature limits for all design conditions of storage.

3.9 References

1. 10 CFR 72, Code of Federal Regulations, "Licensing Requirements for the Independent Storage of Spent Fuel, High Level Radioactive Waste and Reactor-Related Greater than Class C Waste", US Nuclear Regulatory Commission, Washington, DC, January 1996.
2. American National Standard for Radioactive Materials N14.6-1993, "Special Lifting Devices for Shipping Containers Weighing 10,000 Pounds (4500 kg) or More," American National Standard Institute, Inc., Washington, DC, 1993.
3. NUREG 0612, "Control of Heavy Loads at Nuclear Power Plants", U. S. Nuclear Regulatory Commission, Washington, D.C., 1980.
4. ANSI/ANS-57.9-1992, American National Standard Design Criteria for an Independent Spent Fuel Storage Installation (Dry Type), American Nuclear Society, La Grange Park, IL, May 1992.
5. "Code Requirements for Nuclear Safety Related Concrete Structures (ACI 349) and Commentary (ACI 349R)," American Concrete Institute, Farmington Hills, MI.
6. ASME Boiler and Pressure Vessel Code, Section III, Subsection NB, "Class 1 Components," American Society of Mechanical Engineers, New York, NY, 2001 Edition with 2003 Addenda.
7. ASME Boiler and Pressure Vessel Code, Section III Subsection NG, "Core Support Structures", American Society of Mechanical Engineers, New York, NY; 2001, with 2003 Addenda.
8. ASME Boiler and Pressure Vessel Code, Appendix F, "Rules for Evaluation of Service Loadings with Level D Service Limits," The American Society of Mechanical Engineers, New York, NY, 2001, with 2003 Addenda.
9. NUREG / CR-6322, "Buckling Analysis of Spent Fuel Basket", Lawrence Livermore National Laboratory, Livermore, CA, 1995.
10. AFFDL-TR-69-42, "Stress Analysis Manual", Air Force Flight Dynamics Laboratory, Dayton, Ohio, 1969.
11. "Steel Structures Design and Behavior," C.G. Salmon and J.E. Johnson, Harper and Row Publishers, New York, NY, Second Edition, 1980.
12. "Machinery's Handbook", Industrial Press, New York, NY, 25th Edition, 1996.
13. "Roark's Formulas for Stress & Strain", Young, Warren C., McGraw Hill, New York, NY, Sixth Edition, 1989.
14. "Reinforced Concrete Design," Leet, Kenneth, McGraw-Hill, New York, NY, Second Edition, 1991.

15. ACI-349-85, "Code Requirements for Nuclear Safety Related Concrete Structures", American Concrete Institute, Farmington Hills, MI, 1986.
16. "Practical Stress Analysis in Engineering Design," Alexander Blake, Marcel Dekker, Inc., New York, NY, Second Edition, 1990.
17. NUREG – 0800, "Standard Review Plan," U.S. Nuclear Regulatory Commission Draft, Washington, DC, June 1987.
18. ASCE 7-93, "Minimum Design Loads for Buildings and Other Structures," American Society of Civil Engineers, New York, NY, March 12, 1994.
19. NSS 5-940.1, "A Review of Procedures for the Analysis and Design of Concrete Structures to Resist Missile Impact Effects," Nuclear and Systems Sciences Group, Holmes & Narver, Inc., Anaheim, CA, September 1975.
20. BC-TOP-9A, Revision 2, Topical Report, "Design of Structures for Missile Impact," Bechtel Power Corporation, San Francisco, CA, September 1974.
21. "Engineering Fluid Mechanics," Roberson, J.A. and Crowe, C.T. Houghton Mifflin Co., Boston, MA, 1975.
22. ASCE 4-86, "Seismic Analysis of Safety-related Nuclear Structures and Commentary on Standard for Seismic Analysis of Safety-related Nuclear Structures", American Society of Civil Engineers, New York, NY, 1986.
23. "Structural Dynamics," Biggs, John M., McGraw-Hill, New York, NY, 1964.
24. ISG-15, Revision 0, "Materials Evaluation", US Nuclear Regulatory Commission, Washington, DC, January 10, 2001.

Chapter 3 Appendices

Chapter 3 Appendices

Table of Contents

3.A	PWR Fuel Basket Finite Element Models	3.A-1
3.A.1	Load Path Description.....	3.A-1
3.A.2	Finite Element Model Descriptions	3.A-2
3.A.2.1	PWR Basket Periodic Models.....	3.A-2
3.A.2.2	PWR Basket Plane Strain Plastic Model	3.A-3
3.A.3	Finite Element Model Boundary Conditions	3.A-4
3.A.3.1	Thermal Stress Analysis Boundary Conditions	3.A-4
3.A.3.2	Off-Normal Handling Boundary Events	3.A-5
3.A.3.3	Concrete Cask Tip-over Accident Boundary Events	3.A-5
3.A.4	Post-processing Finite Element Analysis Results.....	3.A-6
3.A.4.1	Maximum Thermal Stresses	3.A-6
3.A.4.2	Maximum Stresses for Off-normal Handling Conditions.....	3.A-6
3.A.4.3	Maximum Stresses for Concrete Cask Tip-over Accident.....	3.A-7
3.B	BWR Fuel Basket Finite Element Models.....	3.B-1
3.B.1	Load Path Description.....	3.B-1
3.B.2	Finite Element Model Descriptions	3.B-2
3.B.2.1	BWR Basket Periodic Models	3.B-2
3.B.2.2	BWR Basket Plane Strain Plastic Model	3.B-3
3.B.3	Finite Element Model Boundary Conditions	3.B-4
3.B.3.1	Thermal Stress Analysis Boundary Conditions	3.B-4
3.B.3.2	Off-Normal Handling Boundary Conditions	3.B-5
3.B.3.3	Concrete Cask Tip-over Accident Boundary Conditions.....	3.B-5
3.B.4	Post-processing Finite Element Analysis Results.....	3.B-6
3.B.4.1	Maximum Thermal Stresses	3.B-6
3.B.4.2	Maximum Stresses for Off-normal Handling Condition	3.B-6
3.B.4.3	Maximum Stresses for Concrete Cask Tip-over Accident.....	3.B-7
3.C	TSC Finite Element Model	3.C-1
3.D	Concrete Cask Finite Element Models	3.D-1
3.D.1	Pedestal Finite Element Model for Lift Evalaution	3.D-1
3.D.2	Concrete Cask Finite Element Model for Thermal Stress Evaluation	3.D-1
3.D.3	Pedestal Finite Element Model for 24-inch Drop Evaluation.....	3.D-2
3.D.4	Concrete Cask Finite Element Model for Tip-over Evaluation	3.D-4
3.E	Transfer Cask Finite Element Model	3.E-1

List of Figures

Figure 3.A-1 Expanded View of PWR Basket.....3.A-9
Figure 3.A-2 Bolted Attachment Details.....3.A-10
Figure 3.A-3 Freebody Diagram of PWR Basket Fuel Tube Detail.....3.A-11
Figure 3.A-4 Freebody Diagram of Basket Support Structure3.A-12
Figure 3.A-5 PWR Basket Periodic Model – 0° Basket Orientation.....3.A-13
Figure 3.A-6 PWR Basket Periodic Model – 45° Basket Orientation.....3.A-14
Figure 3.A-7 PWR Basket Plane Strain Plastic Model3.A-15
Figure 3.A-8 Meshing Detail of Fuel Tube in the PWR Basket Plastic Model.....3.A-16
Figure 3.A-9 PWR Basket Model Boundary Conditions For a Transverse Loading –
0° Basket Orientation.....3.A-17
Figure 3.A-10 PWR Basket Model Boundary Conditions for a Transverse Loading –
45° Basket Orientation.....3.A-18
Figure 3.B-1 Expanded View of BWR Basket.....3.B-9
Figure 3.B-2 Bolted Attachment Details.....3.B-10
Figure 3.B-3 Freebody Diagram of BWR Basket Fuel Tube Detail3.B-11
Figure 3.B-4 Freebody Diagram of Basket Support Structure3.B-12
Figure 3.B-5 BWR Basket Periodic Model – 0° Basket Orientation3.B-13
Figure 3.B-6 BWR Basket Periodic Model – 45° Basket Orientation3.B-14
Figure 3.B-7 BWR Basket Plane Strain Plastic Model.....3.B-15
Figure 3.B-8 Meshing Detail of Fuel Tube in the BWR Basket Plastic Model3.B-16
Figure 3.B-9 BWR Basket Model Boundary Conditions for a Transverse Loading –
0° Basket Orientation.....3.B-17
Figure 3.B-10 BWR Basket Model Boundary Conditions for a Transverse Loading –
45° Basket Orientation.....3.B-18
Figure 3.C-1 MAGNASTOR TSC Finite Element Model and Boundary Conditions.....3.C-6
Figure 3.C-2 Identification of Sections for Evaluating Linearized Stresses in TSC3.C-7
Figure 3.D-1 Concrete Cask Pedestal Finite Element Model for Lift Evaluation.....3.D-8
Figure 3.D-2 Concrete Cask Finite Element Model for Thermal Stress Evaluation.....3.D-9
Figure 3.D-3 Concrete Cask Model – Elements for Rebar.....3.D-10
Figure 3.D-4 Concrete Cask Model Boundary Conditions3.D-11
Figure 3.D-5 Concrete Cask Pedestal Finite Element Model for 24-inch Drop
Evaluation3.D-12
Figure 3.D-6 Stress-Strain Curve for A36 Carbon Steel.....3.D-13
Figure 3.D-7 Finite Element Models for Tip-over Evaluation.....3.D-14
Figure 3.E-1 Finite Element Model for the Transfer Cask3.E-2

3.A PWR Fuel Basket Finite Element Models

3.A.1 Load Path Description

This section describes the load paths and interactions between basket components during storage conditions. The MAGNASTOR PWR fuel basket is designed to accommodate thirty-seven PWR fuel assemblies. For the normal conditions of storage, the weight of the fuel assemblies is directly supported by the bottom plate of the TSC. The basket is subjected to its self-weight only. For the off-normal and accident events associated with loadings in the transverse direction of the basket (e.g. off-normal handling load, concrete cask tip-over accident), the weight of the fuel assemblies is supported by the twenty-one fuel tubes, side support weldments, and corner support weldments. Referring to Figure 3.A-1, load transfer between the fuel tubes, '1', is through contact at the tube corners. This contact consists of two types: the connector pins and the region between pins where the tube sections are in contact. The connector pin socket connections at 20-inch center-to-center distance prevent the fuel tubes from sliding past each other. The shear load transmitted across the pins is reacted out in bearing in the fuel tube pin sockets. The tube region between pins transmits bearing directly between fuel tubes. Shear loads between the tube corners can be transmitted by friction. The detailed interaction between fuel tube corners as well as a freebody diagram of a tube section are shown in Figure 3.A-3. As the figure shows, the pin welded to one tube fits into the slots cut into the adjoining tube.

Connector pin assemblies are installed as redundant supports at the top and bottom of the fuel basket. The connector pin assemblies join adjacent fuel tubes to ensure each tube is properly aligned during the assembly process. The connector pin assembly provides an end weldment effect that allows for handling of the assembled basket outside of the TSC without special fixtures. The bottom connector pins also provide a standoff between the TSC bottom plate and basket tubes, and transmit bearing loads from the basket to the TSC bottom plate.

The corner and side support weldments provide rigidity to the basket. The weldments are attached to the fuel tube array by means of bolted boss connections. Bosses welded to the fuel tubes are slotted into the weldments. Connection is made with the use of a washer and bolt combination. Figure 3.A-1 and Figure 3.A-2 show the boss connection details, '2'. To ensure the connection is in tension, the bosses are designed not to penetrate completely through the weldment wall. Therefore, once installed and preloaded, the bolts are always in tension. Shear loads are reacted out by the interaction of the bosses, boss welds, and the support weldments. When the support weldments are in compression, bearing loads are transferred through the

support weldment to the fuel tube array, '3' (Figure 3.A-1 and Figure 3.A-2). Figure 3.A-4 shows a freebody diagram of the fuel tube interaction with the support structure.

3.A.2 Finite Element Model Descriptions

This section describes the finite element models used in the PWR basket structural evaluation. The following describes the finite element models and the applicable ASME Code section.

Finite Element Model	Analysis Usage	Loading Condition	ASME Code Section
Periodic Model	Thermal Stress evaluation of PWR basket for radial temperature distribution	Level A	III-NG
	Off-normal TSC handling	Level C	III-NG
	Concrete cask tip-over accident – support weldment evaluation	Level D	III-NG, App. F
	Concrete cask tip-over accident – basket buckling evaluation	Level D	NUREG/CR-6322
Plane Strain Plastic Model	Concrete cask tip-over accident evaluation – fuel tube evaluation	Level D	III-NG, App. F

3.A.2.1 PWR Basket Periodic Models

For normal conditions and off-normal or accident events; two three-dimensional periodic half symmetry models of the PWR basket are used to evaluate the structural integrity of the basket as shown in Figure 3.A-5 and Figure 3.A-6. These models correspond to the critical basket orientations, 0° and 45°, for the loadings in transverse direction of the basket. The fuel tube support pins and slot joints are spaced on 20.0-inch centers. Therefore, the periodic model extends from the axial center of a fuel tube support pin to the mid-point of the fuel tube between the pins (10.0-inch segment). The end effect of the basket on pinned connections is ignored.

The basket finite element models are constructed using ANSYS SOLID45, SHELL63, and BEAM4 elements. Fuel tube assemblies, pins, and side support weldments are modeled using SOLID45 elements. Corner weldment plates are modeled using SHELL63 elements. BEAM4 elements are used to model the support bars on the corner assemblies. BEAM4 elements are also used to model the welds between the fuel tubes and pins. The interaction between fuel tubes, corner support assemblies, and side support assemblies are modeled with CONTAC52 gap elements. These gap elements allow the transfer of loads between the basket structural

components. CONTAC52 gap elements are used to simulate the total gap between the PWR basket and concrete cask (tip-over accident evaluation) or transfer cask (handling and thermal stress evaluation). The effect of the TSC shell is conservatively not included in the model.

The corner support and side support weldment assemblies are bolted to the fuel tube array at 16 locations around the circumference of the basket. The bolt/boss joints are modeled by coupling nodal degrees of freedom, which permit the transmission of shear and axial loads at the joints.

Loads and boundary conditions are discussed in Section 3.A.3. The weight of the neutron absorbers and the retainers, which are not included in the finite element model, are considered by adjusting the density of the carbon steel for the fuel tube sides.

This model is also used to evaluate the thermal stresses in the basket due to the thermal expansion of the basket in the radial and circumferential direction. A thermal conduction analysis is performed by converting the structural elements to corresponding thermal elements, applying the temperature boundary conditions as discussed in Section 3.A.3.1. The nodal temperatures are then read into the structural model to calculate thermal stresses. Each of the basket components is free to expand in the axial direction; therefore, thermal stresses due to the thermal expansion in the axial direction will be negligible.

3.A.2.2 PWR Basket Plane Strain Plastic Model

A two-dimensional plane strain plastic finite element model is used in the structural evaluation of the PWR basket tubes during a concrete cask tip-over accident. This model allows for nonlinear, inelastic, behavior of the basket components, which eliminates the conservatism of the linear elastic models. A nonlinear model allows higher strain rates than a linear model. The use of a plastic model is permitted in accordance with ASME Code Section III Appendix F. The structural components are modeled using PLANE42 elements. BEAM3 elements are used to model the support bars in the corner support assemblies. The support bars geometric properties are modified to represent a plane strain configuration (2-D, unit length model). A quarter symmetry of the model is shown in Figure 3.A-7. Similar to the three-dimensional periodic model, the full model is used to generate two models for the critical basket orientations, 0° and 45°.

To obtain an accurate solution, a fine mesh is required in the model to allow the development of elastic and inelastic strain regions. Figure 3.A-8 shows the mesh density used in the plastic finite element model. Reviewing the finite element results of the elastic models indicate that the fuel tubes have higher stresses than the side and corner supports. Therefore, the element meshing of

the fuel tubes is finer than the meshing for the side and corner supports. The bending stresses are the highest in the corners of both the fuel tubes and support assemblies. The meshing in the corners of the structural components is finer than the flat regions of the basket.

The interaction between adjacent fuel tubes, between the corner support assemblies and fuel tubes, and between side support assemblies and fuel tubes are modeled with CONTAC52 gap elements. These gap elements allow the transfer of loads between the basket structural components. For the basket structural evaluation, the TSC is not modeled. CONTAC52 gap elements are used to model the total gap between the PWR basket and concrete cask standoffs similar to the periodic model described in Section 3.A.2.1.

The corner support and side support assemblies are bolted to the fuel tube array at 16 locations around the circumference of the basket. The bolt/boss joints are modeled by coupling nodal degrees of freedom, which permit the transmission of shear and axial loads at the joints. The tube array pin joints represented by coupling the degrees of freedom, which will transmit shear (parallel to chamfered tube corner) across the joint but will allow the tubes to separate during basket deflection.

Loads and boundary conditions are discussed in Section 3.A.3. The weight of the neutron absorbers and the retainers, which are not included in the finite element model, are considered by adjusting the density of the carbon steel for the fuel tube sides.

3.A.3 Finite Element Model Boundary Conditions

3.A.3.1 Thermal Stress Analysis Boundary Conditions

The three-dimensional periodic model for 0° basket orientation described in Section 3.A.2.1 is used to calculate the thermal stress due to the thermal expansion in the radial direction. For the thermal conduction solution, a maximum temperature of 700°F is applied to the nodes at the center slot of the basket model, and a minimum temperature of 550°F is applied to the nodes at the exterior surfaces of the basket, thus providing a bounding temperature delta of 150°F in the radial direction of the basket. Note that the applied temperatures are conservatively selected to envelop the maximum temperature, as well as the maximum radial temperature gradient (ΔT) of the basket for all normal conditions and off-normal events of storage and for transfer conditions, determined by the thermal analysis in Chapter 4. For the thermal stress structural analysis, the temperature profile calculated by the thermal conduction solution is used.

Symmetry boundary conditions are applied at the plane of symmetry. In the basket axial direction, the model is restrained at one end.

3.A.3.2 Off-Normal Handling Boundary Events

For off-normal handling events, the three-dimensional periodic models described in Section 3.A.2.1 are used to calculate the stresses due to loading in the transverse direction of the basket. The gap between the basket and the transfer cask is 0.62 inch (0.12 inch basket-TSC and 0.50 inch TSC-cask). To represent the loads from the fuel assemblies, a pressure load is applied to the fuel tubes. The applied pressure is conservatively based on the heaviest fuel assembly being loaded into the shortest basket. The pressure (P) applied to the tubes for a 1g loading is shown below.

$$P = \frac{W}{wL} = 1.24 \text{ psi}$$

where:

- W = 1,680 lb -----Maximum PWR fuel assembly weight
- w = 8.20 inch -----Width of fuel tube flat
- L = 165.5 inch -----Length of fuel pressure load

The boundary conditions for 0° and 45° basket orientations are shown in Figure 3.A-9 and Figure 3.A-10, respectively. For off-normal events, an inertia load of 0.707g (resultant of 0.5g loading in the two transverse directions) is applied in the transverse direction of the basket. Applied pressure loads for fuel assemblies are also multiplied by 0.707g.

The 0° and 45° basket orientations are critical for the PWR basket for loading in the transverse direction. The 0° basket orientation maximizes the stresses in the fuel tube sidewalls and the 45° basket orientation maximizes the bending stresses in the tube corners. Intermediate basket orientations are bounded by the 0° and 45° orientations. Therefore, the basket evaluation is performed using two half-symmetry models for the 0° and 45° basket orientations, respectively. Symmetry boundary conditions are applied at the plane of symmetry. Symmetry boundary conditions are also applied to both ends of the finite element model to represent a periodic section of the basket. Fixed nodes are used to represent the transfer cask. For off-normal events, material properties at 100°F are conservatively used (using the modulus of elasticity for carbon steel at lower temperature results in slightly higher stress results.)

3.A.3.3 Concrete Cask Tip-over Accident Boundary Events

The concrete cask tip-over is evaluated as a side impact for the basket. During the concrete cask tip-over event, acceleration varies from 1g at the bottom of the concrete cask to a maximum acceleration at the top of the TSC. The two-dimensional plane strain plastic model is used for



the evaluation of the basket fuel tubes (Section 3.A.2.2), and the three-dimensional periodic models (Section 3.A.2.1) are used for the evaluation of the basket side and corner support weldments. The three-dimensional models are also used for the buckling evaluation of the basket. A bounding acceleration of 40g is applied to the basket models in the transverse direction. The 40g acceleration bounds the maximum acceleration in the basket, including the dynamic load factor for the concrete cask tip-over accident.

The gap between the basket and the concrete cask is 0.87 inch (0.12 inch basket-TSC and 0.75 inch TSC-cask). Pressure loads are applied to the PWR basket models to represent the fuel assembly weight with a 40g acceleration.

For the tip-over accident (loading in the transverse direction), the 0° and 45° basket orientations are critical for the PWR basket as discussed in Section 3.A.3.2. Therefore, the basket is evaluated using models corresponding to the 0° and 45° basket orientations. Symmetry boundary conditions are applied at the plane of symmetry. Symmetry boundary conditions are also applied to both ends of the three-dimensional periodic finite element model. Fixed nodes are used to represent the concrete cask stand-offs. The boundary conditions for these models are shown in Figure 3.A-9 and Figure 3.A-10. For accident conditions, material properties at 100°F are conservatively used.

3.A.4 Post-processing Finite Element Analysis Results

3.A.4.1 Maximum Thermal Stresses

The post-processing of the finite element analysis results for the thermal stress evaluation is performed by extracting the maximum nodal stress intensities from the model. The maximum nodal stress is obtained for two separate regions: (1) fuel tubes and (2) corner and side support weldments.

3.A.4.2 Maximum Stresses for Off-normal Handling Conditions

The post-processing of the finite element analysis results from the periodic model for the off-normal event is performed by taking section cuts at various locations in the model.

The fuel tube section cuts are divided into two regions. Region 1 is the region between the pin supports. For the periodic model, this region is defined from the base of the model (mid distance between pins) to the base of the pin. Region 2 is the pin region. This region starts at the base of the pin and extends to the top of the finite element model (mid-plane of pin). For both regions, the region just above and below the pin cutout (± 0.25 inch) is omitted from the section cuts to

eliminate stress concentrations in the model. The membrane stresses are calculated by taking a section cut at the center of the tube thickness. The membrane plus bending stress is calculated by taking the maximum of the stresses calculated at the inner or outer surface of the fuel tube. Refer to Figure 3.7-2 and Figure 3.7-4 for the locations of the section cuts.

The section cuts for the corner support weldments are calculated by taking section cuts along the length of the weldment (ten inches for the periodic model). Since the corner weldment is modeled using SHELL63 elements, the membrane stresses are calculated at the mid plane of the element and the membrane plus bending stresses are calculated using the maximum stresses of either the inner or outer surface of the element. Refer to Figure 3.7-5 and Figure 3.7-6 for the locations of the section cuts.

The section cuts for the side weldments are calculated taking section cuts along the length of the weldment (ten inches for the periodic model). The membrane stresses are calculated by taking a section cut at the mid-thickness of the weldment. The membrane plus bending stress is calculated by taking the maximum of the stresses calculated at the inner or outer surface of the weldment. Refer to Figure 3.7-7 and Figure 3.7-8 for the locations of the section cuts.

3.A.4.3 Maximum Stresses for Concrete Cask Tip-over Accident

The post-processing of finite element analysis results for the basket tip-over accident using the three-dimensional periodic model and plane strain plastic model, is performed by calculating stresses at various locations of the basket structure.

The fuel tube stresses are calculated using the plane strain plastic model. The membrane stresses are calculated by extracting the nodal stress intensity at the mid-thickness of the tube thickness. The membrane plus bending stress is calculated by extracting the maximum nodal stress intensity at the inner or outer surface of the fuel tube. Refer to Figure 3.7-2 and Figure 3.7-4 for the locations of the stress sections.

The stresses for the corner and side support weldments are calculated using the 3-D periodic model. The section cuts for the corner support weldments are located along the length of the weldment (ten inches for the periodic model). Since the corner weldment is modeled using SHELL63 elements; the membrane stresses are calculated at the mid plane of the element, and the membrane plus bending stresses are calculated using the maximum stresses of either the inner or outer surface of the element. Refer to Figure 3.7-5 and Figure 3.7-6 for the locations of the section cuts. The section cuts for the side weldments are located along the length of the weldment (ten inches for the periodic model). The membrane stresses are calculated by taking a section cut at the mid-thickness of the weldment. The membrane plus bending stress is

calculated by taking the maximum of the stresses calculated at the inner and outer surface of the weldment. Refer to Figure 3.7-7 and Figure 3.7-8 for the locations of the section cuts. The stresses in the corner support weldment support bars are calculated using the forces and moments extracted from the BEAM4 elements. Classical hand calculations are used to calculate the critical stresses in the support bars.

Figure 3.A-1 Expanded View of PWR Basket

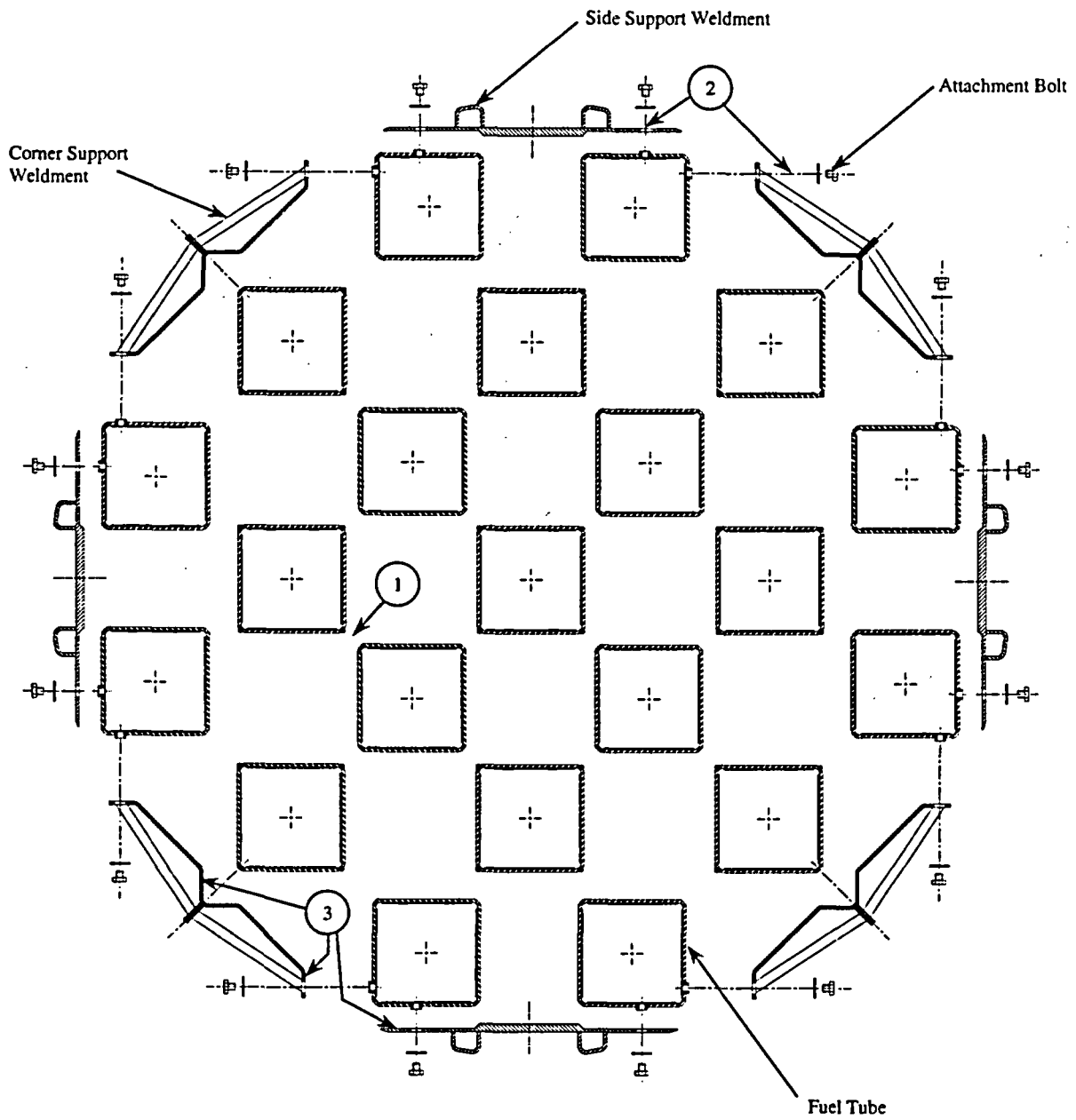


Figure 3.A-2 Bolted Attachment Details

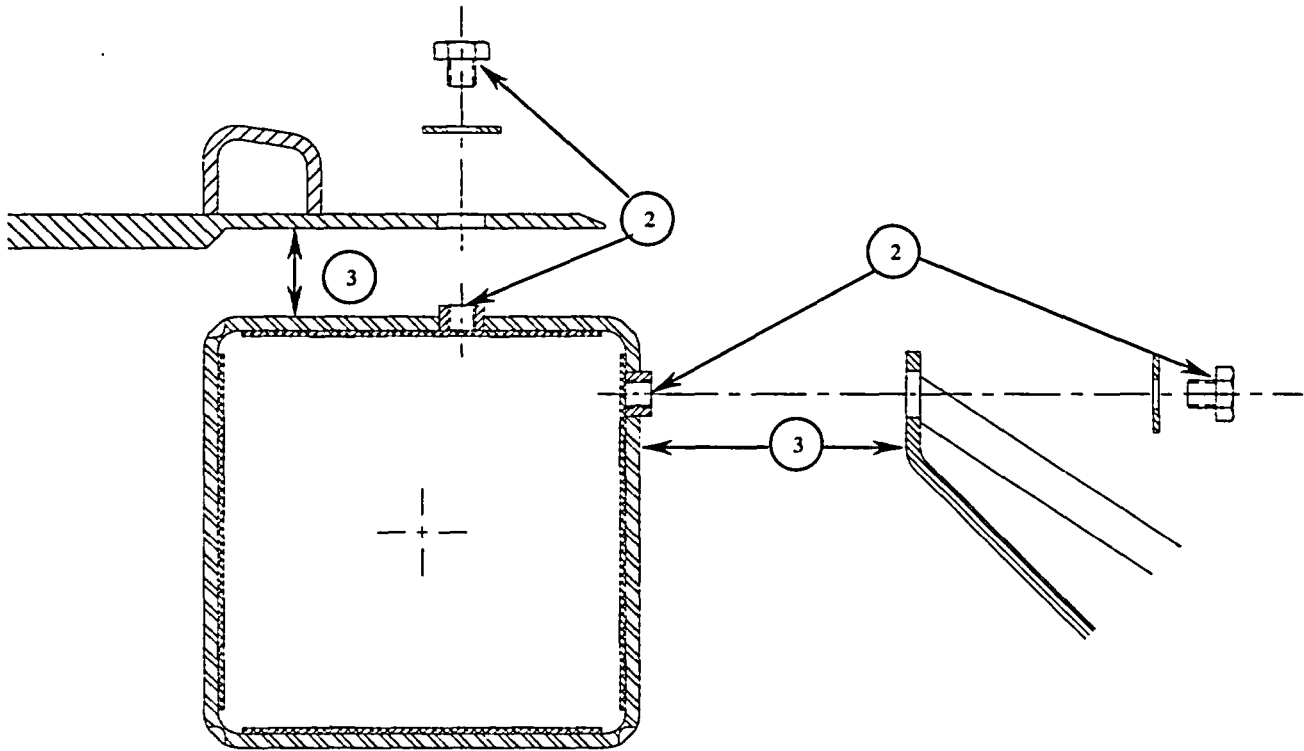
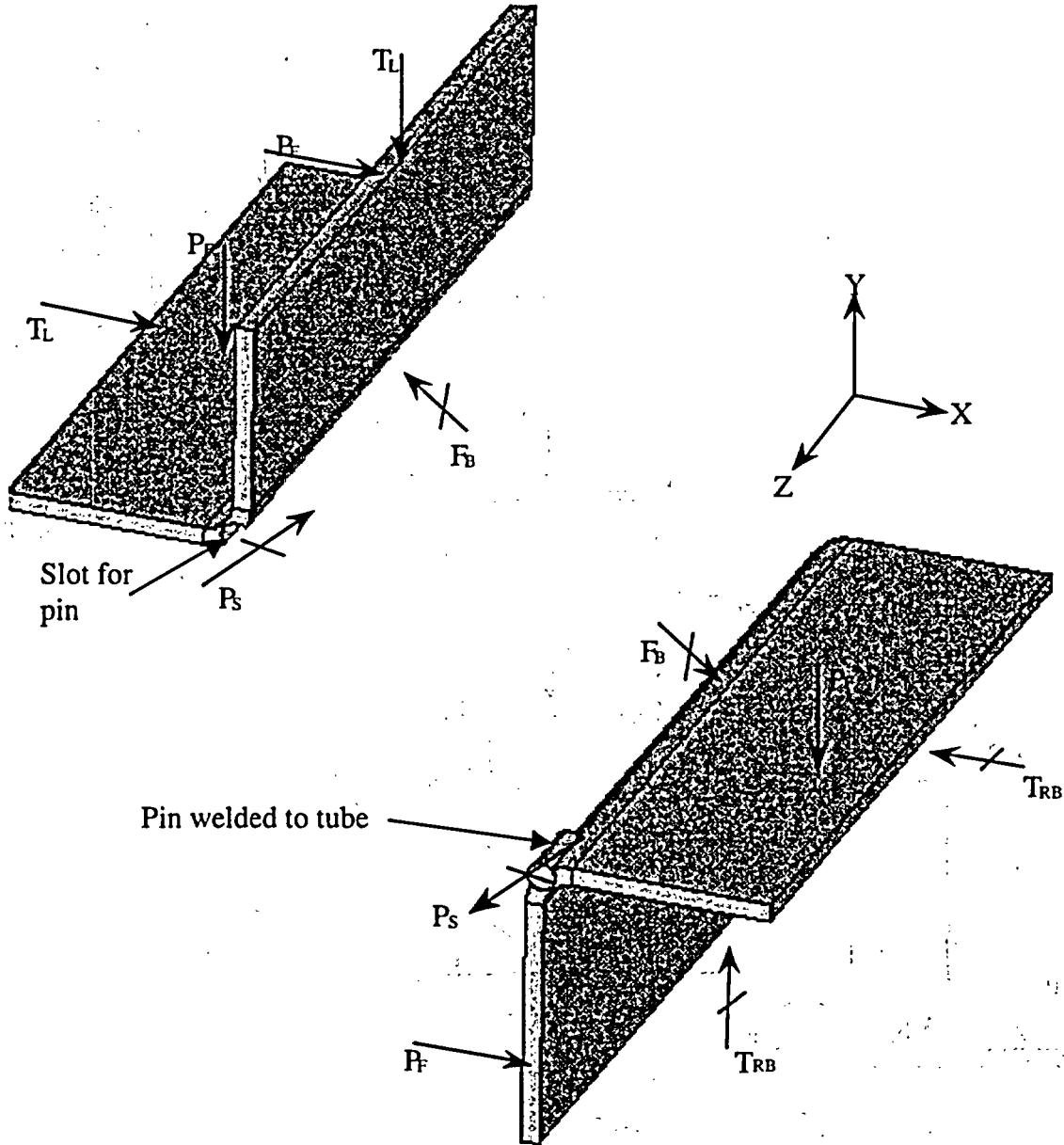
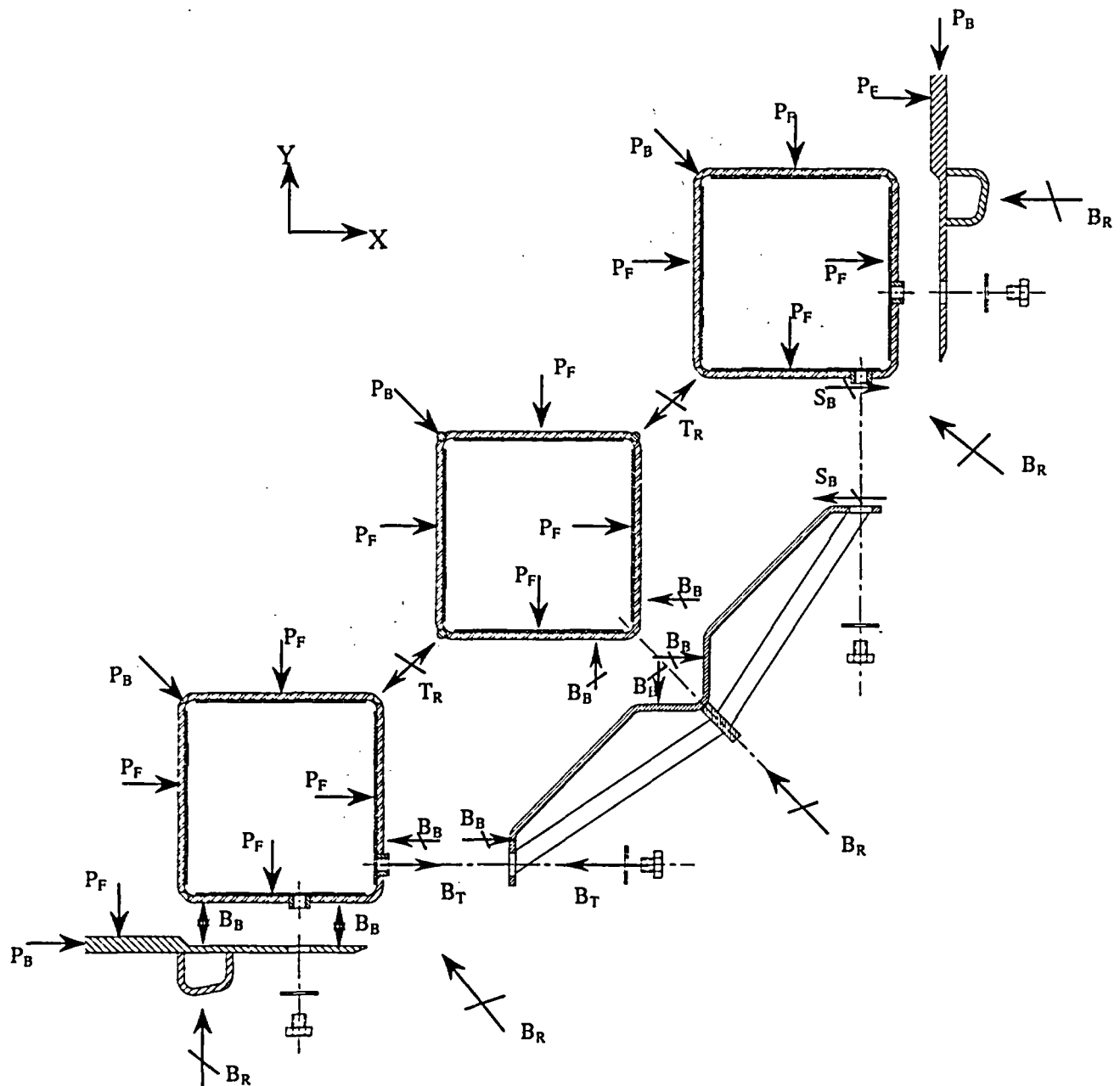


Figure 3.A-3 Freebody Diagram of PWR Basket Fuel Tube Detail



- T_L Loads from adjacent tube or fuel assembly
- P_F Local load due to fuel assembly
- T_{RB} Reaction loads in tubes for equilibrium at symmetry planes of tubes
- P_S Shear Reaction thru pin joint (in the XY plane)
- F_B Bearing Reaction across tube flat

Figure 3.A-4 Freebody Diagram of Basket Support Structure



- P_B Loads due to adjacent basket structure
- P_F Local load due to fuel assembly
- B_R Basket reaction with TSC shell locations
- B_T Tensile load at bolt and tube boss (typical)
- B_B Bearing reaction between tube sidewall and support structure (typical)
- S_B Shear reaction between support structure and tube boss (typical)
- T_R Reactions between tubes detailed in Figure 3.A-3

Figure 3.A-5 PWR Basket Periodic Model – 0° Basket Orientation

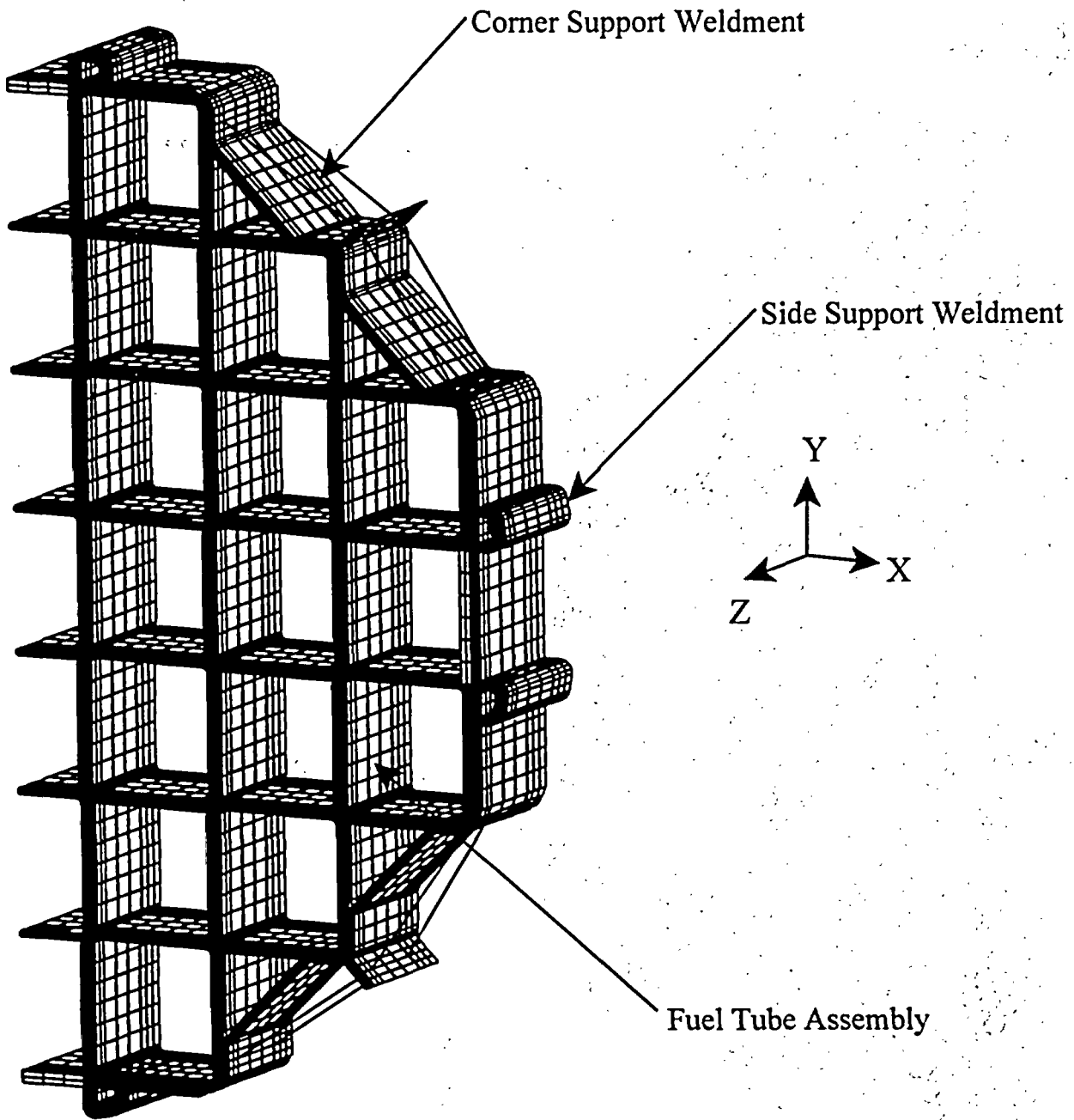


Figure 3.A-6 PWR Basket Periodic Model – 45° Basket Orientation

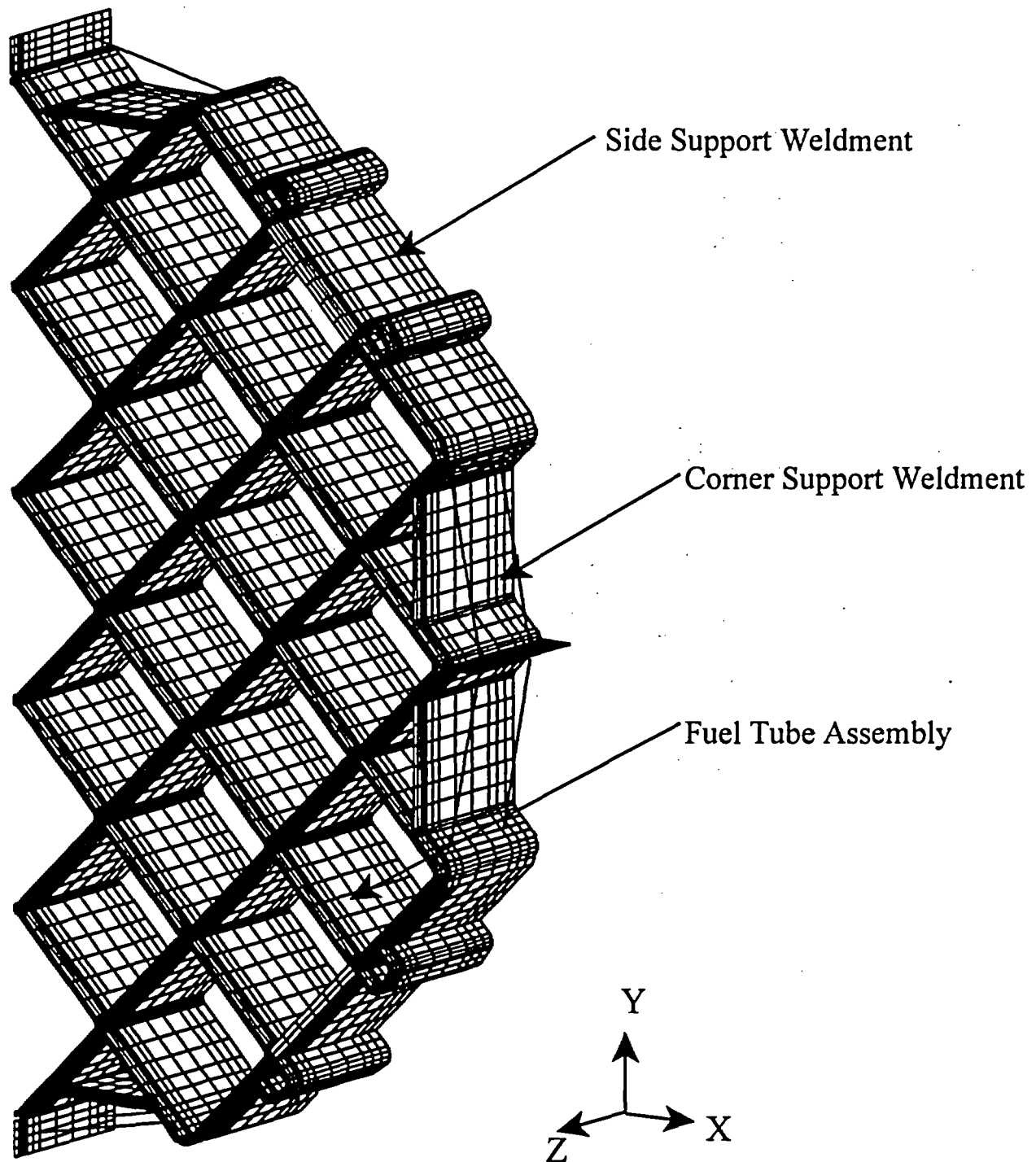
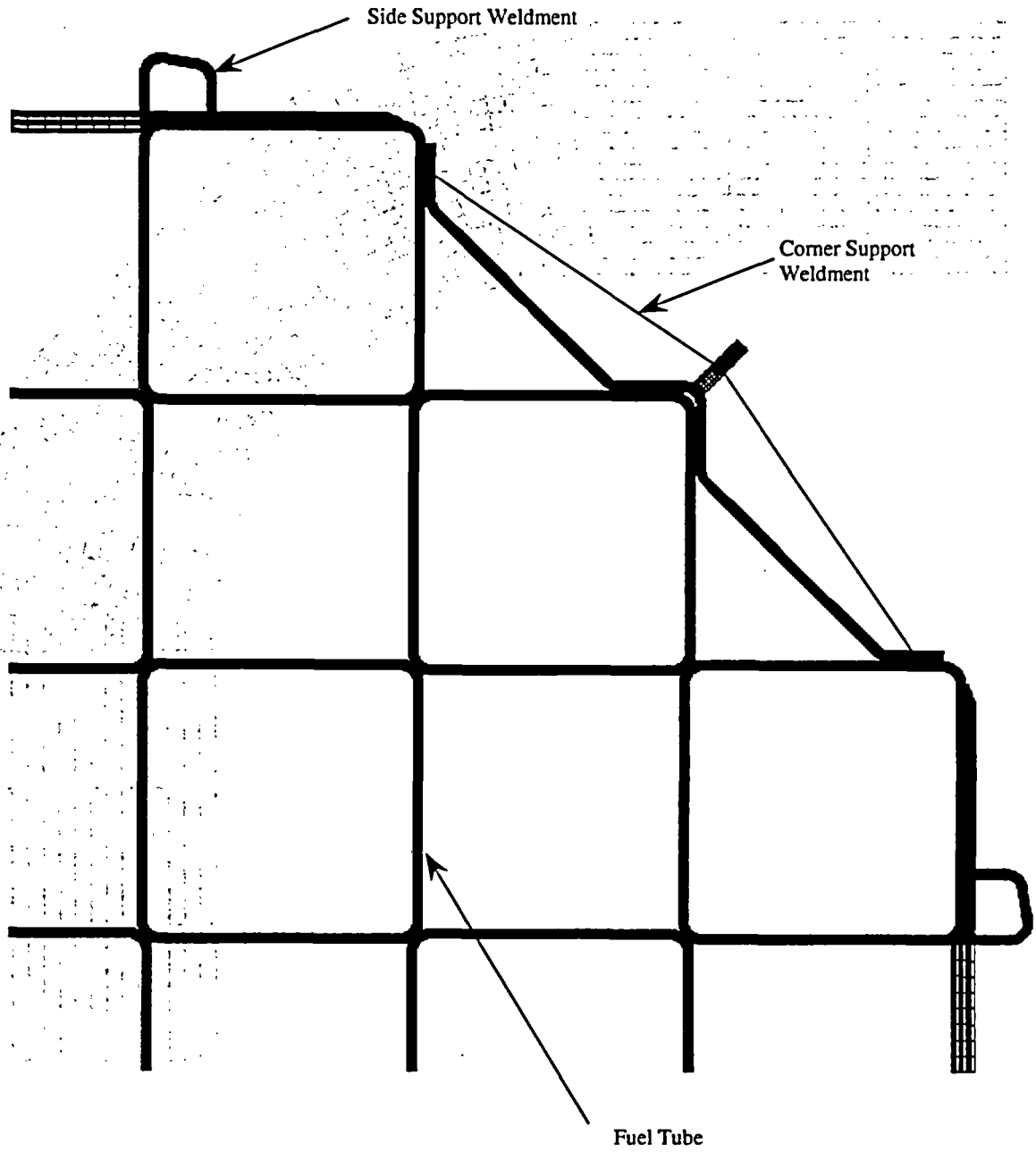


Figure 3.A-7 PWR Basket Plane Strain Plastic Model



(Quarter of model shown)

Figure 3.A-8 Meshing Detail of Fuel Tube in the PWR Basket Plastic Model

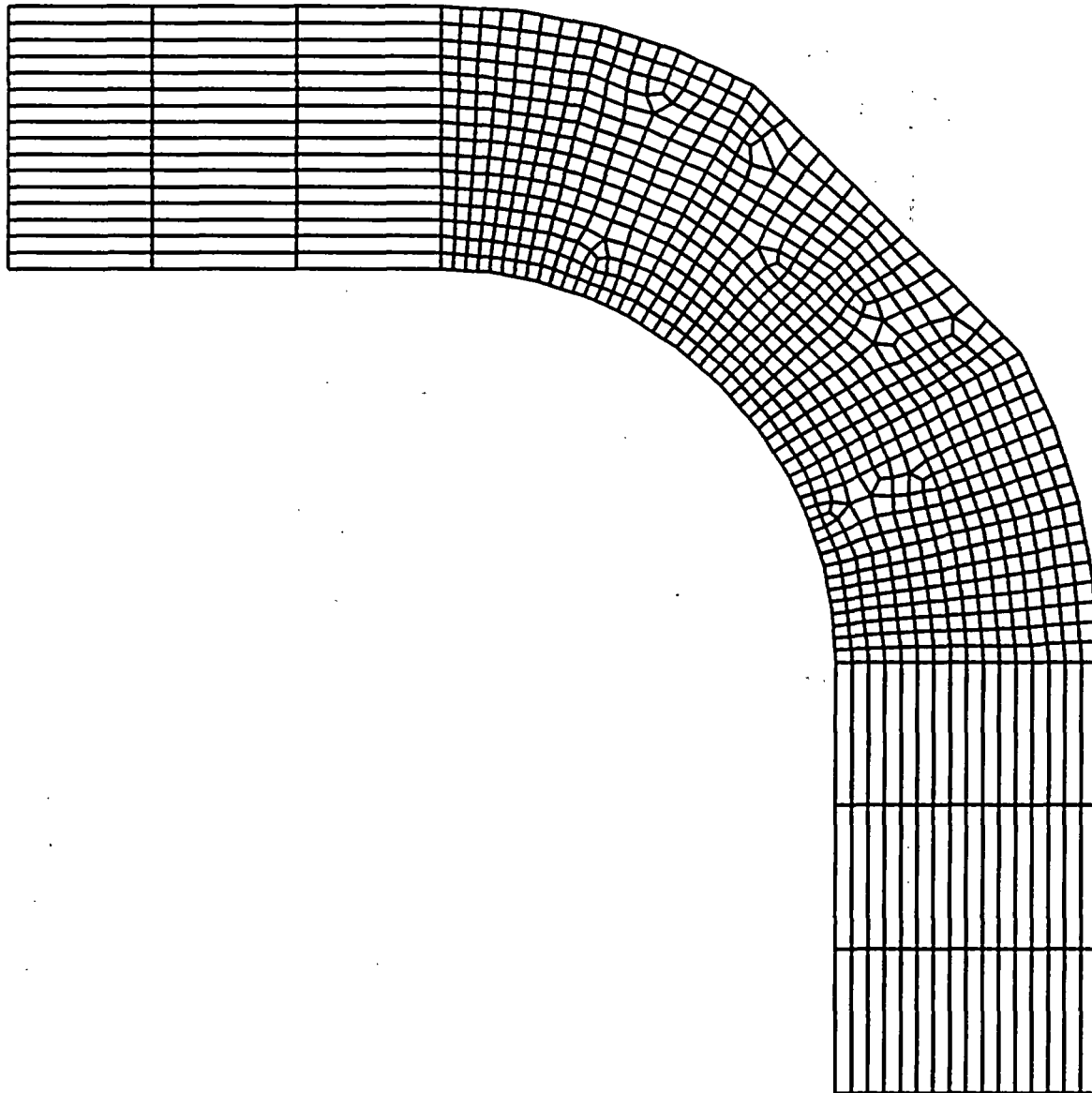


Figure 3.A-9 PWR Basket Model Boundary Conditions For a Transverse Loading – 0°
Basket Orientation

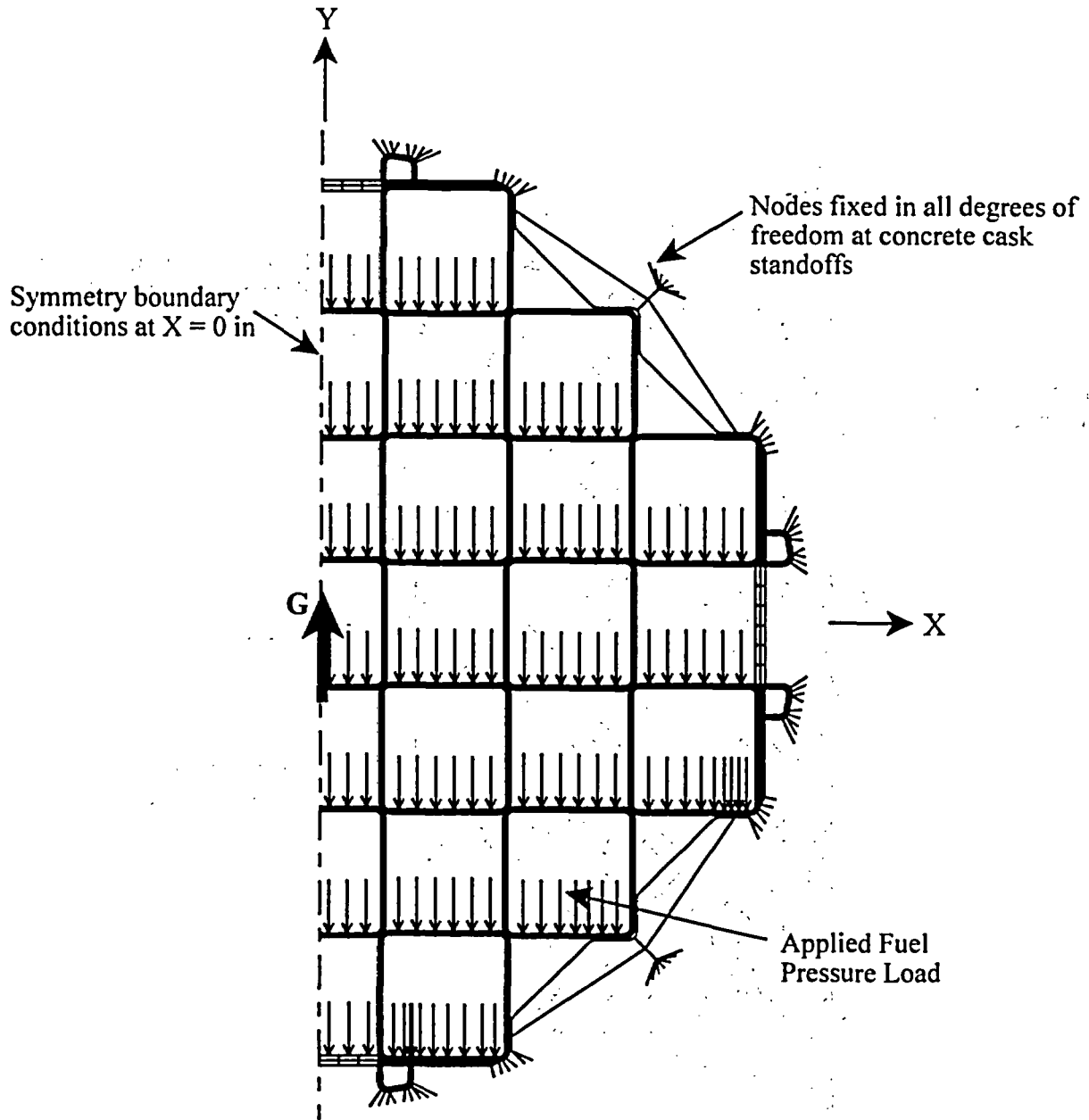
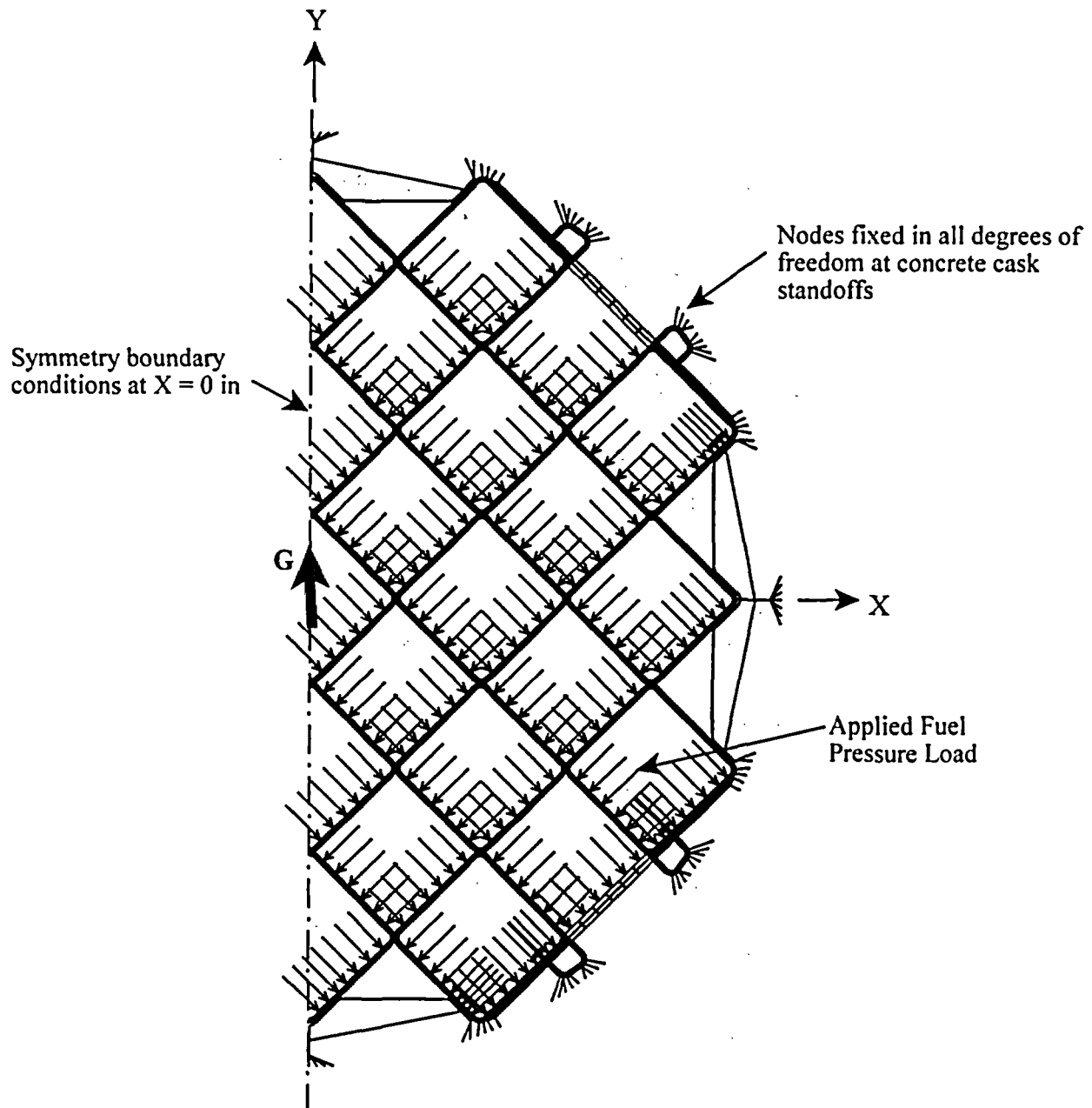


Figure 3.A-10 PWR Basket Model Boundary Conditions for a Transverse Loading – 45° Basket Orientation



3.B BWR Fuel Basket Finite Element Models

3.B.1 Load Path Description

This section explains the load paths in the basket that ensure the structural integrity of the BWR MAGNASTOR during all conditions of storage. The MAGNASTOR BWR fuel basket is designed to accommodate 87 BWR fuel assemblies. For normal conditions of storage, the weight of the fuel assemblies is directly supported by the bottom plate of the TSC. The basket is subjected to its self-weight only. For the off-normal and accident conditions associated with loadings in the transverse direction of the basket (e.g. off-normal handling load, concrete cask tip-over accident), the weight of the fuel assemblies is supported by the 45 fuel tubes, side support weldments, and the corner support weldments. Referring to Figure 3.B-1, load transfer between the fuel tubes, '1', is through bearing contact at the corners. The bearing contact consists of two load paths; the connector pins transmit load directly between each fuel tube; and where the tubes are in contact, bearing loads are transmitted. The shear load transmitted across the pins is reacted out in bearing in the pin sockets. The detailed interaction between fuel tube corners is shown in Figure 3.B-1 and Figure 3.B-3. As the figures show, the pins welded to one tube mate to the slots cut into the adjoining tube. Figure 3.B-3 shows a freebody diagram of the fuel tube pin joint.

At the top and bottom of the fuel basket, connector pin assemblies are used to add additional support to the basket. The end basket configurations do not affect the periodic model analysis of the basket because the connector pin assemblies do not transmit loads in the lateral direction. The connector pin assemblies are installed as a redundant support for the basket system to maintain the structural configuration of the basket. The bottom connector pin assemblies also provide a standoff between the TSC bottom plate and basket tubes, and transmit bearing loads from the basket to the TSC bottom plate.

The corner and side support weldments provide rigidity to the basket. The weldments are attached to the fuel tube array by means of bolted boss connections. Bosses welded to the fuel tubes are slotted in to the weldments. Connection is made with the use of a washer and bolt combination. Referring to Figure 3.B-1 and Figure 3.B-2, the bolted joints, '2', are designed to transmit tensile loads. Therefore, once installed and preloaded the bolts are always in tension. Shear loads are reacted out by interaction of the bosses, boss welds, and the support weldments. If the support weldments are bearing on the fuel tube array the load is transferred through the bearing contact, '3', of the support weldments and fuel tube array (Figure 3.B-1 and Figure

3.B-2). Figure 3.B-4 shows a freebody diagram of the fuel tube interaction with the support structure.

3.B.2 Finite Element Model Descriptions

This section describes the finite element models used in the BWR basket structural evaluation. The following table describes the finite element models and the applicable ASME Code section.

Finite Element Model	Analysis Usage	Loading Condition	ASME Code Section
Periodic Model	Thermal Stress evaluation of BWR basket for radial temperature distribution	Level A	III-NG
	Off-normal TSC handling	Level C	III-NG
	concrete cask tip-over accident – support weldment evaluation	Level D	III-NG, App. F
	concrete cask tip-over accident - basket buckling evaluation	Level D	NUREG/CR-6322
Plane Strain Plastic Model	concrete cask tip-over accident evaluation - fuel tube evaluation	Level D	III-NG, App. F

3.B.2.1 BWR Basket Periodic Models

The two three-dimensional periodic models of the BWR basket are used to evaluate the structural integrity of the basket during normal, off-normal; and accident tip-over conditions as shown in Figure 3.B-5 and Figure 3.B-6. These models correspond to the critical basket orientations, 0° and 45°, for the loadings in the transverse direction of the basket. The fuel tube support pins are spaced on 20.0-inch centers; therefore, the periodic model extends from the axial center of a tube pin to the mid-point of the spacing between the pins, a 10.0-inch segment.

The basket finite element models are constructed using SOLID45, SHELL63, and BEAM4 elements. The fuel tube assemblies, pins, and side support weldments are modeled using SOLID45 elements. The weight of the poison plates is included in the finite element model by adjusting the density of the carbon steel for the fuel tube sides. The corner support weldment is modeled using SHELL63 and BEAM4 elements. The corner support vertical wall is modeled using SHELL63 elements. BEAM4 elements are used to model the support plates on the corner assemblies. BEAM4 elements are also used to model the welds between the fuel tubes and pins. The interaction between fuel tubes, corner support assemblies, and side support assemblies are modeled with CONTAC52 gap elements. These gap elements allow the transfer of loads between

the basket structural components. For the basket structural evaluation, the TSC is not modeled. CONTAC52 gap elements are used to model the total gap between the BWR basket and concrete cask (tip-over accident evaluation) or transfer cask (handling and thermal stress evaluation).

The corner support and side support assemblies are bolted to the fuel tube array at sixteen locations around the circumference of the basket. The bolt/boss joints are modeled by coupling nodal degrees of freedom, which permit the transmission of shear and axial loads at the joints.

Loads and boundary conditions are discussed in Section 3.B.3. The weight of the neutron absorbers and the retainers, which are not included in the finite element model, are considered by adjusting the density of the carbon steel for the fuel tube sides.

This model is also used to evaluate the thermal stresses in the basket due to the thermal expansion of the basket in the radial and axial directions. A thermal conduction analysis is performed by converting the structural elements to corresponding thermal elements, applying the temperature boundary conditions as discussed in Section 3.B.3.1. The nodal temperatures are then read into the structural model to calculate thermal stresses. Each of the basket components is free to expand in the axial direction; therefore, thermal stresses due to thermal expansion in the axial direction are negligible.

3.B.2.2 BWR Basket Plane Strain Plastic Model

A two-dimensional plane strain plastic finite element model is used in the structural evaluation of the BWR basket tubes during a concrete cask tip-over accident. This model allows for non-linear, inelastic, behavior of the basket components, which eliminates the conservatism of the linear elastic models. A non-linear model allows higher strain rates than a linear model. The use of a plastic model is permitted in accordance with ASME Code Section III Appendix F. The structural components are modeled using PLANE42 elements. BEAM3 elements are used to model the support plates in the corner support assemblies. The support plate geometric properties are modified to represent a plane strain configuration (2-D, unit length model). Figure 3.B-7 shows a quarter of the finite element model. Figure 3.B-8 shows the meshing density of the plane strain model. Similar to the three-dimensional periodic model, the full model is used to generate two models for the critical basket orientation, 0° and 45°.

To obtain an accurate solution, a fine mesh is required in the model to allow the development of elastic and inelastic strain regions. Reviewing the finite element results of the elastic models indicate that the fuel tubes have higher stresses than the side and corner supports. Therefore, the element meshing of the fuel tubes is finer than the meshing for the side and corner supports. The

bending stresses are the highest in the corners of both the fuel tubes and support assemblies. The meshing in the corners of the structural components is finer than the flat regions of the basket.

The interaction between adjacent fuel tubes, between the corner support assemblies and fuel tubes, and between the side support assemblies and fuel tubes are modeled with CONTACT52 gap elements. These gap elements allow the transfer of loads between the basket structural components. For the basket structural evaluation, the TSC is not modeled. CONTACT52 gap elements are used to model the total gap between the BWR basket and concrete cask standoffs similar to the periodic model described in Section 3.B.2.1.

The corner support and side support assemblies are bolted to the fuel tube array at sixteen locations around the circumference of the basket. The bolt/boss joints are modeled by coupling nodal degrees of freedom, which permit the transmission of shear and axial loads at the joints. The tube array pin joints are modeled with COMBIN40 gap elements that will transmit shear (parallel to chamfered tube corner) across the joint; the tubes can separate during basket deflection.

Loads and boundary conditions are discussed in Section 3.B.3. The weight of the neutron absorbers and the retainers, which are not included in the finite element model, are considered by adjusting the density of the carbon steel for the fuel tube sides.

3.B.3 Finite Element Model Boundary Conditions

3.B.3.1 Thermal Stress Analysis Boundary Conditions

The three-dimensional periodic model for 0° basket orientation described in Section 3.B.2.1 is used to calculate the thermal stress due to the thermal expansion in the radial direction. For the thermal conduction solution, a maximum temperature of 700°F is applied to the nodes at the center slot of the basket model, and a minimum temperature of 550°F is applied to the nodes at the exterior surfaces of the basket, thus providing a bounding temperature delta of 150°F in the radial direction of the basket. Note that the applied temperatures are conservatively selected to envelop the maximum temperature, as well as the maximum radial temperature gradient (ΔT) of the basket for all normal conditions and off-normal events of storage and for transfer conditions, determined by the thermal analysis in Chapter 4. For the thermal stress structural analysis, the temperature profile calculated by the thermal conduction solution is used. In the basket axial direction, the model is restrained at one end.

3.B.3.2 Off-Normal Handling Boundary Conditions

The three-dimensional periodic models as described in Section 3.B.2.1 are used to calculate the stresses due to loading in the transverse direction of the basket for off-normal handling conditions. The gap between the basket and the transfer cask is 0.62 inch (0.12-inch basket-TSC and 0.50-inch TSC-cask). To represent the loads from the fuel assemblies, a pressure load is applied to the fuel tubes. The applied pressure is conservatively based on the heaviest fuel assembly being loaded into the shortest basket. The pressure (P) applied to the tubes for a 1g loading is shown below.

$$P = \frac{W}{wL} = 0.83 \text{ psi}$$

where:

- W = 704 lb -----Maximum weight of BWR fuel assembly
- w = 5.34 inch -----Width of fuel tube flat
- L = 159.1 inch -----Length of fuel pressure load

The boundary conditions are the models, for 0° and 45° basket orientations, are shown in Figure 3.B-9 and Figure 3.B-10, respectively. For off-normal events, an inertia load of 0.707g (resultant of 0.5g acceleration applied in the two transverse directions) is applied in the transverse direction of the basket. Applied pressure loads for fuel assemblies are also multiplied by 0.707g.

The 0° and 45° basket orientations are critical for the BWR basket for loading in the transverse direction. The 0° basket orientation maximizes the stresses in the fuel tube sidewalls and the 45° basket orientation maximizes the bending stresses in the tube corners. Intermediate basket orientations are bounded by the 0° and 45° orientations. Therefore, the basket evaluation is performed using two half-symmetry models for the 0° and 45° basket orientations, respectively. Symmetry boundary conditions are applied at the plane of symmetry. Symmetry boundary conditions are also applied to both ends of the finite element model to represent a periodic section of the basket. Fixed nodes are used to represent the transfer cask. For off-normal events, material properties at 100°F are conservatively used (using the modulus of elasticity for carbon steel at lower temperature results in slightly higher stress results.)

3.B.3.3 Concrete Cask Tip-over Accident Boundary Conditions

The concrete cask tip-over is evaluated as a side impact for the basket. During the concrete cask tip-over event, the acceleration varies from 1g at the bottom of the concrete cask to a maximum acceleration at the top of the TSC. The two dimensional plane strain plastic model is used for the

evaluation of basket fuel tubes (Section 3.B.2.2), and the three-dimensional periodic models (Section 3.B.2.1) are used for the evaluation of the basket side and corner support weldments and the buckling evaluation of the fuel basket. A bounding acceleration of 40g is applied to the BWR models. The 40g acceleration bounds the maximum acceleration in the basket, including dynamic load factor, for the concrete cask tip-over accident.

The gap between the basket and the concrete cask is 0.87 inch (0.12-inch basket-TSC and 0.75-inch TSC-cask). Pressure loads are applied to the BWR basket models to represent the fuel assembly weight with an applied 40g acceleration.

For the tip-over accident (loading in the transverse direction) the 0° and 45° basket orientations are critical for the BWR basket as discussed in Section 3.B.3.2. Therefore, the basket is evaluated using models corresponding to the 0° and 45° basket orientations. Symmetry boundary conditions are applied at the plane of symmetry. Symmetry boundary conditions are also applied to both ends of the three-dimensional periodic finite element model. Fixed nodes are used to represent the concrete cask stand-offs. The boundary conditions are shown in Figure 3.B-9 and Figure 3.B-10 for the tip-over basket evaluation. For accident conditions, material properties at 100°F are conservatively used.

3.B.4 Post-processing Finite Element Analysis Results

3.B.4.1 Maximum Thermal Stresses

The post-processing of the finite element analysis results for thermal stress evaluation is performed by extracting the maximum nodal stress intensities from the model. The maximum stress is obtained for two separate regions: (1) fuel tubes and (2) corner and side support weldments.

3.B.4.2 Maximum Stresses for Off-normal Handling Condition

The post-processing of the finite element analysis results from the periodic model for the off-normal handling event is performed by taking section cuts at various locations in the model.

The fuel tube section cuts are divided into two regions. Region 1 is the region between the pin supports. For the periodic model this region is defined from the base of the model (mid distance between pins) to the base of the pin. Region 2 is the pin region. This region starts at the base of the pin and extends to the top of the finite element model (mid-plane of pin). For both regions the region just above and below the pin cutout (± 0.25 inch) is omitted from the section cuts to eliminate local stress concentrations in the model. The membrane stresses are calculated by

taking a section cut at the center of the tube thickness. The membrane plus bending stress is calculated by taking the maximum of the stresses calculated at the inner or outer surface of the fuel tube. Refer to Figure 3.7-11 and Figure 3.7-13 for the locations of the section cuts.

The section cuts for the corner support weldments are calculated by taking section cuts along the length of the weldment (ten inches for the periodic model). Since the corner weldment is modeled using SHELL63 elements; the membrane stresses are calculated at the mid plane of the element, and the membrane plus bending stresses are calculated using the maximum stresses of either the inner or outer surface of the element. Refer to Figure 3.7-14 and Figure 3.7-15 for the locations of the section cuts.

The section cuts for the side weldments are calculated taking section cuts along the length of the weldment (ten inches for the periodic model). The membrane stresses are calculated by taking a section cut at the mid-thickness of the weldment. The membrane plus bending stress is calculated by taking the maximum of the stresses calculated at the inner or outer surface of the weldment. Refer to Figure 3.7-16 and Figure 3.7-17 for the locations of the section cuts.

3.B.4.3 Maximum Stresses for Concrete Cask Tip-over Accident

The post-processing of finite element analysis results for the basket tip-over accident using the three-dimensional periodic model and plane strain plastic model is performed by calculating stresses at various locations of the basket structure.

The fuel tube stresses are calculated using the plane strain plastic model. The membrane stresses are calculated by extracting the nodal stress intensity at the mid-thickness of the tube thickness. The membrane plus bending stress is calculated by extracting the maximum nodal stress intensity at the inner or outer surface of the fuel tube. Refer to Figure 3.7-11 and Figure 3.7-13 for the locations of the stress sections.

The stresses for the corner and side support weldments are calculated using the 3-D periodic model. The section cuts for the corner support weldments are located along the length of the weldment (ten inches for the periodic model). Since the corner weldment is modeled using SHELL63 elements; the membrane stresses are calculated at the mid plane of the element, and the membrane plus bending stresses are calculated using the maximum stresses of either the inner or outer surface of the element. Refer to Figure 3.7-14 and Figure 3.7-15 for the locations of the section cuts. The section cuts for the side weldments are located along the length of the weldment (ten inches for the periodic model). The membrane stresses are calculated by taking a section cut at the mid-thickness of the weldment. The membrane plus bending stress is calculated by taking the maximum of the stresses calculated at the inner and outer surface of the

weldment. Refer to Figure 3.7-16 and Figure 3.7-17 for the locations of the section cuts. The stresses in the corner support weldment support plates are calculated using the forces and moments extracted from the BEAM4 elements. Classical hand calculations are used to calculate the critical stresses in the support bars.

Figure 3.B-1 Expanded View of BWR Basket

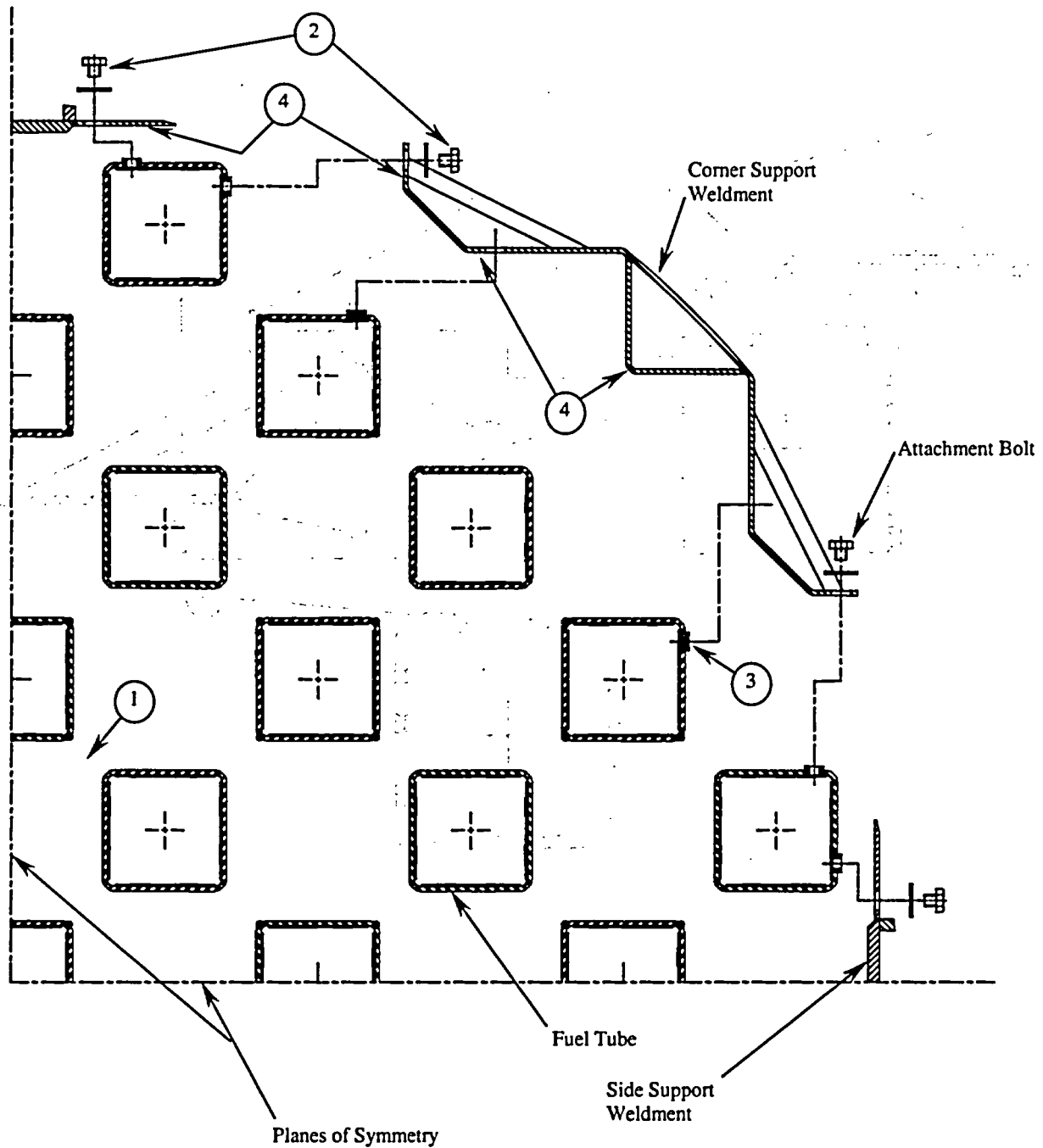


Figure 3.B-2 Bolted Attachment Details

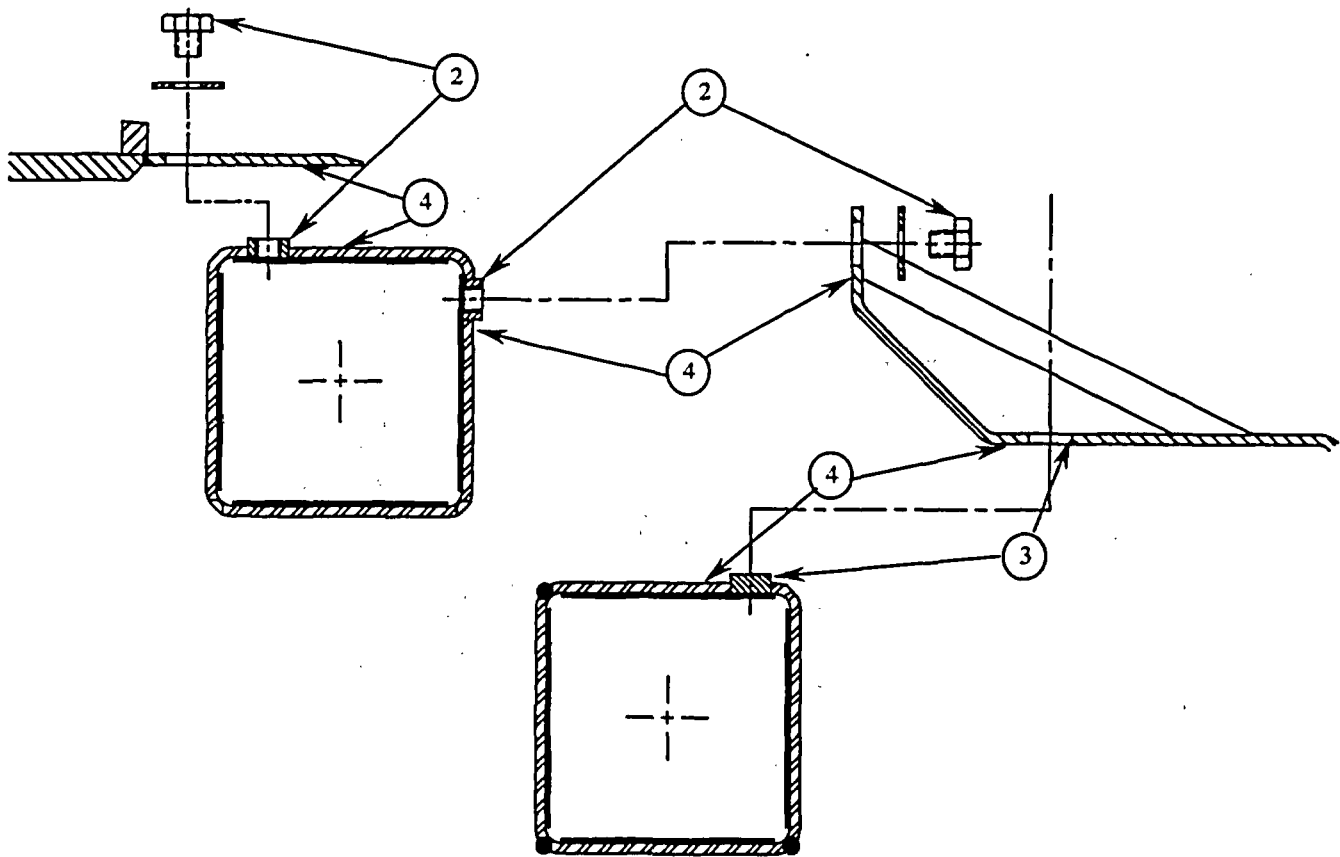
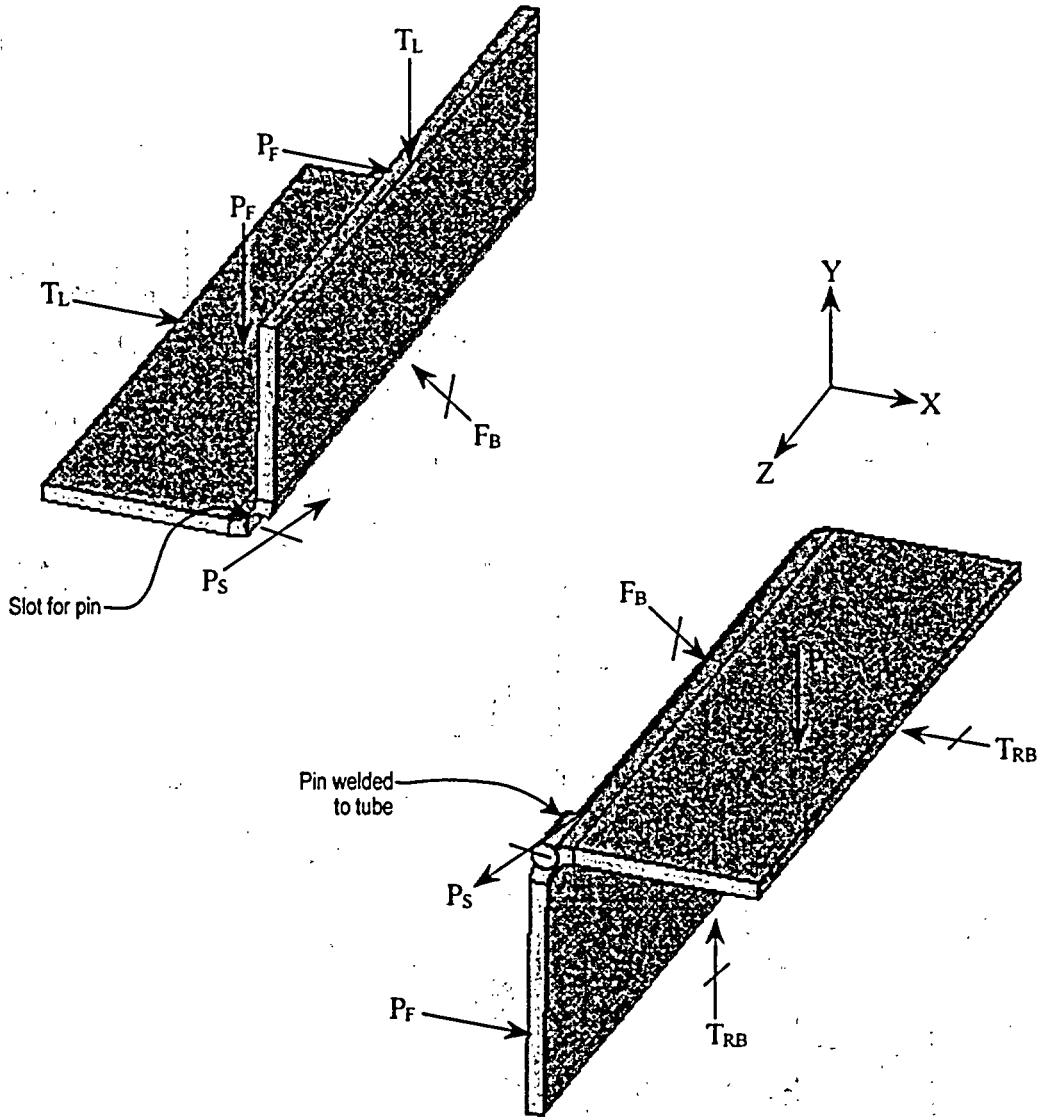
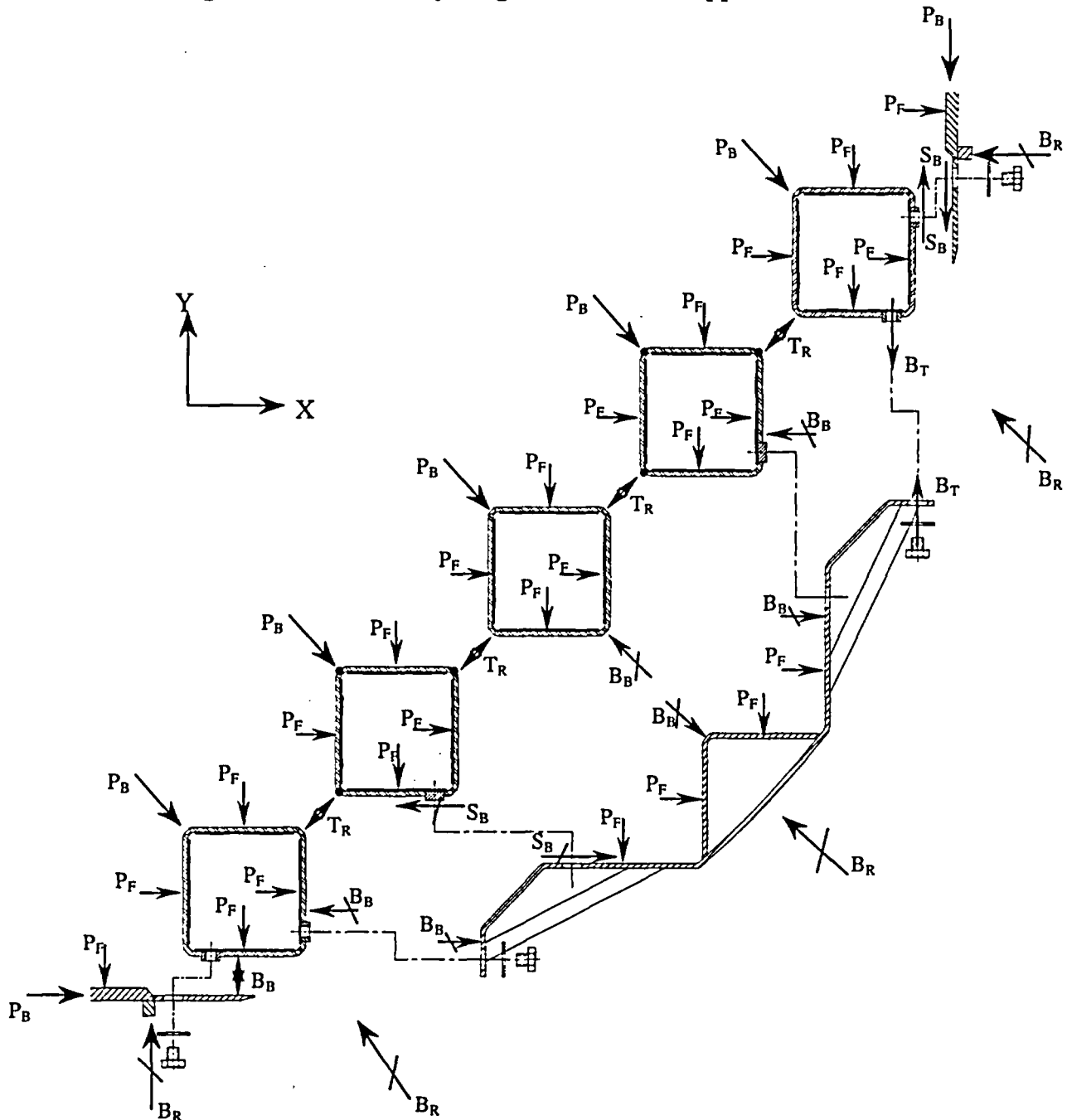


Figure 3.B-3 Freebody Diagram of BWR Basket Fuel Tube Detail



- T_L Loads from adjacent tube or fuel assembly
- P_F Local load due to fuel assembly
- T_{RB} Reaction loads in tubes for equilibrium at symmetry planes of tubes
- P_S Shear Reaction thru pin joint (in the X-Y plane)
- F_B Bearing Reaction across tube flat

Figure 3.B-4 Freebody Diagram of Basket Support Structure



- P_B Loads due to adjacent basket structure
- P_F Local load due to fuel assembly
- B_R Basket reaction with TSC shell locations
- B_T Tensile load at bolt and tube boss (typical)
- B_B Bearing reaction between tube sidewall and support structure (typical)
- S_B Shear reaction between support structure and tube boss (typical)
- T_R Reactions between tubes detailed in Figure 3.B-2

Figure 3.B-5 BWR Basket Periodic Model – 0° Basket Orientation

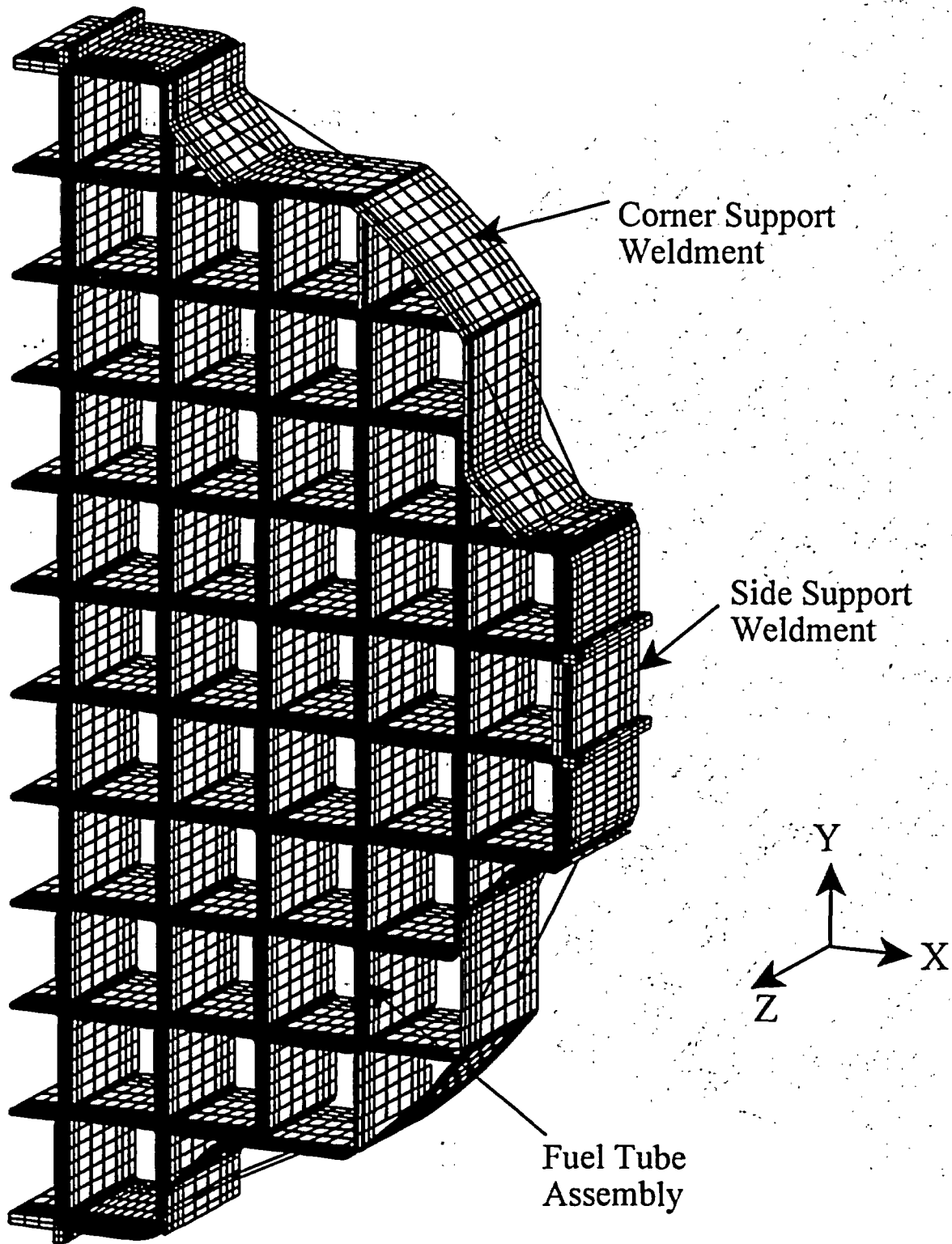


Figure 3.B-6 BWR Basket Periodic Model – 45° Basket Orientation

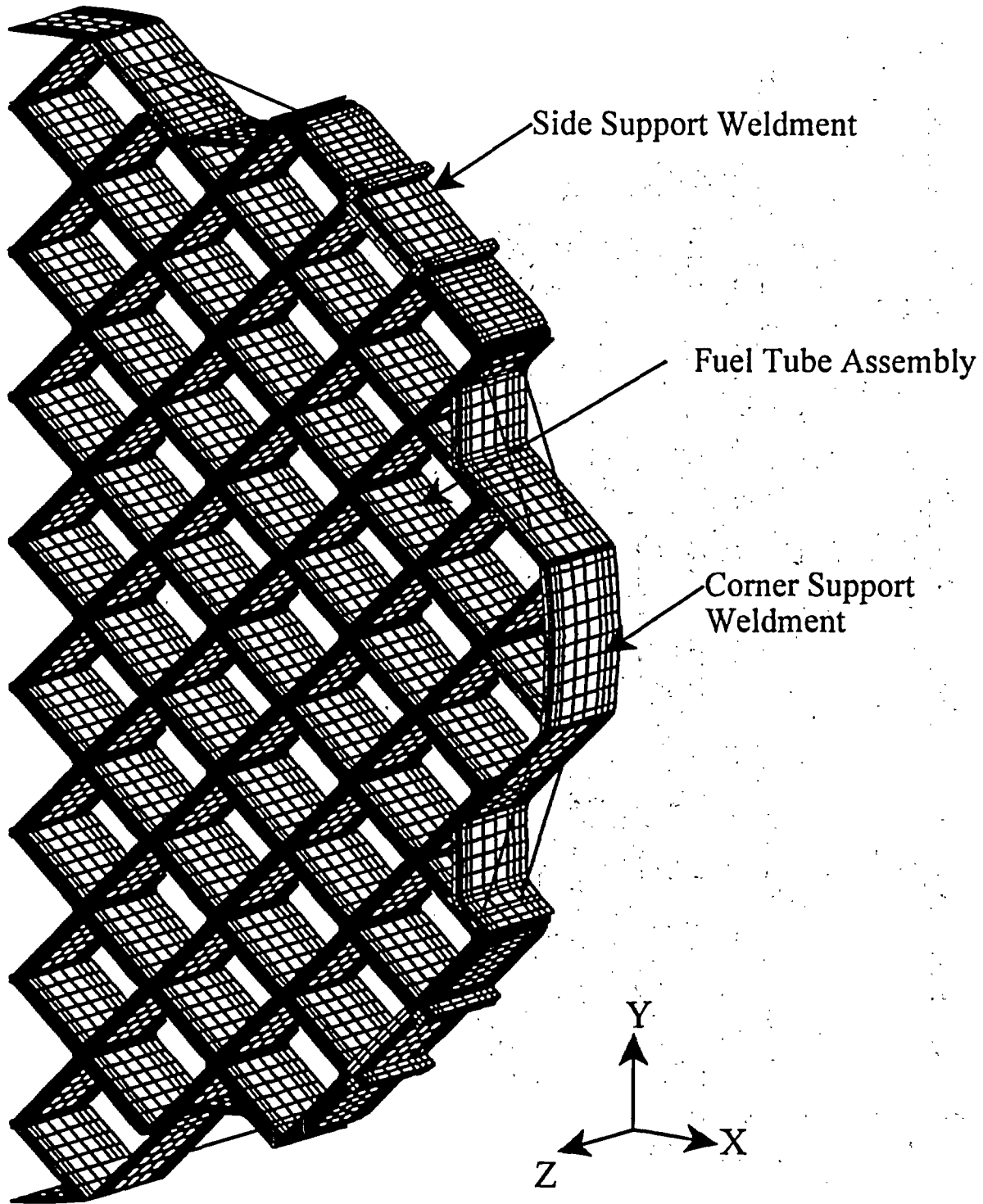
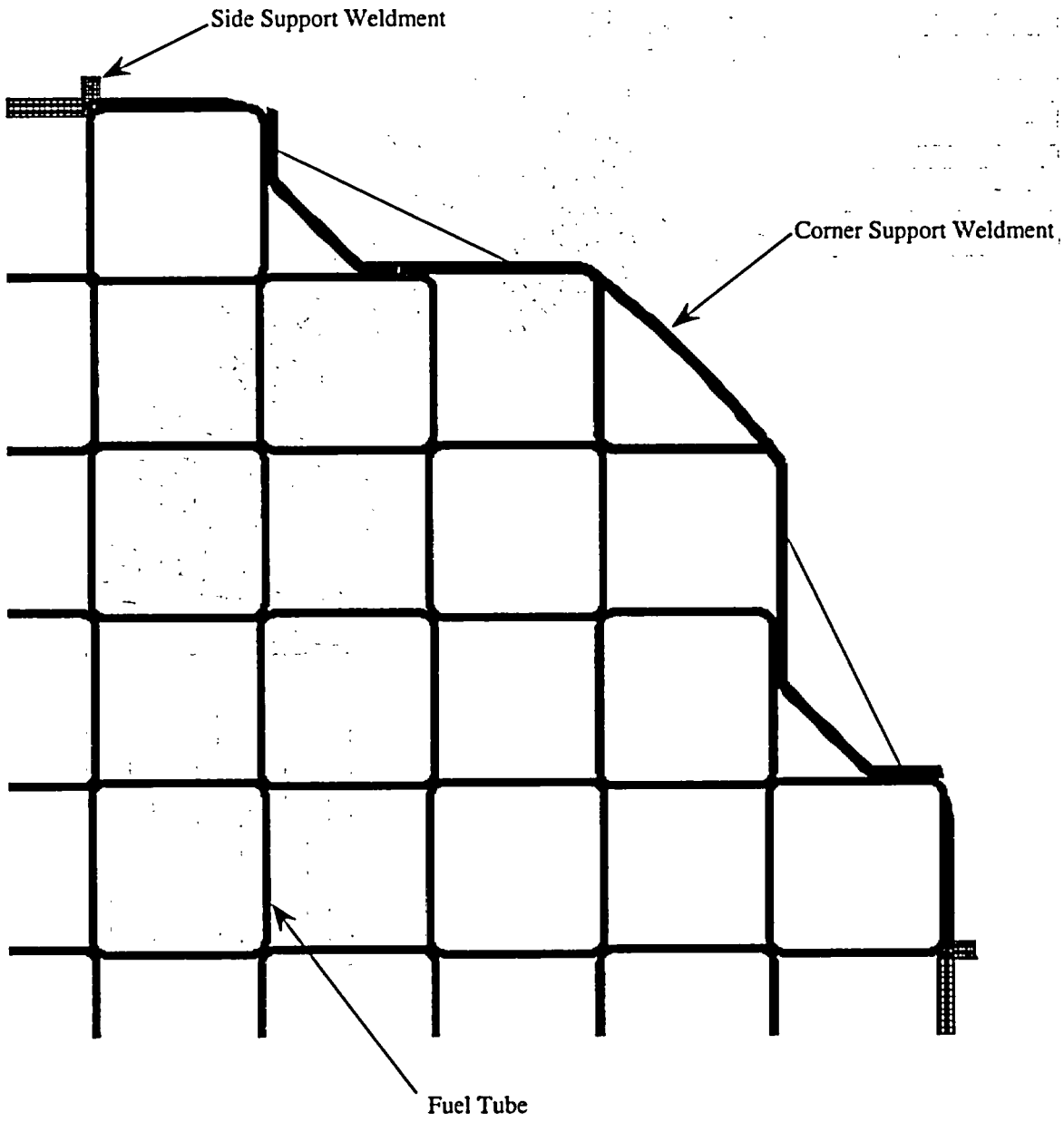


Figure 3.B-7 BWR Basket Plane Strain Plastic Model



(Quarter of model shown)

Figure 3.B-8 Meshing Detail of Fuel Tube in the BWR Basket Plastic Model

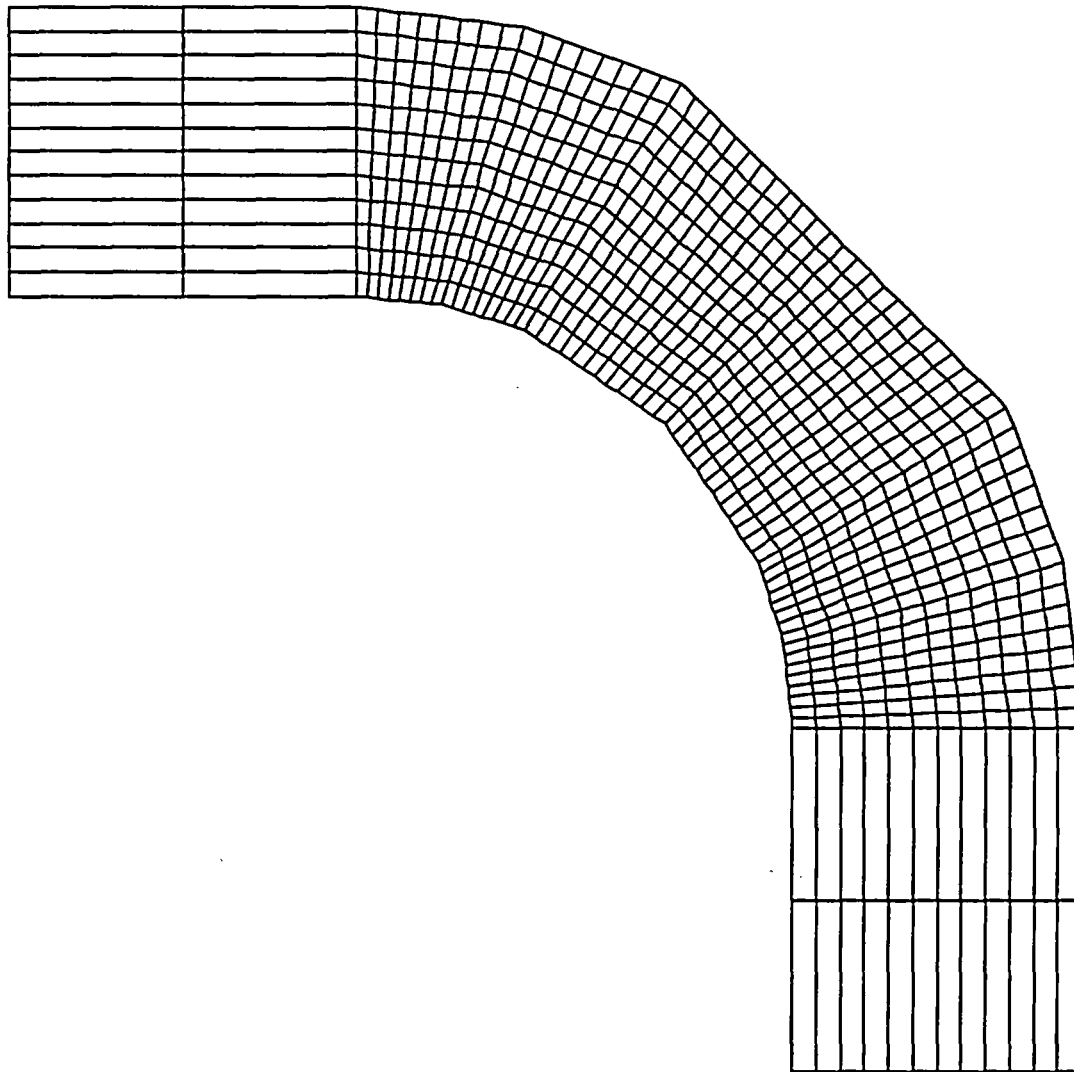


Figure 3.B-9 BWR Basket Model Boundary Conditions for a Transverse Loading – 0° Basket Orientation

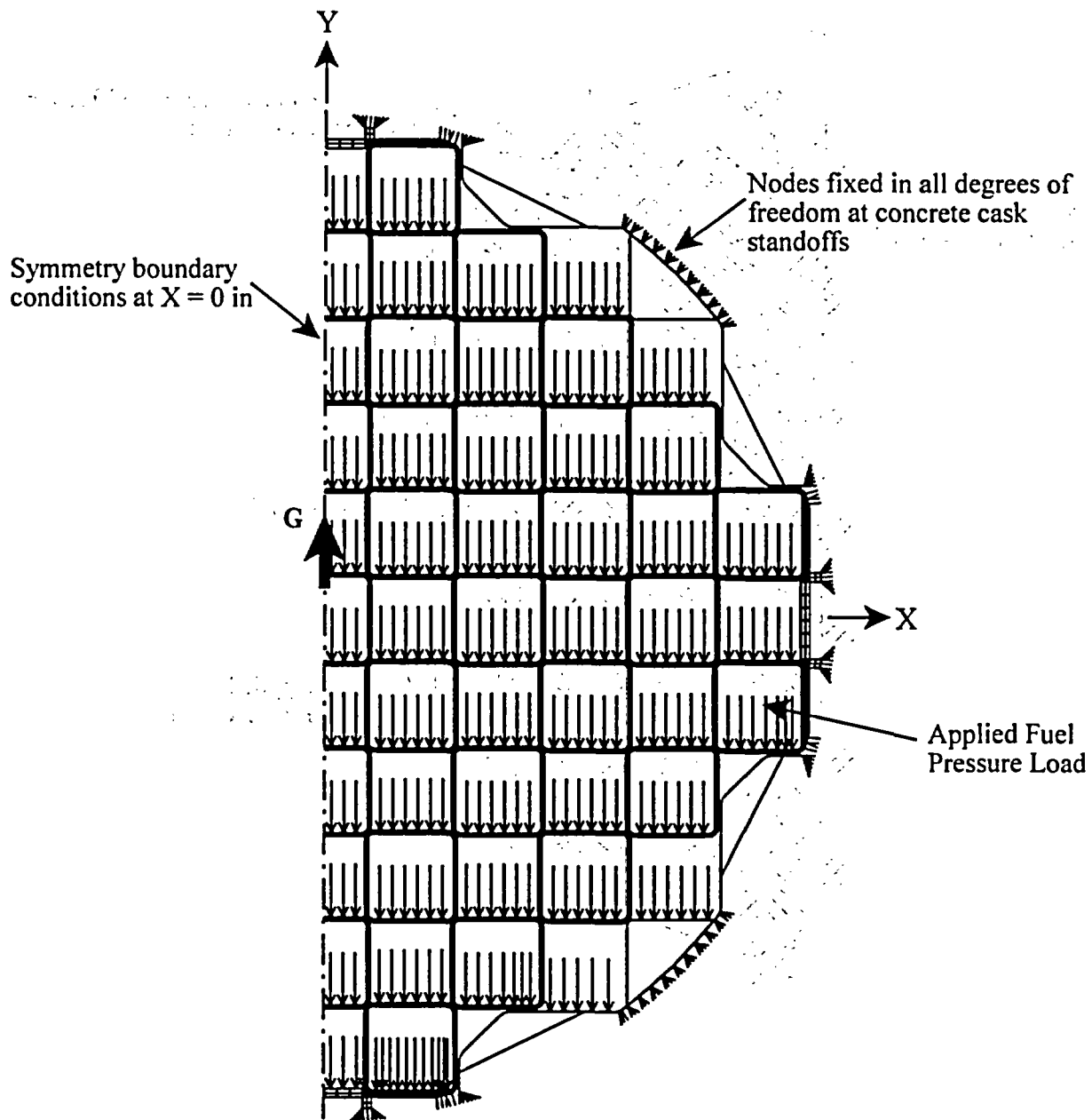
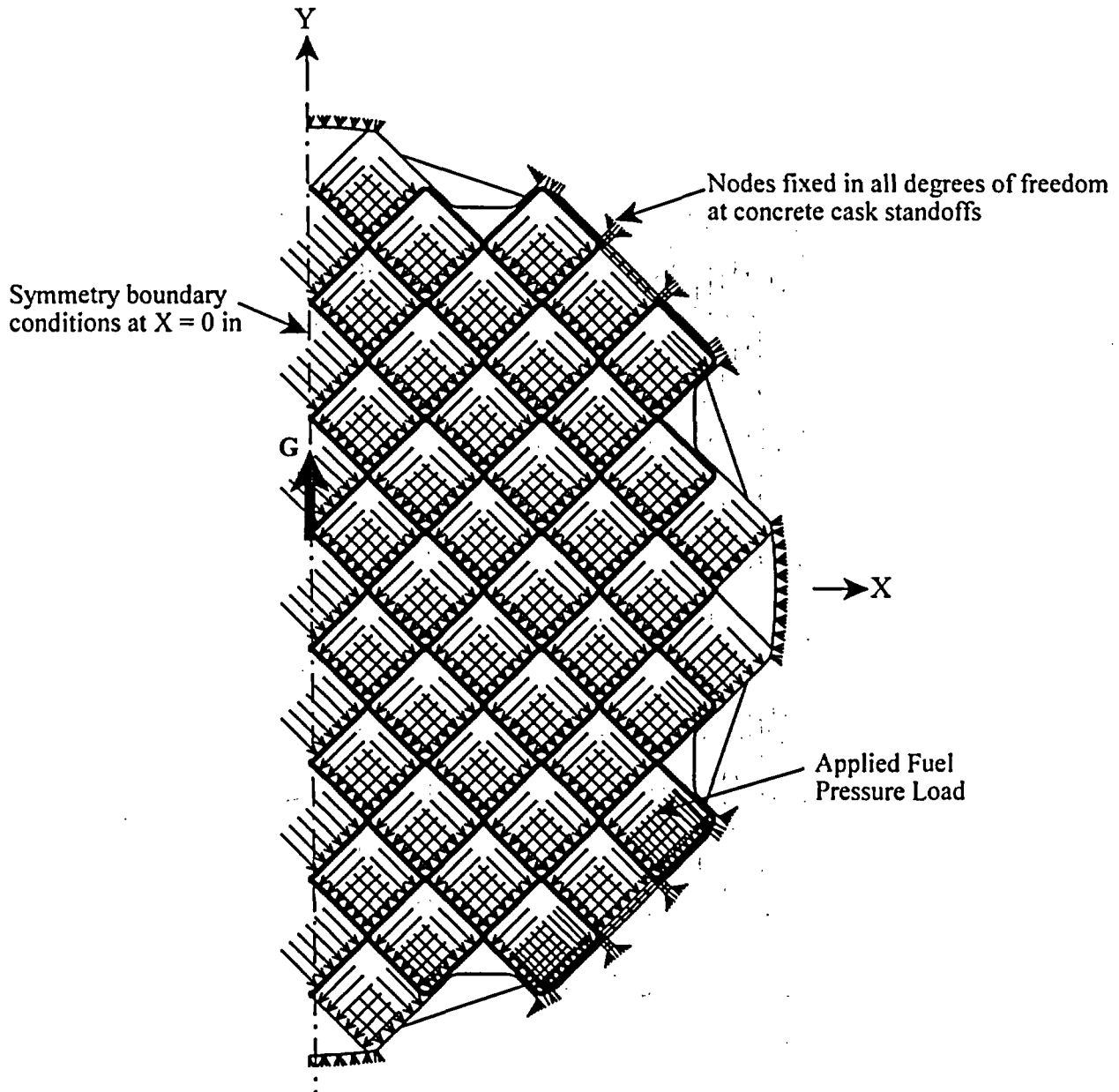


Figure 3.B-10 BWR Basket Model Boundary Conditions for a Transverse Loading –
45° Basket Orientation



3.C TSC Finite Element Model

This appendix presents details on the TSC finite element model used in the structural evaluation of the TSC for lift, normal conditions and off-normal or accident events of storage.

TSC Finite Element Model Description

The three-dimensional finite element model of the TSC is constructed using ANSYS SOLID45 elements. By taking advantage of the symmetry of the TSC, the model represents one-half (180° section) of the TSC including the TSC shell, bottom plate, and closure lid. The finite element model of the TSC is shown in Figure 3.C-1. ANSYS CONTAC52 elements are used to model the interaction between the closure lid and the TSC shell. Gap elements are also used to simulate the interaction with the concrete cask inner liner during a side impact and pedestal during an end impact. The size of the CONTAC52 gaps is determined from nominal dimensions of contacting components. Due to the relatively large gaps resulting from the nominal geometry, these gaps remain open during all loadings considered. All gap elements are assigned a stiffness of 1×10^8 lb/in.

This model represents a “bounding” combination of geometry and loading that envelope the MAGNASTOR PWR and BWR TSCs. Specifically, the longest TSC is modeled in conjunction with a conservative fuel and basket combination. By using the longest TSC with the conservative content weight, bending stresses are maximized at the junction of the shell and lid. Thus, the analysis yields conservative results relative to the expected performance of the actual TSC configurations.

Boundary Conditions for TSC Lift

The lifting configuration for the TSC consists of six hoist rings bolted to the closure lid at equally spaced angular intervals. To simulate the lifting of the TSC, nodes representing the hoist rings on the closure lid are constrained in the Y-direction. For heavy lift evaluation, only three of the hoist rings are considered. Due to the symmetry of the model, only the nodes at 60° and 180° are constrained (see Figure 3.C-1). Symmetry boundary conditions are applied at the plane of symmetry of the model. Pressure representing the weight of the fuel and basket is applied to the TSC bottom. A 1.1g inertia load is applied in the axial direction.

Boundary Conditions for Normal Conditions and Off-normal or Accident Events

Model Constraints:

The model is constrained in the global Z-direction for all nodes in the plane of symmetry. Other constraints for different loading conditions are summarized below. The directions of the coordinate system are shown in Figure 3.C-1

Model Constraint Summary

Condition	Constraint
Dead Weight	Y-direction at TSC bottom
Normal Handling	Y-direction – lift points in TSC lid
Off-normal Handling - axial	Y-direction – lift points in TSC lid
Off-normal Handling – lateral	Gap elements at TSC shell in radial direction
24-inch drop	Y-direction at TSC bottom
Tip-over	Gap elements at TSC shell in radial direction

Inertial Load:

Inertial loads resulting from the weight of the TSC and contents are considered by applying an appropriate deceleration factor (g-load). Inertial loads are summarized below.

Inertial Load Summary

Condition	Inertial Load
Dead Weight	1g – axial
Normal Handling	1.1g – axial
Off-normal Handling	1.5g – axial, 0.707g – lateral
24-inch drop	60g – axial
Tip-over	40g – lateral

Pressure Load – Internal Pressure:

A uniform pressure is applied to all internal surfaces of the TSC. The TSC pressures used for the normal (110 psig), off-normal (130 psig), and accident (250 psig) bound all pressure conditions.

Pressure Load – Dead load, Handling, and 24-inch Drop

For the dead load, handling, and 24-inch drop analyses, the inertial load produced by the contents weight is considered to be uniformly distributed on the inner surface of TSC bottom plate. Based on the contents weight of 100,000 lb and the TSC inside radius of 35.5 inch, the pressure corresponding to the contents weight is shown below.

$$p = \frac{100,000}{(\pi)(35.5)^2} = 25.26 \text{ psi}$$

The pressure load is multiplied by appropriate inertia loading (1g, 1.1g and 60g for dead load, handling, and 24-inch drop, respectively).

Pressure Load—Tip-over:

The inertial load produced by the 100,000 lb (50,000 lb for the half-symmetry model) content weight is represented as an equivalent static pressure applied on the interior surface of the TSC shell. The pressure is uniformly distributed along the cavity length over a section equal to the length of a basket, and is applied in the circumferential direction as a cosine distribution. The maximum pressure occurs at the impact centerline; the pressure decreases to zero at locations that are 36° either side of the impact centerline, as illustrated in Figure 3.C-1. The following formula is used to determine the applied pressures on the elements within the 36° arc. Pressure load is multiplied by appropriate inertia loading. This method uses a summation scheme to approximate the integration of the cosine-shaped pressure distribution:

$$F_{\text{total}} = \sum_{i=1}^6 P_{\text{max}} A_i \cos(\theta_i) \cos(\theta'_i)$$

where:

- F_{total} ----- conservative basket and fuel weight
- P_{max} ----- maximum pressure (at impact centerline)
- θ_i ----- average angle of subtended arc of i^{th} element measured from centerline at point of impact, to obtain vertical component of pressure
- i ----- i^{th} circumferential sector
- θ'_i ----- normalized angle to peak at 0° and to be zero at 36°
- $\theta_i \left(\frac{90}{36} \right) = 2.5(\theta_i)$
- A_i ----- i^{th} circumferential area over which the pressure is applied
- $\Delta\theta_i$ ----- $R(\Delta\theta_i)(\pi/180) L$
- R ----- inner radius of cask
- L ----- basket length
- g ----- deceleration

Temperatures for Thermal Stress Analysis:

The finite element thermal stress analysis is performed with TSC temperatures that envelope the TSC temperature gradients for normal (100°F ambient temperature), off-normal storage (106°F and -40°F ambient temperatures), and transfer conditions for all TSC configurations. Prior to performing the thermal stress analysis, the steady-state temperature distribution is determined using bounding temperature data from the storage and transfer thermal analyses. This is accomplished by converting the SOLID45 structural elements of the TSC model to SOLID70 thermal elements to perform a thermal conduction analysis. Nodal temperatures are applied at key locations for the thermal analysis: top-center of the closure lid, top-outer diameter of the closure lid, bottom-center of the closure lid assembly, bottom-center of the bottom plate, bottom-outer diameter of the bottom plate, and the TSC shell where the maximum temperature occurs.

The temperature distribution used in the structural analyses envelops the temperature gradients experienced by all PWR and BWR TSC configurations under storage and transfer conditions. The temperatures at the key locations are listed below. Temperatures locations (A through F) are defined in Figure 3.C-2. The temperatures for all nodes in the TSC model are obtained by the solution of the steady state thermal conduction analysis.

Top center of the closure lid (C)	=	510°F
Top outer diameter of the closure lid (F)	=	430°F
Bottom center of the closure lid (B)	=	570°F
Bottom center of the bottom plate (A)	=	350°F
Bottom outer diameter of the bottom plate (D)	=	240°F
Canister shell at 168 inch from TSC bottom (E)	=	520°F

Post-processing

The stress evaluation for the TSC is performed in accordance with the ASME Code, Section III, Subsection NB, by comparing the linearized sectional stresses against allowable stresses. The sectional stresses at 12 locations of the TSC model are obtained for each 9° angular division of the model. The locations for the stress sections are shown in Figure 3.C-2. The allowable stresses for normal conditions and off-normal or accident events are taken from Subsection NB.

Bounding temperatures that envelop the maximum temperatures experienced by TSC components during storage and transfer conditions are used to determine allowable stress values. Temperatures used at each stress section are given in Figure 3.C-2. Allowable stress values at

temperature are determined based on mechanical properties for SA-240 Type 304 stainless steel. All stress components are reported in the global cylindrical coordinate system ($X = \text{Radial}$, $Y = \text{Circumferential}$, $Z = \text{Axial}$). Additionally, in accordance with ISG 15, Revision 0, a 0.8 weld reduction factor is applied to the allowable stresses for the closure lid weld (Section 10 of Figure 3.C-2).

Figure 3.C-1 MAGNASTOR TSC Finite Element Model and Boundary Conditions

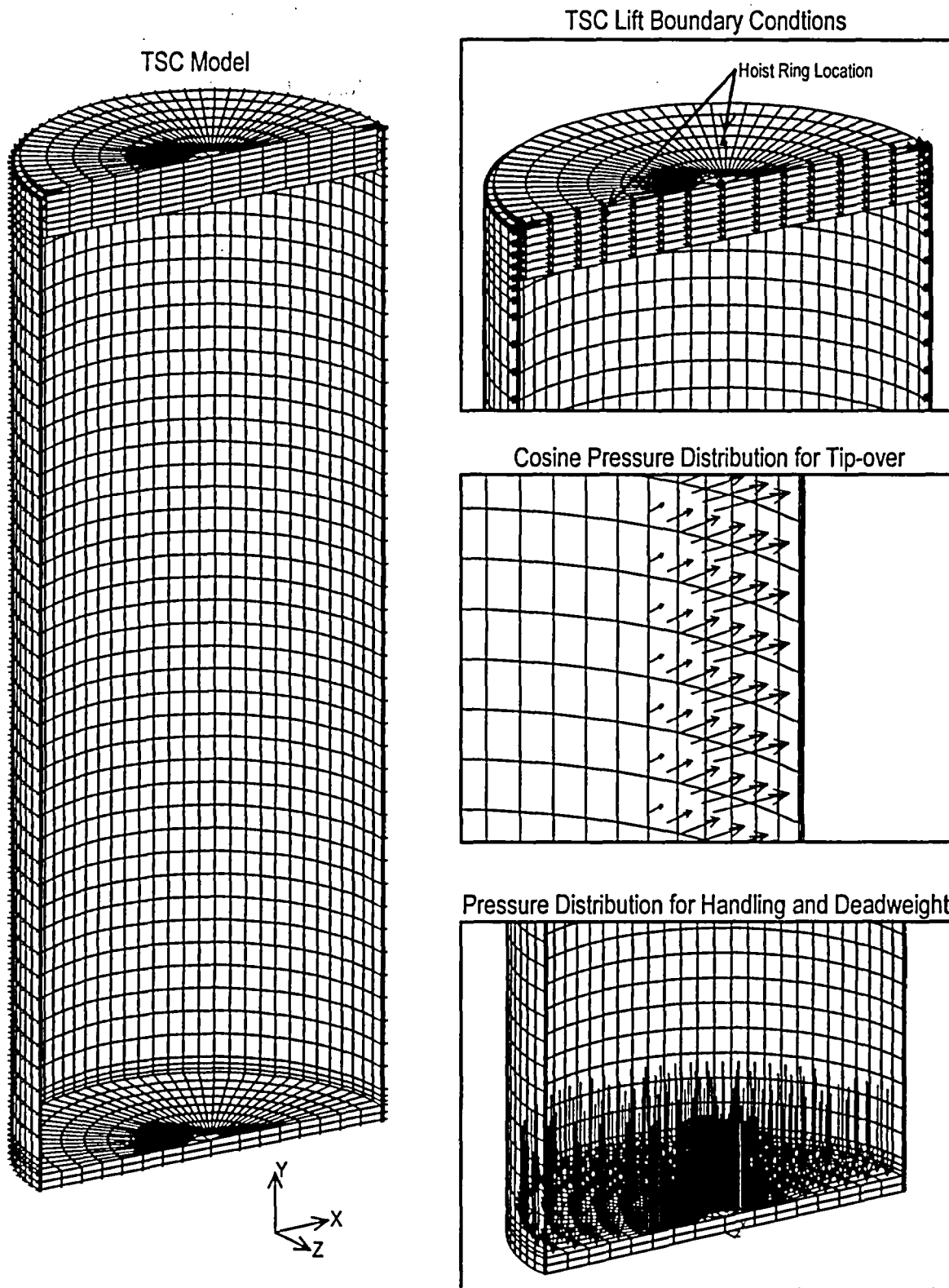
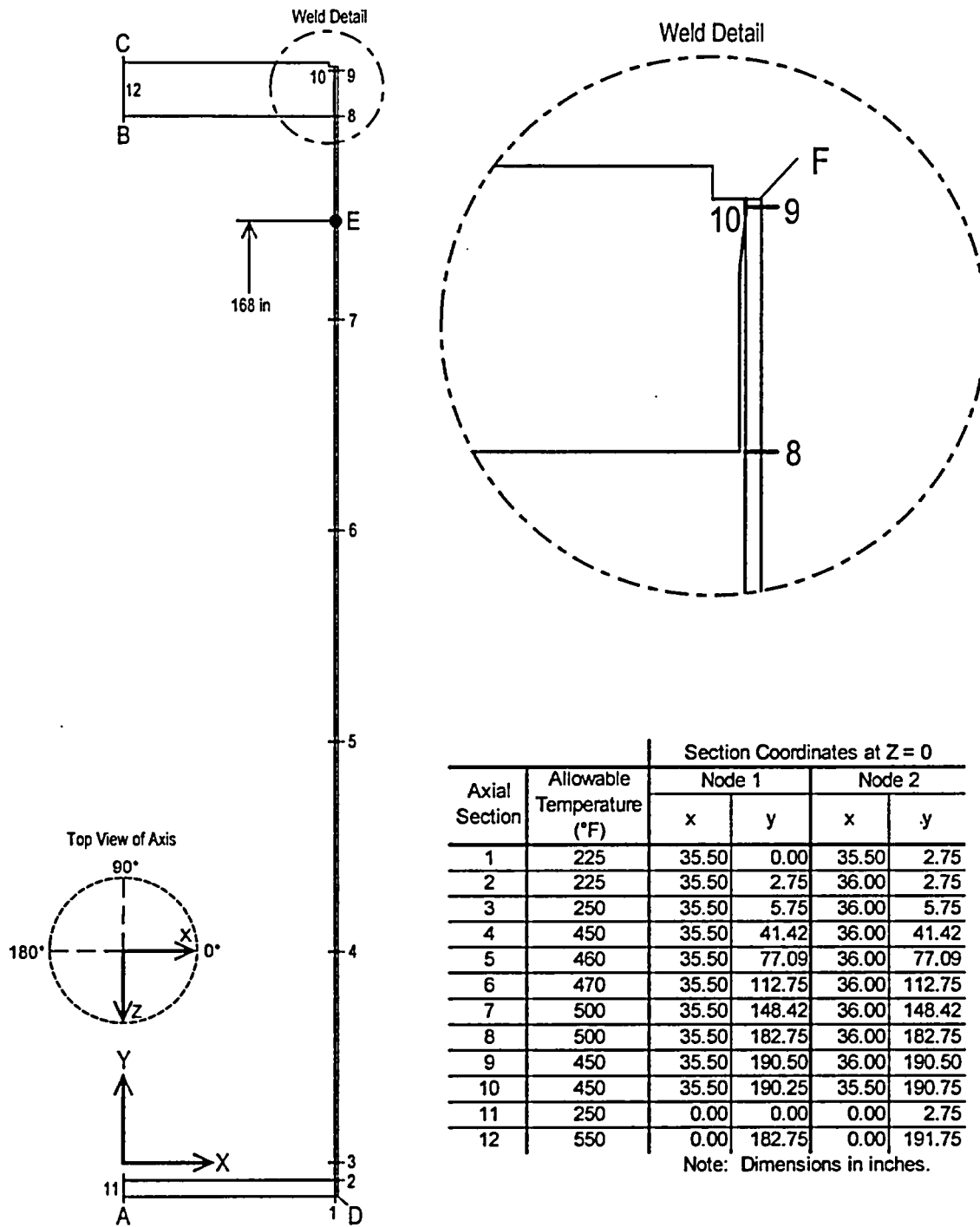


Figure 3.C-2 Identification of Sections for Evaluating Linearized Stresses in TSC



3.D Concrete Cask Finite Element Models

3.D.1 Pedestal Finite Element Model for Lift Evaluation

An ANSYS finite element model of the concrete cask pedestal (Figure 3.D-1) is used to perform the structural evaluation for the lift condition. The model is constructed using SHELL63, LINK8, and CONTAC52 elements. LINK8 elements are used to model the Nelson studs. The model is a quarter symmetry model. Symmetry boundary conditions are used on the XZ and YZ planes. The pedestal is a welded structure. CONTAC52 gap elements are used to model regions where components are not welded together (stand to pedestal plate, and support rails to stand). The gap elements do not close during the analysis, which maximizes the bending stresses in the support rails and inlet tops; therefore, the analysis is bounding. During a concrete cask top-end lift the TSC loads the pedestal plate. A pressure load (P_{can}) is used to apply the TSC weight to the pedestal plate.

$$P_{can} = \frac{1.1 \times W_{can}}{A_{ped}} = \frac{1.1 \times 120,000}{4,071} = 32.4 \text{ psi}$$

The load in the pedestal is reacted out by the Nelson studs, which carry the load into the concrete. The tops of the Nelson studs are restrained in all degrees of freedom. An inertia load of 1.1g (Z-direction) is applied to the finite element model for dynamic load factor (DLF). The 1.1g DLF is applied per ANSI/ASME N45.2.15.

3.D.2 Concrete Cask Finite Element Model for Thermal Stress Evaluation

A thermal stress evaluation of the concrete cask was performed for normal conditions and off-normal or accident events. A three-dimensional finite element model was created using the ANSYS program. The concrete cask contains 56 periodic radial sections with the 56 vertical rebars. Therefore, the model represents 6.4° ($1/56^{\text{th}}$) of the concrete cask. The model contains only the portion of the concrete cask shell and liner between the top of the lower vents and the lid assembly because the circumferential and vertical rebar are located in this region.

The thermal conduction model is constructed using ANSYS SOLID70 elements for the concrete shell and steel liner. The nodes at the liner/shell interface are coincident and are connected using temperature couples. The model is divided into four sections vertically with 0.1-inch gaps. LINK33 elements are used to connect the four sections to allow for thermal conduction across the gaps. The temperatures vary in the vertical and radial directions. Conservatively, the temperature profile corresponding to the 106°F (off-normal) ambient condition is used for the

normal conditions. The temperature profile for the 133°F ambient condition is used for the accident event. Temperatures are applied to nodes on the inner and outer surfaces of the concrete cask.

The thermal conduction model is modified for the structural evaluation. The SOLID70 elements are replaced with SOLID45 elements. COMBIN14 elements are used between the four vertical sections of the model for the steel liner. CONTAC52 gap elements are used between the liner and concrete shell to permit only compressive loads to be transmitted across the gap. Rebar was modeled into the model using LINK8 elements. LINK8 elements were also modeled across the vertical gaps to represent the vertical rebar; therefore, tensile loads are taken by the rebar. There are 24 vertical rebar on the inner radius and 56 on the outer radius. The properties of the inner vertical rebar are determined by a ratio to represent the $1/56^{\text{th}}$ model (24/56 ratio). The finite element model is shown in Figure 3.D-2 and Figure 3.D-3. Boundary conditions are shown in Figure 3.D-4.

3.D.3 Pedestal Finite Element Model for 24-inch Drop Evaluation

Subjecting the concrete cask to a bottom end impact, the TSC produces a force on the base weldment located at the bottom of the cask. The ring above the air inlets is expected to yield. To determine the resulting acceleration of the TSC and deformation of the pedestal, a LS-DYNA analysis is used.

A quarter-symmetry model of the base weldment is shown in Figure 3.D-5. The model is constructed using 4-node shell elements. Symmetry boundary conditions are applied along the planes of symmetry (X-Z and Y-Z plane). Rigid mass 8-node solid elements located in the TSC bottom plate represent the loaded TSC. Rigid mass 8-node solid elements located above the air inlet duct top represent the weight of the inner liner shell. The impact plane is represented as a rigid plane. To determine the maximum acceleration and deformations, impact analyses are solved using LS-DYNA program.

The weldment support rails, weldment pedestal plate, air inlet ducts, and the cylindrical stand materials are modeled using the piece wise linear plasticity model in LS-DYNA. The stress-strain curve used for this analysis was obtained from the Atlas of Stress-Strain Curves and is presented in Figure 3.D-6. To ensure that maximum deformations and accelerations are determined, two analyses are performed. One analysis, which uses the upper bound weight of 105 kips, envelops the maximum deformation of the pedestal. The second analysis employs the lower-bound weight of 60 kips to account for maximum acceleration. The details of the model are described as follows.

- All structural components are modeled using shell elements. A layer of solid elements represents the TSC weight.
- The ground base plate of the pedestal is not modeled since the plate is in contact with the impact plane during impact and has no effect on the deformation of the pedestal.
- The gravitational force is aligned with the Z-axis and is acting in the negative Z direction.
- All components of the pedestal are made of ASTM A36 carbon steel.
- The cylindrical shell under the pedestal plate is separated (not welded) from the support rail to allow buckling to occur at a relative lower g-level.
- The loaded TSC is modeled as a rigid body. The density of the TSC is calculated so that the total weight of the TSC model is equal to 105 kips or 60 kips, bounding values for the maximum and minimum TSC loaded weights.
- The concrete cask liner is modeled as a rigid body. The density of the liner is calculated so that the total weight is equal to 16,900 lb, which envelops the weight of the liner shell and the S-shape steel beams attached to the concrete cask liner.
- The column weight of the concrete portion of the concrete cask projected onto the top of an air inlet plate is represented by a uniformly distributed normal pressure acting on the top of the air inlet plate. The weight is only statically applied to the top of the air inlet. Upon impact, since the air inlet is more flexible than the base plate, all of the impact force of the concrete is transmitted to the base plate. The static pressure is always present during the impact.
- The rigid wall is an infinitive rigid plane. The rigid wall featured in LS-DYNA is used to simulate the rigid ground surface on which the concrete cask is supported or dropped.
- The filter frequency used in the LS-DYNA evaluation is determined by performing natural frequency calculations of the various components in the load path of the base weldment. The component with the lowest natural frequency is the cylindrical stand. This calculation results in a natural frequency of 182 Hz. Therefore, a filter frequency of 200 Hz is selected.

Material Property

The pedestal material is A-36 carbon steel. The LS-DYNA material type 24 (Piecewise_Linear_Plasticity) is used. The true stress-strain curve of A-36 is shown in Figure 3.D-6.

Initial Condition

The body force applied to the TSC and the pedestal assembly is the 1-g acceleration representing the ever-present gravitational force. Body force is a vectored input depending on the angle of drop. The 1-g body force is applied in the -Z direction. Since the 24-inch drop represents the dynamic force input, the initial velocity, V_o is computed as shown below.

$$V_o = \sqrt{2gH} = \sqrt{2(386.4)(24)} = 136.1 \text{ inch/sec}$$

where:

$$g = 386.4 \text{ inch/sec}^2$$

$$H = 24.0 \text{ inch} \text{-----Drop height}$$

Post-processing

To obtain output, a node on the TSC tracks the movements of the TSC as it impacts on the top base plate of the pedestal. Since the TSC is modeled as a rigid body, any node on the TSC is sufficient to track the global movements and deceleration of the TSC. The output database contains a time-series of nodal displacement, velocity, and acceleration. The nodal output file is a text file that the postprocessor of LS-DYNA can convert into time-history plots and apply to the plotted graphs signal-conditioning operations such as filtering and rescaling. The acceleration of the TSC is obtained directly from the output file and then filtered to eliminate the ripples. The filtered acceleration (in-inch/sec²) is rescaled to units of g (386.4 inch-inch/sec²) value.

3.D.4 Concrete Cask Finite Element Model for Tip-over Evaluation

The concrete cask is designed to hold a TSC during long-term storage conditions and is constructed of a steel liner surrounded by reinforced concrete. The critical locations for measuring accelerations are at the top of the fuel basket and top of the TSC closure lid.

Two half-symmetry finite element models of the concrete cask, concrete pad, and soil sub grade are constructed of solid brick elements using the LS-DYNA program for the cask tip-over evaluation. One model uses a standard sized pad, and the other model uses an oversized pad. The difference between the two models reflects the segments in the concrete pad. The finite element models are shown in Figure 3.D-7.

Material Properties

The mechanical properties used in the analyses are described in the following sections. The densities of each part are calculated to account for the total weight of nonstructural components that are not modeled as part of the finite element model.

Concrete:

The concrete is represented as a homogeneous isotropic material. The effect of the reinforcing steel is ignored. The concrete for the cask and the pad are modeled as LS-DYNA material 16 (Mat_Pseudo_Tensor), which represents a concrete constitutive model in LS-DYNA. This material model requires an equation-of-state represented in LS-DYNA as EOS_Tabulated_Compaction. The LS-DYNA input for the cask concrete is shown below.

$$f_c = 4,000 \text{ psi} \text{-----Compressive Strength}$$

$$\rho_c = 148 \text{ pcf} = 0.0002217 \text{ lb-sec}^2/\text{in}^4 \text{-----Density}$$

$$\nu_c = 0.22 \text{-----Poisson's Ratio}$$

$$E_c = 33\rho_c^{1.5}\sqrt{f_c} = 3.758 \times 10^6 \text{ psi} \text{-----Modulus of Elasticity}$$

$$G_c = \frac{E_c}{2(1+\nu_c)} = 1.540 \times 10^6 \text{ psi} \text{-----Shear Modulus}$$

$$K_c = \frac{E_c}{3(1-2\nu_c)} = 2.237 \times 10^6 \text{ psi} \text{-----Bulk Modulus}$$

$$\epsilon_v = \frac{f_c}{K_c} = 0.001788 \text{-----Volumetric Strain}$$

Using the same formulae presented above, the required input data for the pad concrete is shown below.

f_c (psi)	ρ_c (lbs/ft ³)	E_c (psi)	G_c (psi)	K_c (psi)	ϵ_v
5,000	160	4.723×10^6	1.936×10^6	2.811×10^6	0.001779

Soil:

An elastic model with the following properties is used to represent the subgrade soil material of the site.

$$\rho = 100 \text{ pcf} \text{-----Density}$$

$$\nu_s = 0.45 \text{-----Poisson's Ratio}$$

$$E = 30,000 \text{ psi} \text{-----Modulus of Elasticity}$$

Steel Inner Liner:

The steel liner is represented by a rigid material model with the following properties.

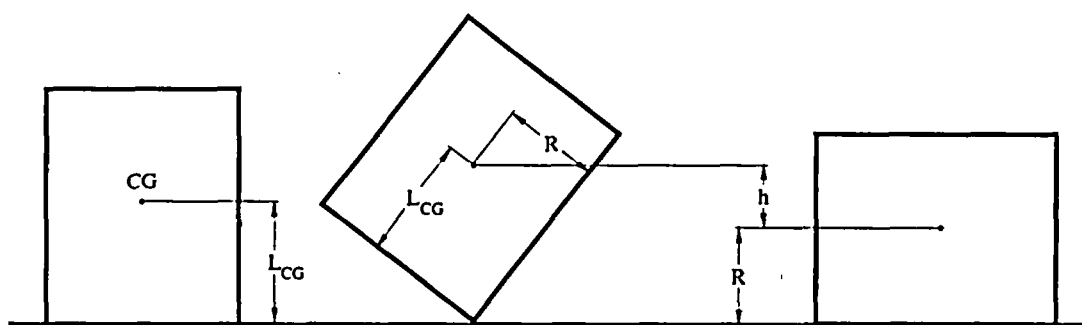
$$\nu = 0.31 \text{-----Poisson's ratio}$$

$$E = 29 \times 10^6 \text{ psi} \text{-----Modulus of elasticity}$$

Boundary Conditions

Automatic_Surface_To_Surface contact conditions are employed between the concrete cask and the pad, between the pad and soil, and between the cask steel liner and concrete. Symmetry boundary conditions are applied to all parts at the plane of symmetry (see Figure 3.D-7). The vertical displacements at the bottom of the soil sub grade and horizontal displacements for the three vertical boundaries of the soil are restrained.

Tip-over is simulated by applying an initial angular velocity, ω , to the entire concrete cask. The angular velocity value is determined by the conservation of energy about the center of gravity as the concrete cask rotates from end to corner to side orientations as shown in the figure below.



To ensure accuracy, the LS-DYNA output kinetic energies are compared to actual calculated potential energy. Equating the potential to the kinetic energy during tip-over

$$mgh = \frac{I\omega^2}{2}$$

where:

- $\omega = 1.527 \text{ rad/sec}$ -----Angular velocity for concrete cask
- $m = 785.6 \text{ lb}_m$ -----Total mass of the concrete cask
- $g = 386.4 \text{ inch/sec}^2$ -----Acceleration due to gravity
- $h = \sqrt{R^2 + L_{CG}^2} - R$ -----Height change of the concrete cask mass center
- I -----Total mass moment of inertia (lb-inch^2) of the concrete cask about the pivot point (automatically calculated by LS-DYNA)
- $R = 68 \text{ inch}$ -----Outside radius of concrete cask

The potential energy due to the height change of the concrete cask's mass center during tip-over is bounded by the kinetic energy of 2.0×10^7 inch-lb.

Load Cases

Bounding load cases are used to evaluate the loaded concrete cask during tip-over conditions. Two concrete pad and subsoil combinations are considered to bound all possible storage configurations: the standard pad configuration and oversize pad configuration. The standard pad represents typical storage pad properties and boundary conditions. The oversized pad is used as a sensitivity study to determine the effect of increased foundation size on accelerations. The dimensions of the standard concrete pad are 30 ft (Length) \times 30 ft (Width) with subsoil measuring 35 ft (Length) \times 35 ft (Width). The dimensions of the oversized concrete pad are 60 ft (Length) \times 30 ft (Width) with subsoil measuring 70 ft (Length) \times 35 ft (Width).

With the exception of pad size, the standard and oversized pads use identical parameters and boundary conditions. The mesh density and element aspect ratio of the oversized pad is maintained from the standard model.

Figure 3.D-1 Concrete Cask Pedestal Finite Element Model for Lift Evaluation

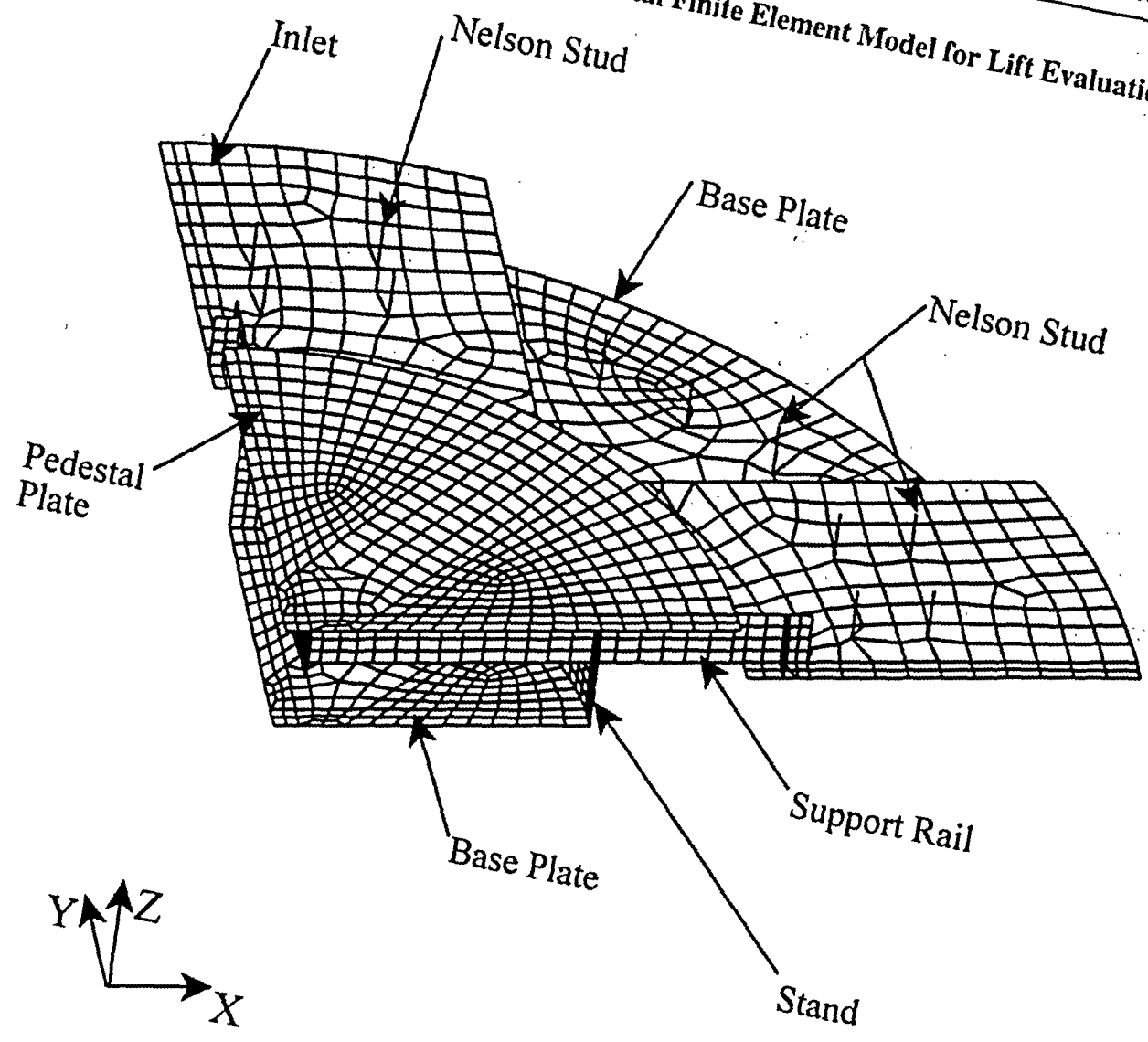


Figure 3.D-2 Concrete Cask Finite Element Model for Thermal Stress Evaluation

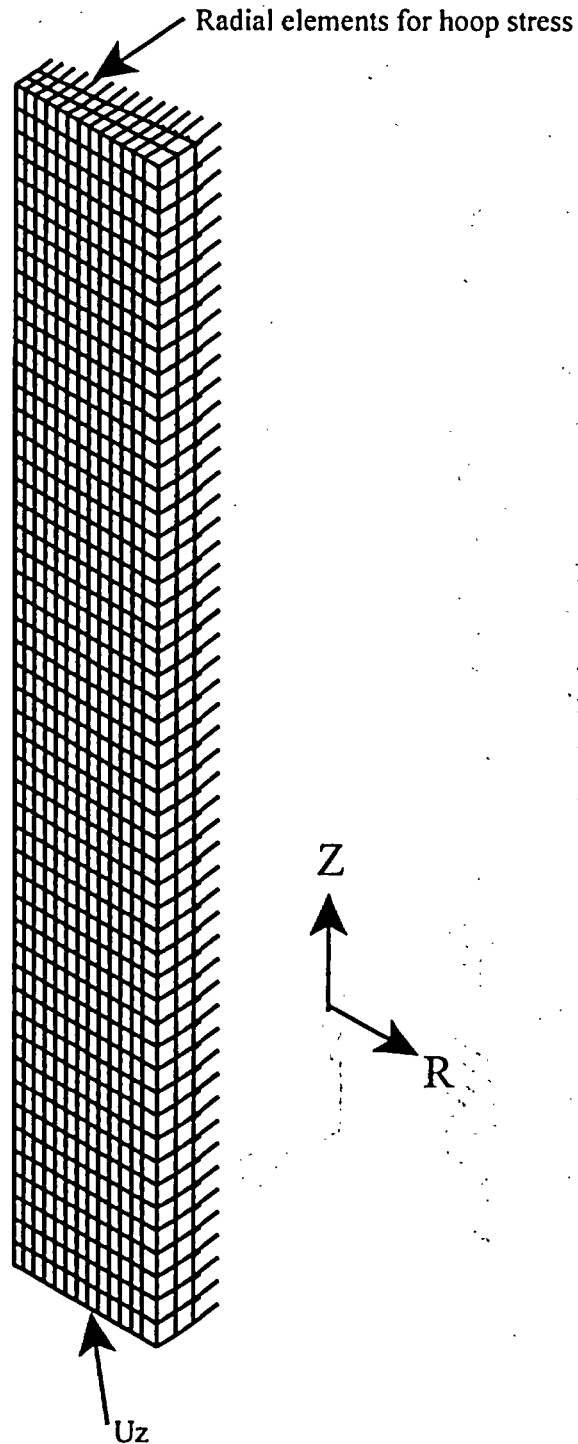


Figure 3.D-3 Concrete Cask Model – Elements for Rebar

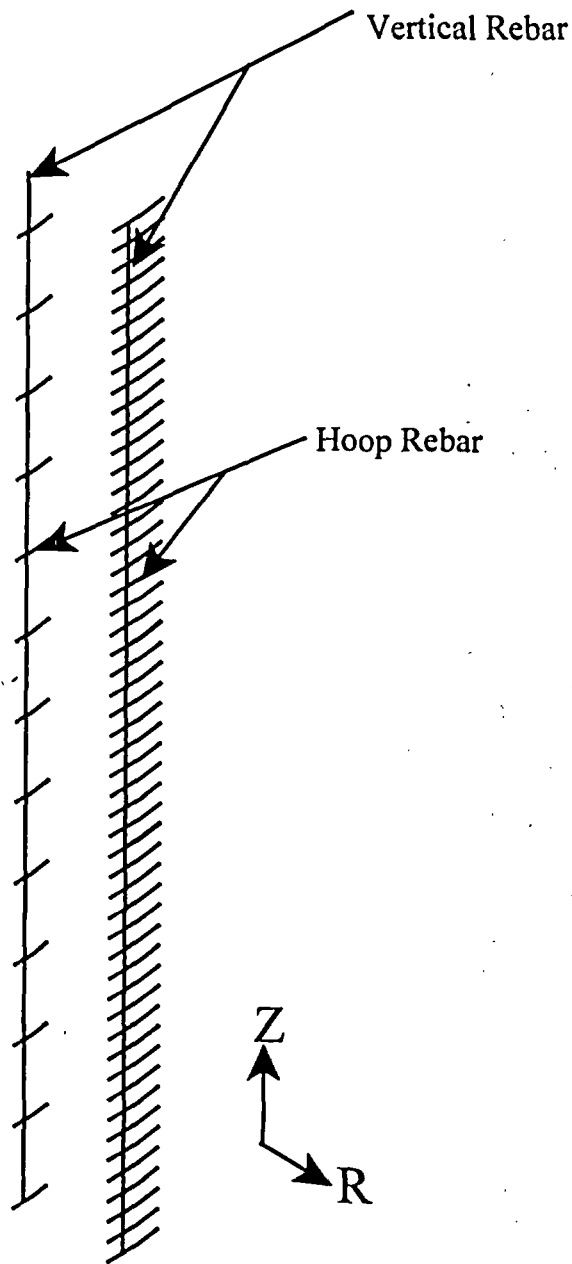


Figure 3.D-4 Concrete Cask Model Boundary Conditions

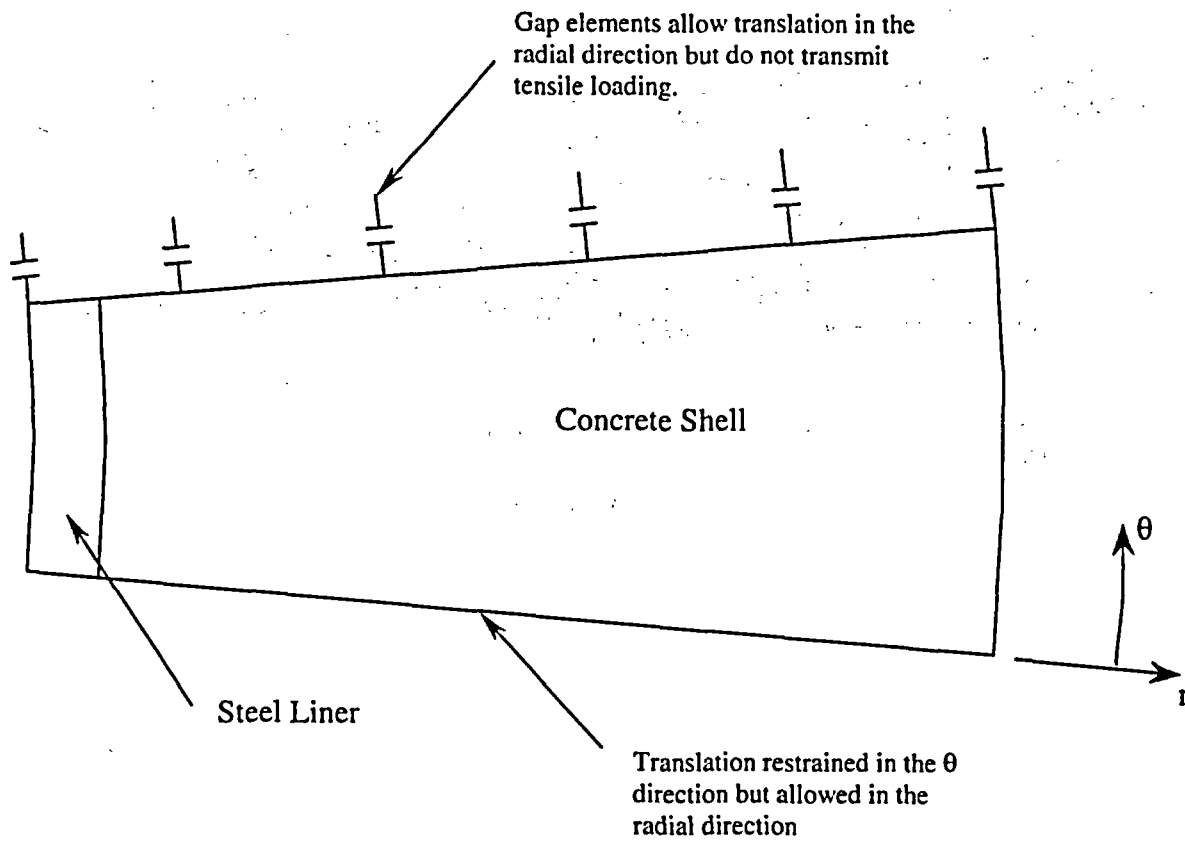


Figure 3.D-5 Concrete Cask Pedestal Finite Element Model for 24-inch Drop Evaluation

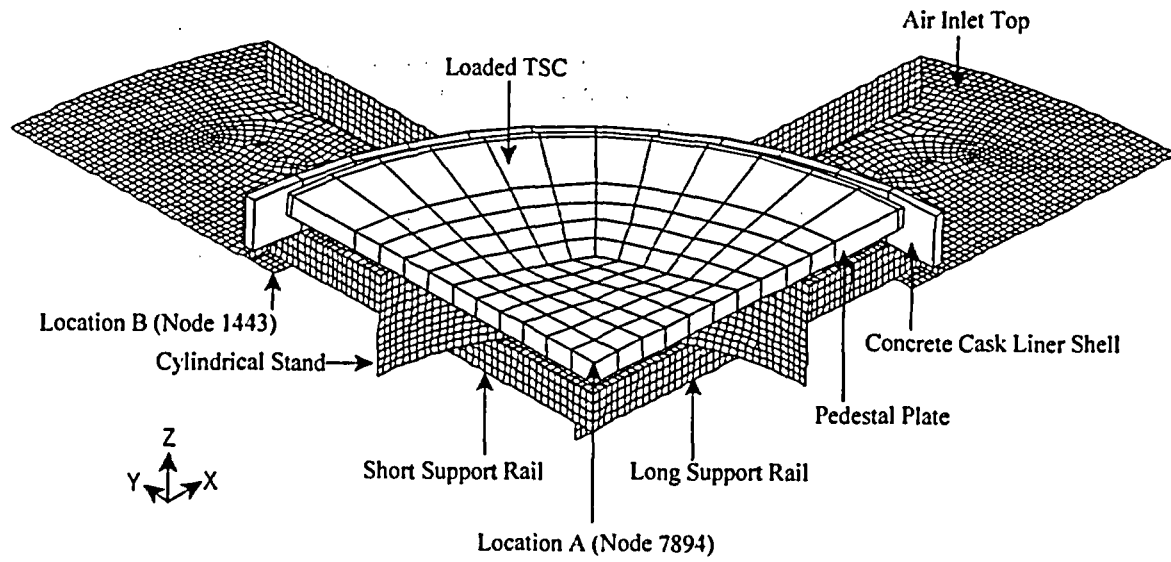


Figure 3.D-6 Stress-Strain Curve for A36 Carbon Steel

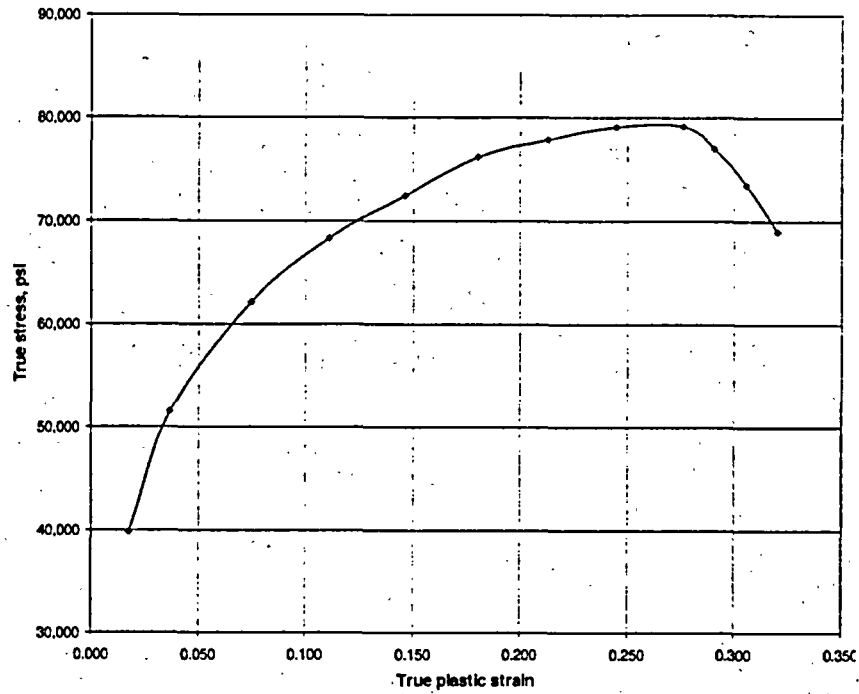
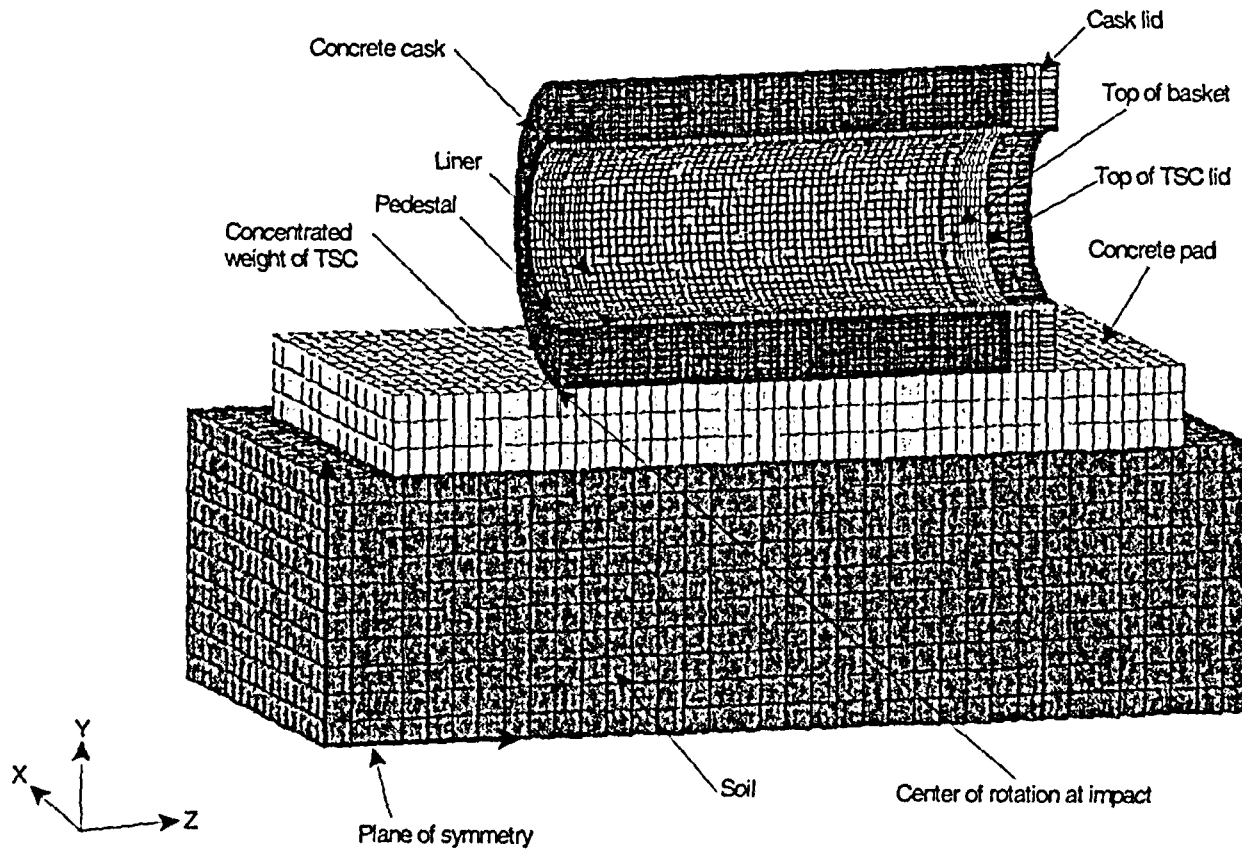
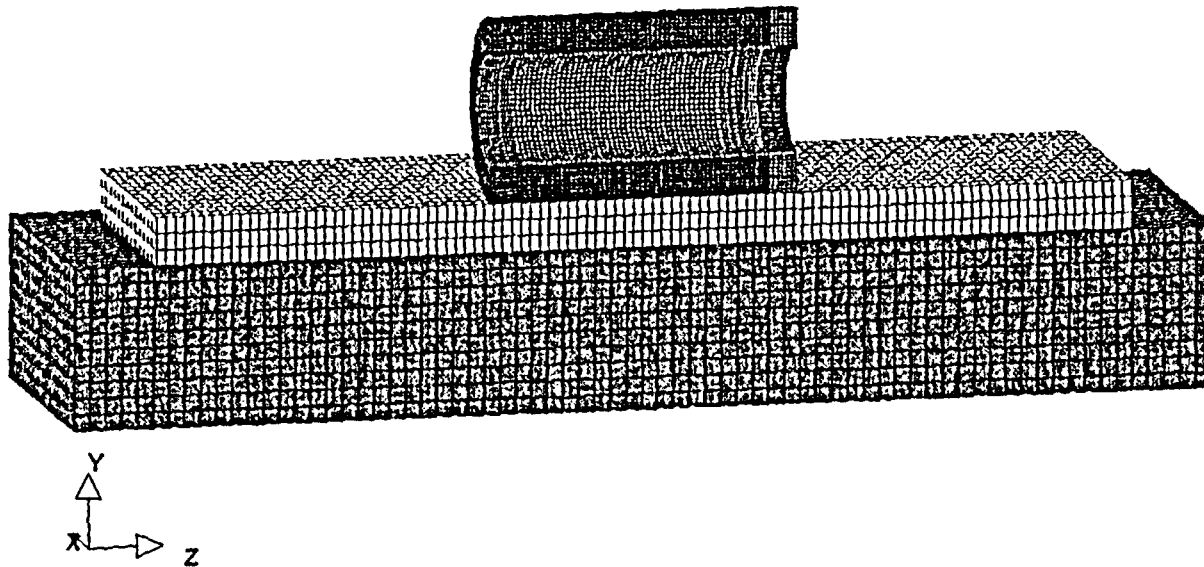


Figure 3.D-7 Finite Element Models for Tip-over Evaluation

Standard Pad Model



Oversized Pad Model



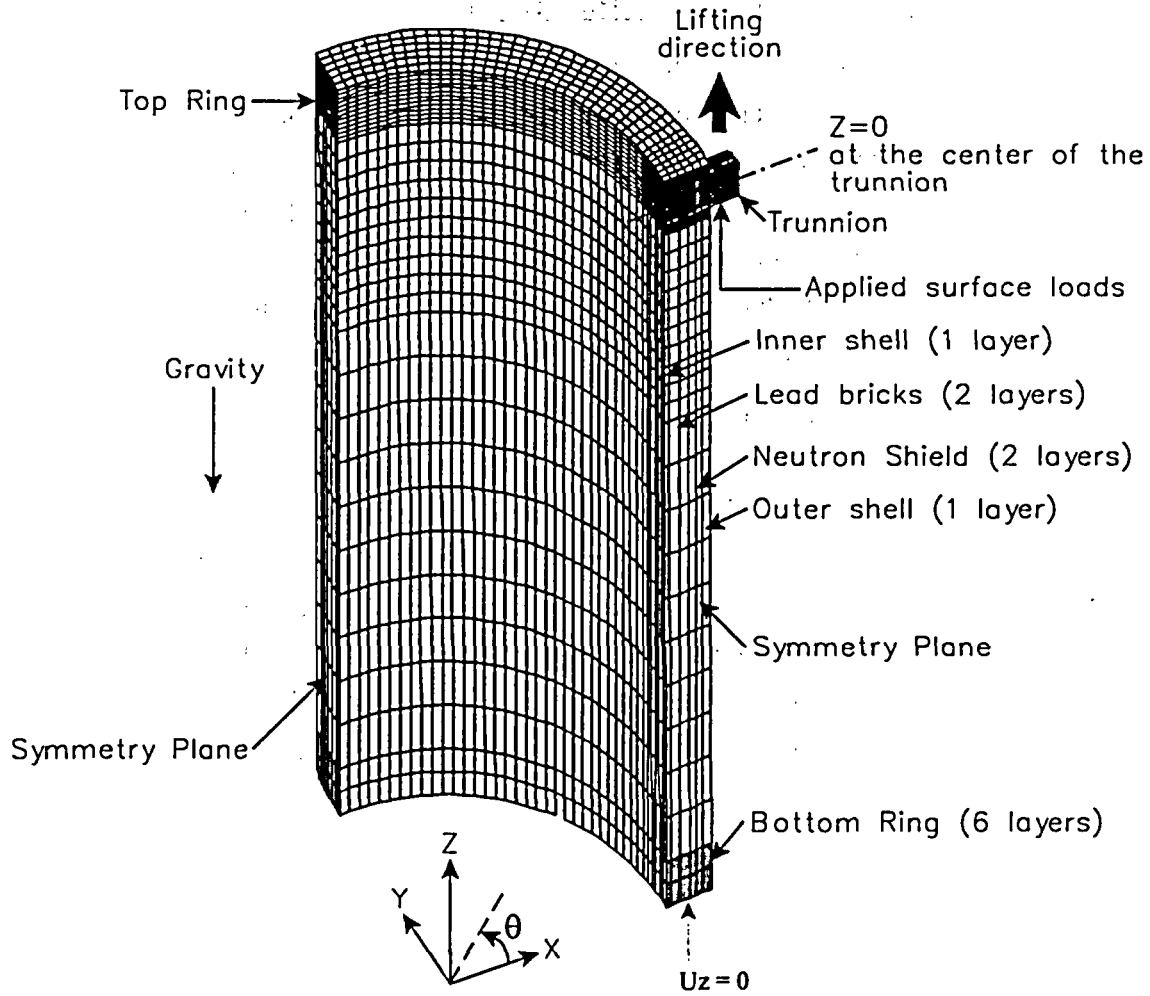
3.E Transfer Cask Finite Element Model

The top section of the transfer cask is a solid ring made of carbon steel. A pair of trunnions, 9-inch in diameter, are mounted 180° apart on this ring. The middle section of the transfer cask is comprised of a steel inner shell, a lead layer, a neutron shield layer, and a steel outer shell. The bottom section is a solid ring made of carbon steel. A pair of rails is welded to the bottom of the solid forging. A pair of steel doors is inserted in the rails. The overall height of the transfer cask is 198.0 inches. The overall diameter of the cask is 88.0 inches. The maximum loaded weight of the transfer cask is 230,000 pounds.

A three-dimensional finite element model is used to evaluate the lifting of a fully loaded MAGNASTOR transfer cask. Because of symmetry, only one-quarter of the transfer cask is modeled, as shown in Figure 3.E-1. The model includes the trunnions, the top ring at the trunnion region, the inner and outer shells, the bottom, and the lead and the neutron shield between the inner and outer shells. ANSYS SOLID45 elements (8-node brick element) are used to model the transfer cask. The trunnions are partial penetration welded to the top ring. CONTAC52 elements are used to model the interface between the trunnion and the top ring. The groove welds attaching the trunnion to the top ring are represented by coupled nodes between the two components.

The total weight of the heaviest loaded transfer cask is less than 115 tons. A conservative load of 120 tons, plus a 10% dynamic load factor, is used in the model. The load used in the quarter-symmetry model is $(240,000 \times 1.1)/4 = 66,000$ pounds. The load is applied upward at the trunnion as a "surface pressure load" whose location is determined by the lifting yoke dimensions. The magnitude of the surface pressure load is calculated so that the total upward force equals to the load of 66,000 pounds. The model is restrained along two planes of symmetry with symmetry boundary conditions. Vertical restraints are applied to the bottom of the model to resist the force applied to the trunnion.

Figure 3.E-1 Finite Element Model for the Transfer Cask



Chapter 4 Thermal Evaluation

Table of Contents

4	THERMAL EVALUATION	4-1
4.1	Discussion	4.1-1
4.2	Thermal Properties of Materials	4.2-1
4.3	Technical Specifications for Components	4.3-1
4.4	Normal Storage Conditions.....	4.4-1
4.4.1	Thermal Analysis Models.....	4.4-1
4.4.2	Test Model	4.4-21
4.4.3	Maximum Temperatures for PWR and BWR Fuel Configurations.....	4.4-21
4.4.4	Maximum Internal Pressures for PWR and BWR TSCs	4.4-23
4.5	Off-Normal Storage Events	4.5-1
4.6	Accident Events	4.6-1
4.6.1	Analysis of Maximum Anticipated Heat Load	4.6-1
4.6.2	Fire Accident.....	4.6-1
4.6.3	Full Blockage of Concrete Cask Air Inlets.....	4.6-3
4.6.4	Maximum TSC Internal Pressure for Accident Events.....	4.6-3
4.7	References.....	4.7-1

Appendices

Table of Contents.....	4.A-i
List of Figures.....	4.A-i

List of Figures

Figure 4.1-1	Definition of the Preferential Loading Pattern for PWR Fuel	4.1-4
Figure 4.4-1	Two-Dimensional Model of Concrete Cask Loaded with PWR TSC	4.4-26
Figure 4.4-2	Computational Mesh for the Two-Dimensional Axisymmetric CFD Model of the Concrete Cask	4.4-27
Figure 4.4-3	Reynold's Number at the Radial Mid-Point of the Concrete Cask Annulus ..	4.4-28
Figure 4.4-4	Axial Power Distribution for the PWR Fuel Assembly	4.4-29
Figure 4.4-5	Axial Power Distribution for the BWR Fuel Assembly	4.4-30
Figure 4.4-6	PWR Peak Fuel Cladding Temperature versus TSC Internal Pressure	4.4-31
Figure 4.4-7	Two-Dimensional Finite Element Model of the PWR Fuel Basket	4.4-32
Figure 4.4-8	Two-Dimensional Finite Element Model of the BWR Fuel Basket	4.4-33
Figure 4.4-9	14 x14 PWR Fuel Assembly Two-Dimensional Model	4.4-34
Figure 4.4-10	10 x10 BWR Fuel Assembly Two-Dimensional Model	4.4-35
Figure 4.4-11	Neutron Absorber Model for PWR Fuel Tube	4.4-36
Figure 4.4-12	BWR Fuel Tube Configuration with Channel and Neutron Absorber	4.4-37
Figure 4.4-13	BWR Fuel Tube Configuration with Channel, but without the Neutron Absorber	4.4-38
Figure 4.4-14	Two-Dimensional Model of Transfer Cask Loaded with a PWR TSC	4.4-39
Figure 4.4-15	Temperature (°F) Distribution for the Concrete Cask and TSC Containing a Design Basis PWR Heat Load	4.4-40
Figure 4.4-16	Air Velocity (m/s) in the Concrete Cask Annulus for the Design Basis PWR Heat Load ($V_{max} = 1.98$ m/s)	4.4-41

List of Tables

Table 4.1-1	Summary of Thermal Design Conditions for Storage for the MAGNASTOR	4.1-5
Table 4.1-2	Maximum Allowable Material Temperatures	4.1-6
Table 4.4-1	Effective Thermal Conductivities for 14x14 PWR Fuel Assemblies for Helium Backfill	4.4-42
Table 4.4-2	Effective Thermal Conductivities for 10x10 BWR Fuel Assemblies for Helium Backfill	4.4-42
Table 4.4-3	Maximum Component Temperatures for Normal Condition Storage of Design Basis PWR and BWR Heat Loads	4.4-43
Table 4.4-4	Maximum Fuel Temperatures for the Transfer Operations for Design Basis Heat Load	4.4-43

4 THERMAL EVALUATION

This section presents the thermal design and analyses of MAGNASTOR for normal conditions and off-normal and accident events of storage. Results of the analyses demonstrate that with the design basis contents, MAGNASTOR meets the thermal performance requirements of 10 CFR 72 [1] and NUREG-1536 [20].

4.1 Discussion

MAGNASTOR consists of a TSC, concrete cask, and a transfer cask. In long-term storage, the fuel is loaded in a basket structure positioned within the TSC. The TSC is placed in the concrete cask, which provides passive radiation shielding and natural convection cooling. The transfer cask is used to handle the TSC. The thermal performance of the concrete cask containing a loaded TSC with design basis fuel, and the performance of the transfer cask containing a loaded TSC with design basis fuel are evaluated in this chapter.

The thermal evaluation considers normal conditions and off-normal and accident events of storage. Each of these conditions can be described in terms of the environmental temperature, use of solar insolation, and the condition of the air inlets as shown in Table 4.1-1. For the transfer operation evaluation, a separate model including the continuous annulus cooling system is used. The evaluation of the different phases of the transfer operation is accomplished by altering the properties of the medium in the canister to correspond to water, helium or vacuum.

In order for the heat from the stored spent fuel assemblies to be rejected to the ambient via the concrete cask or the transfer cask, the decay heat from the spent fuel assemblies must be transferred to the TSC surface. The MAGNASTOR baskets for the PWR and the BWR fuel assemblies rely on all three heat transfer modes—radiation, conduction and convection—to transfer the heat to the TSC surface. The basket design enhances convection heat transfer. Helium is used as the backfill gas in the TSC because its thermal conductivity is better than other backfill gases. Since the basket is comprised of full-length carbon steel tubes, it provides a significant path for conduction heat transfer. Radiation is a significant mode of heat transfer in the fuel region and between the outer surface of the basket and the TSC shell.

The significant thermal design feature of the concrete cask is the passive convective airflow around the outside of the TSC. Cool (ambient) air enters at the bottom of the concrete cask through four air inlets. Heated air exits through the four air outlets in the upper concrete cask body. Radiant heat transfer occurs from the TSC shell to the concrete cask liner, which then transmits heat to the annular airflow. Conduction through the concrete cask, although not significant, is included in the analytical model. Natural circulation of air through the concrete cask annulus, in conjunction with radiation from the TSC surface, maintains the fuel cladding temperature and all component temperatures below their design limits.

The MAGNASTOR design basis heat load is 40 kW for 37 PWR fuel assemblies. The loading pattern for the PWR can accommodate a uniform heat load of 1.08 kW per assembly, or a preferential loading pattern as shown in Figure 4.1-1. The preferential loading pattern identified

in Figure 4.1-1 defines three values of heat generation that place the fuel assemblies with the maximum heat generation rate in an intermediate region of fuel storage locations. This configuration enhances convection, while not incurring the penalty from the maximum heat-generating assemblies being in the center of the basket region. The BWR design can accommodate 87 fuel assemblies with a uniform design basis heat load of 38 kW or 437 W per assembly.

The thermal evaluation applied different component temperature limits and allowable stress limits for long-term conditions versus short-term conditions. Normal storage operation is considered to be a long-term condition. Off-normal and accident events are considered to be short-term conditions. Thermal evaluations are performed for the design basis PWR and BWR fuels for all design conditions. The maximum allowable material temperatures for long-term and short-term conditions are provided in Table 4.1-2.

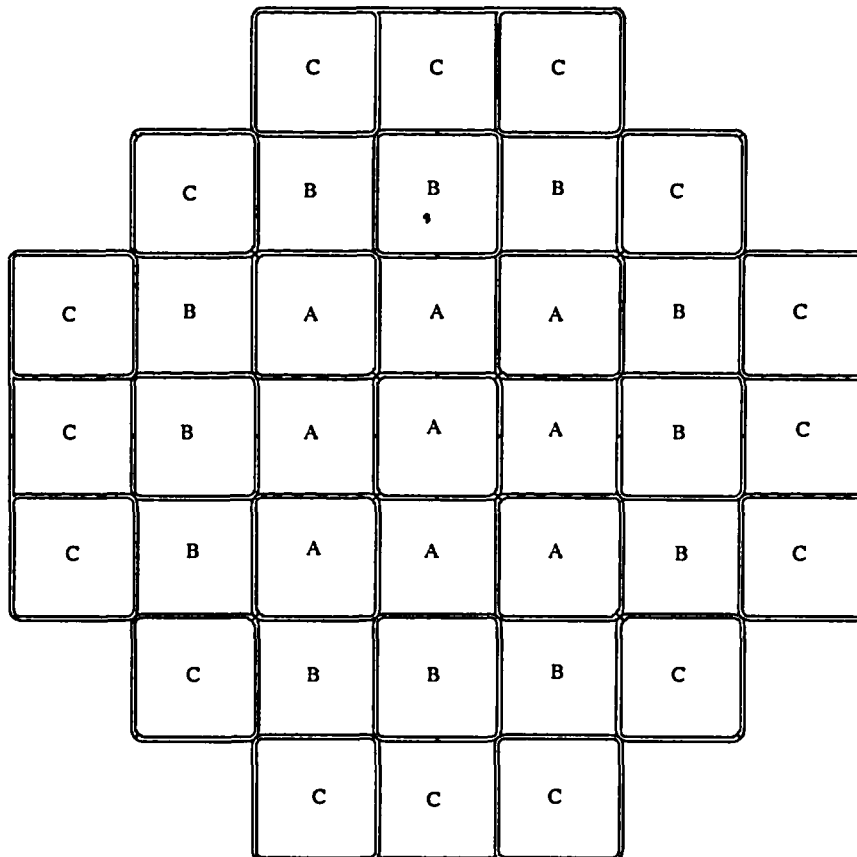
During normal conditions of storage and off-normal and accident events, the concrete cask must reject the decay heat from the TSC to the environment without exceeding the system components temperature limit. In addition, to ensure fuel rod integrity for normal conditions of storage, the spent fuel must be maintained at a sufficiently low temperature in an inert atmosphere to preclude thermally induced fuel rod cladding deterioration. To preclude fuel degradation, the maximum cladding temperature under normal conditions of storage and canister transfer operations is limited to 752°F (400°C) per ISG-11[2]. For either fuel type, the maximum cladding temperature for off-normal and accident events is limited to 1,058°F (570°C). For the structural components of the storage system, the thermally induced stresses, in combination with pressure and mechanical load stresses, are limited to the material allowable stress levels.

Thermal evaluations for normal conditions of storage and canister transfer operations are presented in Section 4.4. The finite element method is used to compute the effective properties for the basket and fuel region. The thermal solutions for the concrete cask and transfer cask are obtained using finite volume methodology. Thermal models used in the evaluation of normal and transfer conditions are described in Section 4.4.1

A summary of the thermal evaluation results for normal conditions of storage is provided in Table 4.4-3 for the PWR and the BWR cases. Table 4.4-4 contains the maximum fuel cladding temperatures for the different phases of the transfer operations. Thermal evaluation results for off-normal and accident events are presented in Section 4.5 and 4.6, respectively. The results demonstrate that the calculated temperatures are less than the allowable fuel cladding and component temperatures for all normal (long-term) storage conditions and for short-term events.

As shown in Chapter 3, the thermally induced stresses, combined with pressure and mechanical load stresses, are also within allowable limits.

Figure 4.1-1 Definition of the Preferential Loading Pattern for PWR Fuel



Zone Identification	A	B	C
Maximum Heat Load per Assembly (kW)	1.08	1.35	0.88
Total Number of Fuel Assemblies	9	12	16

Table 4.1-1 Summary of Thermal Design Conditions for Storage for the MAGNASTOR

Condition		Environmental Temperature (°F)	Solar Insolation ^{a)}	Condition of Concrete Cask Inlets
Normal		100	Yes	All inlets open
Off-Normal - Half Air Inlets Blocked		100	Yes	Half inlets blocked
Off-Normal - Severe Heat		106	Yes	All inlets open
Off-Normal - Severe Cold		-40	No	All inlets open
Accident - Extreme Heat		133	Yes	All inlets open
Accident - All Air Inlets Blocked		100	Yes	All inlets blocked
Accident - Fire	During Fire	1475	Yes	All inlets open
	Before and After Fire	100	Yes	All inlets open

^{a)} Solar Insolation per 10 CFR 71[3]:

Curved Surface: 400 g cal/cm² (1475 Btu/ft²) for a 12-hour period.

Flat Horizontal Surface: 800 g cal/cm² (2950 Btu/ft²) for a 12-hour period.

Table 4.1-2 Maximum Allowable Material Temperatures

Material	Temperature Limits (°F)		Reference
	Long Term	Short Term	
Concrete	200(B)/300(L) ^{a)}	350	ACI-349 [4] NUREG-1536 [20]
Fuel Clad			
PWR Fuel	752	752/1,058 ^{b)}	ISG-11 [2] and PNL-4835 [5]
BWR Fuel	752	752/1,058 ^{b)}	
NS-4-FR	300	300	JAPC [6]
Chemical Copper Lead	600	600	Baumeister [7]
ASME SA693 17-4PH Type 630 Stainless Steel	650	800	ASME Code [8] ARMCO [9]
ASME SA240 Type 304 Stainless Steel	800	800	ASME Code [8]
ASTE SA537 Class 1 Carbon Steel	700	700/1,000 ^{c)}	ASME Code [8]
ASTM A588 Carbon Steel	700	700	ASME Code Case N-71-17 [10] ASTM Standard [19]
ASTM A350 LF2 Carbon Steel	700	700	ASTM Standard [19]
ASTM A36 Carbon Steel	700	700	ASME Code Case N-71-17 [10] ASTM Standard [19]

^{a)} B and L refer to bulk temperatures and local temperatures, respectively.

^{b)} 752°F TSC transfer operations; 1,058°F off-normal and accident events.

^{c)} 700°F TSC transfer operations; 1,000°F off-normal and accident events.

4.2 Thermal Properties of Materials

Material properties used in the analytical model are separated into two categories. One category represents materials specified in the design that are explicitly represented in the model and are tabulated in Chapter 8. The second category represents effective properties of the basket and fuel region, which are calculated using the thermal models presented in Section 4.4.1.

4.3 Technical Specifications for Components

The three major components of MAGNASTOR must be maintained within their safe operating temperature ranges: the concrete cask, the transfer cask, and the TSC with fuel basket. The safe operating ranges for these components are from a minimum temperature of -40°F to the maximum temperatures defined in Table 4.1-2.

The criterion for the safe operating range of the lead in the transfer cask is maintaining the lead temperature below its melting point of 620°F [7]. The maximum operating temperature limit of the NS-4-FR neutron shield material in the transfer cask has been determined by the manufacturer and ensures the stability of the material. The temperature limits for the steel components of the fuel basket and the TSC are defined by ASME Code Section II, Part D [8]. The temperature limits for the steel components of the transfer cask and the concrete cask are defined by ASTM Standards [19]. The temperature limits for concrete are defined by ACI-349 [4] and NUREG-1536 [20].

4.4 Normal Storage Conditions

The finite element and finite volume methods are used to evaluate the thermal performance of MAGNASTOR for normal conditions of storage. The general-purpose finite element analysis program ANSYS [11] is used to perform analyses requiring radiation and conduction. The Computational Fluid Dynamic (CFD) program FLUENT [12], which is based on finite volume methods, is used to perform analysis that includes conduction, radiation and convection. In FLUENT, convection of heat is simulated through motion of fluid, as well as by the specification of a film coefficient for a surface boundary condition.

4.4.1 Thermal Analysis Models

Analysis models used for the thermal evaluation of both the PWR and BWR design configurations are described in the following sections. The methodology inherent in the models conservatively reflects the heat transfer performance provided by the MAGNASTOR design.

The designs for both the PWR and the BWR fuel systems utilize the same method of passive heat rejection to transfer the decay heat from the fuel assemblies to the ambient environment. The TSC is a closed system, whereas the concrete cask and the transfer cask are open to the environment. Internal to the TSC, the decay heat is transferred from the fuel assemblies in each of the fuel tubes to the TSC shell by three modes of heat transfer: convection, conduction and radiation. The fuel baskets designed for PWR and BWR fuel assemblies permit the helium backfill gas to flow up the fuel tubes containing the fuel assemblies and carry the heat away from the fuel assemblies. The region in the TSC just above the fuel basket allows the helium flow upward from the fuel tubes to combine and flow through the downcomer regions formed between the TSC shell and the basket side weldments. The gas exiting the downcomer regions at the bottom of the fuel basket enters a region below the basket tubes. The flow of the helium upward in the fuel basket and downward in the downcomer regions is driven by the buoyancy forces created by the effect of the heated helium rising up through the fuel tubes. To increase the buoyancy force, the density of the helium is increased by raising the helium backfill pressure. Since the fuel tubes are full-length carbon steel tubes, they provide a path for conduction of heat. While the tubes are not welded together, the effect of the gap between the tubes is mitigated by the use of the helium backfill. The side and corner weldments of the fuel basket, which support the fuel basket during a side impact, also provide a path of heat conduction. While a gap is considered between the side and corner weldments and the TSC shell for analysis purposes, the heat transfer across the gap is provided by the radiation from the weldments and conduction through the helium gap to the TSC shell. Radiation is also a mode of heat transfer, which allows heat from the interior of the fuel assembly to be transferred to the outer pins of the fuel assembly.

Additionally, since the fuel assemblies are assumed to be in the center of each fuel tube, radiation also contributes to the heat transfer from each fuel assembly to the fuel tube wall. Radiation is also taken into account for all gaps, such as those between the tubes. Additionally, radiation contributes to the heat being transferred from the outer basket surface to the TSC shell.

As the heat is being transferred to the TSC shell, the airflow up the annulus region between the TSC and the concrete cask carbon steel liner is removing heat from the TSC outer surface and rejecting it to the ambient environment. This annulus airflow is also driven by the buoyancy of the heated air. The air entering the air inlets at the base of the concrete cask provides a supply of cooler air into the annulus region. The heated air rises and exits the air outlets. Since the TSC shell faces the concrete cask liner, it radiates heat to the liner, which allows heat from the liner to be transferred to the annulus airflow. The liner also serves to distribute the heat along the length of the liner. Heat not rejected into the airflow is conducted through the concrete cask wall to the outer surface. At the surface, both convection and radiation modes of heat transfer reject the heat to the ambient.

Due to the convection of the fuel decay heat into the downcomer, the temperature distribution along the length of the TSC shell inner surface is not uniform, but increases monotonically from the base of the TSC to an elevation near to the top of the basket. This indicates that the heat flux due to the heated helium along the TSC wall is not uniform, and that this heat flux actually can be considered to be a boundary condition to the airflow in the annulus region of the concrete cask. For this reason, it is more efficient to consider a model in which both the TSC fuel basket and fuel region are considered in conjunction with the airflow in the annulus region of the concrete cask. The model used to represent the TSC and the concrete cask is a two-dimensional axisymmetric model, which is described in Section 4.4.1.1.

The fuel basket and fuel regions inside the TSC are modeled as homogeneous regions incorporating all modes of heat transfer. Effective thermal conductivities are used to represent the conduction and radiation in the fuel region and fuel basket, which require a two-step modeling process. A series of two-dimensional planar models is generated to determine the effective conductivities for the fuel assembly (Section 4.4.1.3) and the neutron absorber (Section 4.4.1.4). Using the effective conductivity for the fuel region and the neutron absorber, the effective conductivity for the fuel basket is determined using the two-dimensional fuel basket model as presented in Section 4.4.1.2.

The flow of helium in the fuel region is affected by the wetted perimeter associated with the fuel pins. To represent the flow of helium in the fuel region, which is represented as a homogenized entity, porous media is used in the modeling. The porous media model allows the effect of the

reduced flow area to be considered in representing the momentum of the helium flow by including a pressure drop based on the geometry of the fuel assembly, i.e., the pitch of the fuel rods and the fuel rod diameter. Computations of the constants inherent in the porous media use standard methodology for flow between cylindrical-shaped fuel rods. The determination of porous media constants is presented in Appendix 4.B. The flow of helium in the downcomer regions in the TSC does not require special consideration of effective flow conditions. To confirm that the use of a two-dimensional model for the TSC is an acceptable and conservative methodology, a benchmark is provided in Appendix 4.A.

The thermal evaluation for the transfer conditions is performed using the two-dimensional axisymmetric models of the transfer cask and TSC, as presented in Section 4.4.1.5. Similar to the model of the concrete cask and TSC, the fuel basket and fuel assemblies inside the TSC in the transfer cask are modeled as homogeneous regions using effective thermal properties.

4.4.1.1 Two-Dimensional Axisymmetric Concrete Cask and TSC Models

This section describes the finite volume models used to evaluate the thermal performance of the concrete cask and TSC for the PWR and BWR fuel configurations. As shown in Figure 4.4-1, the two-dimensional axisymmetric concrete cask and TSC model includes the following:

- Concrete cask, including lid, liner, pedestal and stand
- Air in the air inlets, the annulus and the air outlet
- TSC shell, lid and bottom plate
- Basket with fuel and neutron absorber
- Helium internal to the TSC

The fuel basket, fuel and neutron absorber are modeled as homogeneous regions with effective properties. The effective thermal conductivities for the TSC internals in the radial and axial directions are determined using the two-dimensional models as detailed in Section 4.4.1.2.

The two-dimensional axisymmetric concrete cask and TSC model is used to perform computational fluid dynamic analyses to determine the mass flow rate, velocity and temperature of the airflow in the annulus region, as well as for the helium flow internal to the TSC. Since the concrete cask and its components are contained in the model, the temperature distributions in the concrete and the concrete cask steel liner are also determined. Two models are generated for the evaluations—the PWR system and the BWR system, respectively. These models are identical, except for differences in dimensions of the active fuel region and the effective properties of the TSC internals. Figure 4.4-2 shows an overall view of the cells employed in the model representing both the concrete cask and the TSC containing a design basis fuel heat load.

Modeling of the Concrete Cask

The concrete cask body has four air inlets at the bottom and four air outlets at the top. Since the configuration is symmetrical, it can be simplified into a two-dimensional axisymmetric model by using equivalent dimensions for the air inlets and outlets, which are assumed to extend around the concrete cask periphery. The vertical air gap is an annulus, with a radial width of 3.5 inches. This radial dimension of the air annulus between the TSC shell and the concrete cask liner is modified to a smaller effective value to account for the reduction of the airflow cross-sectional area due to the standoffs welded to the liner. The bottom ends of the standoffs are more than 63 inches from the bottom of the TSC, which means that for over 30% of the length of the annulus, the standoffs do not exist. The model conservatively represents them as being the full length of the TSC. The additional axial conductance from the standoffs is conservatively neglected. Thermal radiation across the annulus gap is considered in the model, and the emissivities of the TSC surface and the concrete cask liner are reported in Chapter 8. Heat being radiated to the concrete cask liner is transferred into the annulus by convection, as well as being conducted through the concrete cask wall.

The most significant mechanism for rejecting heat into the environment is through the movement of air up through the annulus. The airflow in the vertical annulus is modeled as turbulent flow.

To determine if such conditions exist in the annulus flow, the Reynold's number (Re), a common metric to determine if the flow is considered to be turbulent, is calculated. It is computed as follows.

$$Re = \frac{\rho DV}{\mu} \quad [14]$$

where:

ρ	-----	density of the air (lb/in ³)
μ	-----	viscosity (lb-sec/in ²)
V	-----	velocity (in/s)
D	-----	hydraulic diameter of the annulus region (m)

The Reynold's number was computed for the normal condition in the annulus region. A plot of the Reynold's number along a vertical line at the midpoint of the annulus is shown in Figure 4.4-3. The value for the Reynold's number is shown to be significantly above the threshold value 2,300, SMITS [17] considered for turbulent flow, which validates the use of the turbulent model for the annulus region.

The mesh corresponding to the annulus for the analysis is shown in Figure 4.4-2. Increased cell density is used in the annulus region. In modeling turbulent conditions, FLUENT can employ a “law of the wall” in the row of the cells adjacent to the wall. The purpose of the “law of the wall” is to simulate the fluid behavior for the boundary layer, which is considered to be comprised of three layers: the viscous sublayer, the buffer layer and the log layer (FLUENT, [12]). This is taken into account in the k-ε model, which incorporates a standard wall function. In these analyses, the k-ε model with the standard wall function is used with a y+ of approximately 30.

Cell thicknesses are varied in the radial direction through the annulus to allow the y+ to be between 20 and 30, ensuring proper turbulent modeling.

The TSC model is included with the concrete cask model as shown in Figure 4.4-1. Boundary conditions at the edges of the model to the ambient are applied to the concrete cask surfaces. The heat flux being transferred from the helium internal to the TSC through the TSC shell and into the air annulus region is not considered to be a boundary condition for the concrete cask since all of these components are included in the same model. The boundary conditions applied to the outer surface of the concrete cask include the following.

- Solar insolation to the outer surfaces of the concrete cask.
- Natural convection heat transfer at the outer surfaces of the concrete cask.
- Radiation heat transfer at the concrete cask outer surfaces.

Solar Insolation

The solar insolation on the concrete cask outer surfaces is considered in the model. The incident solar energy is applied based on 24-hour averages as shown:

$$\text{Side surface: } \frac{1475\text{Btu/ft}^2}{24\text{hrs}} = 61.46\text{Btu/hr} \cdot \text{ft}^2$$

$$\text{Top surface: } \frac{2950\text{Btu/ft}^2}{24\text{hrs}} = 122.92\text{Btu/hr} \cdot \text{ft}^2$$

Natural Convection

Natural convection heat transfer at the outer surfaces of the concrete cask is evaluated by using the heat transfer correlation for vertical and horizontal plates. This method assumes a surface temperature and then estimates Grashof (Gr) or Rayleigh (Ra) numbers to determine whether a heat transfer correlation for a laminar flow model or for a turbulent flow model should be used. Since Grashof or Rayleigh numbers are much higher than the values defining the transition from

laminar to turbulent flow, correlation for the turbulent flow model is used as shown in the following.

Side surface (Kreith) [13]:

$$Nu = 0.13(Gr \cdot Pr)^{1/3} \quad \text{for } Gr > 10^9$$

$$h_c = Nu \cdot k_f / H_{vcc}$$

Top surface (Incropera)[14]:

$$Nu = 0.15Ra^{1/3} \quad \text{for } Ra > 10^7$$

$$h_c = Nu \cdot k_f / L$$

where:

- Gr -----Grashof number
- h_c -----Average natural convection heat transfer coefficient
- H_{vcc} -----Height of the concrete cask
- k_f -----Conductivity
- L -----surface characteristic length,
----- L = area / perimeter
- Nu -----Average Nusselt number
- Pr -----Prandtl number
- Ra -----Rayleigh number

All material properties required in these equations are evaluated based on the film temperature defined as the average value of the surface temperature and the ambient temperature.

Radiation Heat Transfer

The radiation heat transfer between the outer surfaces of the concrete cask and the ambient environment is evaluated in the model by calculating an equivalent radiation heat transfer coefficient.

$$h_{rad} = \frac{\sigma(T_1^2 + T_2^2)(T_1 + T_2)}{\frac{1}{\epsilon_1} + \frac{1}{\epsilon_2} + \frac{1}{F_{12}} - 2} \quad [14]$$

where:

- h_{rad} -----Equivalent radiation heat transfer coefficient
- F₁₂ -----View factor

T_1 & T_2	-----	Surface (T_1) and ambient (T_2) temperatures
ϵ_1 & ϵ_2	-----	Surface (ϵ_1) and ambient ($\epsilon_2=1$) emissivities
σ	-----	Stefan-Boltzmann Constant

At the concrete cask side, an emissivity for a concrete surface of $\epsilon_1 = 0.9$ is used and a calculated view factor (F_{12}) = 0.182 [14] is applied. The view factor is determined by conservatively assuming that the cask is surrounded by eight casks. At the cask top, an emissivity, ϵ_1 , of 0.8 is conservatively used (emissivity for concrete is 0.9), and a view factor, F_{12} , of 1 is applied.

Modeling of the TSC

The TSC is a closed system designed so that pressurized helium can circulate inside the TSC and transfer heat from the fuel in the basket to the TSC shell. Additionally, the basket permits heat to be conducted from the interior regions of the basket to the periphery of the basket, then radiated and convected to the TSC shell surface. The stiffeners at the periphery of the basket do provide a path of conduction to the TSC shell, even though a small gap exists between the stiffeners and the TSC shell. The heat conduction through these stiffeners is neglected in the evaluation, which is considered to be conservative. Radiation is modeled in the fuel assemblies, as well as in gaps in the basket. Heat transfer to the TSC lid and bottom plate is considered in the analysis, but it is not a major contributor to the heat-rejection process. Two separate models are generated—one for the PWR fuel configuration and one for the BWR fuel configuration. The differences between the two models are in the dimensions of the basket region and the effective properties derived for each basket and fuel region.

The TSC region consists of the following: the TSC shell, the TSC bottom plate, the TSC lid, the fuel basket region, and the helium-filled volume outside the fuel basket region. The fuel basket region is subdivided into three sections to reflect the location of the active fuel region with the associated heat generation and the fuel regions above and below the active fuel regions. These three separate regions are shown in Figure 4.1-1.

The cross-section of the flow path for the helium in the fuel basket and TSC significantly changes between the flow up through the basket region and the flow down in the downcomer region next to the TSC shell. For the flow up through the basket, the outline of the cross-sectional area is comprised of the area between the square basket tubes and circular fuel pins. Additionally, as the helium flows up through the basket tube, the fuel assembly grids will provide resistance to the flow. In the downcomer region, the exterior boundary is circular, while the interior boundary is the edge of the square fuel tubes. This is also an irregular shaped area. In a two-dimensional representation of these areas, the concept of the hydraulic diameter is

employed, which is commonly used to determine an equivalent cross-sectional area for a cross-section with complex shapes.

To account for the resistance to flow in the fuel region in the basket due to the wetted perimeter of the fuel region in the basket, the porous media option for fluids is used. The resistance to flow due to the fuel pins and the fuel assembly grids is represented in terms of a pressure drop included in the momentum equations for each cell in the model associated with porous media.

The expression for the pressure drop is given by:

$$\frac{\Delta P}{L} = \frac{\mu}{\alpha} V + C \left(\frac{1}{2} \rho V^2 \right)$$

where:

$\Delta P/L$	-----	pressure drop per unit length (Pa/m)
V	-----	superficial fluid velocity (m/s)
μ	-----	fluid viscosity (kg/m-s)
ρ	-----	fluid density (kg/m ³)
α	-----	permeability parameter (m ²)
C	-----	inertial resistance factor (m ⁻¹)

In this expression, the viscosity is input as a temperature dependent material property for the helium and the density is computed during the solution based on the ideal gas law. The permeability is based on the geometry of the fuel rods and the inertial resistance factor. Details of the calculation of the permeability and the inertial resistance factor are contained in Appendix 4.B. The values used for the evaluation are based on the bounding fuel parameters.

The downcomer region of the TSC does not use a porous media model. The areas of the downcomer regions are calculated to be 600 inches² and 550 inches² for the PWR and the BWR fuel baskets, respectively. Area is used to calculate the effective outer diameter of the fuel basket region, which serves as the radial boundary for the porous media region for the fuel.

Due to the large cross-section for the flow up through the fuel basket, the helium velocity is expected to be sufficiently low to correspond to laminar flow. In the downcomer region, the gas velocities would result in the flow being in a transitional regime. Conservatively, all helium flow in the TSC is taken to be laminar.

The porous media representation of the fuel basket region incorporates orthotropic effective thermal conductivities. The axial conductance in the fuel basket region is due to the significant cross-sectional area of the fuel tubes and the fuel assemblies. The in-plane conductance is associated with the conductance of the fuel tubes, as well as the effective conductivities of the fuel assembly and neutron absorber. The effective conductivity of the fuel basket region is determined in two steps. Separate effective thermal conductivities for the two-dimensional fuel assembly and the neutron absorber are computed for the axial and the in-plane directions using two finite element models. Details for these models are described in Section 4.4.1.3 for the fuel assemblies and Section 4.4.1.4 for the neutron absorber. In these sections, both the PWR and the BWR effective properties calculations are performed.

The resulting conductivities for the fuel assemblies and neutron absorber are then used in a single two-dimensional planar model of the cross-section of the basket, which is used to determine the axial and in-plane conductivities for the fuel basket region associated with the porous media. This model is described in Section 4.4.1.2. The effective conductivity for the porous media model uses two conductivities (k_f , k_s), as identified in the following equation.

$$K_{eff} = \epsilon \times k_f + (1 - \epsilon) \times k_s$$

where:

- ϵ ----- porosity factor
- k_f ----- thermal conductivity of the helium
- k_s ----- thermal conductivity associated with the solid portion of the porous media model

Heat Generation

The heat generation for the fuel is applied to the active fuel region of the TSC model (see Figure 4.4-1) for the PWR and the BWR fuel assemblies. The maximum design basis heat loads to be considered for the PWR and the BWR fuel basket configurations are 40 kW and 38 kW, respectively.

For the PWR fuel basket, two patterns of heat generation are considered. A uniform loading of 40 kW or 1.08 kW in each fuel location is considered. The axial power distribution for PWR fuel, as shown in Figure 4.4-4, is included in applying the heat generation. An optional heat generation pattern, as shown in Figure 4.1-1 is also considered and has the same total heat load of 40 kW. The application of the heat generation for this condition incorporates an axial distribution and a radial distribution. The area over which each fuel assembly heat load is distributed in Figure 4.1-1 is determined on the basis of the cross-section of the fuel tubes

containing the specific heat loads identified as A, B and C in Figure 4.1-1. The heat generation values specified in Figure 4.1-1 are considered to be the maximum permissible heat generation in each fuel location.

For the BWR fuel basket, only a uniform thermal loading pattern is considered. The design basis heat load for BWR fuel is 38 kW, which corresponds to a maximum heat load of 437 Watts for each of the 87 fuel assemblies. The axial power distribution for the BWR fuel is shown in Figure 4.4-5. For some BWR fuel assembly enrichments, the five fuel locations in the center of the BWR basket will not be loaded. In this configuration, the fuel assembly decay heat is limited to 437 Watts. Fuel storage locations not containing a fuel assembly will have an effective fuel cell insert installed to prevent the helium flow from bypassing the fuel locations containing fuel assemblies. The configuration with a partially loaded fuel basket containing BWR fuel assemblies with a maximum heat load of 437 Watts per assembly is considered to be bounded by the fully loaded BWR fuel basket configuration. Temperatures obtained from analyses performed using the maximum heat load in conjunction with a fully loaded BWR basket are considered to bound the results for a partially loaded basket.

Pressure of the Helium Backfill

To drive the convection internal to the TSC it is necessary to increase the density of the helium. Since the free volume in the TSC remains constant, the density of the backfill gas can be increased by backfilling the TSC to a range of pressures and temperatures which would result in an increase in the density. In the MAGNASTOR design, the TSC is pressurized to 7 atm (gauge) for the helium backfill for normal conditions. Since the gas in the model is characterized as an ideal gas, the increased density in the analysis can be indirectly obtained by specifying a pressure in the TSC region. For the PWR normal condition, the density of helium in the TSC associated with a pressure of 7 atm (g) is 0.047 lbm/in³. It is important to assess the effect of the helium density on the performance of the system. The evaluation of the sensitivity of the peak fuel temperature to the pressure is performed using the PWR model described in this section. The condition requiring a change is the pressure which is applied to the TSC region of the model. The results of the model solutions for pressures of 1 atm (g), 3 atm (g), 5 atm (g) and 7 atm (g) are shown as a graph in Figure 4.4-6. As shown in Figure 4.4-6, the variation of the peak cladding temperature with the pressure specified inside the TSC is a nonlinear function. The peak cladding temperature decreases sharply when the pressure increases from 1 atm to 3 atm. Subsequent increases in the pressure to 5 atm and 7 atm do not result in the same rate of decrease of the clad temperature as for the 1 atm and 3 atm cases. The model of the TSC in the concrete cask has two regions of convection separated by a TSC shell. Heat can only be transferred

through the shell from the TSC internal region to the annulus region outside the TSC. The flow characteristics in the annulus region are primarily affected by the total heat generation being transferred through the TSC shell, as well as the geometry of the annulus. As the pressure (and the associated mass) of the gas in the TSC is increased, the buoyancy force inside the TSC is increased. This increases the mass flow rate of the TSC gas so that the ability to reject heat from the fuel is also increased. This would tend to reduce the maximum clad temperature. However, the flow in the annulus is not expected to be significantly affected by the velocity of the gas internal to the TSC. Therefore, regardless of the buoyancy force inside the TSC, the maximum clad temperature is limited by the shell temperature, which is controlled by the annulus flow. At some pressure level, an increase in the TSC pressure (and mass) of the gas would not significantly decrease the fuel clad temperature, which would imply a reduced derivative of the clad temperature with respect to the pressure. This is the characteristic of the curve in Figure 4.4-6, which implies that further increase in the pressure does not result in a significant reduction of the clad temperature. There is an advantage in operating in this regime of the curve in that the sensitivity of the clad temperature due to a reduction in the helium density is reduced. This evaluation demonstrates that even with a 10% loss of density, the fuel and basket temperatures remain under 700°F.

Mesh Sensitivity Evaluation

With respect to the sensitivity of the calculated fuel cladding, concrete cask and TSC temperatures to the number of divisions of the finite volume cells, this need only be addressed for the regions containing fluid flow. For the solid regions, such as the concrete or the steel components, the sensitivity evaluation of cell refinement is not required.

There are two fluid regions in the model: the airflow annulus region outside the TSC, and the helium region inside the TSC. Each of these fluid regions uses a different fluid flow model. The TSC internal flow is modeled utilizing a laminar flow model; the airflow in the annulus region is modeled using a turbulent flow model.

In the concrete cask annulus region, the modeling accuracy of the turbulent flow depends not on the usual refined mesh near the wall, as for a laminar flow condition, but on the value of y^+ , as previously discussed. Over-refining the model to reduce the y^+ does not improve the accuracy of the model. The cell divisions in the annulus region have been set to permit the y^+ to be between 20 and 30, which is acceptable according to FLUENT documentation. Therefore, further refinement of the annulus region would not provide a more accurate temperature result.

For the helium flow in the TSC (laminar flow), the largest velocities are in the downcomer regions and, essentially, the entire heat load must be transferred to the TSC shell. The focus of

the sensitivity evaluation is the number of cell divisions in the downcomer region. The largest velocity gradients in the downcomer regions occur in the radial direction, not in the axial direction. To determine the sensitivity of the radial divisions in the downcomer region, the number of radial divisions modeled was increased by a factor of two. The axial divisions in the downcomer region remain the same. The mesh refinement in the air annulus and in the concrete cask remain unchanged. The condition used in the evaluation corresponded to the normal condition using a uniform heat loading of 40 kW. The results of this evaluation showed that the maximum fuel temperature changed by less than 1°F for the increased refinement mesh. The temperature of the TSC shell showed a decrease of 2°F for the mesh with the increased refinement. This indicates that the maximum fuel temperature is relatively insensitive to the mesh refinement in the downcomer region.

Heat Transfer by Radiation

Thermal radiation in all fluid (air and helium) regions has been considered in the model, specifically the following.

- Thermal radiation across the air annulus between the TSC shell and the concrete cask liner.
- Thermal radiation across the air gap above the TSC lid and in the isolated air region below the pedestal of the concrete cask.
- Thermal radiation across the helium downcomer region between the fuel basket and the TSC shell.

The discrete ordinates (DO) radiation model in FLUENT is used to solve the radiative heat transfer equation with emissivity values applied on the solid material surfaces.

Radiation in the porous media fuel region is modeled by using equivalent thermal conductivities that include the effects of heat transfer by radiation.

4.4.1.2 Two-Dimensional Fuel Basket Models

The purpose of the two-dimensional fuel basket model is to determine the effective thermal conductivity of the basket region in the axial and radial directions. The effective conductivities are used in the two-dimensional axisymmetric concrete cask and TSC models and the two-dimensional axisymmetric transfer cask and TSC models. Three types of media are considered in the TSC: helium, water and vacuum. The fuel assemblies and neutron absorbers in the fuel basket model are shown as homogeneous regions with effective thermal properties, which are determined by the two-dimensional fuel assembly models and the two-dimensional fuel tube models described in Sections 4.4.1.3 and 4.4.1.4, respectively. The analyses performed in

Section 4.4.1.3 identify that the PWR fuel assembly with the minimum conductivity is the 14×14. The properties of the PWR 14×14 fuel assembly are used in the evaluation of the effective properties for the PWR basket in this section. For the BWR assembly, the bounding fuel assembly type is the 10×10, which is used to determine the effective properties for the BWR basket.

Since the effective properties for the fuel basket correspond to the basket region, which is comprised of full-length fuel tubes, it is only necessary to consider a cross-section of the basket with a two-dimensional planar model. Due to symmetry of the basket designs, only a 1/8th section model is required for the PWR and the BWR fuel baskets. ANSYS is used to perform the conduction analysis using the models shown in Figure 4.4-7 for the PWR fuel basket and Figure 4.4-8 for the BWR fuel basket. The models include only radiation and conduction heat transfer. Radiation heat transfer is incorporated into the effective properties for the fuel assemblies and the neutron absorbers. Each fuel basket model takes into account the size of the cells in the basket - i.e., those cells formed directly by the fuel tube, and those cells formed by adjacent fuel tubes. The neutron poison is contained only in the inner surface of the basket tubes. The exterior tubes, which form the boundary of the downcomer region, may not have neutron absorbers on the inner surface of those fuel tubes. In the condition where the neutron absorbers are not present, aluminum plates may be substituted, but are not required. The PWR and BWR fuel basket models evaluated in this section use the conductivity of the neutron poison defined in Chapter 8. The absence of neutron absorber on the exterior fuel tubes has an insignificant effect on the radial transfer of heat. The removal of the neutron absorber actually increases the flow area in the tubes.

Additionally, it is conservatively assumed for both the PWR and BWR fuel baskets that a gap between the fuel tubes exists for the full length of the tube without any contact, as shown in Figure 4.4-7 and 4.4-8. The gap between the fuel tubes is modeled as being 0.01 inch, and the conduction through the gap is based on the presence of either helium or water, depending on the condition.

The effective thermal conductivity (K_{eff}) of the fuel basket region in the radial direction is determined by considering the basket region as a solid cylinder with heat generation.

Considering the temperature at the center of the TSC to be T_{max} , the effective thermal conductivity (K_{eff}) as shown:

$$K_{eff} = \frac{Q}{4\pi H(T_{max} - T_o)} = \frac{Q}{4\pi H\Delta T} \quad [15]$$

where:

Q	-----	total heat generated by the fuel (Btu/hr)
H	-----	length of the active fuel region (in)
T_o	-----	boundary temperature of the basket
ΔT	-----	$T_{max} - T_o$ (°F)

The value of ΔT is obtained from thermal analysis using the two-dimensional models shown in Figure 4.4-7 and Figure 4.4-8 with the boundary temperature constrained to be T_o . The effective conductivity (K_{eff}) is then determined by using the stated expression. The analysis is repeated by applying different boundary temperatures so that temperature-dependent conductivities can be determined.

4.4.1.3 Two-Dimensional Fuel Assembly Models

The two-dimensional fuel assembly models include the fuel pellets, cladding, and the media occupying the space between fuel rods. The media is considered to be helium for storage conditions, and water, vacuum or helium for transfer conditions. The two-dimensional finite element models of the fuel assemblies are used to determine the effective conductivities for the PWR and BWR fuel assemblies. The effective conductivities are used in the two-dimensional fuel basket models described in Section 4.4.1.2. For the PWR fuel assemblies, four separate types are considered: 14×14, 15×15, 16×16 and 17×17. For the BWR fuel assemblies, four separate types are considered: 7×7, 8×8, 9×9 and 10×10. For the BWR fuel assembly, a fuel channel is considered since it may be present and it will result in bounding fuel cladding temperatures. Therefore, it is only necessary to address a single fuel configuration for each of the fuel assembly types.

The two-dimensional fuel assembly models include the fuel pellets, cladding, media between fuel rods, media between the fuel rods and the inner surface of the fuel tube (PWR) or between the fuel rods and the inner surface of the fuel channel (BWR), and helium in the gap between the fuel pellets and cladding. The media are considered to be helium for storage, and water, vacuum or helium for transfer conditions. Modes of heat transfer modeled include conduction and radiation between individual fuel rods for the steady-state condition. ANSYS PLANE55 conduction elements and MATRIX50 radiation elements are used to model conduction and radiation. (Radiation is not considered for the water condition.) Radiation elements are defined between fuel rods and between the fuel rods and the fuel tube (PWR) or the fuel channel (BWR). A typical PWR fuel assembly finite element model is shown in Figure 4.4-9, which corresponds to the 14×14 fuel assembly. The BWR fuel assembly model only considers the region up to the

inner surface of the channel, and a typical BWR fuel assembly is shown in Figure 4.4-10, which corresponds to the 10x10 fuel assembly.

The effective conductivity for the fuel is determined by using an equation defined in a Sandia National Laboratory Report [15]. The equation is used to determine the maximum temperature of a square cross-section of an isotropic homogeneous fuel with a uniform volumetric heat generation. At the boundary of the square cross-section, the temperature is constrained to be uniform. The expression for the temperature at the center of the fuel is given by:

$$T_c = T_e + 0.29468 (Qa^2 / K_{eff})$$

where:

- T_c ----- the temperature at the center of the fuel (°F)
- T_e ----- the temperature applied to the exterior of the fuel (°F)
- Q ----- volumetric heat generation rate (Btu/hr-in³)
- a ----- half length of the square cross-section of the fuel (inch)
- K_{eff} ----- effective thermal conductivity for the isotropic homogeneous fuel (Btu/hr-in-°F)

Volumetric heat generation (Btu/hr-in³) based on the design heat load is applied to the pellets. The effective conductivity is determined based on the heat generated and the temperature difference from the center of the model to the edge of the model. Temperature-dependent effective properties are established by performing multiple analyses using different boundary temperatures. The effective conductivity in the axial direction and the effective density of the fuel assembly is calculated on the basis of the material area ratio. The effective specific heat is computed on the basis of a weighted mass average.

For the PWR fuel assemblies, the 14x14 fuel assembly is shown to have the effective properties that correspond to the minimum values, as shown in Table 4.4-1 for both fuel tube configurations.

For the BWR fuel assemblies, the 10x10 fuel assembly is shown to have the effective properties that correspond to the minimum values, as shown in Table 4.4-2.

4.4.1.4 Two-Dimensional Neutron Absorber Models

The two-dimensional neutron absorber model is used to calculate the effective conductivities of the neutron absorber, the neutron absorber retainer, and the fuel channel (for BWR only). These effective conductivities are used in the two-dimensional fuel basket models (Section 4.4.1.2). A

total of three neutron absorber models is required: one PWR model (for the PWR 14×14) and two BWR models—one with the neutron absorber plate and channel and one with the channel but without the neutron absorber plate, corresponding to the enveloping configurations of the 10×10 BWR fuel assembly.

The configurations shown in the neutron absorber models in Figure 4.4-11 and Figure 4.4-12 for PWR and BWR fuel, respectively, incorporate the neutron absorber (and the channel for the BWR). The configuration shown in Figure 4.4-13 is for the BWR fuel tube with the channel, but without the neutron absorber.

As shown in Figure 4.4-11, the PWR fuel tube model includes the neutron absorber, the stainless steel retainer, and the gaps between the neutron absorber and the stainless steel retainer and the surface of the fuel tube. Three conditions of media are considered in the gaps: helium vacuum and water.

ANSYS PLANE55 conduction elements and LINK31 radiation elements are used to construct the model. The model consists of four layers of conduction elements and two sets of radiation elements (radiation elements are not used for the water condition) that are defined at the gaps (two for each gap). The thickness of the model (x-direction) is the distance measured from the outside surface of the stainless steel retainer to the inside surface of the fuel tube (assuming the neutron absorber is centered between the retainer and the fuel tube, and there is no contact for the length of the basket). The gap size between the neutron absorber and the adjacent surfaces is 0.002 inch.

The BWR fuel assemblies may include a fuel channel, as compared to the PWR assemblies, which have no fuel channel. Therefore, two effective conductivity models are necessary for the BWR: one model with the neutron absorber plate (a total of six layers of materials) and a fuel channel; and the other model with a fuel channel, but with a gap replacing the neutron absorber plate (a total of two layers of materials).

As shown in Figure 4.4-12, the first BWR neutron absorber model includes the fuel channel, the retainer, the neutron absorber and associated gaps. As shown in Figure 4.4-13, the second BWR neutron absorber model includes the fuel channel and the gap between the fuel channel and the fuel tube surface.

Heat flux is applied at the left side of the model (retainer for PWR model and fuel channel for BWR model), and the temperature at the right boundary of the model is specified. The heat flux is determined based on the design heat load. The maximum temperature of the model (at the left boundary) and the temperature difference (ΔT) across the model are calculated by the ANSYS model. The effective conductivity (K_{xx}) is determined using the following formula.

$$q = K_{xx} (A/L) \Delta T$$

or

$$K_{xx} = q L / (A \Delta T)$$

where:

K_{xx}	-----	effective conductivity (Btu/hr-in-°F) in X direction in Figure 4.4-11 through Figure 4.4-13
q	-----	heat rate (Btu/hr)
A	-----	area (in ²)
L	-----	length (thickness) of model (in)
ΔT	-----	temperature difference across the model (°F)

The temperature-dependent conductivity is determined by varying the temperature constraints at one boundary of the model and solving for the temperature difference. The effective conductivity for the parallel path (the Y direction in Figure 4.4-11) is calculated by the following.

$$K_{yy} = \frac{\sum K_i t_i}{L}$$

where:

K_i	-----	thermal conductivity of each layer (Btu/hr-in-°F)
t_i	-----	thickness of each layer (in)
L	-----	total length (thickness) of the model (in)

4.4.1.5 Two-Dimensional Transfer Cask and TSC Model

During the transfer condition, the TSC in the transfer cask is subjected to four separate conditions.

- The water phase when the lid is being welded to the TSC.
- The drying phase in which pressurized helium drying or vacuum drying can be used to remove moisture from the TSC.
- The helium backfilled phase when the TSC closure is completed and the transfer cask annulus flow system is operating.
- The operation of loading the helium-backfilled TSC into the concrete cask without the transfer cask annulus flow system operating.

Except for the final operation of placing the TSC into the concrete cask, the first three steps are considered to be steady-state conditions, if pressurized helium drying is used to remove the

moisture. Since vacuum drying is an optional method to lower heat load fuel, the time in vacuum drying is administratively controlled to maintain the maximum fuel cladding temperatures less than the allowable temperature. For all operations, except for the final step to load the TSC into the concrete cask, the transfer cask annulus cooling system continuously supplies water at a specified temperature, with a minimum flow rate to the annulus between the TSC and the transfer cask. The annulus cooling system is designed to remove the design basis heat load from the TSC without any dependence on the transfer of heat to the ambient environment from the transfer cask.

The two-dimensional axisymmetric transfer cask and TSC model is used to evaluate the transfer operation for PWR fuel with the design basis heat load of 40 kW. Since the PWR fuel heat load and calculated temperatures in the steady-state condition bound those for the BWR fuel, the bounding configuration is considered to be the TSC containing a design basis PWR fuel heat load. The components comprising the transfer cask and TSC model are shown in Figure 4.4-14. The TSC portion of the model is identical to the model employed in Section 4.4.1.1, with the exception that one of the conditions in the transfer operations uses water in the TSC instead of helium. The transfer cask and the water annulus between the transfer cask and the TSC are also included in the model. The transfer cask inner shell is represented by effective properties. The model also contains the shield doors of the transfer cask. While the inlets to the transfer cask are tubes in the side walls of the transfer cask, they are included in the model as straight sections parallel to the annulus.

Evaluation of the Water Phase

The model that includes water in the TSC treats the entire cavity as though it is filled with water, whereas, it is necessary to remove water from the TSC during the closure lid welding operation. Since the water level in the TSC may be below the top of the fuel basket, the fuel tubes are designed with holes in the sides to permit the water to flow from the center of the TSC to the downcomer region of the TSC. The model for the TSC, described in Section 4.4.1.1, uses effective properties for the fuel basket region. For the water condition, the methodology described in Sections 4.4.1.2, 4.4.1.3, and 4.4.1.4 is used to determine the effective properties for the fuel basket region. For the condition of water in the TSC, no contribution due to radiation was considered; only conduction was taken into account for the effective properties. The porous media constants for the fuel basket region need not be recomputed since they are dependent on the fuel assembly and fuel basket geometry only. However, during the analytical evaluation of the water phase, the pressure drop in the fuel basket region due to the water requires the use of the viscosity, which is input as a material property. Since the maximum water temperature in the

TSC is significantly below 212°F, the water is expected to remain in the liquid state, and the use of properties for the liquid state is acceptable. The following conditions are applied to the model for the steady-state evaluation of the water condition.

- The outer surfaces of the transfer cask are considered to be adiabatic and without the application of solar insolation.
- The inlet water temperature for the annulus between the TSC and the transfer cask is specified to be 125°F.
- The driving force for the water flow in the annulus between the TSC and the transfer cask is natural convection.
- The heat generation internal to the TSC is 40 kW using the preferential loading pattern shown in Figure 4.1-1 and as described in Section 4.4.1.1.
- The flow in the TSC and in the annulus region is treated as being laminar for both the water and helium conditions of the TSC.
- Radiation heat transfer is removed from the solution.

Evaluation of the Drying Phase

During the drying phase, pressurized helium is forced to circulate between the pressurized helium drying (PHD) system and the TSC, entering through the drain tube to the bottom of the TSC and exiting from the vent port. The circulation of the helium in the TSC during this time will result in helium flowing up through the fuel assemblies. The pressure employed in the system for the drying and recirculation of the helium will result in the helium mass flowing up through the fuel region in the same manner as it does during the normal conditions of storage. For this reason, the properties developed for the storage condition are applied for the condition of the drying phase using pressurized helium. Since the water in the annulus will maintain the TSC shell temperatures to be less than 180°F, the temperatures for the fuel region will be significantly less than those determined for normal conditions of storage. The following conditions are applied to the model for the steady-state evaluation of the drying condition.

- The outer surfaces of the transfer cask are considered to be adiabatic and without the application of solar insolation.
- The inlet water temperature for the annulus between the TSC and the transfer cask is specified to be 125°F.
- The driving force for the water flow in the annulus between the TSC and the transfer cask is natural convection.
- The heat generation internal to the TSC is 40 kW using the preferential loading pattern shown in Figure 4.1-1 and as described in Section 4.4.1.1.
- The flow in the TSC and in the annulus region is treated as being laminar for both the water and helium conditions of the TSC.

- Radiation heat transfer is included in the solution.

For the alternative method of drying the TSC cavity using vacuum drying, the transfer cask model using the effective properties corresponding to the vacuum condition is applied. This determines the allowable time in vacuum, depending on the heat load, to ensure that the fuel cladding temperature limit of 752°F (400°C) is not exceeded.

Evaluation of the Helium Phase

Upon completing the drying operation, the TSC is backfilled and pressurized with helium for the normal condition of storage. The transfer cask and TSC remain in this helium phase condition until the TSC is placed into the concrete cask. During the helium phase, the transfer cask annulus cooling system will be in continuous operation. Since the water in the annulus will maintain the TSC shell temperatures to be less than 180°F, the temperatures for the fuel region will be significantly less than those determined for normal conditions of storage. The evaluation of this condition is required to determine the initial conditions for the operation in which the TSC is placed into the concrete cask with the transfer cask annulus flow system not in operation. Since the conditions are identical to those for the drying phase, an additional evaluation is not required. The results obtained for the evaluation of the drying phase are applicable for the helium phase.

Evaluation of Moving the TSC into the Concrete Cask

The transfer cask is used to load the TSC into the concrete cask. During this phase, the transfer cask annulus cooling system is disconnected from the transfer cask, and the annulus is drained. This results in the annulus being filled with air instead of water; therefore, this operation is time-limited, since the annulus between the TSC and the transfer cask is not designed for natural convection cooling. The thermal performance of the transfer cask in this condition is similar to the concrete cask accident event in which all of the air inlets are blocked. The TSC for this operational condition is identical, with one exception, to the condition of the TSC in the concrete cask for the condition of all air inlets blocked. The exception is that the initial fuel and TSC component temperatures for this operational condition are significantly lower than the design basis temperatures for the normal conditions of storage. While the concrete cask has significantly more mass than the transfer cask to absorb heat, the conductivity of the concrete is only approximately 4% of the conductivity of lead or carbon steel. Thus, the transfer cask has the ability to effectively absorb more heat than the concrete cask for a limited period of time. The transient solution for the concrete cask for the all air inlets blocked condition provides bounding fuel temperatures for this TSC transfer condition. The transient solution performed for the all inlets blocked condition can be used to identify a "temperature rate change," which

establishes the time limit for moving the TSC into the concrete cask once the transfer cask annulus water cooling system has been shut off. During this TSC transfer condition, the duration of time to complete the movement and lid installation on the concrete cask will be limited to assure that the fuel temperatures remain less than 752°F (400°C).

4.4.2 Test Model

MAGNASTOR is conservatively designed by analysis. Therefore, no physical model is employed for thermal analysis. The benchmark provided in Appendix 4.A provides confirmation that the analysis methodology employed for the MAGNASTOR design is conservative.

4.4.3 Maximum Temperatures for PWR and BWR Fuel Configurations

Normal Conditions of Storage

The temperature distribution and maximum component temperatures for MAGNASTOR for normal conditions of storage are provided in this section. System components containing PWR and BWR fuels are addressed separately. The temperature distributions for the BWR design basis fuel are similar to those of the PWR design basis fuel and are, therefore, not presented.

The temperature distribution for the concrete cask and the TSC containing the PWR design basis fuel for normal conditions of storage, with a uniform heat load, is shown in Figure 4.4-15. The air velocity distribution in the annulus between the TSC and the concrete cask liner for the normal conditions of storage for PWR fuel is shown in Figure 4.4-16. The maximum component temperatures for the normal conditions of storage for the PWR and BWR design basis fuel are shown in Table 4.4-3.

As shown in Figure 4.4-15, the peak fuel temperature for the normal storage condition occurs near the top of the fuel basket and, based on the uniform spacing of the isotherms at the centerline of the TSC, the temperature varies monotonically from the TSC bottom to the peak near the top of the fuel basket. This is indicative that the dominant mode of heat rejection from the fuel is by convection due to the helium flow circulating within the TSC.

The calculated temperatures at the TSC surface for the normal storage condition are higher than the concrete liner or surface, indicating that radiation heat transfer occurs across the concrete TSC cask annulus. As shown in Table 4.4-3, the local temperature in the concrete is directly affected by the radiation heat transfer across the concrete cask annulus and can reach 266°F for PWR design basis fuel, which is less than the 300°F allowable temperature.

Transfer Condition

The maximum component temperatures for MAGNASTOR during the transfer operation are reported in this section. Since the PWR fuel configuration is considered to be bounding, it is conservative to identify these temperature results for the PWR fuel design basis heat load as the maximum temperatures for the BWR fuel design basis heat load. The transfer operation is comprised of four separate phases: the water phase, the drying phase, the helium phase, and the TSC loading phase. The only phases considered to be limited by time are vacuum drying of the TSC and the final phase of loading the TSC into the concrete cask. The reason that indefinite time limits are permitted for the water phase, the helium drying phase, and the helium phase is the use of the transfer cask annulus cooling water system. The annulus cooling water system maintains the canister shell at a temperature significantly lower than the temperature corresponding to the normal conditions of storage. The maximum temperature for the PWR fuel cladding is reported for each of the separate transfer phases in Table 4.4-4. It is observed that the PWR fuel cladding temperatures shown in Table 4.4-4 are bounded by the PWR fuel cladding temperatures for the normal storage steady-state conditions in Table 4.4-3. This indicates that the normal condition PWR fuel cladding and component temperatures, such as for the fuel basket and the TSC, bound the maximum temperatures for any phase of the transfer condition for the fuel basket and TSC components. The times for the vacuum drying are administratively controlled to maintain the fuel cladding temperature below the 752°F limit. The TSC loading phase is administratively limited to 48 hours to ensure that the maximum fuel cladding temperature is bounded by the normal condition storage temperature. The 48 hours is determined using the fuel cladding temperature rise for the "all air inlets blocked" accident event and the peak fuel cladding temperature limit of 752°F.

During the vacuum drying operations, the vacuum drying times will be administratively controlled to ensure that the fuel temperatures are below the temperature limit of 752°F.

4.4.4 Maximum Internal Pressures for PWR and BWR TSCs

The maximum TSC internal operating pressures for normal conditions of storage are calculated in the following sections for the TSCs containing PWR and BWR design basis fuel assemblies.

Maximum Internal Pressure for the TSC Containing PWR Fuel

The internal pressure of a TSC containing PWR fuel assemblies is a function of fuel type, burnup, initial enrichment, cool time, fuel condition (failure fraction), presence or absence of nonfuel hardware, TSC length, and the backfill gases in the TSC. Gases included in the pressure evaluation of a TSC containing PWR fuel include fuel rod fission, decay and backfill gases, gas generated by the nonfuel hardware components (assembly control components contain boron as the absorber material), and TSC backfill gases. Each of the PWR fuel types is separately evaluated to determine a bounding pressure for a TSC containing PWR fuel assemblies.

Fission gases include all fuel material generated gases including helium generated by long-term actinide decay. Based on detailed SAS2H calculations, the quantity of fission and decay gases rises as burnup and cool time are increased and enrichment is decreased. The maximum gas available for release is conservatively calculated based on 70,000 MWd/MTU burnup cases at an enrichment of 1.9 wt% ^{235}U and a cool time of 40 years for maximum fissile material assemblies in each major PWR fuel class. For other PWR fuel assembly types, fission and decay gases are determined by ratioing the fissile material mass to the maximum fissile material mass assemblies.

Fuel rod backfill pressure varies significantly among the PWR fuel types. Based on a literature review, a 500 psig backfill is assigned to Westinghouse and CE core fuel types. A maximum backfill pressure of 435 psig is assigned to B&W core assemblies. Backfill gas quantities are based on the fresh fuel free volume between the fuel pellet stack and the fuel rod cladding, including the plenum volume, and a backfill temperature of 68°F.

Burnable poison rod assemblies (BPRAs) placed within the TSC may contribute additional gas quantities due to n-alpha reaction of ^{10}B during in-core operation. A portion of the neutron poison population is formed by ^{10}B . Other neutron poisons, such as gadolinium and erbium, do not produce a significant amount of helium nuclides (alpha particles). The principal BPRAs in use include the Westinghouse Pyrex (borosilicate glass) and WABA (wet annular burnable absorber) configurations, as well as B&W BPRAs and shim rods used in CE cores. The CE shim rods replace standard fuel rods to form a complete assembly array. The quantity of helium available for release from the BPRAs is directly related to the initial boron content of the fuel rods and the release fraction of gas from the matrix material. The gas released from either of the

low-temperature, solid matrix BPRA materials is likely to be limited, but no release fractions were available in open literature. Consequently, a 100% release fraction is applied. Initial boron content in the Westinghouse and B&W BPRAs is based on a uniform absorber concentration of 0.0063 g/cm ¹⁰B. The maximum number of poison rods is 16 for Westinghouse 14×14 fuel assemblies, 20 for Westinghouse and B&W 15×15 fuel assemblies, and 24 for Westinghouse and B&W 17×17 fuel assemblies. The length of the absorber rods is conservatively taken as the active fuel length. CE core shim rods are modeled at 0.0126 g/cm ¹⁰B for 16, 12, and 12 rods applied to CE-manufactured 14×14, 15×15, and 16×16 fuel assemblies, respectively.

Under normal operating conditions, the helium backfill for a TSC containing PWR fuel assemblies is at a maximum average gas temperature of 477°F and a maximum pressure of 103 psig. Free volumes inside the two classes of TSCs containing PWR fuel are 10,000 and 10,400 liters. The free volumes do not include PWR fuel assembly and nonfuel hardware components, since these vary for each assembly type. The free volume of the TSC is obtained by subtracting the assembly volume (with BPRA, TP or CEA insert). For the Westinghouse BPRAs, the Pyrex volume is employed since it displaces more volume than the WABA rods.

The TSC internal pressure is determined by summing the partial pressures of the TSC helium backfill gas and the released gases from the fuel and the poison rods. The partial pressure due to the fuel and neutron poison rod gases is determined by the ideal gas correlation ($PV=nRT$) and the applicable rod release fractions and failure rates. For normal conditions, a 1% rod failure fraction is applied. For failed fuel rods, the releasable molar quantity of the fission and actinide decay gas is 30%, with 100% of the rod backfill gas being released. The normal condition average temperature of the gases released from the fuel rods and neutron poison inserts is conservatively set to 485°F (525 K) in the partial pressure calculation.

The TSC is evaluated for normal condition pressure for each of the PWR fuel types, with insert. The maximum normal condition pressure for a TSC containing PWR fuel assemblies is 104 psig. At a 1% rod failure fraction, the quantity of gas released from the fuel and neutron poison rods is minimal, resulting in no significant effect on system pressure.

Maximum Internal Pressure for the TSC Containing BWR Fuel

Maximum internal pressures are determined for the BWR fuel in the same manner as those documented for the TSC containing PWR fuel. Primary differences for the BWR evaluations, versus those for the PWR, include a rod backfill gas pressure of 132 psig, a maximum burnup of 60,000 MWd/MTU used to generate fission gases, and the absence of neutron poison gases (no nonfuel hardware in the BWR system). The 132 psig rod backfill pressure used in this analysis is significantly higher than the 6 atmosphere (g) maximum pressure reported in open literature.

Free volumes, without fuel assemblies, in the TSC containing BWR fuel types are 9,900 and 10,300 liters.

A bounding normal condition average temperature of 525 K is used for the partial pressure analysis of the fuel rod gases. The maximum normal condition pressure for a TSC containing BWR fuel is 104 psig.

Figure 4.4-1 Two-Dimensional Model of Concrete Cask Loaded with PWR TSC

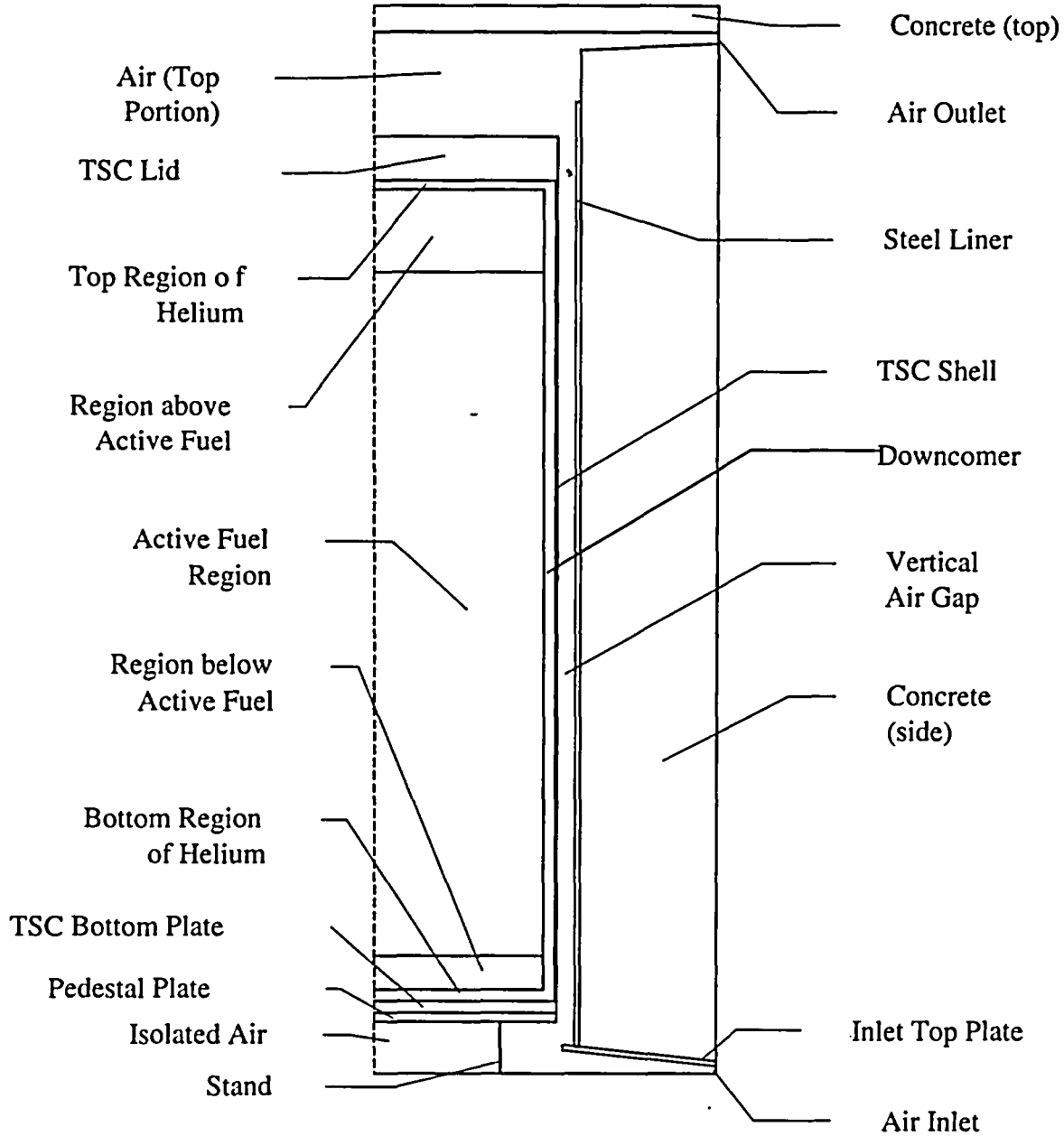


Figure 4.4-2 Computational Mesh for the Two-Dimensional Axisymmetric CFD Model of the Concrete Cask

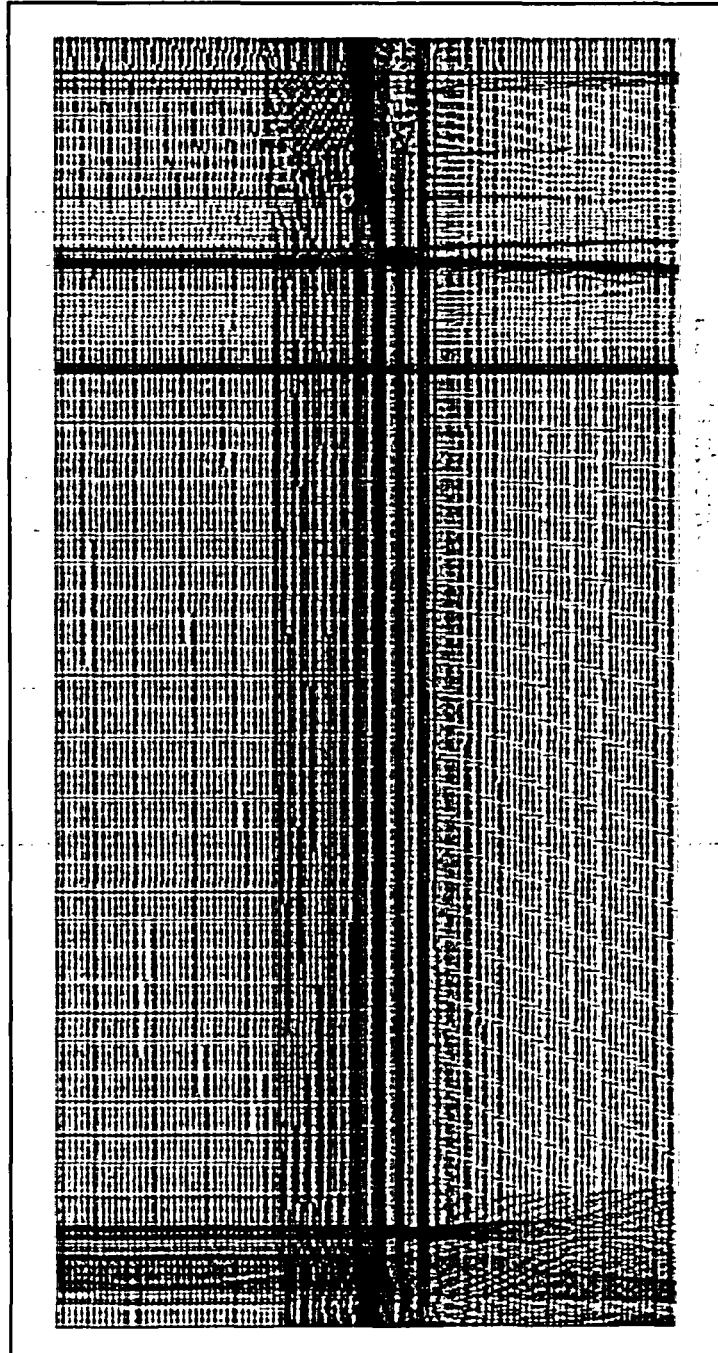


Figure 4.4-3 Reynold's Number at the Radial Mid-Point of the Concrete Cask Annulus

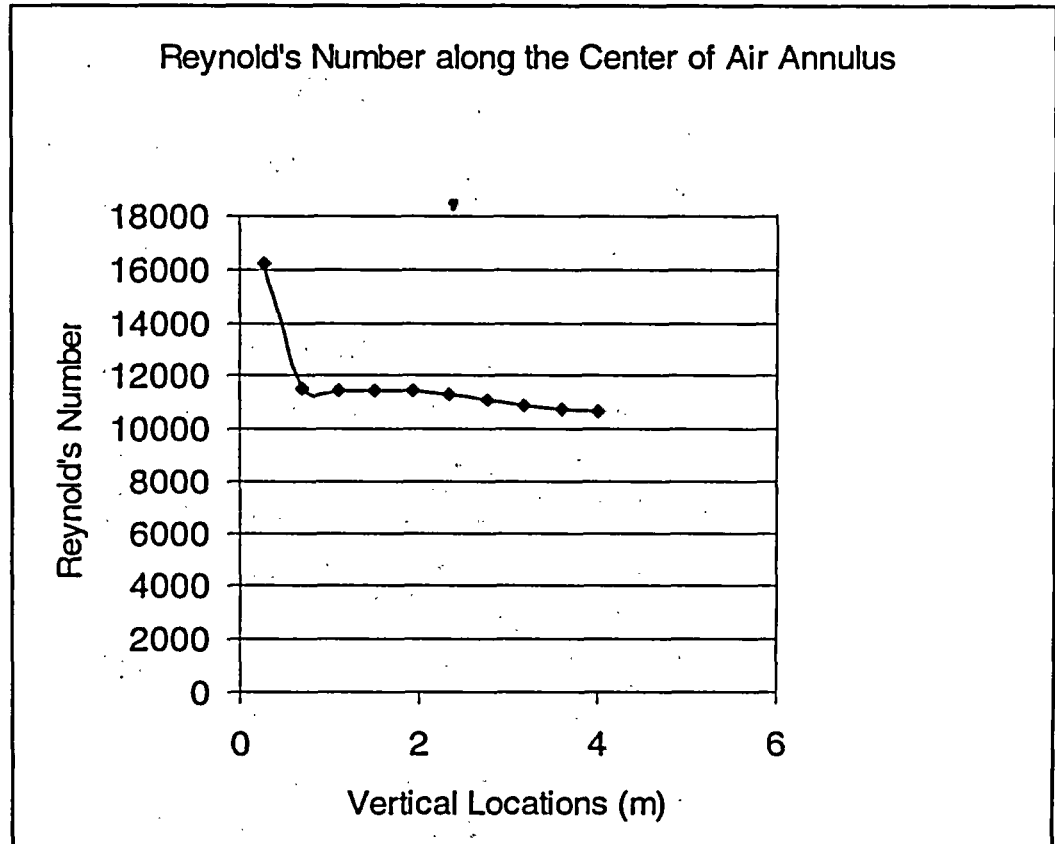


Figure 4.4-4 Axial Power Distribution for the PWR Fuel Assembly

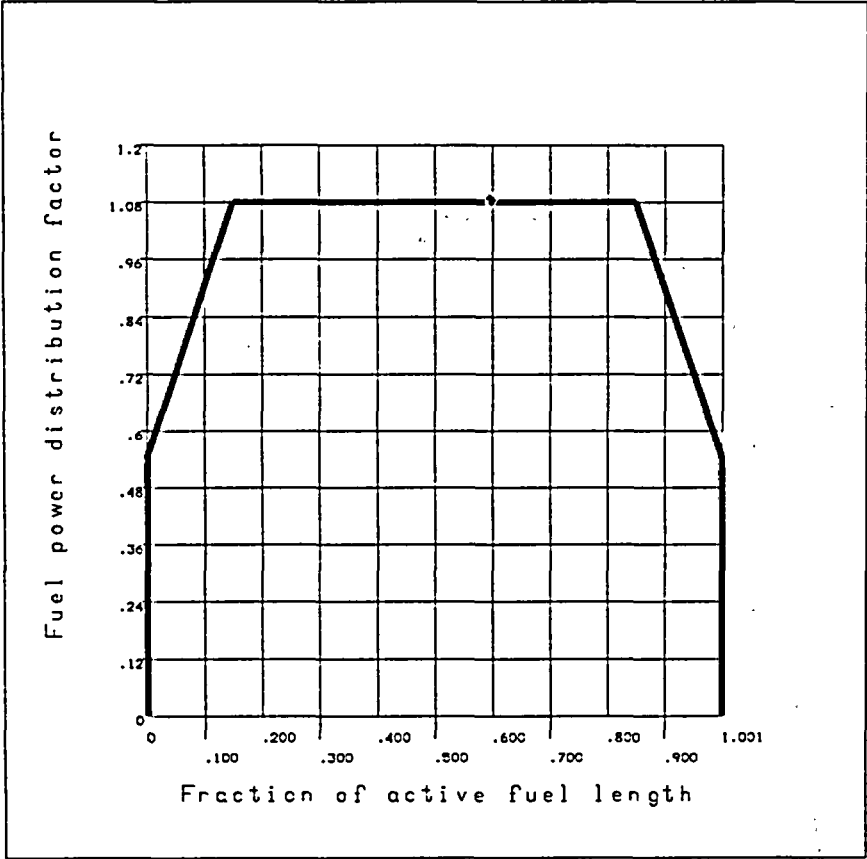


Figure 4.4-5 Axial Power Distribution for the BWR Fuel Assembly

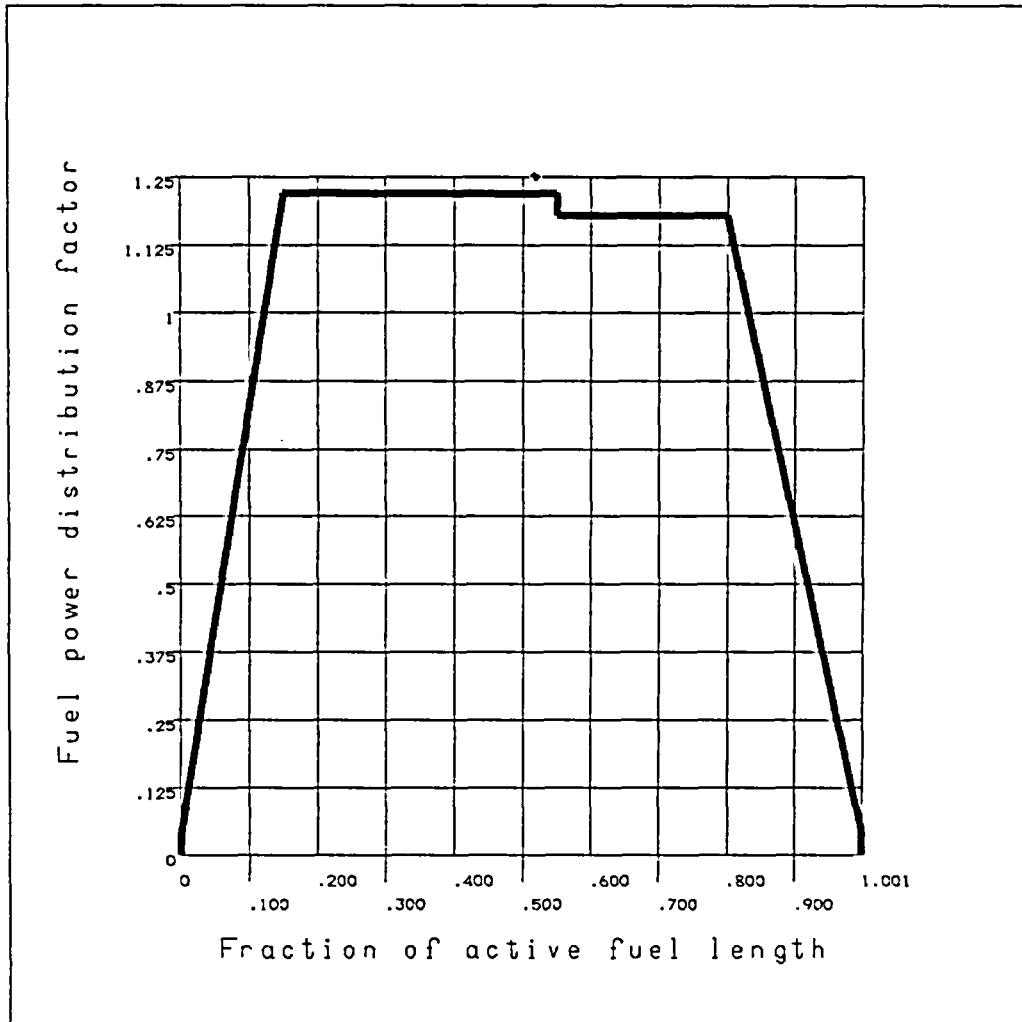


Figure 4.4-6 PWR Peak Fuel Cladding Temperature versus TSC Internal Pressure

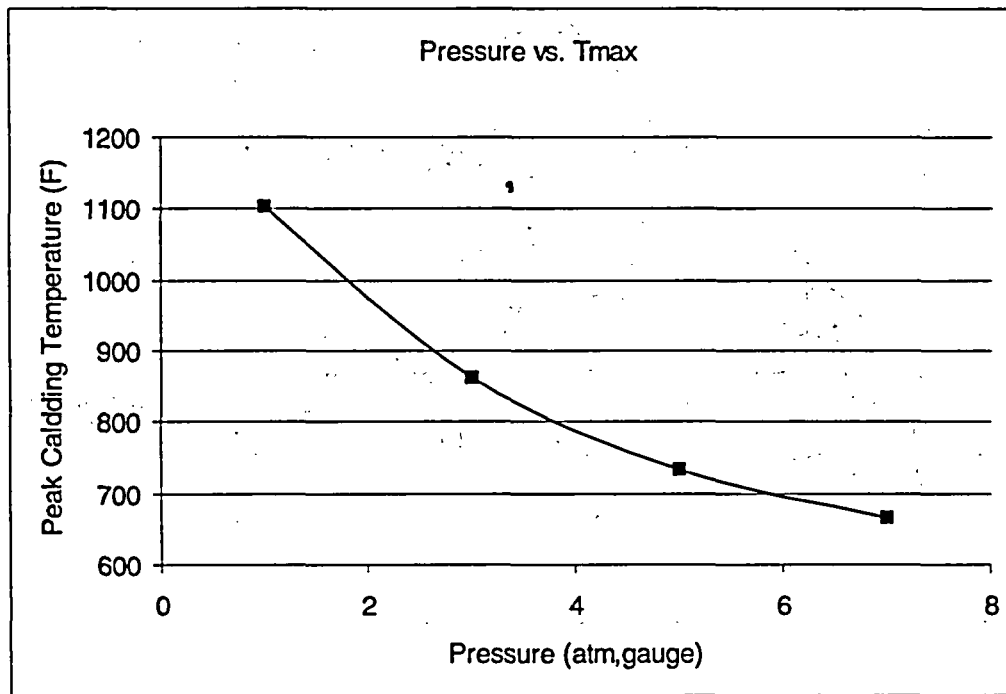


Figure 4.4-7 Two-Dimensional Finite Element Model of the PWR Fuel Basket

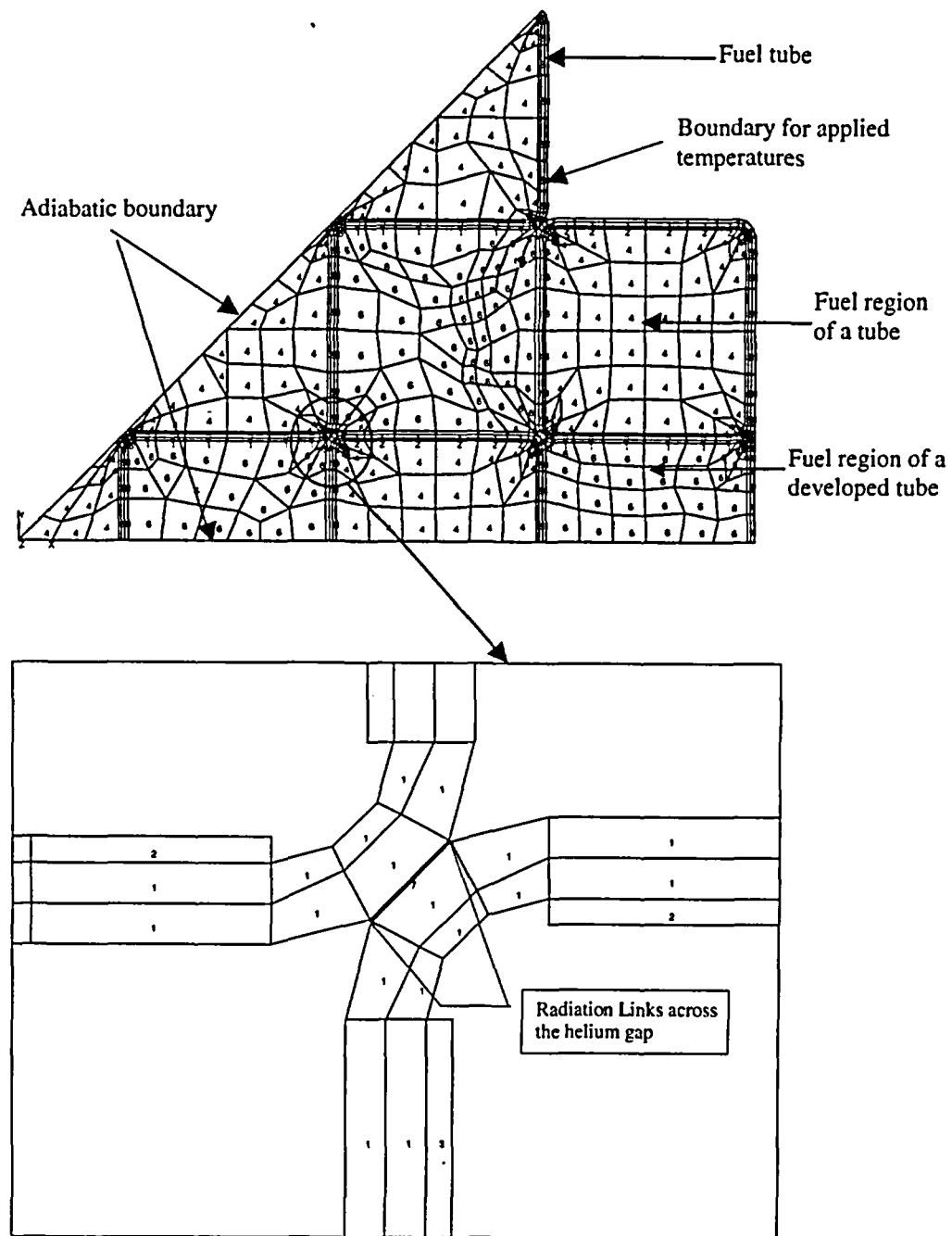


Figure 4.4-8 Two-Dimensional Finite Element Model of the BWR Fuel Basket

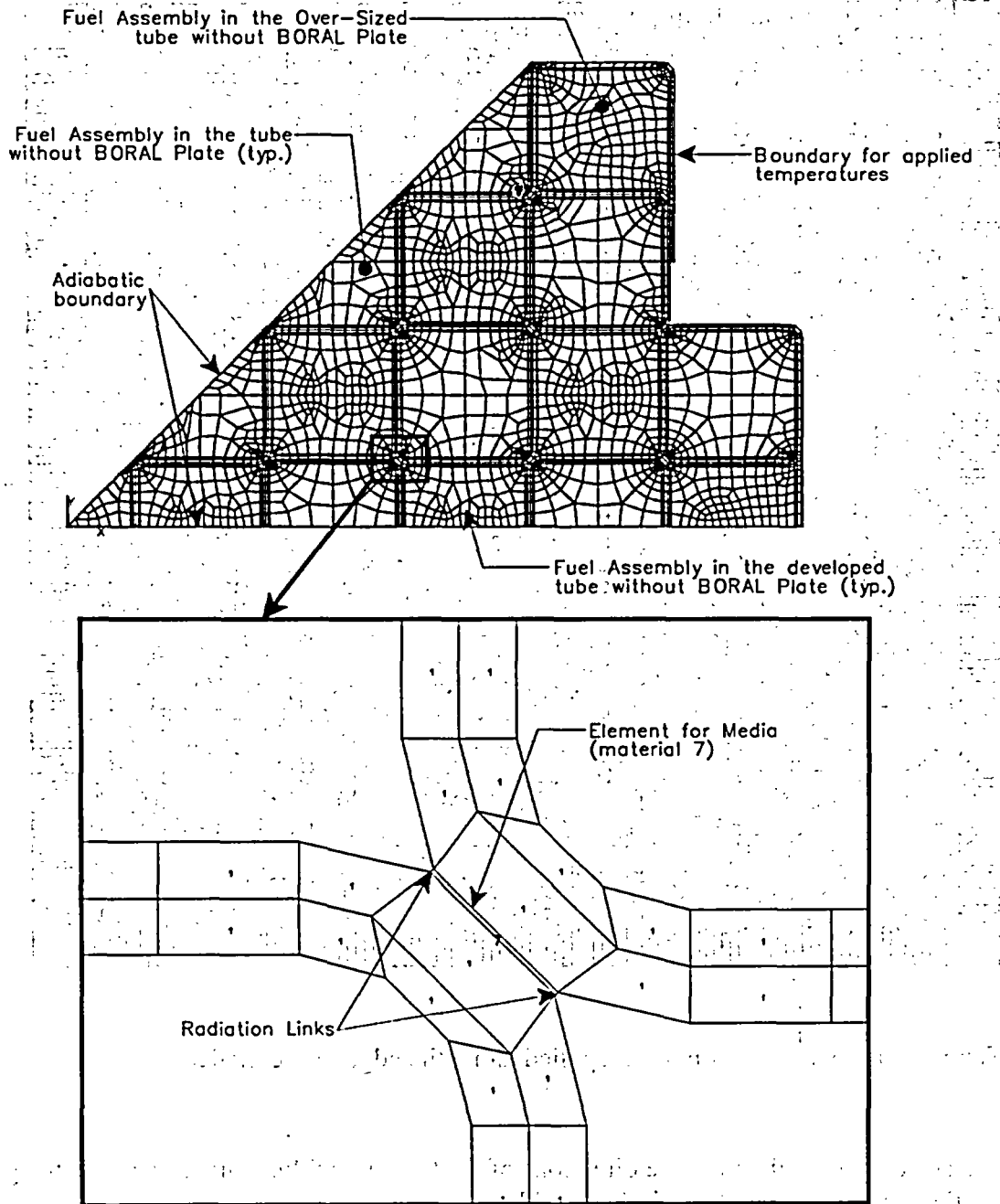
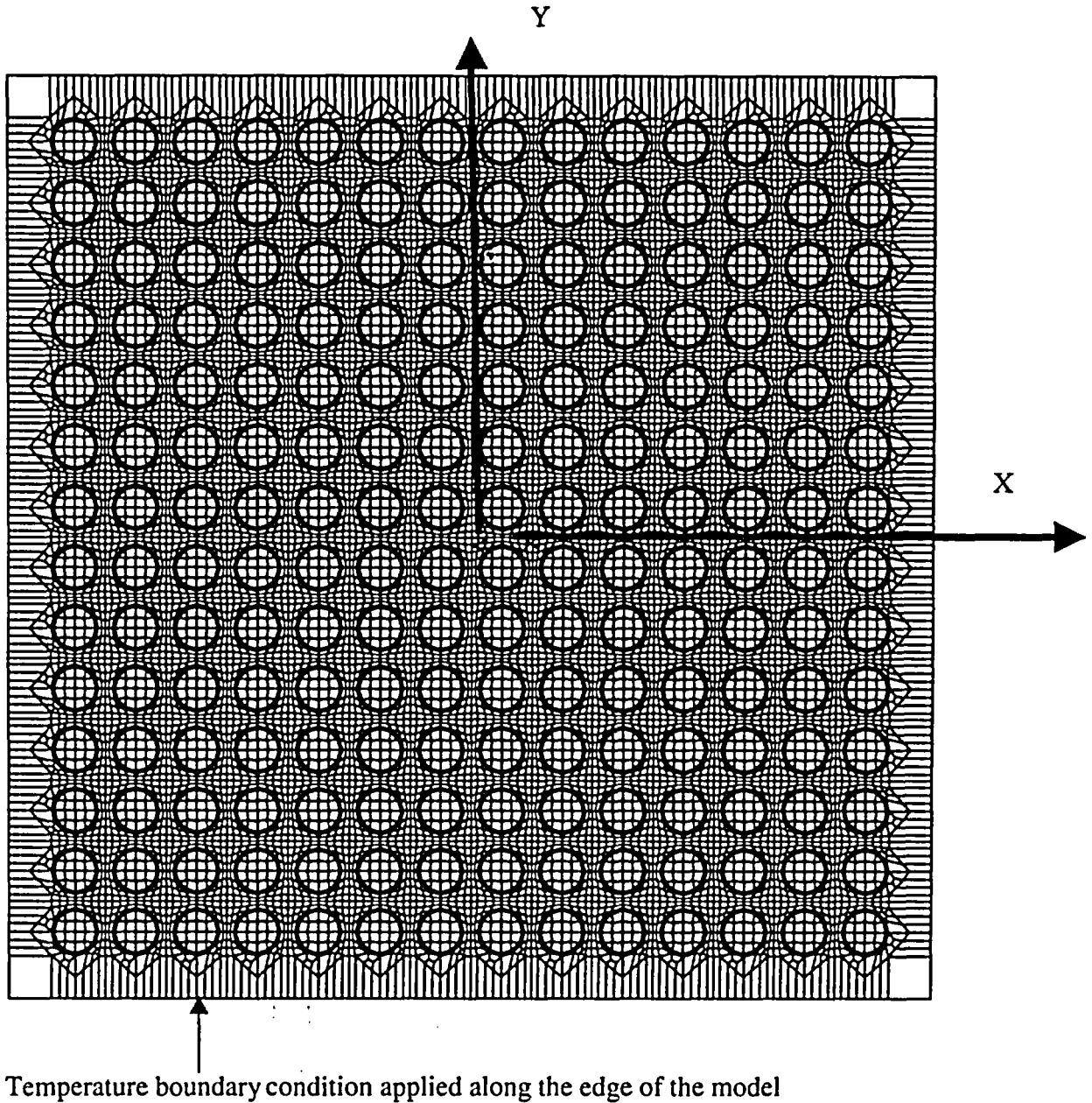


Figure 4.4-9 14 x14 PWR Fuel Assembly Two-Dimensional Model



Note: X and Y correspond to the in-plane directions of the fuel assembly, while Z is out of the plane and corresponds to the axial direction of the fuel assembly.

Figure 4.4-10 10 x 10 BWR Fuel Assembly Two-Dimensional Model

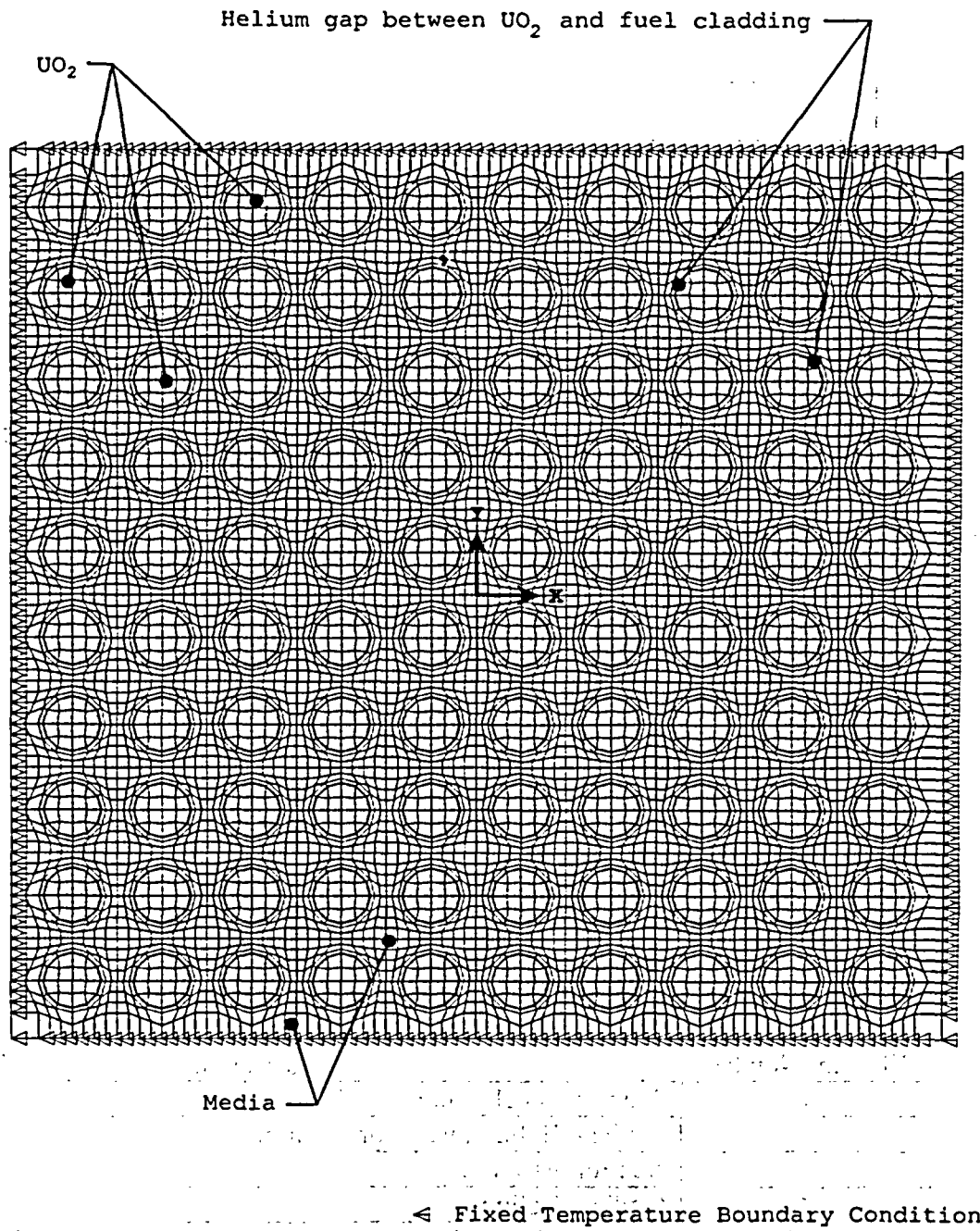
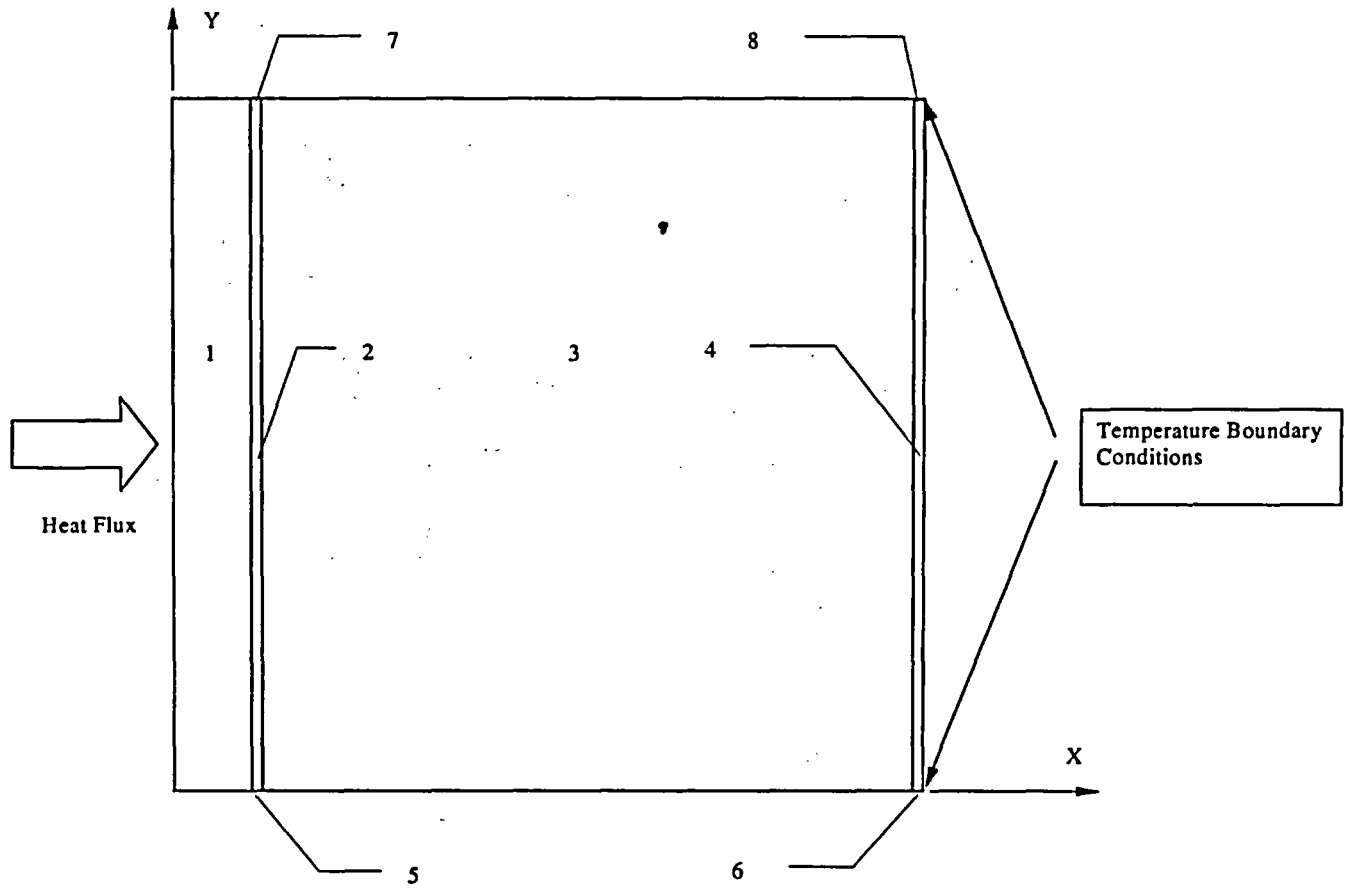
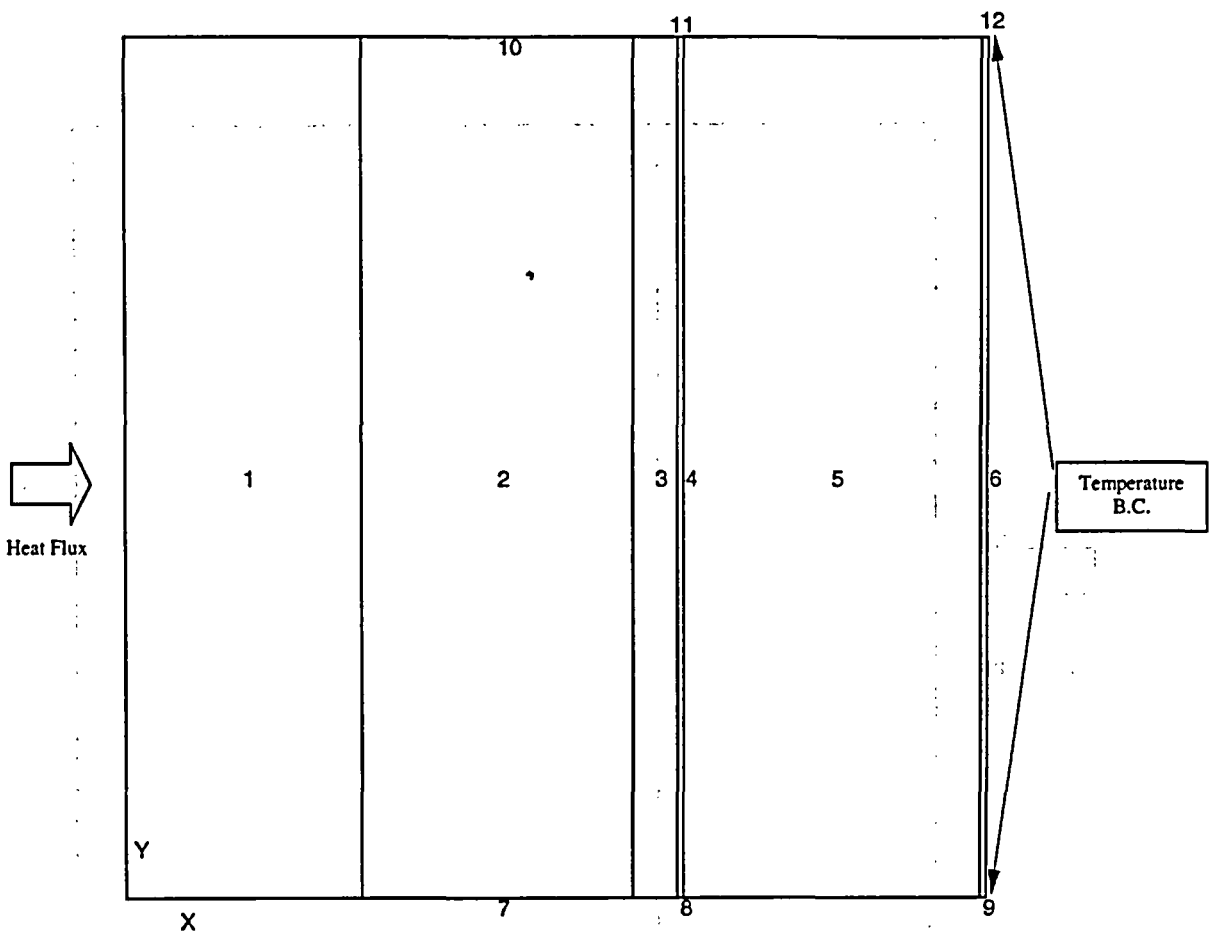


Figure 4.4-11 Neutron Absorber Model for PWR Fuel Tube



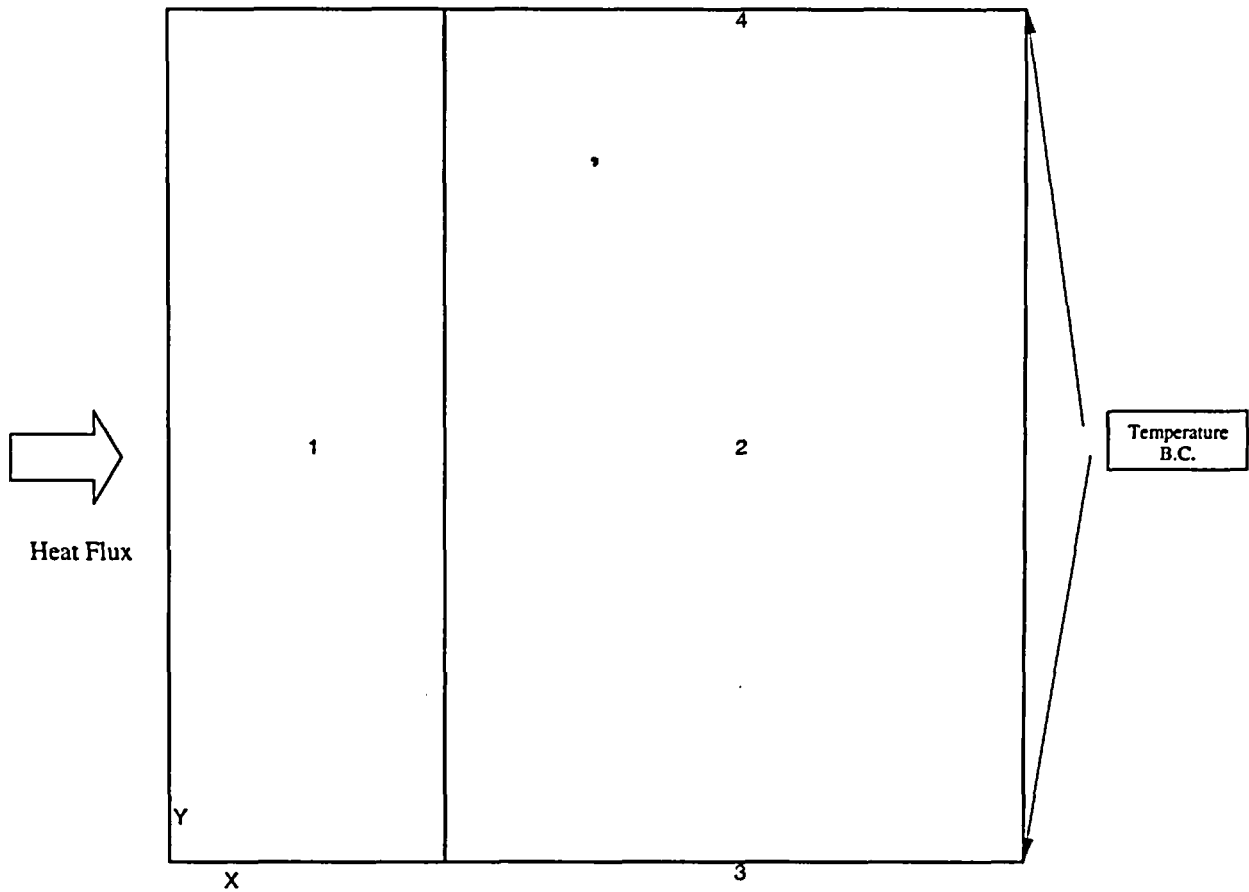
Element Number	Description
1	Stainless Steel Retainer Strip
2	Media – Helium, water or vacuum
3	Neutron Absorber
4	Media – Helium
5,7	Radiation Links (between stainless steel and neutron absorber)
6,8	Radiation Links (between aluminum and nickel plated carbon steel)

Figure 4.4-12 BWR Fuel Tube Configuration with Channel and Neutron Absorber



Element Number	Description
1	Zirconium-based alloy (BWR fuel channel)
2, 4, 6	Media – Helium, water or vacuum
3	Stainless Steel Retainer Strip
5	Neutron Absorber
7, 10	Radiation Links (between zirconium-based alloy and stainless steel)
8, 11	Radiation Links (between stainless steel and aluminum)
9, 12	Radiation Links (between aluminum and nickel-plated carbon steel)

Figure 4.4-13 BWR Fuel Tube Configuration with Channel, but without the Neutron Absorber



Element Number	Description
1	Zirconium-based alloy (BWR fuel channel)
2	Media ---- Helium, water or vacuum
3, 4	Radiation Links (between zirconium-based alloy and nickel-plated carbon steel)

Figure 4.4-14 Two-Dimensional Model of Transfer Cask Loaded with a PWR TSC

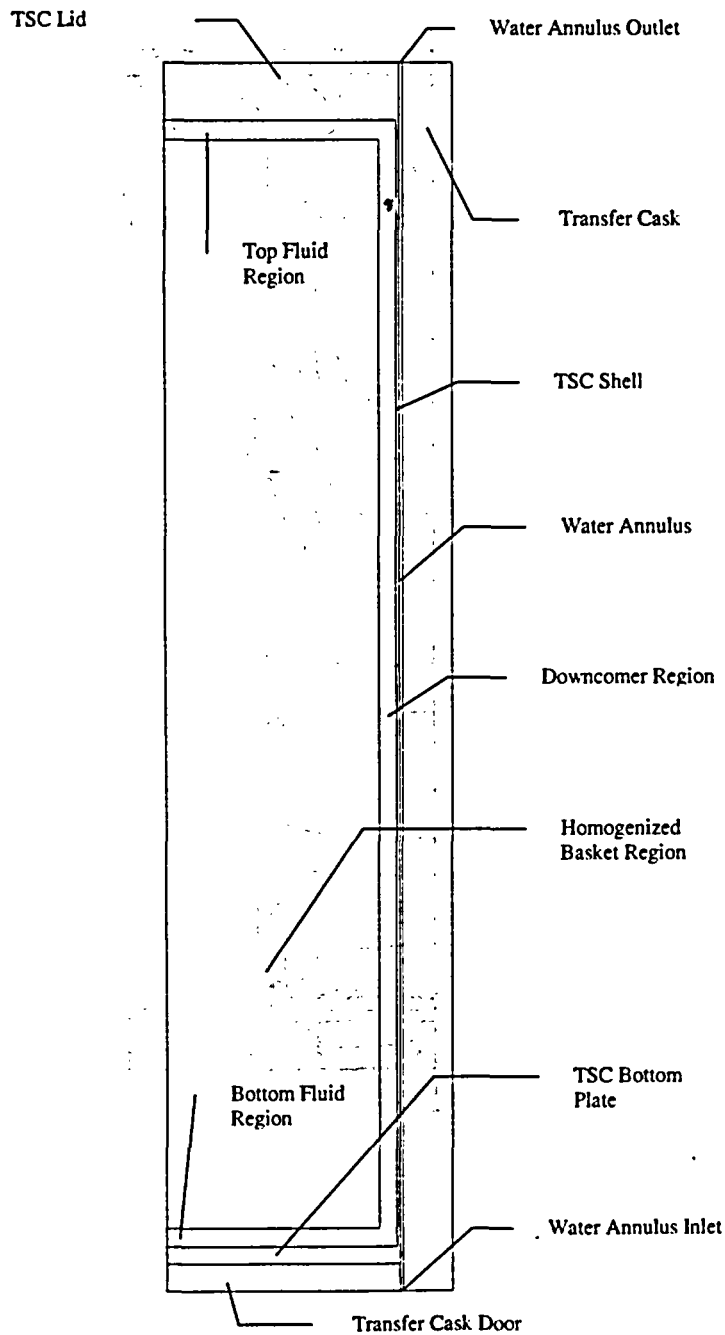


Figure 4.4-15 Temperature (°F) Distribution for the Concrete Cask and TSC Containing a Design Basis PWR Heat Load

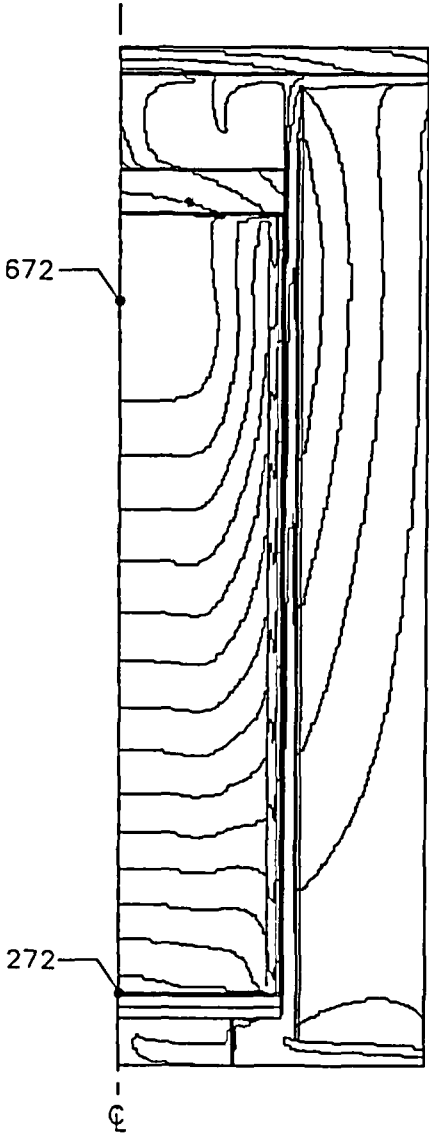


Figure 4.4-16 Air Velocity (m/s) in the Concrete Cask Annulus for the Design Basis PWR Heat Load ($V_{max} = 1.98$ m/s)

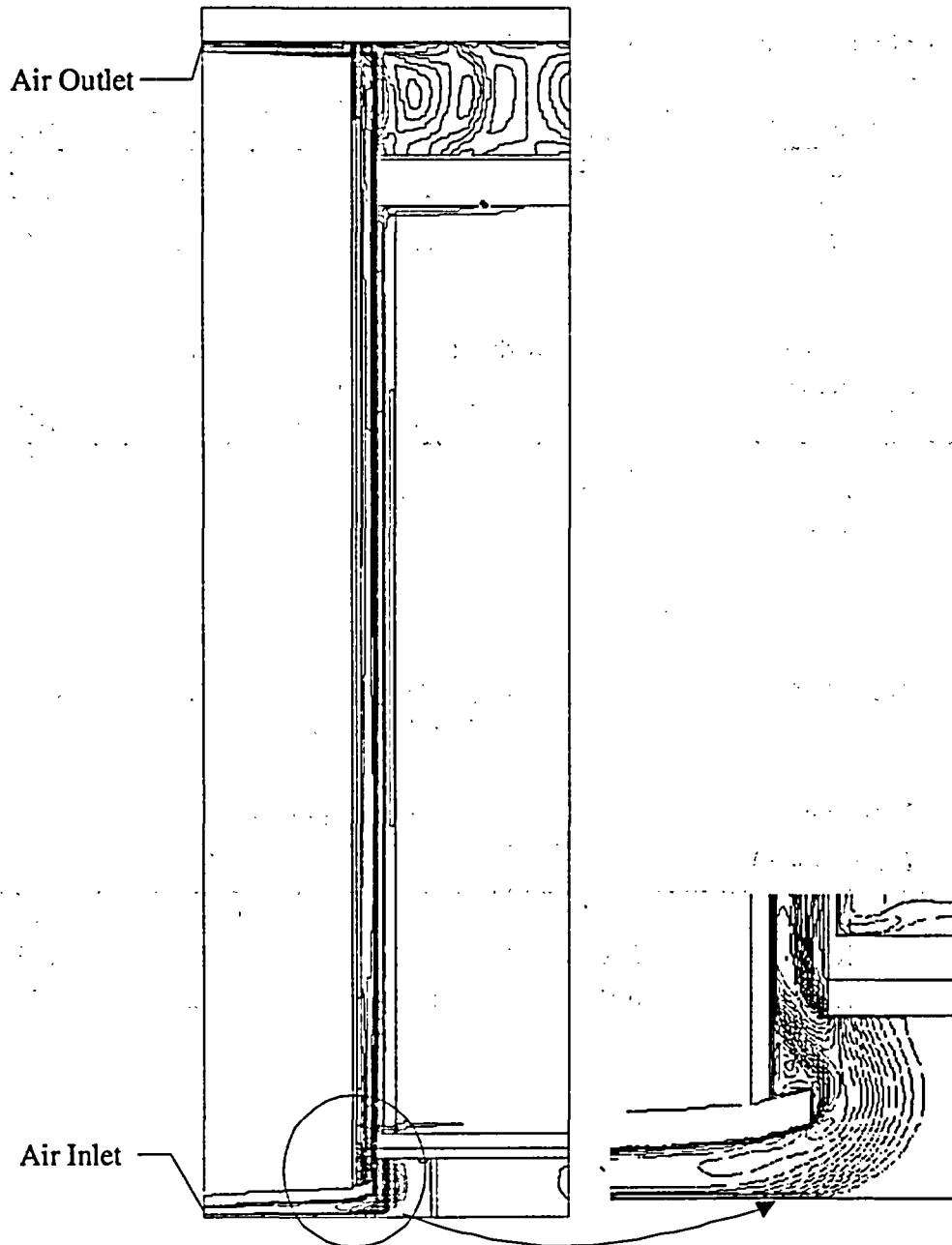


Table 4.4-1 Effective Thermal Conductivities for 14×14 PWR Fuel Assemblies for Helium Backfill

For fuel assemblies in fuel tubes with the neutron absorber:

Conductivity ^{a)} (Btu/hr-in-°F)	Temperature (°F)			
	228	421	619	819
Kxx	0.019	0.025	0.035	0.045
Kyy	0.019	0.025	0.035	0.045
Kzz	0.172	0.155	0.146	0.143

For fuel assemblies in positions without the neutron absorber:

Conductivity ^{a)} (Btu/hr-in-°F)	Temperature (°F)			
	227	419	615	815
Kxx	0.020	0.027	0.037	0.049
Kyy	0.020	0.027	0.037	0.049
Kzz	0.169	0.152	0.143	0.140

Table 4.4-2 Effective Thermal Conductivities for 10×10 BWR Fuel Assemblies for Helium Backfill

Conductivity ^{a)} (Btu/hr-in-°F)	Temperature (°F)			
	192	394	597	801
Kxx	0.021	0.028	0.039	0.053
Kyy	0.021	0.028	0.039	0.053
Kzz	0.176	0.161	0.152	0.151

^{a)} Kxx and Kyy correspond to the in-plane conductance, and Kzz correspond to the axial conductance (see Figure 4.4-9).

Table 4.4-3 Maximum Component Temperatures for Normal Condition Storage of Design Basis PWR and BWR Heat Loads

Principal Component Temperatures (°F)			
Component	PWR	BWR	Allowable Temperature (°F)
Fuel Cladding	672	657	752
Fuel Basket ^{a)}	672	657	700
TSC Shell	455	438	800
Concrete	266 (local)	248 (local)	300 (local)
	181 (bulk)	176 (bulk)	200 (bulk)

Table 4.4-4 Maximum Fuel Temperatures for the Transfer Operations for Design Basis Heat Load

Transfer Phase	Maximum Fuel Cladding Temperature (°F)
Water	157
Pressurized Drying	467
Helium	467
TSC Loading into Concrete Cask	650

^{a)} The maximum fuel cladding temperature is conservatively used.

4.5 Off-Normal Storage Events

This section evaluates postulated off-normal storage events that might occur once during any calendar year of operations. The actual occurrence of any of these events is, therefore, infrequent.

The concrete cask and TSC model described in Section 4.4.1.1 is used for the evaluation of the concrete cask and TSC for the off-normal events: severe ambient temperature conditions (106°F and -40°F) and the half-blocked air inlets condition. The evaluation of the off-normal events for variations in the ambient temperature only requires a change to the boundary condition temperature. For the half-blocked air inlets condition, the air inlet condition is modified to permit only half of the air flow into the inlet. The design basis heat loads of 40 kW and 38 kW are used in the evaluations of the concrete cask and TSC containing PWR and BWR fuels, respectively.

The principal component temperatures for each of the off-normal events, discussed previously, are summarized in the following tables, along with the allowable temperatures. Note that the maximum fuel cladding temperatures are conservatively used as the maximum fuel basket temperatures. As the tables show, the component temperatures for the concrete cask and TSC containing PWR and BWR fuels are within the allowable values for the off-normal storage events.

Principal Component Temperatures – Off-Normal Storage of PWR Fuel

Component	106°F Ambient, Maximum Temperatures (°F)	-40°F Ambient, Maximum Temperatures (°F)	100°F Ambient/Half Blocked Air Inlets Temperatures (°F)	Allowable Temperature (°F)
Fuel Cladding	670	524	676	1,058
Fuel Basket	670	524	676	1,000
TSC Shell	460	304	458	800
Concrete	273	67	271	350

Principal Component Temperatures – Off-Normal Storage of BWR Fuel

Component	106°F Ambient, Maximum Temperatures (°F)	-40°F Ambient, Maximum Temperatures (°F)	100°F Ambient/Half Blocked Air Inlets Temperatures (°F)	Allowable Temperature (°F)
Fuel Cladding	657	509	662	1,058
Fuel Basket	657	509	662	1,000
TSC Shell	446	292	444	800
Concrete	256	47	252	350

There are no adverse consequences due to these off-normal events. The maximum component temperatures are less than the allowable temperature limits.

Off- Normal Event TSC Internal Pressures

Off-normal event TSC internal pressures are evaluated using the method and inputs documented in the normal condition pressure evaluations (Section 4.4.4). The off-normal event TSC internal pressure analysis considers a 10% rod failure fraction and a TSC backfill temperature and pressure to 485°F and 104 psig. The higher backfill temperature, and associated pressure, is the result of the “severe heat” off-normal thermal evaluation. The maximum TSC internal pressures calculated for off-normal events are 114 psig for the PWR system and 110 psig for the BWR system.

4.6 Accident Events

This section presents the evaluations of the thermal accident design events, which address very low probability events that might occur once during the lifetime of the ISFSI or hypothetical events that are postulated because their consequences may result in the maximum potential impact on the surrounding environment. Three thermal accident events are evaluated in this section: maximum anticipated heat load, fire accident and full blockage of the air inlets. The maximum TSC internal pressure for the bounding accident conditions is evaluated in Section 4.6.4.

The concrete cask and TSC model described in Section 4.4.1.1 is used for the evaluation of the concrete cask and TSC for these thermal accident events.

4.6.1 Analysis of Maximum Anticipated Heat Load

This section evaluates the concrete cask and the TSC for the postulated accident event of an ambient temperature of 133°F. A steady state condition is considered in the thermal evaluation of the system for this accident event.

Using the same methods and thermal models described in Section 4.4.1.1 for the normal conditions of storage, thermal evaluations are performed for the concrete cask and the TSC with its contents for this accident condition. All boundary conditions in the model are the same as those used for the normal condition evaluation, except that an ambient temperature of 133°F is used. The maximum calculated temperatures of the principal PWR and BWR cask component, with the corresponding allowable temperatures, are as follows.

Component	PWR Maximum Temp (°F)	BWR Maximum Temp (°F)	Allowable Temp. (°F)
Fuel Cladding	716	701	1058
Fuel Basket	716	701	1000
TSC Shell	493	474	800
Concrete	313	293	350

Note that the maximum fuel cladding temperatures are conservatively considered to be the maximum basket temperatures. This evaluation shows that the component temperatures are within the allowable temperatures for the extreme ambient temperature conditions.

4.6.2 Fire Accident

A fire may be caused by flammable material or by a transport vehicle. While it is possible that a transport vehicle could cause a fire while transferring a loaded storage cask at the ISFSI, this fire

will be confined to the vehicle and will be rapidly extinguished by the persons performing the transfer operations or by the site fire crew. Fuel in the fuel tanks of the concrete cask transport vehicle and/or prime mover (maximum 50 gallons) is the only flammable liquid that could be near a concrete cask, and potentially at, or above, the elevation of the surface on which the cask is supported. The fuel carried by other onsite vehicles or by other equipment used for ISFSI operations and maintenance, such as air compressors or electrical generators, is considered not to be within the proximity of a loaded cask on the ISFSI pad. Site-specific analysis of fire hazards will evaluate the specific equipment used at the ISFSI and determine any additional controls required.

The analyzed area is a 15×15-foot square, less the 128-in-diameter footprint of the concrete cask, corresponding to the center-to-center distance of the concrete casks on the ISFSI pad. The potential depth (D) of the 50-gallon pool of flammable liquid is calculated as follows.

$$D = \frac{50 \times 231}{15 \times 15 \times 144 - 3.14 \times 128^2 / 4} = 0.6 \text{ in.}$$

With a burning rate of 5 in/hr, the fire would continue for 7.2 minutes. The fire accident evaluation in this section conservatively considers an 8-minute fire. The temperature of the fire is taken to be 1,475°F, which is specified for the fire accident event in 10 CFR 71.73c [3].

The fire condition is an accident event and is initiated with the concrete cask in a normal operating steady-state condition. To determine the maximum temperatures of the concrete cask components, the two-dimensional axisymmetric model of the concrete cask and TSC for the PWR configuration described in Section 4.4.1.1 is used to perform a transient analysis.

The initial condition of the fire accident transient analysis is based on the steady-state analysis results for the normal condition of storage, which corresponds to an ambient temperature of 100°F in conjunction with solar insolation (as specified in Section 4.4.1.1). The fire condition is implemented by applying a boundary temperature condition of 1,475°F at the air inlet and the lower surface of the steel plate forming the top of the air inlet for eight minutes. This boundary condition temperature is applied as a stepped boundary condition. During the eight-minute fire, solar insolation is also applied to the outer surface of the concrete cask. At the end of the eight minutes, the temperature at the inlet is reset to the ambient temperature of 100°F. The cooldown phase is continued for an additional 10.7 hours to observe the maximum TSC shell temperature and the average temperature of the TSC contents.

The maximum fuel temperature increased by less than 3°F, thus remaining well below the accident event temperature limit of 1,058°F. The maximum temperature of the TSC shell increases to 512°F due to the fire condition. The limited duration of the fire, the large thermal

capacitance of the concrete cask, and the minimal thermal conductivity limit the local region where the concrete temperatures exceed 300°F to less than 10 inches above the top surface of the air inlets. These results confirm that the operation of the concrete cask is not adversely affected during and after the fire accident condition.

4.6.3 Full Blockage of Concrete Cask Air Inlets

This section evaluates the concrete cask for the transient condition of full blockage of the air inlets at the normal storage condition temperature (100°F).

The accident temperature conditions are evaluated using the concrete cask and TSC thermal models described in Section 4.4.1.1. The transient analysis assumes initial normal storage conditions, with the sudden loss of convective cooling of the TSC. This is simulated by removing the inlet and outlet conditions from the model. Heat is then rejected from the TSC to the concrete cask liner only by radiation and convection. The loss of convective cooling to the ambient environment results in a sustained heat-up of the TSC and its contents and the concrete cask. The maximum fuel cladding temperature, maximum basket temperature, and the maximum concrete bulk temperature remain less than the allowable accident temperatures for approximately 72 hours after the initiation of the event. However, the internal pressure in the TSC cavity will reach the analyzed maximum pressure condition of 250 psig in approximately 58 hours after the initiation of a complete blockage event.

The evaluation demonstrates that there are no adverse consequences due to this accident, provided that debris is cleared from at least two air inlets within 58 hours based on the steady-state evaluation of the half-blocked air inlet condition in Section 4.5.

4.6.4 Maximum TSC Internal Pressure for Accident Events

Accident event pressures are evaluated with the method and inputs documented in the normal condition pressure evaluation (Section 4.4.4). Differences incorporated in the accident condition analysis are use of a 100% rod failure fraction and an increase in the TSC backfill temperature and pressure to 677°F and 128 psig. The higher backfill temperature, and associated pressure increase, is the result of the full air inlets blocked thermal evaluation. Maximum calculated TSC internal pressures under these conditions are 246 psig for the PWR system and 195 psig for the BWR system.

4.7 References

1. 10 CFR 72, "Licensing Requirements for the Independent Storage of Spent Nuclear Fuel and High Level Radioactive Waste and Reactor-Related Greater than Class C Waste," Code of Federal Regulations, US Government, Washington, DC.
2. ISG-11, Revision 3 – "Cladding Considerations for the Transportation and Storage of Spent Fuel," US Nuclear Regulatory Commission, Washington, DC, November 17, 2003.
3. 10 CFR 71, "Packaging and Transportation of Radioactive Material," Code of Federal Regulations, US Government, Washington, DC.
4. ACI-349-85, "Code Requirement for Nuclear Safety Related Concrete Structures and Commentary," American Concrete Institute, Farmington Hills, MI.
5. PNL-4835, Johnson, A.B., and Gilbert, E.R., "Technical Basis for Storage of Zirconium-based alloy-Clad Fuel in Inert Gases," 1985.
6. "NS-4-FR Fire Resistant Neutron and/or Gamma Shielding Material" - Product Technical Data, The Japan Atomic Power Company, Tokyo, Japan.
7. Standard Handbook for Mechanical Engineers, Baumeister T. and Mark, L.S., 7th Edition, New York, McGraw-Hill Book Co., 1967.
8. ASME Boiler and Pressure Vessel Code, Section II, Part D, "Properties," American Society of Mechanical Engineers, New York, NY, 2001 Edition with 2003 Addenda.
9. ARMCO Product Data Bulletin No. S-22, "17-4PH, Precipitation Hardening Stainless Steel," ARMCO, Inc., 1988.
10. ASME Code Case N-71-17, "ASME Boiler and Pressure Vessel Code, Code Cases - Boilers and Pressure Vessels," American Society of Mechanical Engineers, New York, NY, 1996.
11. ANSYS, Revision 6.0, ANSYS INC, Canonsburg, PA
12. FLUENT, Revision 6.1, Fluent Inc, Lebanon, NH
13. "Principles of Heat Transfer," Krieth F., Bohn M.S., , Fifth Edition, West Publishing Company.
14. "Fundamentals of Heat and Mass Transfer," F.P. Incropera and D.P. DeWitt, 1981.
15. "A Method for Determining the Spent-Fuel Contribution to Transport Cask Containment Requirements," TTC-1019, UC-820, Sandia 90-2406, Sanders, T. L., et al., November 1992.

16. EPRI NP-5128, "The TN-24P PWR Spent-Fuel Storage Cask: Testing and Analyses," Pacific Northwest Laboratory, Virginia Power Company and EG&G, Idaho National Engineering Laboratory, April 1987.
17. "A Physical Introduction to Fluid Mechanics," 1st Edition, Alexander J. Smits, 2000.
18. "Fluid Mechanics," 2nd Edition, Frank M. White, 1979.
19. "Annual Books for ASTM Standards," Section 1, Volume 01.04, American Society for Testing and Materials, West Conshohocken, PA.
20. "NUREG-1536, Standard Review Plan for Dry Cask Storage Systems," US Nuclear Regulatory Commission, Washington, DC, January, 1997.

Chapter 4 Appendices

Appendix 4 Thermal Evaluation

Table of Contents

4.A	Benchmark of the Two-Dimensional Axisymmetric Methodology for TSC Thermal Analyses For MAGNASTOR	4.A-1
4.A.1	Introduction.....	4.A-1
4.A.2	Purpose.....	4.A-2
4.A.3	Description of the Thermal Test	4.A-2
4.A.4	FLUENT Model Description	4.A-2
4.A.4.1	Effective Properties for the Basket and Fuel Regions	4.A-2
4.A.4.2	Boundary Conditions	4.A-3
4.A.5	Analysis Results.....	4.A-4
4.A.6	Application of the Benchmark to the MAGNASTOR Evaluation	4.A-4
4.A.7	Conclusions.....	4.A-6
4.B	Methodology to Compute the Porous Media Constants	4.B-1

List of Figures

Figure 4.A-1	Two-Dimensional Model of the 24 PWR Assembly Thermal Test Configuration	4.A-7
Figure 4.A-2	ANSYS Model for Determination of the Benchmark Basket Thermal Properties	4.A-8
Figure 4.A-3	Temperature Profile from the Benchmark Cask Cavity Inner Surface.....	4.A-9
Figure 4.A-4	Axial Power Distribution Curve for the 15 x15 PWR Fuel Assembly.....	4.A-9
Figure 4.A-5	Temperature Contours for the Benchmark Cask Thermal Test	4.A-10

4.A Benchmark of the Two-Dimensional Axisymmetric Methodology for TSC Thermal Analyses For MAGNASTOR

In this Appendix, a benchmark evaluation is performed. A thermal evaluation using two-dimensional modeling methodology is performed for a system for which a thermal test has been conducted. Convection, conduction and radiation within the confinement boundary are considered in this evaluation. The thermal test is described in EPRI NP-5128 [16]. The results of the thermal evaluation using the two-dimensional methodology performed in this Appendix shows that the two-dimensional methodology is conservative and, therefore, acceptable for use in the thermal evaluation of MAGNASTOR.

4.A.1 Introduction

The thermal design of MAGNASTOR involves all three modes of heat transfer to reject heat from the fuel into the ambient. The most dominant mode of heat transfer is by convection, which involves helium removing heat from the fuel assembly as it flows up through the fuel tubes and transferring the heat to the TSC shell as it flows down through the basket weldment (downcomer) region. The heat transferred to the TSC shell is then rejected into the concrete cask annulus airflow and transported to the ambient environment. The design of the concrete cask annulus to permit airflow between the TSC and the concrete cask to transfer heat to the ambient is in numerous licensed spent fuel storage system designs. The most significant difference with the MAGNASTOR design is the inclusion of convection in the TSC as a means of removing heat from the fuel assemblies.

The geometry of the MAGNASTOR fuel basket is an array of square tubes in a cylindrical outer boundary, the TSC shell. This implies that the flow of the helium upward in the basket is through a complex cross-section of squares, less the circular cross-sections of the fuel rods. The downward flow of the helium on the outside of the fuel basket next to the TSC shell is also through an area with a complex cross-section, since the outer boundary is circular and the inner boundary of the downcomer is the outer perimeter of the square array of fuel tubes. While this has the characteristics of a three-dimensional system, it is evaluated as a two-dimensional axisymmetric system. Even as a three-dimensional system, the complex flow area for the fuel region is impractical to be incorporated into a fluid flow analysis with detailed modeling for each fuel rod. Additionally, due to the design of the fuel basket and the range of fuel temperatures expected, conduction and radiation heat transfer throughout the fuel basket cannot be neglected. The methodology adopted for this analysis includes the determination of effective properties for thermal conduction and radiation, as well as for fluid flow resistances, which are to be implemented in a two-dimensional axisymmetric model. The end result of the two-dimensional evaluation is to determine the maximum temperatures for the fuel rod cladding.

For this reason, a benchmark is performed to demonstrate that two-dimensional methodology is acceptable to determine the maximum fuel cladding temperatures for MAGNASTOR.

4.A.2 Purpose

The purpose of this appendix is to provide a benchmark, which demonstrates that the two-dimensional methodology employed in the MAGNASTOR thermal evaluation is conservative.

4.A.3 Description of the Thermal Test

In EPRI NP-5128 [16], thermal testing was performed for a vertical metal cask containing 24 PWR (15×15) assemblies with a total heat load of 20.6 kW. The variation of the heat loads between the assemblies was less than 6%, which can be approximated as a uniform heat load. The basket contained in the cask during testing was comprised of an array of 24 square slots in which the basket walls were constructed of aluminum. While there were a series of tests performed, the test of interest for this evaluation was the test corresponding to vertical orientation of the cask in which the cask was backfilled with nitrogen to one atmosphere. Axial profiles of the temperature data were obtained in the tests for the inner surface of the cask, as well as for various radial locations in the basket. Temperature data was not obtained for the center of any fuel assembly, but rather on the basket.

4.A.4 FLUENT Model Description

The two-dimensional axisymmetric model for this evaluation only needs to consider the cavity of the metal cask. Modeling of the cask wall and surface is not considered necessary since the temperatures at the cask inner surface from the test are being applied as the boundary conditions for the model. The various regions of the model are shown in Figure 4.A-1. Regions 2 through 5 comprise the full length of the basket of the cask. Regions 2 through 4 represent the fuel in the basket, and Region 3 corresponds to the 144-inch active fuel region. Region 5 is considered to be within the length of the basket, but outside the length of the fuel assembly. Regions 1, 6 and 7 correspond to the backfill gas, nitrogen. For Regions 1, 6 and 7, it is only necessary to input the material properties for nitrogen to simulate the flow of nitrogen in the cask cavity. The gas is modeled as an ideal gas in FLUENT and all regions in the model utilized laminar flow conditions.

4.A.4.1 Effective Properties for the Basket and Fuel Regions

For the regions corresponding to the basket, effective properties are employed in the analysis. To account for the flow resistance of the wetted perimeter of the fuel and the fuel assembly grids, the porous media option in FLUENT is used. The determination of the porous media constants

depends on the radius assigned to the basket region, which also must be associated with the effective cross-section area of the downcomer region. The cross-section for the downcomer region is used to compute the outer radius of the basket region in the two-dimensional axisymmetric model (Regions 2 through 5). Calculation of these constants for the porous media is described in Appendix 4.B. The methodology applied for this benchmark follows the same methodology described for the MAGNASTOR TSC model in Section 4.4.1.1.

The effective thermal properties for the basket region are computed using an ANSYS model shown in Figure 4.A-2. This model contains the aluminum basket and the fuel regions, which are modeled with homogeneous orthotropic thermal conductivities. To determine the temperature-dependent effective thermal conductivity of the basket region, a series of temperatures is applied to the boundary of the model. Solutions for each boundary condition determine the maximum temperature of the basket and the associated change in temperature from the boundary to the maximum temperature location. The effective thermal conductivities are determined using the same expression employed for MAGNASTOR in Section 4.4.1.2.

4.A.4.2 Boundary Conditions

The outer edges of the model correspond to the inner surface of the cask cavity. The following boundary conditions were applied to the model.

Temperature Specification

To remove any uncertainties in the model due to the cask wall conductance, the convection condition at the cask surface, or the variations in the ambient conditions, the temperatures from the test corresponding to the inner surface of the cavity were applied to the outer surface of the model. The temperature profile is shown in Figure 4.A-3.

Heat Generation

The total heat load applied to Region 3 of the model in Figure 4.A-1 was 20.6 kW. The heat generation was assumed to be uniformly distributed over the radial direction from the basket centerline to the outer radius of the porous media region (Region 3). In the axial direction, the power distribution as shown in Figure 4.A-4 was applied, which shows a peaking factor of 1.2.

Buoyancy

Since the backfill gas was specified as an ideal gas, the only condition required to enact buoyancy as a driving force for the nitrogen is to set the gravity acceleration as -9.8 m/sec^2 .

Cavity Pressure

To be consistent with the boundary conditions used in the analyses for MAGNASTOR, a pressure was applied to the cavity region. For the benchmark, the pressure in the cavity was set to zero (gauge).

4.A.5 Analysis Results

The temperature contour corresponding to the applied conditions is shown in Figure 4.A-5. The distribution of the contours along the centerline shows the maximum temperature is close to the top of the basket, which is characteristic of baskets in which the dominant heat transfer is by convection. The maximum basket temperature reported in the thermal test was 232°C, as compared to a maximum basket temperature of 233°C obtained from the analysis. This indicates that the analysis temperature is 1°C conservative with respect to the test data.

4.A.6 Application of the Benchmark to the MAGNASTOR Evaluation

The benchmark thermal test cask contained PWR assemblies and was backfilled with nitrogen. The force driving the movement of the backfill gas is buoyancy. A common metric employed to compare buoyancy driven systems is the Rayleigh Number (Ra), which can be computed for both systems. The Ra is expressed as follows.

$$Ra = (\rho^2 \beta g \Delta T L^3 / \mu^2) \times Pr \quad [15]$$

where:

- ρ ----- density (kg/m³)
- β ----- coefficient of expansion (1/K)
- g ----- gravitational constant = 9.8 m/sec²
- ΔT ----- temperature difference = max. centerline temperature - basket bottom temperature (K)
- L ----- height of basket (m)
- μ ----- viscosity (N-sec/m²)
- Pr ----- Prandlt number

Using the data from the benchmark thermal test and the analysis of the normal condition for MAGNASTOR, the Ra of the backfill gas can be computed for each analysis.

Design	Gas T _{ave} (K)	ρ (kg/m ³)	β (1/K)	ΔT (K)	μ (N-sec/m ²)	Pr	L (m)	Ra
MAGNASTOR	520	0.7501	1/520	222	2.63x10 ⁻⁵	0.668	4.420	1.97x10 ¹¹
Benchmark	426	1.213	1/426	142	2.30x10 ⁻⁵	0.703	4.076	4.33x10 ¹¹

Note: T_{ave} is the average gas temperature (helium for MAGNASTOR and nitrogen for the benchmark) used to evaluate the properties in this table.

As indicated by the preceding table, the Ra for MAGNASTOR is the same order of magnitude as that for the benchmark. This indicates that the buoyancy forces driving the flow in the benchmark are essentially identical to the buoyancy force in the MAGNASTOR design. Additionally, both models employ a laminar flow model inside the cavity. While the benchmark cask thermal test design stores 24 PWR fuel assemblies and the MAGNASTOR PWR design can store 37 PWR fuel assemblies, the arrays of both designs are comprised of square slots of nearly the same dimensions. The geometry of the flow area in the basket region is similar for both, since PWR fuel assemblies occupy a square slot in a square design. This is indicated in the following table, which contains the slot dimensions. These values indicate that the porous media parameters would also be similar, and in both analyses, the porous media parameters are computed using the same methodology.

Design	Fuel Assembly Width (inch)	Slot Size (inch)
MAGNASTOR	8.426	8.86/8.76
Benchmark	8.304	8.99

This indicates the high degree of similarity of both configurations. Additionally, in both designs, the downcomer region is comprised of a circular outer boundary and an inner boundary consisting of a series of edges of squares.

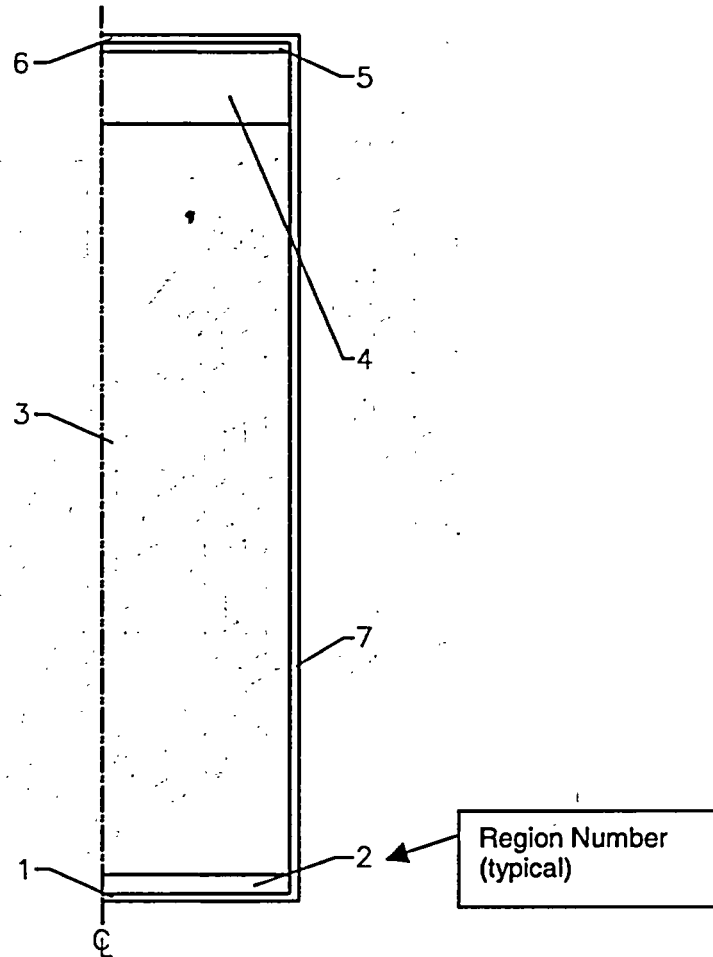
In both designs, the basket is formed of plates (or tubes for MAGNASTOR), which also serve as conductors to the periphery of the basket. In the benchmark evaluation and in the MAGNASTOR evaluation, the porous media material is modeled to represent the conduction in the basket as well, since the basket plates were not modeled explicitly. The conductivity for the porous media region represents the radial conductance, as well as the axial conductance of the baskets. The method used to compute the effective thermal conductivities for both baskets was identical.

The reported results of the thermal test indicate that the two-dimensional modeling using FLUENT is conservative since the FLUENT simulation of the benchmark predicted a higher temperature than the reported test data. It is important to note that the thermal boundary conditions for the FLUENT analysis of the benchmark thermal test employed the temperatures from the benchmark test directly, which eliminates any uncertainties in the analysis due to the conduction through the benchmark cask body, convection from the cask surface, or variations in the ambient conditions over the cask. The analysis associated with the thermal test focused only on the convection internal to the cask cavity. This confirms that the axisymmetric modeling, in conjunction with the use of porous media material characterization, is an acceptable methodology for the computation of maximum fuel cladding temperatures.

4.A.7 Conclusions

In this appendix a thermal evaluation has been performed for the thermal test described in EPRI N-5128 [17]. The analysis results indicate that the two-dimensional axisymmetric modeling methodology incorporating effective thermal properties and the flow resistance in the fuel region is acceptable to determine a bounding maximum fuel temperature. The benchmark also confirms the use of the hydraulic diameter for the representation of the non-axisymmetric downcomer region, as well as the use of orthotropic properties for the basket conductance.

Figure 4.A-1 Two-Dimensional Model of the 24 PWR Assembly Thermal Test Configuration



Region Number	Description	Dimension (mm)
1	Bottom nitrogen region	45
2	Region below active fuel region in the basket	152
3	Active fuel region	3658
4	Region above active fuel region in the basket	248
5	Basket region without fuel	18
6	Top nitrogen region	29
7	Equivalent radial gap (downcomer region)	64

Figure 4.A-2 ANSYS Model for Determination of the Benchmark Basket Thermal Properties

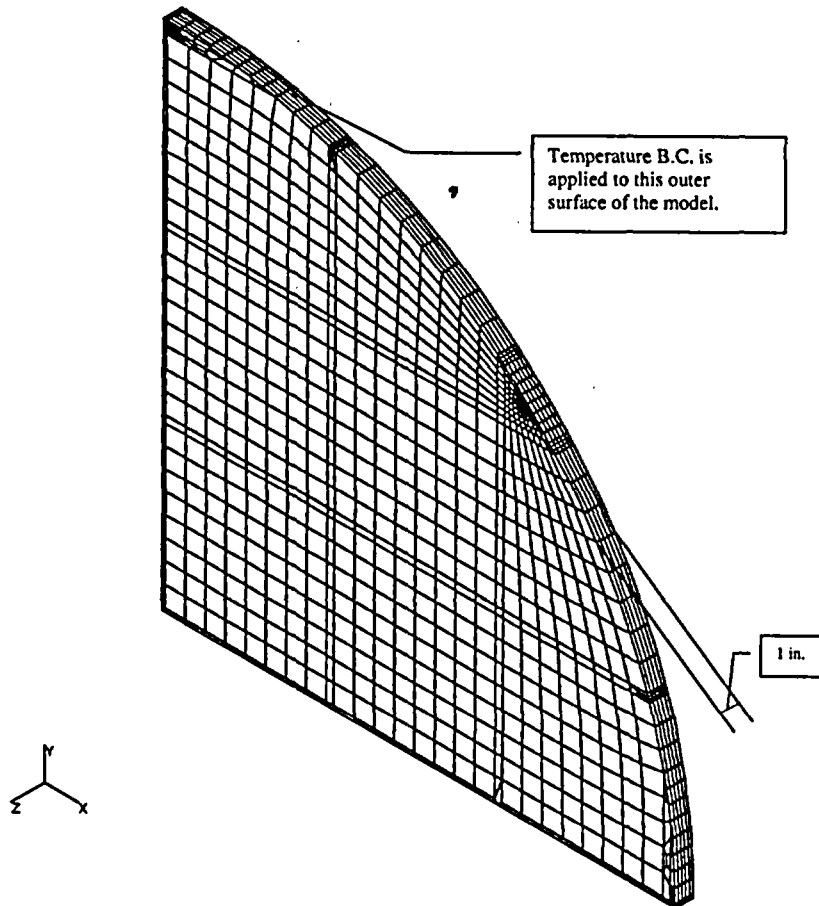


Figure 4.A-3 Temperature Profile from the Benchmark Cask Cavity Inner Surface

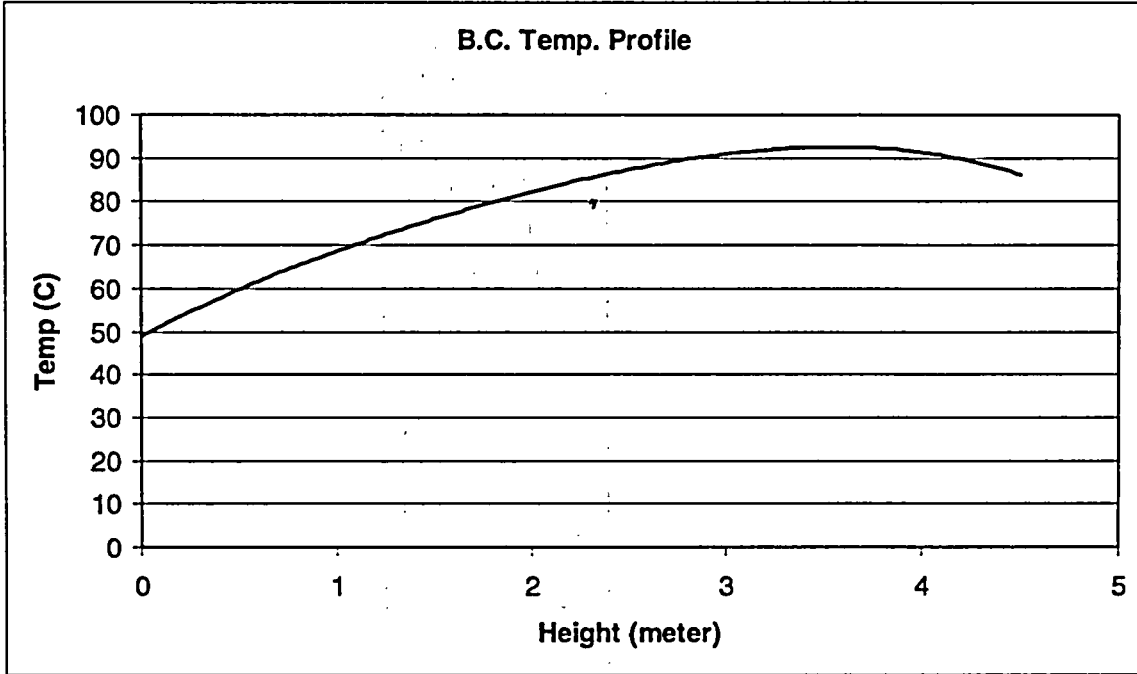


Figure 4.A-4 Axial Power Distribution Curve for the 15 x15 PWR Fuel Assembly

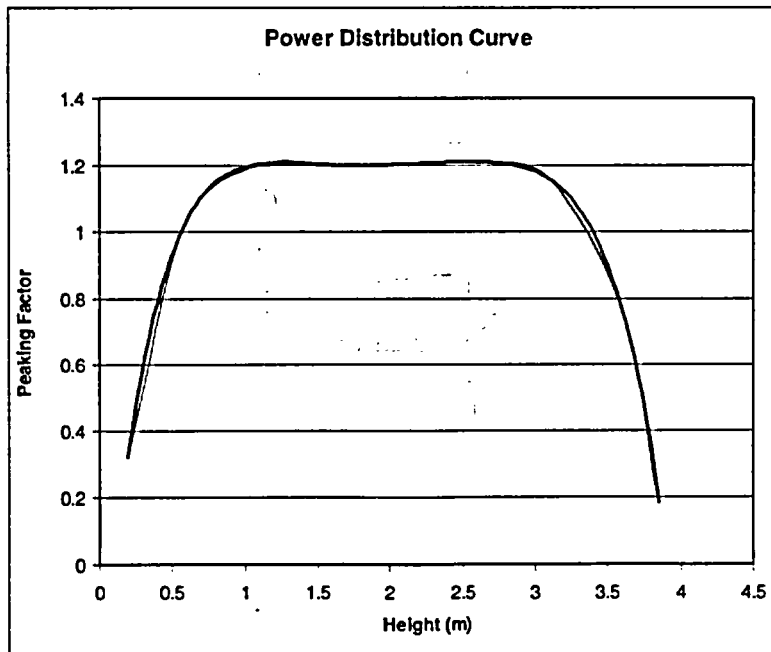
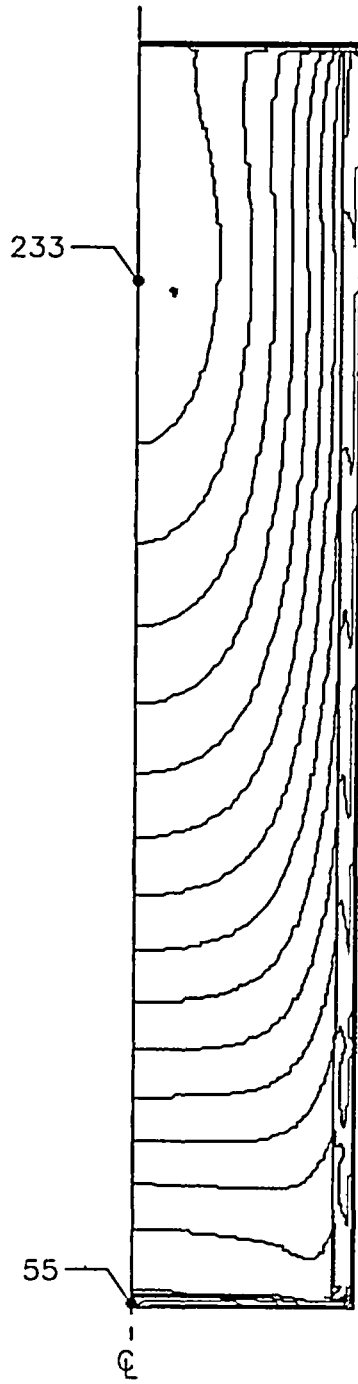


Figure 4.A-5 Temperature Contours for the Benchmark Cask Thermal Test



4.B Methodology to Compute the Porous Media Constants

This appendix presents the methodology used to determine the porous media constants, which will simulate the flow resistance due to the fuel assembly and fuel assembly grids to be taken into account for the basket tube/fuel region of the two-dimensional axisymmetric TSC model. To simulate the flow resistance in the porous media models, the following FLUENT porous media pressure drop [12] is employed.

$$\frac{\Delta P}{L} = \frac{\mu}{\alpha} V + C \left(\frac{1}{2} \rho V^2 \right)$$

where:

$\Delta P/L$	-----	pressure drop per unit length (Pa/m)
V	-----	superficial fluid velocity (m/s)
μ	-----	the fluid viscosity (kg/m-s)
ρ	-----	fluid density (kg/m ³)
α	-----	permeability parameter (m ²)
C	-----	inertial resistance factor (m ⁻¹)

In this representation, the pressure drop for the porous media consists of two terms: one being proportional to the velocity and the other proportional to the velocity squared. For the first term, the viscosity (μ) is obtained from the material properties defined for the gas, while the factor (α), referred to as the permeability, is computed on the basis of laminar pipe flow for a constant cross-sectional area. For the second term, the density (ρ) is obtained from the material properties defined for the gas, while the factor (C), referred to as the inertial resistance, is due to the pressure loss associated with the fuel assembly grids.

The porous cells in FLUENT are 100% open in the porous media model [12]. Therefore, the values specified for $1/\alpha$ and C are adjusted based on the porosity of the porous media [12].

Permeability (α)

To determine the permeability, neglect the loss due to the inertial resistance and consider the steady-state flow of fluid in a pipe.

The pressure drop of the porous media model then reduces to Darcy's Law:

$$\frac{\Delta P}{L} = \frac{\mu}{\alpha} V \tag{a}$$

The average velocity for a laminar pipe flow [18] is:

$$V = \frac{D^2}{32\mu} \left(\frac{\Delta P}{L} \right) \quad (b)$$

where, D is hydraulic diameter.

From equation (b), we can get

$$\frac{\Delta P}{L} = \frac{32\mu}{D^2} V \quad (c)$$

Comparing equation (a) with equation (c), we can get

$$\frac{1}{\alpha} = \frac{32}{D^2}$$

Considering the porosity of the porous media (ϵ), the $1/\alpha$ becomes

$$\frac{1}{\alpha} = \frac{32}{\epsilon D^2}$$

Inertial Resistance (C)

The fuel assembly grids occur at discrete locations over the fuel assembly, but they are not modeled explicitly in the model. The pressure loss is to be taken into account over the length of the assembly, and the inertial resistance factor is proportional to the velocity square (V^2). Since the porous media is being considered, the physical velocity must be employed. This implies that the velocity must be divided by the porosity (ϵ) and, since the pressure drop due to the inertial resistance occurs over a length L, the expression for C is as follows.

$$C = \frac{K}{L} \frac{1}{\epsilon^2} = \frac{K}{\epsilon^2 L}$$

The quantity K is the inertial resistance factor, which is dependent on the geometry. The pressure loss due to the flow through the grid is represented in terms of the loss due to contraction of the flow as the flow enters the grid (K_c) and due to expansion as the flow leaves the grid (K_e). To provide a bounding value for K_c , the loss associated with entering the grid is taken to 0.5, which is for the contraction from an infinite reservoir to finite cross-sectional area [19]. Likewise, to provide a bounding value for K_e , the loss associated with flow leaving the grid is taken to 1.0, which is for the expansion from a finite cross-sectional area to an infinite

reservoir [19]. These losses are considered to be additive over eight grids for a typical PWR fuel assembly, which yield the following expression for K:

$$K = N \times (K_c + K_e) = 8 \times (1.5) = 12$$

This value for K, which is determined based on the limiting values for K_c and K_e , is considered to be conservative, since the geometry of the grid does not represent these extreme conditions.